The University of Nottingham
UNITED KINGDOM · CHINA · MALAYSIA
School of Pharmacy

Novel Thermoresponsive Particle Gels For Tissue Engineering Applications

Racha Cheikh Al Ghanami, MPharm

Thesis submitted to the University of Nottingham for

the degree of Doctor of Philosophy
September 2011

ABSTRACT

Biomaterials play an important role in tissue engineering, where they are used as scaffolds for the 3D culture of cells, to help the generation of neo tissues *in*-vitro and achieve superior tissue engraftment and regeneration *in*-vivo.

The work presented in this thesis describes how thermoresponsive particle gels, a class of materials not previously investigated for tissue engineering applications, can find important applications in this field.

The main gels developed and studied were the aqueous thermoresponsive particle gels prepared from poly(poly(ethylene glycol) methacrylate ethyl ether) (polyPEGMA$_{246}$-EE) together with polycaprolactone (PCL) microparticles.

The thermoresponsive polymer polyPEGMA$_{246}$-EE, synthesised by free radical polymerisation, was employed as an adsorbing steric stabiliser for polycaprolactone microparticles prepared by the single emulsion solvent evaporation method. The resulting suspensions exhibited reversible temperature induced gelation based on incipient flocculation, where they switched from being free flowing at temperatures below 19°C to form space filling gels at body temperature (37°C) over periods of ~1 minute. On cooling, the suspensions returned to a fluid state.

The viscoelastic properties of the particle gels could be controlled by varying the temperature and composition, enabling these gels to be tailored for specific applications.

Using NIH3T3 as a model cell line, PCL/polyPEGMA$_{246}$-EE particle gels exhibited key characteristics advantageous for the 3D culture of cells. These were mainly the ability to

assemble around the cells at temperatures, above the LCST of polyPEGMA$_{246}$-EE, and the provision of a supportive scaffold with appropriate mechanical properties for growth, along with good cytocompatibility enabling cell spreading and proliferation over extended culture times, as well as the rapid return to a flowable state on cooling allowing for suspension transfer, for cell subculture and harvesting, without the need for enzymes. The latter property would also allow for the injectable delivery of the *in*-vitro conditioned cell-gel constructs for therapeutic applications.

Another variant of thermoresponsive particle gels has also been presented in this thesis. Thermoresponsive magnetic-particle gels were developed from the combination of magnetic polystyrene microparticles and the thermoresponsive polymer polyPEGMA$_{246}$-EE. These exhibited reversible thermogelling behaviour which allowed for cell encapsulation, while their magnetic sensitivity allowed for cell recovery through simple magnetic particle separation.

The novel concept of scaffold deconstruction by temperature, and cell recovery through magnetic-particles separation is significant for applications where a scaffold-free outcome would be desired such as the commercial expansion of therapeutic cells.

In this thesis, the preparation and application of first generation biocompatible thermoresponsive particle gels is described.

The combination of ease of preparation, the potential for scale-up and positive cell response make thermoresponsive particle gels promising as a new class of materials for applications in cell culture, as supports for tissue growth and in cell delivery systems.

The materials developed and studied in this thesis are believed to represent a significant contribution to the fields of biomaterials, drug delivery and tissue engineering.

LIST OF PUBLICATIONS

The work presented in this thesis has given rise to the following publications:

- Wang, W., Liang H., Cheikh Al Ghanami R., et al. (2009). "Biodegradable Thermoresponsive Microparticle Dispersions for Injectable Cell Delivery Prepared Using a Single-Step Process." Advanced Materials 21(18): 1809-1813.

- Cheikh Al Ghanami R., Saunders B R., et al. (2010). "Responsive particulate dispersions for reversible building and deconstruction of 3D cell environments." Soft Matter 6(20): 5037-5044.

- Patent application: “Responsive Magnetic Particulate Dispersion for Ex-vivo Cellular Expansion on 2D and 3D Cell Culture and Cell Recovery via Magnetic Separation” (under submission to patenting authorities, 8/2011)

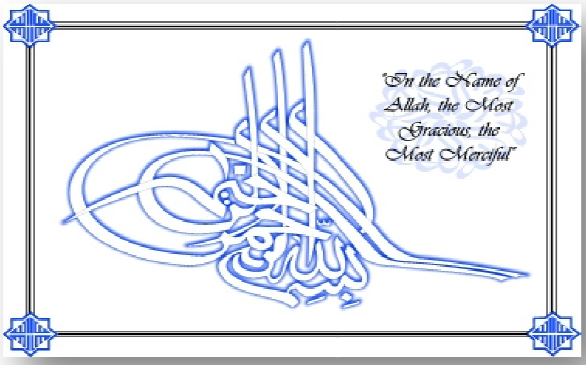

To my beloved Parents,

And the Syrian Martyrs of freedom, 2011

"27 Have you not considered how God sends water down from the sky and that We produce with it fruits of varied colours; that there are in the mountains layers of white and red of various hues, and jet black; 28 that there are various colours among human beings, wild animals, and livestock too? It is those of His servants who have knowledge who stand in true awe of God. God is almighty most forgiving." Noble Quran 35:28-29

ACKNOWLEDGEMENTS

First and foremost, all praise and thanks are due to ***Allah***, the Most Gracious, and the Most Merciful for all his blessings and for making me able to produce this PhD thesis.

I would like to express gratitude to my supervisors Professor Cameron Alexander and Professor Kevin Shakesheff for the inspiration, guidance and support they offered throughout my time in Nottingham.
I would also like to thank Dr. Brian Saunders, University of Manchester, and Dr Michael Fraylich for their help and input over the period of this project.

I am deeply appreciative of the help I received from my colleagues in the Tissue engineering and Drug delivery groups, especially Catherine, Sabrina, Omar, Kapil, Lloyd, Aram, Mahmood, Felicity, Samer, Paco and Andrea who were willing to provide help and advice in the lab whenever I needed. Thanks also to Teresa Marshall, Christy Gringer-Boulbty and Sue Dodson for all the technical help.

I must thank my friends Nanis and Sabrina, Alaae, Romaissa and Klara for the lovely lunch, coffee & chocolate breaks which helped me cheer up after some stressful times in the Lab!

I am indebted, and words can never express my gratitude, to my Father and Mother and my brothers, Riad and Tarek, for their love, encouragement and for all their prayers, which have been the drivers for all what I have achieved so far. The prayers of my extended family and friends are equally appreciated. Special thanks to Issam for his help and encouragement.

Lastly, I would like to acknowledge the funding and financial support I received throughout my postgraduate study at the University of Nottingham from the Algerian Ministry of Higher Education.

TABLE OF CONTENTS

LIST OF FIGURES

LIST OF ABBREVIATIONS

$\%_{v/v}$	% volume per volume
$\%_{w/v}$	% weight per volume
$\%_{w/w}$	% weight per weight
2D	Two dimensional
3D	Three dimensional
BMP	Bone morphogenetic protein
CAM	Cell adhesion molecules
CAMs	Cell adhesion molecules
Da	Dalton
DAPI	4',6-diamidino-2-phenylindole
DCM	Dichloromethane
DMEM	Dulbecco's modified Eagles medium
DNA	Deoxyribonucleic acid
EDTA	Ethylene diamine tetraacetic acid
Ex/Em	Excitation/Emission
FBS	Fetal bovine serum
FDA	Food and drug administartion
FITC	Fluorescein isothiocyanate
G'	Storage (elastic) modulus
G''	Loss (viscous) modulus
GAGs	Glycosaminoglycans
GPC	Gel permeation chromatography
HBSS	Hank's balanced salt solution
kDa	Kilo Daltons
LVE	Linear viscoelastic region
MACS	Magnetic activated cell sorting
Micro-CT	micro computed tomography
Mn	Number average molecular weight
Mw	Weight average molecular weight
NaOH	Sodium hydroxide

NMR	Nuclear magnetic resonance
Pa	Pascals
PBS	Phosphate buffered saline
PCL	Poly (caprolactone)
PEG	Poly(ethylene glycol)
$PEGMA_{246}$-EE	poly(ethylene glycol) methacrylate ethyl ether (Mn=246)
$PEGMA_{475}$-ME	poly(ethylene glycol) methacrylate methyl ether (Mn=475)
PGs	Proteoglycans
PLC	Phospholipase C
PLGA	Poly (lactic-co-glycolic) acid
PolyNIPAm	poly(N-isopropylacrylamide)
$polyPEGMA_{246}$-EE	poly(poly(ethylene glycol) methacrylate ethyl ether)
$polyPEGMA_{475}$-ME	poly(poly(ethylene glycol) methacrylate methyl ether)
ppHEX	Plasma polymerised hexane
PS	Polystyrene
PVA	Poly(vinylalcohol)
RAFT	Reversible addition fragmentation transfer reaction
RGD	Arginine-Glycine-Aspartic acid
Rpm	Revolutions per minute
SD	Standard deviation
SEM	Scanning electron microscopy / Standard error of the mean
TCP	Tissue culture plastic
TGF-β	tumour growth factor- β
TRITC	tetramethyl rhodamine isothiocyanate
WCA	Water contact angle

CHAPTER 1

General introduction

1.1 Regenerative medicine and tissue engineering

Bio/chemical interventions and the use of various drug molecules have revolutionised health care and disease management over the last century, where several deadly disease states that claimed millions of lives have became readily curable. However, there still remain certain disease conditions where those interventions are insufficient to restore normal tissue function or grant a cure. Examples include diabetes, stroke, muscular dystrophy, liver cirrhosis and renal failure where organ transplantation remains the mainstay of therapy. Not only does organ transplantation put the recipient at increased risk of infections and further complications from the associated immunosuppressive therapy, but the large shortage of donated organs compared to the long waiting lists, means that the disease is often fatal before therapy becomes available(Atala, 2007).

Regenerative medicine holds promise for those diseases involving functional or structural tissue loss. It aims at restoring the functions of diseased or damaged tissues or organs, using approaches that include: cell therapy, tissue engineering, and gene therapy or employing medical devicesf(Yannas, 2005, Prokop, 2001, Polak and Bishop, 2006).

Tissue engineering, a term first coined at the National Science Foundation Worksop in 1988, was defined by Langer and Vacanti as: “An interdisciplinary field that applies the principles of engineering and life sciences towards the development of biological substitutes

that restore, maintain or improve tissue function or a whole organ" (Langer and Vacanti, 1993).

The basic tissue engineering paradigm is based on combining three key elements: cells, biomaterials and growth factors to achieve neo-tissue formation and regeneration. Traditionally, the process starts by harvesting cells from a patient, expanding them in culture, and then seeding them onto a scaffold to provide a biomechanical environment that supports tissue formation. The tissue can be grown on a scaffold that will completely resorb as the new tissue grows, or on a permanent scaffold and the bio-composite would then be implanted. After implantation, the tissue engineered construct must be able to survive, restore normal function, and integrate with the surrounding tissues (see figure 1.1) (Dvir et al., 2010).

Various cell types have been used by tissue engineers to identify the best cell source for constructing a particular tissue. These include primary cells and stem cells. Primary cells are tissue specific mature cells, harvested from explant material. Primary cells are most desirable with regard to immunological compatibility, but are differentiated and post-mitotic. Their widespread use is faced with limitations related to the tendency of some cell types to de-differentiate during *ex*-vivo cultivation and express an inappropriate phenotype (e.g. articular chondrocytes in culture often produce fibrocartilage as opposed to hyaline cartilage)(Freemont and Hoyland, 2006). In addition, harvesting some phenotypes, e.g., spinal cord neurons from patients or donors is not practical (Polak and Bishop, 2006).

Stem cells, on the other hand, are undifferentiated cells that can proliferate and have the capacity both to self-renew and to differentiate to one or more types of specialised cells. These cells offer a huge potential to the field of tissue engineering, thanks to their ability to self-renew, providing a theoretically inexhaustible supply, and to differentiate to any cell type when grown under the appropriate conditions.

Stem cells can be isolated from embryos, foetuses, or from adult tissue, and the range of cell types they can differentiate into varies accordingly.

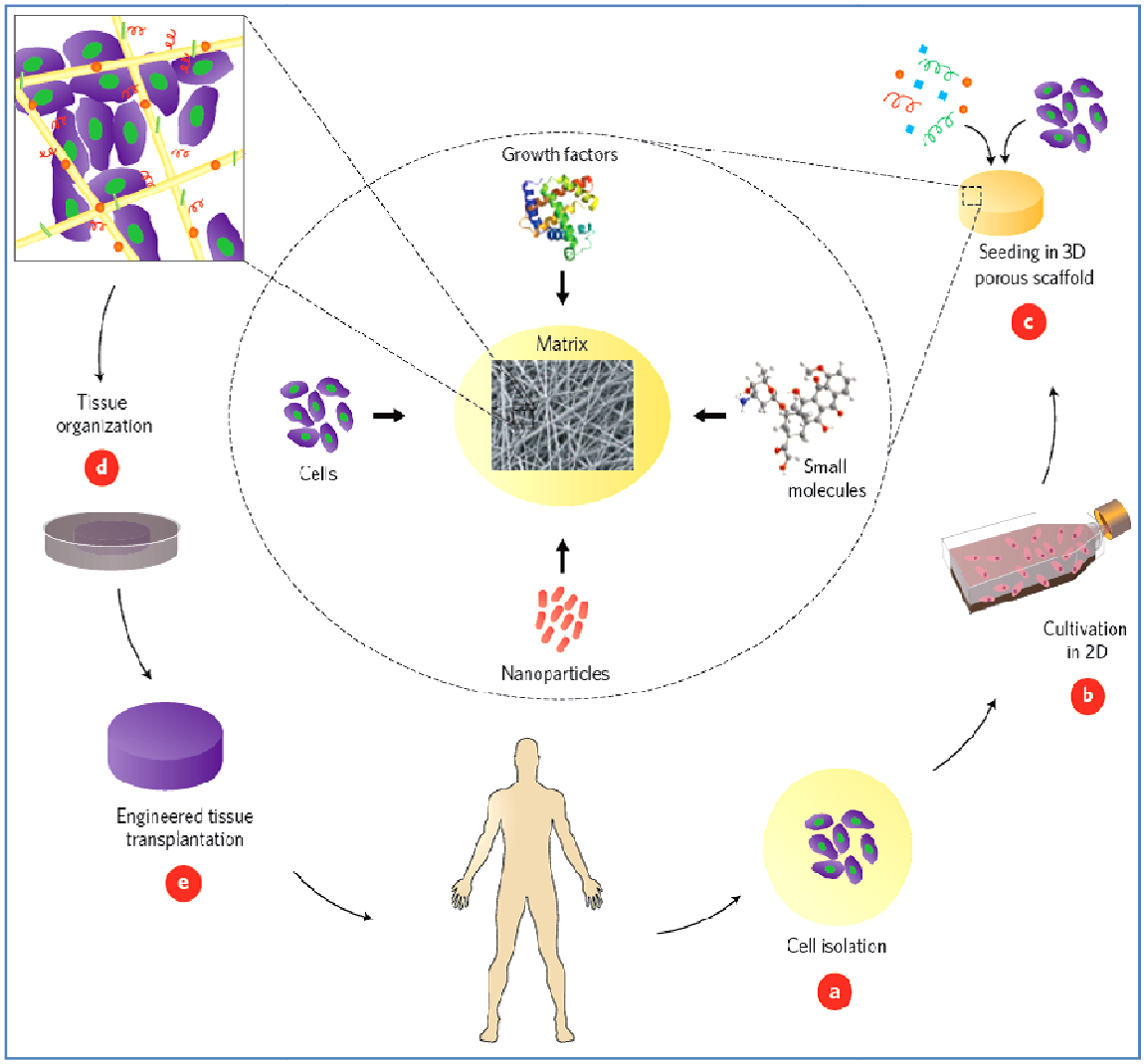

Figure 1.1: The key stages of tissue engineering.

(**a**) Cells isolated from the patient, or other sources (**b**) are cultivated *in vitro* on two-dimensional surfaces for efficient expansion. (**c**) The cells are next seeded in porous scaffolds together with growth factors, small molecules, and micro- and/or nanoparticles. The scaffolds serve as a mechanical support and a shape-defining material (**d**). The cell constructs are further cultivated (in bioreactors) under optimal conditions for organisation into a functioning tissue. (**e**) Once a functioning tissue has been successfully engineered, the construct is transplanted in the defect to restore function. Figure taken from (Dvir et al., 2010).

Embryonic stem cells have been shown to be pluripotent, differentiating to all lineages, including the germ line and trophoblast. An adult (or postnatal somatic) stem cell is an undifferentiated cell found among differentiated cells in a tissue or organ, of which there is an extensive repository located in various tissue niches throughout the body, including bone marrow, brain, liver, and skin as well as in the circulation. In adulthood, tissue homeostasis and regeneration are critically dependent on both the self-renewal and the differentiation capacity of these stem cells.

In addition to optimising cell isolation, proliferation and, in the case of stem cells, differentiation, a key challenge facing tissue engineers is the design of scaffolds that promote and support the coordinated growth of three-dimensional tissues.

To maximise their chances of success, tissue engineers attempt to replicate as far as possible the natural microenvironment in which cells would normally grow and function within the body. The study of cellular behaviour and tissue homeostasis identified a range of physical and chemical factors impacting on cell function. These can be broadly divided into physical (insoluble macromolecules, e.g., collagen), chemical (soluble macromolecules, e.g., growth factors), and cell– cell interactions (proteins on adjacent cells) (figure 1.2) (Polak and Bishop, 2006, Lutolf and Hubbell, 2005). Accordingly, some of the strategies attempted to reproduce the natural cell microenvironment include the controlled delivery of growth factors, three dimensionality, bio-functionalisation of synthetic materials, controlling the scaffold elasticity in addition to the development of cell co-culture protocols (Lutolf and Blau, 2009). Scaffolds where such design complexity can be achieved are, therefore, highly desirable.

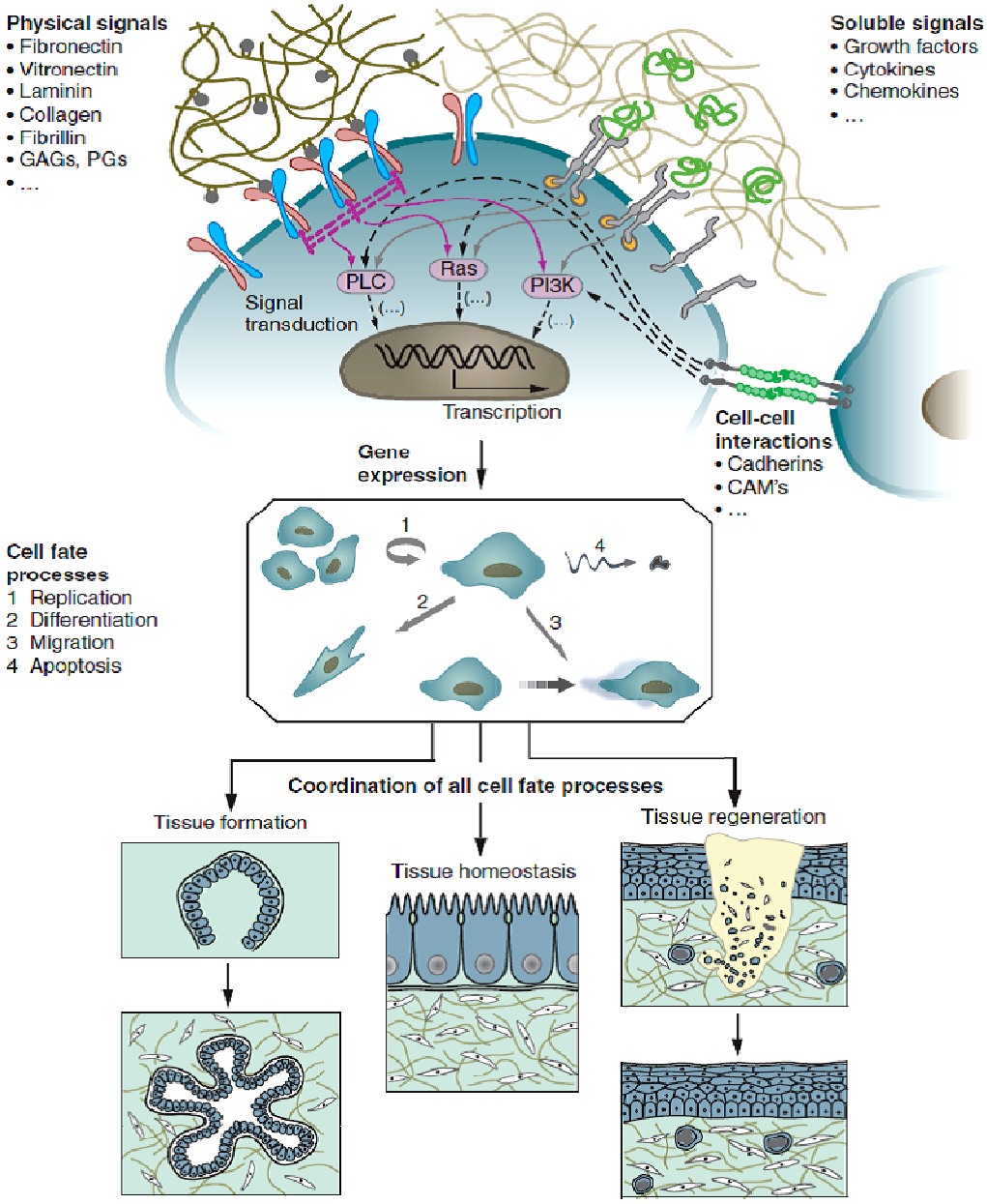

Figure 1.2: The reciprocal molecular interactions between cells and their surroundings and their impact on cell behavior and tissue homeostasis.

The cues within the cells microenvironment include support for cells and their secreted transmembrane cell–cell adhesion proteins, soluble factors, and the surrounding ECM. Specific binding of these signaling cues with cell-surface receptors induces complex intracellular signaling cascades that converge to regulate gene expression, establish cell phenotype and direct tissue formation, homeostasis and regeneration. Figure taken from (Lutolf and Hubbell, 2005).

PLC: phospholipase C, GAGs: glycosaminoglycans, PGs: proteoglycans, CAMs: cell adhesion molecules

1.2 Importance of biomaterials in tissue engineering

Cells naturally exist in an extracellular matrix (ECM), a soft, tough and elastomeric proteinaceous network that provides mechanical stability and structural integrity to tissues and organs. In tissue engineering the natural design of a tissue is emulated to obtain replacement functional tissues *in vitro* and also *in vivo*, based on the combination of three key elements: a specific living cell type (or several cell types), a material scaffold and active biomolecules such as growth factors.

The three dimensional (3D) scaffolds (matrices) serve as temporary substrates that mimic the natural ECM, providing the supporting architecture for the cells to guide tissue formation into the desired shape, while allowing for adequate transport of nutrients and growth factors to promote tissue growth. Scaffolds can be engineered with built-in capabilities to deliver soluble/insoluble molecules as well as temporal and spatial cues. This ultimately provides a physical support and a local bio-inductive environment for the cells, to enable and facilitate the development of a functional tissue (Langer and Vacanti, 1993).

The importance of using scaffolds *in vivo* stems from the limited success of cell therapy when free cells in suspension were injected to an area of functional or structural loss. This is mainly due to poor cell engraftment, where it was as low as 1-5% of the injected cells in certain conditions (Mooney and Vandenburgh, 2008). Post-injection, all control over cell fate is lost and since the cells lack a template to guide restructuring, they become incapable of histological reorganisation and tissue formation, leading eventually to the vast majority of them to die (Kim and Mooney, 1998, Vacanti et al., 1998). Besides, lack of cell attachment is known to induce cell apoptosis. This is a homeostatic mechanism referred to as *anoikis*, that ensures the viability and function of cells solely in their native environment (Frisch and Screaton, 2001).

Biomaterial scaffolds are also important *in vitro* for the 3D culture of cells. Traditionally cells have been cultured on planar surfaces, a practice that does not mirror the natural environment cells exist in. Various recent studies have emphasised the importance of 3D culture environments, especially with regards to stem cells where temporal and spatial cues are critical in deciding cell fate (Lutolf and Blau, 2009).

These 3D environments are crucial for the engineering of tissue models for drug testing or further biological studies (Fischbach et al., 2007), as well as the generation of tissue substitutes that can be used to replace failing tissues *in*–vivo.

1.3 The properties required in biomaterials scaffolds

The goal of employing biomaterials in tissue engineering is to support tissue regeneration *in vitro* and *in vivo* at sites often compromised by infection and loss of structure. Scaffolds not only serve to guide tissue formation to the desired shape, but also provide adequate transport of nutrients and growth factors to promote tissue growth and vascularisation.

The choice of biomaterial is an important consideration for any scaffold design. Scaffolds must have certain characteristics as an absolute minimum for use with cells, these include (Jagur-Grodzinski, 2006):

1. **Biocompatibility:** When within the body**,** the material and its degradation products must not be toxic to the cells or surrounding tissues, nor elicit any significant inflammatory, immunological, thrombogenic or any response that detracts from its desired function.

2. **Biodegradability**: For transplantation purposes it is often desirable to have the material biodegrade after cell delivery and incorporation into the host environment

has been accomplished. The regeneration of fully functional tissue ideally coincides in time with complete scaffold degradation and resorption, where over time the cells produce and deposit their own extracellular matrix (ECM), while the scaffold degradation products are eliminated from the body.

3. **Adequate mass transfer**: to allow for nutrients, metabolite and gas exchange, and is generally governed by pore size and free volume.

4. **Appropriate physical properties**: The scaffold should possess adequate mechanical properties, ideally matching those of the original tissue, that allow for sufficient cell in-growth and maintenance of appropriate extracellular matrix. Additionally, some level of bioactivity should be provided by the scaffold surface to accommodate cell adhesion and migration (Goldberg et al., 2007).

1.4 Common materials used for scaffolding in tissue engineering

The last half century of biomaterials research has witnessed a shift from the use of permanent metallic implants, to temporary synthetic materials which contributed to the current tissue engineering ideology. More recently the shift has become more towards the use of biologically inspired synthetic polymers, where the wealth of knowledge acquired in cell biology is being employed in developing more sophisticated biologically relevant materials (Lutolf and Hubbell, 2005, Salih, 2009), drawing the biological and material science fields closer. Some of the common materials that have been employed in tissue engineering are briefly listed below.

1.4.1 Natural materials

These are advantageous due to their inherent properties of biological recognition and susceptibility to cell-triggered proteolytic degradation and remodelling. However their application has been limited by complexities associated with sourcing, processing and purification, limited mechanical properties, immunogenicity and pathogen transfer (Ratner and Bryant, 2004).

Collagen has been used as a tissue scaffold, being a natural component of the extracellular matrix of mammalian tissues (Cen et al., 2008). Collagen and fibrin are clinically well-established and FDA-approved matrices for wound healing (to treat burns and chronic wounds) and as tissue sealants, respectively. Hyaluronic acid (Esposito et al., 2006) and gelatin (Yamamoto et al., 1999), Chitosan (Madihally and Matthew, 1999) and alginates (Dvir-Ginzberg et al., 2003) have also been widely studied as scaffolds for tissue engineering.

Another source for natural scaffolds is the decellularisation of donor organs such as heart, liver, and lung to obtain scaffolds with in-built bioactivity. These can provide an acellular, naturally occurring three dimensional biologic scaffold material that can then be seeded with selected cell populations (Crapo et al., 2011). This approach was recently confirmed as being at the forefront of whole-organ tissue engineering, when a 30-year old woman became the first person to receive a tissue engineered tracheal segment that saved her left lung. A decellularised human donor trachea was repopulated with the patient's own cells expanded from a biopsy. The decellularisation protocol removed virtually all traces of human leukocyte antigens, which obviated the need for immunosuppressive drugs. As well as immediately restoring airway patency, the engineered tissue facilitated the rapid development of an internal cellular lining and blood vessel network (Macchiarini et al., 2008).

The full potential of such biological scaffolds, however, will only be realised if optimal methods of decellularization are employed to overcome potential immunogenic reactions to cell remnants or antigens in allogenic and xenogenic tissue-derived scaffolds (Crapo et al., 2011)

1.4.2 Synthetic materials

Synthetic materials have been widely used for tissue engineering. Polymers have been particularly employed thanks to their adaptable chemistries, reproducibility and lack of infection transmission risk. These could be processed into highly porous 3-dimensional scaffolds of variable designs, fibres, sheets, blocks or microspheres (Reinout, 2008).

The poly(α-hydroxy acid) polymers are among the most commonly used polymers in drug delivery and tissue engineering scaffolds (figure 1.3). They have the advantages of low toxicity, good biocompatibility, biodegradability, and being approved by the USA Food and Drug Administration (FDA) for clinical use (e.g., sutures). Characteristically, these gradually degrade into water soluble, non-toxic, by-products which are eliminated from the implant site by the normal metabolic pathways (Jagur-Grodzinski, 2006). Poly(glycolic acid)(PGA) scaffolds seeded with chondrocytes formed cartilage-like tissue after 20 weeks in culture, with relatively high resistance to loading (Ma and Langer, 1999). Poly(lactic-co-glycolic acid) (PLGA) scaffolds have also been widely used as scaffolds for various tissue engineering applications.(Pattison et al., 2005)

Polycaprolactone (PCL) is another aliphatic polyester that has been investigated as a biomaterial for tissue engineering. It is a semi-crystalline polymer with low glass transition temperature (-60°C), and is therefore highly permeable for many therapeutic drugs at room temperature. Compared to PGA and poly(lactic acid)(PLA) the degradation of PCL is significantly slower, which makes it suitable for the design of long-term, implantable

systems. Its improved resistance to hydrolytic attack and its low cost make PCL an attractive polymer for scaffold fabrication (Pachence et al., 2007, Ng et al., 2004).

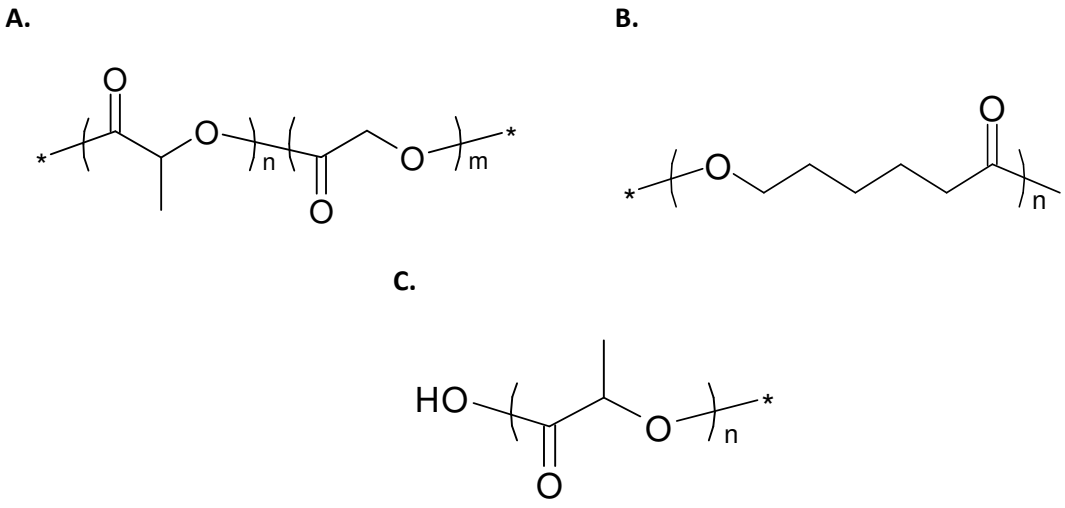

Figure 1.3: Chemical structures of common poly(α-hydroxyacid)s employed in tissue engineering.
(**A**) Polycaprolactone (**B**) Poly (lactic-co-glycolic acid) (PLGA) (**C**) Poly (lactic acid) (PLA).

The use of scaffolds made from synthetic polymers, can be limited by their lack of bio-functionality and hydrophobicity which affects the ability of cells to adhere to them. Moreover, the potential increase in the local pH from the accumulation of degradation products can also be detrimental to cells (Lutolf and Hubbell, 2005).

Various approaches have been devised to improve the cellular response to polyesters. Surface modification techniques led to significant improvements in cell adhesion and further aspects of cell behaviour (Jiao and Cui, 2007). Other groups combined synthetic materials with biological substances, to yield superior materials tailored to induce cell responses (Quirk et al., 2001).

1.5 Different types and designs of scaffolds used in tissue engineering

Biomaterials can be processed by a variety of techniques to generate different types of scaffolds, with variable designs and properties. Some of the common scaffold fabrication techniques and scaffold designs are listed below.

1.5.1 Electrospinning

Electrospinning is an economical, and easily set-up technology for the fabrication of 3D, highly porous scaffolds composed of nano- and microscale fibres. Electrospun fibres have found a broad range of applications in drug delivery, cosmetics, wound dressing (Lu and Ding, 2008) as well as tissue engineering where they have been shown to support cellular activities and tissue formation (Pham et al., 2006, Li et al., 2006).

Various materials can be electrospun into fibrous scaffolds. These include biodegradable polymers such as PLGA, PLA and PCL, water-soluble materials such as poly(ethylene glycol) (PEG) polyvinyl alcohol (PVA), and natural polymers such as collagen, silk protein, and other peptides.

Scaffolds are prepared by dissolving the polymer in an appropriate solvent. The polymer solution is loaded into a syringe and then expelled through a metal capillary at a constant rate via a syringe pump. A high voltage is applied to the capillary (10-15Kv) charging the polymer. When the electric charge overcomes the surface tension of the polymer solution droplet a polymer jet is ejected. As the solvent evaporates, it leaves solid nanofibres that ground on a collecting surface. Non woven porous scaffolds are obtained, with porosities greater than 90%. Fiber thickness, scaffold diameter and average pore diameter can be adjusted by changing polymer concentration, choice of solvent, ejection rate, applied voltage, capillary diameter, collecting plate material or the distance between

the capillary and the collecting plate. Also, composite scaffolds can be created, by sequentially spinning different polymer solutions to obtain scaffolds with different layers.

Various studies have demonstrated the successful use of electrospun scaffolds in tissue engineering. Bone marrow-derived human MSCs seeded onto PCL electrospun nanofibre scaffolds were shown to be able to differentiate into adipogenic, chondrogenic, or osteogenic lineages depending on the culture media selected (Li, 2005). In another study, a contractile cardiac graft was obtained from cardiomyocytes seeded onto an electrospun **PCL** mesh. The cardiomyocytes expressed cardiac-specific proteins such as myosin, connexin, and cardiac troponin I, after 14 days of culture (Shin, 2004).

However, concerns regarding fibre diameter uniformity, the precise control of fibre morphology and the generation of designer scaffolds with clinically relevant dimensions and achieving homogeneous and efficient distribution of cells, in addition to their limited mechanical properties need to be addressed before the widespread application of electrospun scaffolds in tissue engineering.

1.5.2 High-pressure processing

This process is performed by applying a gas, such as carbon dioxide, to dry polymer at high pressure forming a single polymer/gas phase. As the pressure is decreased, nucleation and pore formation occur in the polymer matrix based on the amount and the reduction rate of the pressure. This technique was pioneered by Mooney *et al* who utilised it to fabricate highly porous sponges of PLGA (Mooney et al., 1996).

The main advantage of high-pressure processing, also known as supercritical fluid technology, is avoiding the use of organic solvents, the remnants of which might lead to inflammatory responses after implantation. This also allows for growth factor and

biomolecule incorporation into 3D scaffolds without the risk of solvent-induced denaturation (Watson et al., 2002).

The scaffolds fabricated by this method have pore sizes of 100-500µm. The main drawback, however, is their closed-pore morphology. Harris *et al* showed that this could be addressed through the incorporation of leaching particles (Harris et al., 1998).

1.5.3 Hydrogels

Hydrogels are highly hydrated materials (with a water content at least $\geq 30\%_{w/w}$). The ability of hydrogels to retain a large quantity of water, their biocompatibility, low interfacial tension, and minimal mechanical and frictional irritation are all appealing features, that favoured their application in tissue engineering (Drury and Mooney, 2003). Hydrogels are composed of hydrophilic polymer chains, which are either synthetic or natural in origin. Their structural integrity depends on the crosslinks formed between polymer chains, these being either covalent chemical bonds or physical interactions. A variety of materials may be used to form hydrogels:

- Synthetic materials which include PEG, polyvinyl alcohol (PVA), polyacrylic acid (PAA), poly(propylene furmarate-co-ethylene glycol) (PPF-co-EG), and polypeptides.
- Naturally derived polymers include agarose, alginate, chitosan, collagen, fibrin, gelatin and hyaluronic acid (HA).

Although pre-fabricated scaffolds for surgical implantation are useful in most tissue-engineering applications, injectable *in*-situ polymerising or gelling materials are attracting more interest. These are able to take the shape of the tissue defect, avoiding the need for patient specific scaffold prefabrication, in addition to the clinical benefits of avoiding surgical implantation with its associated risk of infection, scar formation, patient morbidity and cost of treatment. Hence, *in*-situ forming hydrogels have been particularly interesting for

injectable scaffold applications (Kretlow et al., 2007, Klouda and Mikos, 2008). These include hydrogels that are formed through:

- ***In*-situ chemical polymerisation and cross linking:** solidification of a series of polymers is achieved via a thermally activated polymerisation or crosslinking that occurs on heating to body temperature. For example, a cytocompatible water soluble thermal radical initiator system ammonium persulfate/ *N,N,N',N'*-tetramethylethylenediamine (APS/TEMED), was successfully used to prepare cell-OPF (oligopolyethylene fumarate) hydrogel construct at 37°C within 10 minutes of injection (Kretlow et al., 2007).
- **Photinitiated polymerisation and crosslinking**: examples include the photopolymerisation of PPF, although such applications are limited by light penetration to the site of interest *in vivo*.
- **Temperature**: gelation occurs as a result of temperature induced phase transition (see 1.6).

1.6 Common temperature responsive materials used in tissue engineering

Thermoresponsive hydrogels have been particularly investigated for drug delivery and tissue engineering applications. This is thanks to their mild sol-gel transition and their physical cross-links, which form with negligible heat production and with no by-products, compared to materials gelling through chemical covalent crosslinks, where the slow kinetics and precursor toxicity issues make them less attractive (He et al., 2008, Klouda and Mikos, 2008). These properties make thermoresponsive hydrogels ideal for use as injectable scaffolds (Hou et al., 2004).

Below are listed common thermoresponsive polymers used in tissue engineering.

1.6.1 PEO/PPO/PEO copolymers (polyethers)

Poly(ethylene oxide)(PEO)/poly(propylene oxide) (PPO)/ PEO copolymers are a family of more than 30 different nonionic surfactants with molecular weights ranging from 1,000 to 14,000 Da. Concentrated solutions of PEO/PPO/PEO copolymers form reversible gels at elevated temperatures and revert to a liquid state on lowering the temperature. Gelation temperature depends on polymer composition, with Poloxamer 407 (Pluronic F-127) forming gels at 37°C in solutions containing 20%$_{w/v}$ or more of polymer (Gutowska et al., 2001).

At low temperatures, polypropylene oxide (PPO) chains are soluble in water. The PEO-PPO-PEO triblock is wholly hydrophilic and takes a coil conformation. Increase in temperature renders PPO hydrophobic (LCST transition) which leads to the formation of micelles with a PPO core and a hydrophilic PEO shell. The temperature at which this occurs is termed the critical micelle temperature (CMT). As the temperature increases, the equilibrium shifts from unimers to spherical micelles, until the system becomes a gel by micellar packing (Wanka et al., 1990).

Pluronics have found wide applications in drug delivery with regards to TE. Pluronics represent a mainly bio-inert environment, attributed to the flexibility of PEG chains, and most cells do not grow on these polymers (Higuchi et al., 2003). Nevertheless, pluronics found applications as tissue adhesion barriers and also in some tissue engineering applications, where they were investigated for burn wound healing (Schmolka, 1972) and for drug, protein/peptide delivery. In a study by Cortiella *et al* Pluronic F-127 gels were found superior to polyglycolic acid in supporting lung tissue development *in vivo*, as they did not induce an inflammatory response to the extent seen with polyglycolic acid (Cortiella et al., 2006).

Solutions of Pluronic F-127, at 20%$_{w/v}$ concentrations and higher, with isolated chondrocytes were also used as an injectable cartilage formulation. Cartilage formation was tested after subcutaneous injections of the polymer/cell suspension in athymic mice. Histological examination of all samples demonstrated the presence of new cartilage formation. The volume of new cartilage was significantly greater than that obtained by injecting cells suspended in saline only, and after 8 weeks, mature, hyaline-like cartilage was present. The authors concluded that polymer/cell suspension approach holds great promise for orthopaedic and reconstructive surgery (Saim et al., 2000).

The main limitations facing the widespread use of Pluronics in tissue engineering are:

- limited mechanical integrity and stability, with rapid dilution and dissolution at physiological conditions (within few hours) (He et al., 2008)
- non biodegradability and
- the high concentrations needed to form gels.

Some attempts that have been made to address these limitations including the use of Pluronics in combination with other materials, or the synthesis of polymers consisting of multiblocks of Pluronics or multiple blocks of PPO and PEO which showed superior rheological properties and improved biodegradability (Cohn et al., 2003).

1.6.2 PEG/biodegradable polyesters copolymers

Inspired by the thermosensitive behaviour of Pluronics, another group of copolymers combining PEG with polyester blocks were developed by *Jeong* and co-workers as novel injectable thermogelling systems (Jeong et al., 1997). In addition to their biocompatibility and biodegradability, these are water soluble and free flowing at room temperature, but form insoluble gels at body temperature with solubilising properties towards lipophilic compounds.

Both triblock copolymers of PLGA-PEG-PLGA and PEG-PLGA-PEG exhibited reversible temperature dependent sol-to-gel behaviour. The sol-to-gel transition temperature of these triblock copolymers in aqueous solution could be controlled over a temperature range of 15°C to 45°C by changing their molecular parameters such as PLGA length, PEG length and the ratio of lactic acid (LA) to glycolic acid (GA) in the middle block (Jeong and Gutowska, 2002). The likely gelation mechanism of PEG/polyester triblock copolymers is through micellar growth and number expansion with temperature increase, which leads eventually to micellar packing (Jeong et al., 1999).

PEG-PLGA-PEG was used as a dressing and a stem cell scaffold for diabetic wounds, and was found to significantly enhance healing (Lee et al., 2007). Low molecular weight PLGA-PEG-PLGA (1500–1000–1500) has been commercialised under the trade name ReGel®, for use as a drug delivery depot with delivery times ranging from 1 to 6 weeks (Zentner et al., 2001, Elstad and Fowers, 2009). Block copolymers of PEG and other biodegradable aliphatic polyesters have also shown thermoreversible (sol–gel) transition in aqueous solutions. Examples include mPEG–poly(ε-caprolactone) which supported adipose derived stem cell myogenic differentiation for muscle regeneration (Kim et al., 2010).

1.6.3 Thermoresponsive peptides

Engineered elastin-like polypeptides (ELPs) are a class of artificial repetitive polypeptides which are polymers of the pentapeptide motif *VPGVG* that is observed to recur in the **tropoelastin** gene across species.

ELPs undergo *reversible* sharp phase changes as a result of interchain hydrophobic aggregation with changes in temperature. At the transition temperature, the ELPs solutions transform into highly viscous fluids or coacervates. ELPs can be genetically engineered and can be expressed from a plasmid-borne gene in *Escherichia coli* to relatively high yields (~500 mg/L growth), and they can then be readily purified from *E. coli* and other cell lysates,

in a batch process, by exploiting their inverse temperature phase transition without the need for chromatography. These molecular biology techniques has enabled fine tuning of the ELPs properties, potentially allowing controlled aggregation or degradation of polypeptide particles across very narrow pH (less than one pH unit) and temperature ranges (<1°C). ELPs are also deemed biocompatible, biodegradable, and non-immunogenic (Nettles et al., 2010). ELPs have been extensively investigated as drug delivery systems and for applications as ECM mimics in tissue engineering including cartilage and intervertebral disks, vascular grafts, ocular, liver as well as cell-sheet engineering (Nettles et al., 2010).

Limitations of ELPs coacervates include their limited mechanical strength. This could be addressed by engineering of ELPs with crosslinkable moieties to obtain gels or films, especially if the ELPs are intended for load bearing applications such as cartilage tissue engineering. Upon crosslinking, the viscoelastic properties of ELPs can match those of native elastin. Moreover, the ELP sequence is non-cell adhesive, and the incorporation of RGD peptides into the polypeptide structure was suggested to improve cell adhesion (Liu and Tirrell, 2008).

1.6.4 Synthetic polymers with an LCST behaviour

Smart or responsive polymers have intriguing properties that lead to dramatic conformational changes in response to slight changes in their environment. They include polymers responsive to light, pH, ionic strength or temperature. Polymer responses may include precipitation, gelation, and reversible adsorption onto a surface, collapse of a hydrogel or surface graft, and alternation between hydrophobic and hydrophilic states.
Such properties can be harnessed to interconvert a stimulus into a function, and smart polymers are therefore interesting for a variety of biomedical applications, such as switching surfaces, protective coatings that adapt to the environment, artificial muscles, biosensors, drug delivery devices and tissue engineering (Stuart et al., 2010).

Thermoresponsive smart polymers are water soluble polymers with a fine hydrophobic-hydrophilic balance in their structure, which leads them to separate from solution when heated to above their PT (phase transition) temperature, known as the *lower critical solution temperature* (**LCST**). This temperature corresponds to the region in the phase diagram where the enthalpic contribution of the water, hydrogen bonded to the polymer chains, becomes less than the entropic gain of the system as a whole. This makes hydration unfavourable, leading to polymer chain dehydration and the formation of precipitates or physical gels (Dimitrov et al., 2007).

1.6.4.1 poly(N-isopropylacrylamide) (*polyNIPAm)* polymers

The typical example of polymers with LCST is poly(N-isopropylacrylamide) (polyNIPAm) (figure 1.4), which undergoes a *sharp coil-to-globule* transition in water at 32°C, changing from a hydrophilic state below this temperature to a hydrophobic state above it (Schild, 1992). At temperatures below the LCST, polyNIPAm chains are soluble in water and adopt an open coil conformation. This is driven by the enthalpic gain from the binding of water molecules to the polar regions of the chains (the amide side groups), which compensates for the entropic loss of the system as the water molecules have to reorient around the non-polar regions of polyNIPAm chains, being unable to hydrogen bond with them. However, at temperatures above the LCST, the enthalpic term can no longer compensate for the entropy loss, with regards to the free energy of the system. Hence, at these temperatures the entropy term dominates, leading to the *dehydration* of the isopropyl moieties, and the polymer chains to collapse and aggregate into globular structures (Schild, 1992).

PolyNIPAM based polymers have found various applications in tissue engineering. polyNIPAm and copolymers have been used as surface modifiers for cell-sheet tissue engineering. PolyNIPAm-functional surfaces promote cell attachment and growth under

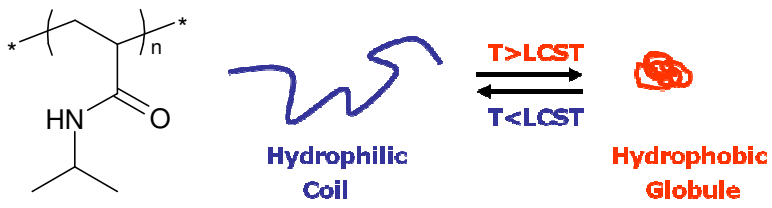

Figure 1.4: Illustration of poly(N-isopropylacrylamide) polyNIPAm temperature induced coil to globule transition in water. Below the LCST the isopropyl moieties in the polymer side chains are hydrated, while above the LCST polymer-polymer interactions dominate, leading to polymer precipitation.

normal physiological temperatures (i.e., at 37°C when the polymer is chain-collapsed and hydrophobic) but allow cell detachment at temperatures below the LCST because of chain extension and hydration of the polymer brush layer. This provides an enzyme and shear free method to harvest cells as an intact monolayer sheet including deposited ECM, an approach referred to as cell-sheet engineering (Matsuda et al., 2007).

PolyNIPAm polymers have also found applications as hydrogel scaffolds. Chrondocytes, dexamethasone and growth factors were encapsulated in poly(NIPAM-co-acrylic acid) hydrogels, and had shown promising results for their application as injectable scaffolds for cartilage tissue engineering (Na et al., 2006). Pancreatic cells, encapsulated within poly(NIPAM-co-acrylic acid), showed continued insulin secretion in response to glucose over 26 days of culture (Vernon et al., 1999).

Recently, polyNIPAm hydrogel and PLGA were combined to yield thermoresponsive 3D foamed scaffolds. Cell attachment to these scaffolds could be controlled with temperature, where on cooling the scaffolds to 4°C most of the cells were detached (Duarte et al., 2010).

The widespread use of polyNIPAm has been limited due to concerns over the monomer N-isopropylacrylamide's high cytotoxicity (Ron and Bromberg, 1998). The polymer

showed less cytotoxicity, but since it is not biodegradable and its *in vivo* fate is unclear, there still exist concerns about its biocompatibility (Vihola et al., 2005).

1.6.4.2 Poly(poly(ethylene glycol) methacrylate) –poly(PEGMA)

Some polymers of poly(ethylene glycol) methacrylate have also been shown recently to possess thermoresponsive properties. The non-linear PEG polymers are composed of up to 85% in weight of PEG and are therefore water soluble and biocompatible (Hu et al., 2010). Their LCST in water was found to increase with the length of the poly(ethylene glycol) side chain and could be tuned to be around physiological temperature. These polymers are considered ideal structures that combines the lack of toxicity and immunogenicity of PEG, and the environment-independent thermosensitivity of polyNIPAm in a single macromolecule(Lutz, 2008).

Lutz *et al* prepared a thermosensitive copolymer, consisting of 2-(2-methoxyethoxy)ethyl methacrylate and poly(ethylene glycol)methacrylate (PEGMA, Mn=475g/mol) (Lutz et al., 2006). This polymer was successfully grafted to gold surfaces, offering temperature control over cell adhesion to the underlying substrate, and showed promising results for cell-sheet engineering (Wischerhoff et al., 2008) and embryonic stem cell culture with enzyme-free passage(Dey et al., 2011).

1.7 The applications of polymeric microparticles in tissue engineering

Microparticles made from various materials have found multiple applications in tissue engineering (see figure 1.5 for a summary).

1.7.1 The use of polymeric microparticles for the delivery of biomolecules

Combining scaffolds, cells and growth factors has synergistic effects on accelerating tissue regeneration (Babensee et al., 2000). Growth factors, such as tumour growth factor- β

(TGF-β) and bone morphogenetic proteins (BMPs), are important signalling molecules in both tissue healing and development.

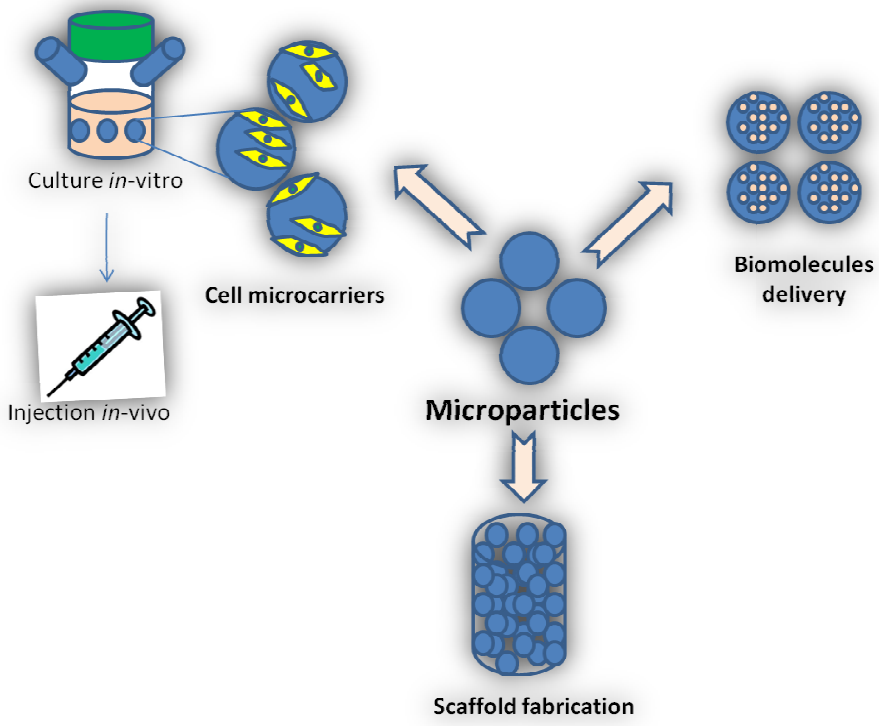

Figure 1.5: The various applications of polymeric microparticles in tissue engineering.

These typically have a short half-life in the circulation, and are rapidly eliminated when delivered systemically. Therefore, vehicles that locally deliver growth factors to the target cell population, in a controlled fashion over a specific time frame are required. The increased retention of such delivery vehicles can also induce the migration of regenerative tissue-forming cells to the area of injury, where they would differentiate and proliferate.

Biodegradable polymeric microparticles have been widely used as delivery vehicles for therapeutic proteins and drugs (Freiberg and Zhu, 2004). Microparticles encapsulating proteins, commonly fabricated by the single or double emulsion methods, release encapsulated proteins from aqueous pockets within the particles (Jain, 2000, Rosca et al., 2004). These have been adapted in tissue engineering for the delivery of growth factors and

other molecules that support cell growth or differentiation (Jaklenec et al., 2008). For example, the delivery of TGF-β1 from PLGA microparticles increased the proliferation and differentiation of marrow stromal cells toward osteoblasts (Lu et al., 2001). Injectable systems of PLGA microspheres delivering BMP-2 were also shown to promote osteoblast differentiation and mineralisation *in vitro* and ectopic bone formation *in vivo* (Woo et al., 2001). In another example, BMP-7 loaded PLGA nanoparticles incorporated into a nanofibrous PLA scaffold, showed promising results of ectopic bone formation in a rat subcutaneous implantation model. After 6 weeks, there was significant bone formation in the BMP-7 containing scaffolds but only fibrous tissue in scaffolds without BMP-7, or those only pre-soaked in a BMP-7 solution (Wei et al., 2007).

PCL microparticles were also used for the encapsulation of nerve growth factor (NGF). The particles achieved controlled release of the peptide in its active form over 91 days, which make them promising for the enhancement of axonal regeneration following injury to the central nervous system (Cao and Schoichet, 1999).

1.7.2 The use of polymeric microparticles as cell scaffolds

Microparticles have been used as scaffolds for cells (in their own right) or as the building blocks for the fabrication of 3D scaffolds

1.7.2.1 Microparticles as microcarriers for cells

Microparticles have been employed *in vitro* as microcarriers for the culture of cells, and also *in vivo* as vehicles for the delivery of adhered cells to repair and regenerate tissues (Martin et al., 2010).

The use of microparticles as injectable scaffolds/or drug delivery carriers obviates the need for invasive surgical procedures. Such injections can contain the combination of particles only, drug/biomolecules encapsulating particles and particles with attached cells, as

a comprehensive implant to fill cavities and promote *de novo* tissue formation. Biodegradable PLGA microspheres have been studied for the delivery of chondrocytes for cartilage engineering. Non-porous PLGA microspheres were used as microcarriers for cell expansion *in vitro* and then used as injectable carriers for the cultured cells for cartilage regeneration *in vivo* (Chun et al., 2004). In another study, Newman and McBurney developed biodegradable PLGA microparticles (60-80μm) which could serve the dual role of a delivery system for retinoic acid, while acting as a scaffold for pluripotent stem cells. Culturing pluripotent embryonic cells on these particles promoted their differentiation into neurons (Newman and McBurney, 2004).

In a more recent study by Bible *et al*, PLGA particles were prepared and functionalised with adhesive proteins to enhance cell attachment for applications as carriers for intra-cerebral injection of neural stem cells (MHP36) through a thin needle. These showed promising results for brain tissue regeneration in an animal-model of stroke (Bible et al., 2009).

1.7.2.2 The use of microparticles as the building blocks of 3D scaffolds

Microparticles have been used for the fabrication of 3D scaffolds using heat sintering, which involves placing the polymeric particles in a mould and then heating them to above their glass transition temperature (Tg) or melting temperature (Tm) to cure them into a scaffold (Jabbarzadeh et al., 2007, Luciani et al., 2008).

By using biocompatible plasticisers the glass transition temperature (Tg) of polyesters could be dropped, so that heat sintering could be performed at lower temperatures, without compromising the stability of encapsulated bioactives. The Tg of PLGA was dropped to 37°C by using PEG as a plasticiser. Therefore, PLGA scaffold fabrication could potentially take place *in vivo* following the injection of concentrated particulate slurry, where the particles would be expected to coalesce at body temperature and generate a hardened scaffold (Suciati et al., 2006, Hamilton, 2008).

Particles can be used to construct scaffolds also by inducing suspended particles to self-assemble. This transforms the particle suspensions into gels that could be employed as tissue scaffolds (see 1.8b).

Scaffolds can also be obtained from particulate suspensions, where the particles are induced to self-assemble. In addition to using environmental stimuli to induce particle self-assembly (see 1.8), this could be achieved using biotin-avidin crosslinking. Biotinylated conjugated particles were induced to self assemble by adding avidin molecules, which cross-linked the particles generating porous scaffolds (Salem et al., 2003).

1.8 Particulate suspensions as a class of materials

Various classes and forms of materials have been used in the biomedical field. In this section the properties of particulate suspensions are discussed with regards to the potential applications they can find in tissue engineering.

1.8.1 The stability of suspensions

Colloidal systems, such as suspensions, consist of a dispersed phase (colloid) of size ranges between 1nm-10μm, and a continuous phase. Concentrated suspensions have found a wide range of applications in various industries including: food, coatings and pharmaceuticals.

Being a system of a large surface area, surface interactions dominate the stability of suspensions. Various forces contribute to the particle interaction potential, therefore to suspension stability (Tadros, 1996).

Universal attractive van der Waals forces between particles drive particle aggregation on collisions caused by Brownian motion, when temporary dipoles in the molecules of a particle induces dipoles in neighbouring particles. Particle flocculation results in system in-homogeneities, leading eventually to the total segregation of the dispersed

from the continuous phases. Therefore, colloidal dispersions must be stabilised by counteracting the attractive van der Waals forces. Electrostatic and/or steric stabilisations are two strategies that introduce a repulsive component to the total interparticle potential, balancing the attractive effects of van der Waals forces.

Electrostatic stabilisation results from charged groups on the surface of each particle. Repulsion between the surface charges prevents close particle approach, and balances the attractive van der Waal forces as first described by the DLVO (Derjaguin and Landau, Verwey and Overbeek) theory (Hughes, 2010). Steric stabilisation, on the other hand, involves grafting or adsorbing a polymer with a lyophilic portion to the surface of a colloidal particle. The lyophobic portion extends into the solvent, providing a steric barrier to particle aggregation. Steric stabilisation balances the van der Waals attractions by two mechanisms:

- The first is the repulsive, entropic contribution arising from the loss of configurational freedom associated with interpenetration or compression of particle stabilising layers as inter-particle distance decreases.
- The second is the enthalpic contribution arising from the change in free energy associated with the partial demixing of chain segments and solvent as the stabilising layers overlap. This contribution can be either attractive or repulsive depending on the polymer-solvent interaction parameter (χ) for the particular system (Napper, 1983) (see chapter 3).

Hence, for dispersed systems the total particle interaction potential, which determines suspension stability, is the sum of the van der Waals attraction and the repulsive interactions (electrostatic and/or steric repulsions, see figure 1.6).

1.9 Controlling inter-particle interactions using an external stimulus

The ability to control interparticle interactions through the prudent variation of certain solution conditions can lead to innovative applications of suspensions in various fields including ceramic processing, water processing as well as biomedical applications (Franks, 2005). Generally, particle aggregation can be induced by changes in particle interaction potential, as a result of changes in pH, ionic strength or the characteristics of the stabilising polymer.

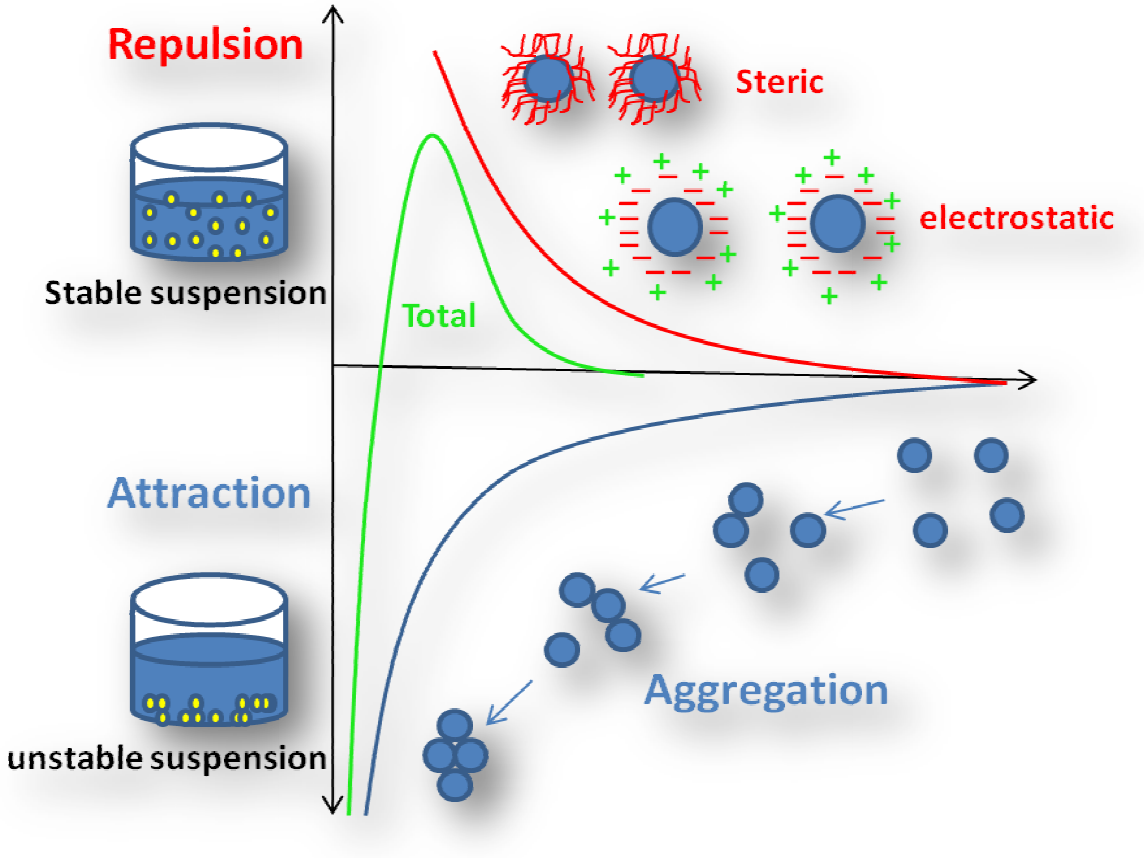

Figure 1.6: A graphical description of particle interaction potential.

Interparticle repulsion incurred by electrostatic or/and steric stabilisations (red line) resists the Van der Waals attraction (blue line), that can lead to particle aggregation. The sum of the repulsive and attractive forces gives the total interaction potential, with an energy barrier to prevent the particles to get into small separation distances, where the Van der Waals forces would dominate (green line).

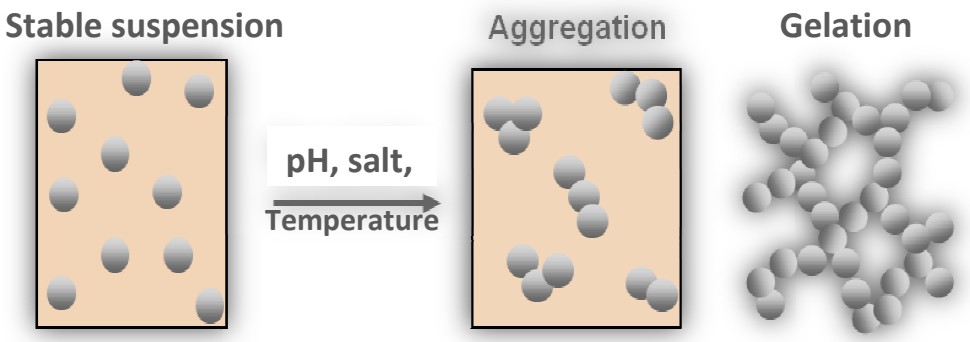

Figure 1.7: A graphical description on how triggered particles aggregation can lead to gelation.

Aggregation of suspended particles destabilises the system with the formation of particle flocks that sediment quickly. However, if the particle concentration and strength of attraction are sufficiently high, the aggregating particles can form a percolating space-filling three dimensional network, leading to gelation (figure 1.7). The obtained gels constitute a unique class of materials termed *particle gels*.

Neutralisation of the surface charge in electrostatically stabilised suspensions abolishes the repulsive forces, leading to particle aggregation and eventually gelation. This is a common practice in food industry, where yoghurt is made by lowering the pH of milk leading to the aggregation of electrostatically stabilised casein micelles forming colloidal gels. Gelation tends to be irreversible in electrostatically stabilised systems(Larson, 1999).

In sterically stabilised suspensions, the stabilisation fails when the solvent quality for the stabilising moieties deteriorates leading to particle flocculation. This can occur on addition of a non-solvent, or by changing the temperature to near the theta temperature when the polymer becomes insoluble in the solvent. This is referred to as ***incipient flocculation***. Particle aggregation is *reversed* on improving the solvent quality for the stabilising chains.

In both cases, gels are obtained if the particle concentration and strength of interaction are sufficiently high.

Temperature can be used as a trigger for particle aggregation, in sterically stabilised suspensions if the stabilising moieties have a temperature dependent solubility in the continuous phase. Franks *et al* suggested that stable suspensions can be made with an appropriate quantity of a temperature sensitive polymer in its soluble state (for example at room temperature for polyNIPAm). Changing the temperature to that at which the polymer becomes insoluble (40°C for polyNIPAm) provides a driving force for the polymer to simultaneously adsorb on the particles and aggregate with other polymer molecules, and particle aggregation will rapidly follow. If the temperature is altered back to the temperature at which the polymer is soluble, repulsion is re-established. The author suggested such a system would have important industrial applications such as dewatering (Franks, 2005).

Particles bearing thermoresponsive polymer layer have been investigated for biomedical applications. Examples include polycaprolactone nanoparticles with polyNIPAm shell (Choi et al., 2006), as well as silica, polystyrene and gold particles bearing thermoresponsive polymers at their surface (Vihola et al., 2007, Elaissari, 2006). These particles have interesting switchable surface properties for use in biomedical diagnostics, where they exhibit outstanding capability for the immobilisation of biomolecules such as proteins and nucleic acids. Protein adsorption occurs when the polymer shell is collapsed above the LCST, while desorption occurs on cooling offering by that a means for protein concentration and purification. Nucleic acid extraction, purification, concentration and amplification can also be achieved in a similar way using cationic particles bearing a thermoresponsive polymer shell, where if adsorption is performed below the LCST, nucleic acids would be selectively adsorbed driven by the charge attraction, but not proteins (Elaissari, 2006). In addition to their use in diagnostics and drug delivery, these particles can also form suspensions with switchable properties, and which can be transformed into gels by varying the temperature.

1.9.1 Current tissue engineering-related applications of particle gels

Particle gels have been widely utilised in various industries. However, a literature search finds much fewer studies exploring their biomedical applications, and specifically as scaffolds in tissue engineering, these being mainly limited to shear responsive particle gels. In one example, thixotropic (shear-thinning) particle gels were used to print 3D scaffolds for tissue engineering. Pluronic F-127 solutions mixed with polyacrylate latex particles gave rise to thixotropic particle gels. The colloidal gels were formed by physical associations between the pluronic-coated particles, through hydrogen-bonds between the extending PEO strands on neighbouring particles. This gel network is disrupted when subjected to high shear conditions, and the attrition of particle clusters frees trapped solvent and leads to shear-thinning. Upon returning to a quiescent state, the network is re-established rapidly and the colloidal suspension returns to the gel state. These gels were well suited for scaffold-fabrication through their direct writing as polymer colloidal-gel-based inks since they could flow through a deposition nozzle and rapidly recover their elasticity, to maintain the shape of the deposited filaments (Lee et al., 2005, Xie et al., 2006).

In another example, colloidal particle gels were obtained from particle networks formed between negatively and positively charged PLGA nanoparticles interacting electrostatically. The gels exhibited pseudoplastic behaviour, facilitating the fabrication of shape specific micrometer scale materials and their potential use as injectable scaffolds. These gels supported the culture of umbilical cord derived stem cells, demonstrating the usefulness of such materials for tissue engineering applications (Wang et al., 2008). Colloidal gels have also been prepared from the assembly of fumed silica particles, yielding thixotropic gels that supported the 3D culture of mammalian cells and allowed for cell subculture without the use of enzymes (Pek et al., 2008).

1.10 Thesis aims and objectives

In this chapter, the importance of biomaterials in tissue engineering was emphasised, and the common materials and processing methods used for scaffold fabrication were discussed with regards to their advantages and disadvantages.

Polymeric microparticles were particularly considered, since those have been used for drug delivery applications for some time, an experience that can be built upon to achieve controlled growth factor delivery in tissue scaffolds.

Also discussed were stimuli-responsive materials used to achieve control over scaffold properties. Using thermoresponsive polymers on culture substrates, for example, provided a means to control their cell adhesive properties with temperature, which led to the development of cell sheet engineering.

Biomaterials can be generally employed to induce regeneration alone or in combination with cells. Acellular material scaffolds, which may contain biological growth factors and other mediators, have been used in a number of studies to initiate repair *in*-situ by recruiting native host cells (Salih, 2009, Stevens et al., 2005). However, the cells-scaffold combined approach remains the most popular in tissue engineering, where single or multiple cell populations are co-cultured within a suitable scaffold. Generally, the maturation of the cell-scaffold construct *in vitro* is required, prior to any implantation procedure. Hence, materials that would support the pre-conditioning of cell-scaffold constructs *in vitro*, and their simple processing for *in vivo* implantation or injection subsequently, are highly desirable.

Accordingly, the aim of this thesis was to prepare thermoresponsive particle gels and explore their application as tissue scaffolds. The proposed particle gels were based on the innovative combination of materials already used in tissue engineering.

The interest in thermoresponsive particle gels stems from their unique properties, highly relevant for tissue engineering, these being:

1. High liquid content.
2. Elasticity matching that of soft tissues.
3. Reversible temperature gelation, a property that can be harnessed for developing these materials as injectable scaffolds where the colloidal mixture of cells and particles is injectable at low temperatures but aggregates into a gel at body temperature.
4. Their building blocks are microparticles, which are interesting in their own right for tissue engineering with regards to the controlled delivery of growth factors.
5. Since microparticles are the major constituent of the gels rather than soluble polymeric networks, these gels are expected to have minimum swelling and osmotic effects on the surrounding tissues if used *in vivo*.

With such properties, the thermoresponsive particle gels are highly amenable to modifications that would allow them to better emulate the natural microenvironment of cells. The strategies commonly adopted to reproduce the natural cellular microenvironment in synthetic scaffolds include the controlled delivery of growth factors, three dimensionality, bio-functionalisation of synthetic materials and controlling the scaffold elasticity. All of these are potentially applicable in thermoresponsive particle gels.

The aim of the thesis was realised in three parts. The first part, described in chapter 3, aimed at the preparation of thermoresponsive particle gels from biocompatible materials. This involved the preparation of suspensions composed of polymeric microparticles as well as a thermoresponsive “smart” polymer. The latter was to be used as a steric stabiliser under one set of temperature conditions and as a flocculent under another, with the ability to switch it between the two states over a physiologically suitable temperature range (figure

1.8). Once made, the physical and mechanical properties of the developed particle gels were characterised.

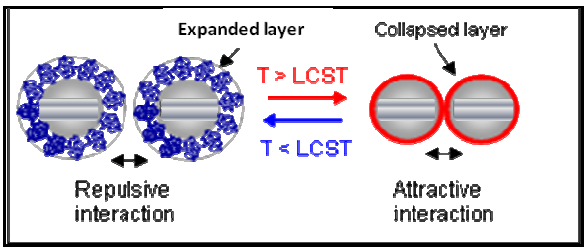

Figure 1.8: Schematic representation of the effect of temperature on particle interactions. While the thermosensitive surfactant layer is hydrated and extended below the LCST preventing the particles aggregation, above the LCST this layer collapses and the particles aggregate.

The second part was concerned with investigating the applicability of the prepared particle gels as scaffolds using a model mammalian cell line (chapters 4 and 5). Firstly, the ability of the gels to support the basic cellular functions of viability, adhesion and proliferation was evaluated. Once successful outcomes were obtained, cell encapsulation within the particle gels and their ability to support the 3D culture of cells was demonstrated. The thermoresponsive behaviour could be harnessed for enzyme-free cell subculture and processing of the cell population cultured within as described in chapter 5 (figure 1.9).

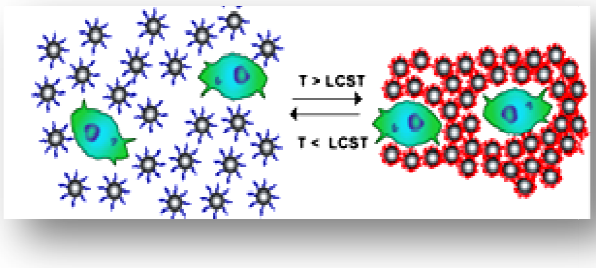

Figure 1.9: **Gel formation and cell encapsulation within temperature responsive dispersions in response to temperature increase.**

In the last part of this thesis, the versatility and the range of properties that could be engineered into thermoresponsive particle gels were exemplified by preparing thermoresponsive gels from magnetic particles. Evidence for the advantages such materials would offer if used as scaffolds, particularly with regards to simplifying cell recovery, was presented in chapter 6.

The thesis was ended by a discussion of the complexity and the repertoire of applications thermoresponsive particle gels can have, based on the data presented in this thesis, with suggestions for further optimisation of the gels and future work.

CHAPTER 2

General materials and methods

The common materials and methods used for the experimental work described in this thesis are given in this chapter. More detailed experimental procedures are given in the relevant chapters that follow.

2.1 Materials

2.1.1 General Chemicals

All general chemicals and reagents were purchased from Sigma-Aldrich (Poole,UK) and used as received except where stated. All solvents were of analytical grade and obtained from Fischer Scientific (Loughborough, UK)

2.1.2 Cell culture reagents

High glucose Dulbecco's modified Eagle medium (DMEM) and media supplements were supplied by Invitrogen, UK, and so were Trypan Blue, Hank's balanced salt solution (HBSS), heat inactivated bovine serum albumin (BSA), Trypsin, L-glutamine, Tween-20 and Alamar Blue. Phosphate buffered saline (PBS), industrial methylated spirits (IMS) and T75/25 Nunc Flasks were purchased from Fischer Scientific and chemicals, UK.

2.1.3 Cell culture vessels and plates

Nunclon cell culture T25, T75, T175 flasks from Nunc (Roskilde, Denmark) were used for cell culture and expansion. Cell culture polystyrene 6, 24, 48-well plates were also obtained from Nunclone. Costar® flat bottom polystyrene 96-well assay plates were from Corning (NY, USA).

2.2 Methods

2.2.1 3T3 fibroblast culture

All cell culture manipulations were performed using aseptic procedures in a Class II microbioology safety cabinet (Class II MST walker safety cabinets, Glossop, Derbyshire).

Mouse NIH3T3 fibroblast were obtained from the European Collection of Cell Cultures (ECACC, ECACC No. 93061524) and 3T3 swiss albino mouse embryo fibroblast cell line (SW3T3, CCL-92^{TM}) cells were from ATCC.

The 3T3 cells were cultured in Dulbecco's Modified Eagle Media supplemented with 10% Foetal bovine serum (FBS), 100 units/mL penicillin, 100 µg/mL streptomycin-, and 250 ng/ml amphotericin B and 2 mM L-glutamine. This culture medium is referred to as *complete medium throughout this thesis*.

They were maintained in T75 Nunc Flasks, in a humidified incubator at 37°C and with 5% CO_2. When the cells reached 70-90% confluence, they were passaged by rinsing once with PBS and incubation with 3ml trypsin/EDTA solution (0.25%$_{w/v}$ trypsin, 2mM EDTA in PBS) for 5 minutes followed by addition of 7 ml of growth media to stop the activity of trypsin. The cells were collected by centrifugation at 250*xg* using a Sigma Laboratory centrifuge 3K15 (Scientific Laboratory Supplies, UK) for 5 minutes. The cell pellet was re-dispersed in fresh media, and the cells were transferred to fresh tissue culture flasks. Cells used in all experiments were between passages 10-25 (NIH 3T3) and 154-160 (SW3T3).

2.2.2 Cell count and viability assessment

Cell counts and viability estimate were performed using Trypan blue exclusion assay and a haemocytometer. Equal volumes of cell suspension and the Trypan blue solution (Invitrogen, UK) were mixed in an eppendorf and left for 5 minutes at room temperature. The mixture was then placed in a Neubauer haemocytometer chamber viewed under a light microscope (10× objective). Dead cells, which lost membrane integrity, stained blue due to uptake of the dye, while live cells remained colourless.

2.2.3 Scanning electron microscopy (SEM)

The samples (dry microparticles or gel sections) were loaded on to aluminium stubs with carbon tabs pre-fixed. These were then gold coated using an SCD 030 Blazers sputter coater for 4 minutes at 30mA. The coated samples were transferred into a JEOL JSM 6060 LV Scanning electron microscope and imaged at 10-15kV. Samples containing cells were treated prior to gold coating, in $5\%_{w/v}$ glutaraldehyde solution in PBS overnight. The samples were then washed three times with PBS each wash for 5 minutes. For further fixation and dehydration the samples were incubated with $1\%_{v/v}$ osmium tetroxide solution for 3 hours. The osmium solution was then removed by aspiration and the samples were left to air dry.

2.2.4 Statistical analysis

All the results are presented as mean ± standard deviation (SD) or mean ± standard error of the mean (SEM) and N refers to the number of samples assayed. The mean, SD and SEM were calculated using statistical Microsoft Excel® 2007 software. The statistical package GraphPad-Prism.v5.01 was used for statistical analysis and statistical significance was set at significant $p < 0.05$ (*), very significant $p < 0.01$ (**) and highly significant $p < 0.001$ (***).

CHAPTER 3

Preparation and characterisation of aqueous thermoresponsive particle gels for bio-applications

3.1 Introduction

Concentrated particulate suspensions have found a wide variety of applications in various industries such as paints, dyestuff, inks, ceramics and cosmetics. Although suspensions have also been widely used in the pharmaceutical industry as oral or injectable dosage forms, there are limited reports regarding their applications as biomaterials, compared to other systems such as foams (Barry et al., 2004), polymeric gels (Drury and Mooney, 2003) or fibres (Brosworth and Downes, 2009). However, some unique properties can be engineered into suspensions, which would make them highly relevant to the field of biomaterials, particularly for tissue engineering and drug delivery applications.

An important consideration, with regards to suspension design, is the maintenance of stability within these systems of high surface area, to ensure that particle aggregation or coagulation is prevented. The stability of a suspension is mainly determined by the balance of inter-particle forces (Tadros, 1992). In general, strong attractive interactions exist between any pair of colloidal particles in a suspension and unless the attractive forces are counteracted by some repulsive forces, the particles will aggregate rapidly. The main forces leading to particle

aggregation are the *universal* van der Waals attractions between the elements of matter composing the particles. These forces become significant at smaller inter-particle separations and lead to strong particle attractions at close contact or following Brownian collisions, the latter being more pronounced in more concentrated suspensions. Van der Waals attractions can be counteracted by repulsive forces such as those encountered by charged particles surrounded by an electrical double layer. Steep repulsion forces are generated at particle separation distance where the electrical double layers overlap. Steric forces imparted by adsorbed or grafted polymeric chains on the particle surface can also counteract the van der Waals attractions (see chapter 1, section 1.8.1).

Accordingly, two main strategies have been employed in practice to incur and maintain stability in suspensions:

1. **Electrostatic stabilisation**: whereby introducing a surface charge to the particles prevent their close approach due to **electrostatic repulsion**.
2. **Polymeric stabilisation**: Polymers of high molecular weights, $\geq 10^4$ Da, have chain dimensions that are comparable to, or exceed the inter-particle distance range of Van Der Waals attractions. Therefore polymers are of the right dimensions to achieve colloid stability by **steric stabilisation.** Polymers can either be grafted or physically adsorbed to the particle surface (Napper, 1983b).

Electrostatic stabilisation suffers from many limitations such as the need for a polar solvent, sensitivity to added salts and pH, and poor freeze-thaw stability. On the other hand, steric stabilisation has the advantages of insensitivity to the presence of electrolytes (except *near the coil-globule transition region*), and the equal efficacy in both aqueous and non-aqueous

dispersion media at both high and low solids contents, and therefore allows for obtaining more concentrated stable dispersions.

Polymeric stabilisation of suspensions is not only advantageous for maintaining stability, but also for offering a way to induce particle aggregation or flocculation in a reversible manner, if required. Aggregation in electrostatically stabilised suspensions is, on the other hand, mostly irreversible (Larson, 1999).

Particle aggregation is of a substantial importance in food industry (for the manufacture of milk products, (Dickinson and Van Vliet, 2003)), ceramic processing (Bergström and Sjöström, 1999) and also in academia (Alava and Saunders, 2006). Particle aggregation is particularly interesting from a materials point of view as it can lead to gelation in concentrated suspensions (Larson, 1999). Suspension aggregation in sterically stabilised systems can be induced by decreasing the solvency of the dispersion medium for the stabilising moieties, a phenomenon referred to as *incipient flocculation* (Napper, 1983b, Tadros, 1996). One way of achieving this in aqueous systems is by altering the temperature or/and pressure to reduce the solvent power of water to the stabilising moieties. Spontaneous re-dispersion occurs on making the dispersion medium a better solvent for the stabilising chains (Napper, 1970).

Based on the above, aqueous suspensions can be prepared where a thermoresponsive polymer is used to address the issue of stability by acting as a steric stabiliser, while at the same time offering a way to control the properties of the suspension by acting as a temperature-induced flocculent. This would yield suspensions that can be reversibly transformed into particle gels with a temperature stimulus.

Previous reports of aqueous suspensions that show temperature dependent gelation were limited to industrially relevant materials. Alava and Saunders showed how a polymeric stabiliser whose solubility in water is temperature dependent, poly(PEGMA-co-NIPAM) (NIPAM and PEGMA are *N*-isopropylacrylamide and poly(ethylene glycol) methacrylate respectively), was used to induce temperature triggered gelation in an industrial latex (Alava and Saunders, 2006). Temperature triggered suspension gelation based on incipient flocculation has also been used in ceramics suspensions for ceramics processing (Bergström and Sjöström, 1999).

An interesting example was that reported by Shay *et al,* who showed how aqueous dispersions of polystyrene colloidal particles bearing grafted poly(ethylene glycol) chains exhibited temperature reversible gelation (Shay et al., 2001).

Although some types of particle gels have been previously developed as biomaterials (Wang et al., 2008, Pek et al., 2008, Xie et al., 2006), *thermoresponsive* particle gels based on the incipient flocculation mechanism, has not been previously reported to be employed in the biomedical field.

In this chapter the development of novel thermoresponsive particle gels prepared from biocompatible materials is described.

3.2 Aim and objectives

The overall aim of the work described in this chapter was "To prepare aqueous suspensions, which can undergo reversible temperature-induced gelation".

This was achieved through the realisation of the following objectives:

1. The preparation and characterisation of biodegradable polymeric microparticles of a mean diameter 2-5µm.

2. The synthesis and characterisation of thermoresponsive polymers to be used as steric stabilisers for the particles.
3. The study of suspensions combining the prepared particles and thermoresponsive polymer.
4. The study of the temperature induced aggregation and gelation behaviour of these suspensions.
5. The characterisation of the mechanical properties of the temperature responsive particle gels, particularly at 37°C.

3.3 Materials and Methods

3.3.1 Synthesis of thermoresponsive polyPEGMA polymers

Two thermoresponsive polymers were prepared by free radical polymerisation (FRP). The monomers (in the case of polyPEGMA$_{246}$-EE PEGMA$_{246}$-EE - (Mn =246) (10 g, 40mmoles, Aldrich -UK) and in the case of the copolymer poly(PEGMA$_{246}$-EE-co-PEGMA$_{475}$-ME) PEGMA$_{246}$-EE (Mn=246) (9.365 g, 38mmoles, Aldrich-UK) and PEGMA$_{475}$-ME (Mn=475) (0.95 g, 2mmoles, Aldrich -UK), were weighed into a round bottom flask. 1-dodecanethiol (0.05 g, 0.25mmoles, Aldrich -UK) and butanone (15ml, Fisher-UK) were then added. The radical initiator azobisisobutyronitrile (AIBN) (0.05 g, 0.3mmoles) was added last, and the mixture was degassed with argon for 15 minutes. The flask was then immersed in an oil bath, and the polymerisation was conducted at 70°C for 1 hour. The homopolymer polyPEGMA$_{246}$-EE was precipitated into 500ml of hexane (Fisher-UK) while the copolymer poly(PEGMA$_{246}$-EE-co-PEGMA$_{475}$-ME) was precipitated into 500ml of hexane: diethylether (1:8 $_{v/v}$). Both polymers were further purified by dialysis in deionised water for a week at 5°C (dialysis membrane of a molecular weight cut off: 6000). Polymers were freeze dried for 2 days and stored at 4°C.

3.3.2 Spectroscopy

^{1}H NMR spectra were recorded on a Bruker 400 spectrometer at 399.8 MHz (^{1}H) in $CDCl_3$. All chemical shifts are reported in ppm relative to tetramethylsilane (TMS). Bruker Topspin 2 software was used to process the data.

3.3.3 Gel permeation chromatography

The number average molecular weight (Mn), weight average molecular weight (Mw) and polydispersity (Mw/Mn) of the synthesised PEGMA-polymers were measured by Gel permeation chromatography (PL-50 Polymer Labs, UK) with an RI detector. The columns (30 cm PLgel Mixed-

C, 2 in series) were eluted with chloroform and calibrated with polystyrene standards (Mw=162–371100Da) (PolymerLabs, UK). All calibrations and analyses were performed at 40°C and at a flow rate of 1ml/min. All samples were dissolved in chloroform for chromatography and were filtered (0.2 µm filter) before injection.

3.3.4 Preparation of PCL microparticles

The single emulsion solvent evaporation method was used. Poly(caprolactone) (Mn=10000, Sigma-UK) (1.5g) dissolved in dichloromethane (DCM) (50ml, Fisher-UK) was added to 500ml of polyvinylalcohol (PVA, Mw=13-23KDa, 87-89% hydrolysed, Aldrich-USA) solution in water (0.3 $\%_{w/v}$). The mixture was homogenised (IKA-Werke T25 basic ultra Turrax) at 24000 rpm for 2 minutes. This was then left to stir at 400rpm for 6 hours, for DCM evaporation and microparticles hardening. The microparticles were collected by centrifugation at 3000 rpm for 4 minutes, and then freeze dried (figure 3.1).

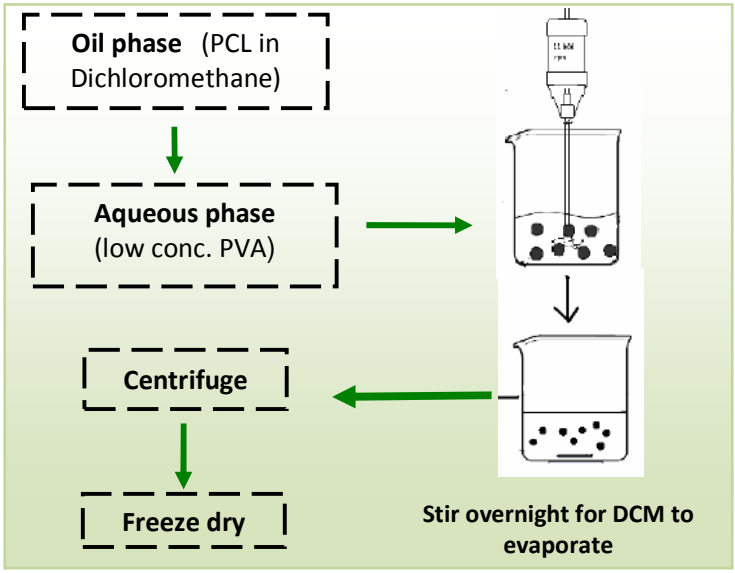

Figure 3.1: Schematic of the PCL particles preparation by the single emulsion solvent evaporation method.

3.3.5 Surface treatment of PCL microparticles

To improve the surface wettability and cell adhesive properties of the PCL microparticles these were immersed in ($30\%_{v/v}$: $70\%_{v/v}$) 0.5N NaOH: Ethanol solution (Fischer-UK) for 30 minutes at 37°C at 1g of PCL/ml. The particles were then washed extensively with deionised water through centrifugation/redispersion, and finally freeze dried**.**

3.3.6 Preparation of the thermoresponsive suspensions

All suspensions studied were obtained by mixing a known weight of PCL microparticles (NaOH treated as described above) with polyPEGMA$_{246}$-EE (or poly(PEGMA$_{246}$-EE-co-PEGMA-$_{475}$-ME)) dissolved in complete cell medium (see chapter 2, 2.2.1). This vehicle was selected to provide an optimum medium for cell culture and is referred to as *complete medium* in what follows.

3.3.7 Particle size measurements

Microparticles were analysed for their size distribution using a Coulter LS230 (Beckman, Coulter Corporation, USA) particle size analyser, which uses a 750nm laser and a double Fourier lens focusing the scattered light on the detector setup. Particle size is determined in this instrument based on the angle and intensity of scattered light. The detection range is 40nm-2000μm and therefore covers the expected size range of PCL particles.

The volume population distribution of the particles was obtained using the Fraunhofer approximation model, and a Garnet standard (Malvern, UK) was used to calibrate the instrument. Microparticles (10 mg) were typically suspended in double-distilled water (10 ml) and a few drops of the dispersion were added to the sizer cell gradually, until an obscuration

value between 8 and 12% was obtained. Size distribution plots based on volume distribution was generated.

3.3.8 Zeta potential measurement

Zeta potential of PCL microparticles was measured using a Malvern Zetasizer 2000 (Malvern Instruments, USA) based on the principle of phase analysis light scattering. The instrument measures electrophoretic mobility (μ) of particles which is converted into zeta potential using the Smoluchowski relation (Zeta potential= μη /ε, where η and ε, are the viscosity and the permittivity of the suspending solution respectively). The buffer used was 10mM PBS and the instrument was calibrated using Malvern Zeta potential transfer standard (-68mV±6.8mV). The mean value and standard deviation for each sample was calculated from at least five measurements.

The samples analysed were:

- Unmodified PCL particles and NaOH-treated PCL particles to determine the effect of NaOH treatment on the particles surface charge
- Surface treated PCL particles from suspensions containing polyPEGMA$_{246}$-EE compared to particles from suspensions not containing polyPEGMA$_{246}$-EE.

All samples were diluted in 10mM PBS, the buffer used for the analysis.

3.3.9 Water contact angle (WCA) measurement

PCL particle films were prepared by dissolving PCL particles in DCM (300mg/ml). 0.3 ml of the solution was thinly spread on a glass slide and left to air dry. Some films were then NaOH-treated as described for the PCL particles (see 3.3) and then left to air dry. The static WCA of films made of PCL particles was measured using a CAM 200 sessile drop video capture apparatus

(KSV Instruments LTD, Helsinki, Finland). A drop of ultrapure water was gently placed onto the sample surface using a micro-syringe and 20 images were taken at 1s intervals. The drop profile was fitted using the Young/Laplace equation and a linear regression was used to estimate the initial WCA at the point the drop first contacted the surface. Measurements were taken from triplicate samples.

3.3.10 Construction of the adsorption isotherm of polyPEGMA$_{246}$-EE on PCL microparticles

3.3.10.A Preparation of polyPEGMA$_{246}$ by Reversible Addition Fragmentation Transfer, RAFT.

In order to introduce a chemical functionality to the polyPEGMA$_{246}$-EE chains that would allow for their detection using UV spectroscopy, the polymer was prepared by Reversible Addition Fragmentation Transfer (RAFT), using the RAFT agent 4-cyanopentanoic acid dithiobenzoate (CPADB) synthesised by Dr Joannes Mangsun Pall (Drug Delivery Group, University of Nottingham) as described by Rizzardo *et al* (Thang et al., 1999). The chemicals used at the ratios and amounts given in table 3.1, were charged into a round bottom flask (100ml) and degassed for 20 minutes under argon. The polymerisation was conducted for 7 hours at 70°C. The resulting polymer was precipitated into a large excess (10 folds) of hexane (Fisher, UK) and then dialysed against deionised water for 5 days (using a dialysis membrane of a Mw cut-off of 6000Da). The polymer was then freeze dried and stored at 4°C.

		ratio	Mmol ratio	Mw	Weight (g)
Monomer	**PEGMA-EE 246**	150	0.014227642	246	3.5
RAFT agent	**CPADB**	1	8.92857E-05	280	0.025
Initiator	**4,4'-AzoBis(4-CyanoValeric Acid) (V501)**	0.5	4.48029E-05	279	0.0125
solvent	**THF**				10.5

Table 3.1: Ratios and amounts of chemicals used during the RAFT polymerisation of polyPEGMA$_{246}$-EE

3.3.11 Quantification of the adsorption of polyPEGMA$_{246}$-EE on PCL particles

PCL particles (100mg) were weighed into seven plastic eppendorfs. polyPEGMA$_{246}$-EE (synthesised by RAFT, 200µl) dissolved in deionised water to different concentrations was then added to each eppendorf. The concentrations of polyPEGMA$_{246}$-EE solutions used were: 0.5, 1, 5, 10, 30, 50, 70 or 100mg/ml of polyPEGMA$_{246}$-EE in deionised water. The amount of polyPEGMA$_{246}$-EE adsorbed to PCL microparticles at each concentration.

The polyPEGMA$_{246}$-EE/PCL microparticles mixtures were incubated at 4°C for 24 hours, after which the suspensions were transferred into eppendorfs attached to 0.2µm filter inserts, using 500µl of deionised water for washing and transfer. The particles were filtered out of the suspensions through centrifugation at 16000rpm for 20 minutes at 4°C. The flow through was carefully collected and made up to 1 ml by adding 300µl of deionised water. The concentration of polyPEGMA$_{246}$-EE in the collected solutions was determined spectroscopically by measuring the solutions absorbance at 300nm a wavelength selected from an absorbance scan of the polymer, using a DU 800 spectrophotometer. The amount of polymer remaining free in solution (i.e. unadsorbed to PCL) was determined from the absorbance value based on a standard curve. The adsorbed amount of polymer was calculated as follows:

Adsorbed polymer (mg) = Total added polymer (mg) - remaining polymer (mg)

Data were collected from 3 separate experiments.

3.3.12 Tube inversion assay

Typically 200µl of particle suspension was added to a 2ml glass vial (8mm diameter, Fisher scientific, UK) and adjusted to the desired temperature for 1 minute. The mobility of the dispersions was assessed by inverting the vial, if no flow occurred after 10 seconds, the suspension was said to have gelled.

3.3.13 SEM

See chapter 2 section 2.2.3

3.3.14 Cryo-SEM

Cryo-SEM was employed to investigate the internal structure of the particle gels. Oxford CT 1500, a cryo-preparation transfer system, was interfaced with and used in conjunction with a JEOL 6060LV scanning electron microscope.

The samples for cryo-imaging were prepared according to the standard operating procedure for the Oxford CT 1500 unit. The surface of frozen gel was fractured (after a rapid pre-freezing in nitrogen slush) with a cold knife on the cold block of the cryo-chamber.

3.3.15 Calculation of porosity

The porosity was determined from the void volume of the particles gels as was reported previously for colloidal gels (Pek et al., 2008). The percentage porosity was determined from the weight percentage of the PCL particle content within the gels as described by the following equation:

$$\text{Porosity}\% = 100 - \%_{w/v}\ \text{PCL microparticles}$$

3.3.16 The characterisation of the mechanical properties of PCL/polyPEGMA$_{246}$-EE suspensions using rheology

Rheology is the technique used for the characterisation of the mechanical properties of viscoelastic materials. Anton Paar Physica MCR 301 rheometer, with 25mm diameter serrated parallel plate at 0.6mm gap was used for the characterisation of the particle gels. To minimise solvent evaporation a solvent trap was used and the external chamber was filled with water. Typically, chilled particle suspensions (~300µl) were loaded onto the bottom plate, the temperature of which was set to 10°C, and the upper plate was then lowered slowly until the

desired gap was reached. Optimal filling of the gap by the sample was ensured and any excess was removed.

Information on the particle suspensions and gels were obtained from two types of rheological tests (Shay, 1999):

A. Steady shear experiments were performed to determine the suspensions viscosity (η) as a function of shear rate. In these tests, a shear deformation (γ) is imposed at a particular rate ($\dot{\gamma}$) and the resulting shear stress (**τ**) can be measured. Shear stress and shear deformation are related by the steady shear viscosity (η):

$$\tau = \eta . d\gamma/dt = \eta \dot{\gamma}$$

In the tests performed the viscosity (η), an indicator for intermolecular forces, was measured at shear rates ($\dot{\gamma}$) between 0.1-100 s^{-1}.

B. Dynamic (oscillatory) rheological experiments were performed at low strain amplitudes in order to obtain further information on the particle gels microstructure and mechanical properties. Unlike steady shear tests, these are nondestructive and can be performed without disrupting the microstructure of a sample. These tests mainly aim at determining the storage modulus (G'), which is an indicator of the solid like character of the material, and the loss modulus (G'') the indicator for the fluid like character, of the material.

Controlled oscillatory strain tests were used, where a sinusoidally varying strain (**γ**) was applied to the material, as described by the following equation:

$$\gamma(t) = \gamma_0 \sin(\omega t)$$

where $\boldsymbol{\gamma_0}$ is the maximal strain amplitude [%], **ω** is the angular frequency of strain oscillation [rad/sec], and **t** is time (sec).

The resulting stress response (τ) of the material to the applied strain, is a phase shifted sin function: $\boldsymbol{\tau(t) = \tau_0 \sin(\omega t+\delta)}$

where τ_0 is the maximal stress and δ is the phase shift angle or loss angle.

In this case, Hook's Law applies in the complex form to relate the applied stress to the material response (strain): $\boldsymbol{\tau(t)= G^* \gamma(t)}$

where **G*** is the complex modulus, and is the complex sum of **G'** (storage modulus) and **G''** (loss modulus):

$$\boldsymbol{G^*=G' + iG''} \quad \text{where } i = \sqrt{-1}$$

The stress response can therefore be expressed (following employment of complex mathematics) as a sum of in-phase and out-of-phase components as follows**:**

$$\boldsymbol{\tau(t) = G'\gamma_0 \cos(\omega t) + G''\gamma_0 \sin(\omega t)}$$

G' , the elastic or storage modulus, is the stress that is in phase with the strain and is a measure of the deformation energy stored during the shear process which reflects the solid-like or structured nature of a material. ***G'',*** the viscous or loss modulus, is the stress that is 90° out of phase with the strain and is a measure of the deformation energy used by the sample as viscous dissipation and therefore reflects the liquid-like nature of a material.

Initially a strain sweep at an angular frequency, ω= 10rad/sec, was performed to determine the linear viscoelastic (LVE) region of the gelled suspensions. In this region, the stress

is linearly related to the strain, and the moduli are not dependent on strain amplitude. After determining the LVE region of the gels the following tests were carried out:

1. Frequency sweeps to obtain plots of the elastic (G') and viscous (G'') moduli as a function of frequency (10^{-1} - 10^{2} rad.s^{-1}) at a strain value of 0.05 %. These reflect the behaviour of the material at different timescales. Particle gels with various concentrations were characterised at different temperatures,

2. Strain amplitude sweeps between 0.1 and 100% (at an angular frequency (ω), ω=10 rad/sec, a commonly selected frequency for such tests (Kwon et al., 2000)).
   These were performed at 37°C on a series of gels of different compositions. G' values recorded at 0.0316% were selected as representative values of G' within the LVE.

3. Temperature ramp experiments were performed at 0.05% strain at ω= 10rad/s, with a heating /cooling rate of 1°C/min.

In all experiments, the samples were equilibrated at the specified temperature for 4 minutes before starting the runs.

3.4 Results

Novel reversibly thermogelling suspensions applicable to the biomedical field were prepared. The component materials and the temperature ranges over which the suspensions exhibited sensitivity were carefully selected to suit their intended application. The suspensions consisted of two main components: polymeric microparticles and a thermoresponsive polymer. The design concept for these suspensions is given in figure 3.2, followed by a detailed description of the experimental steps conducted to realise it.

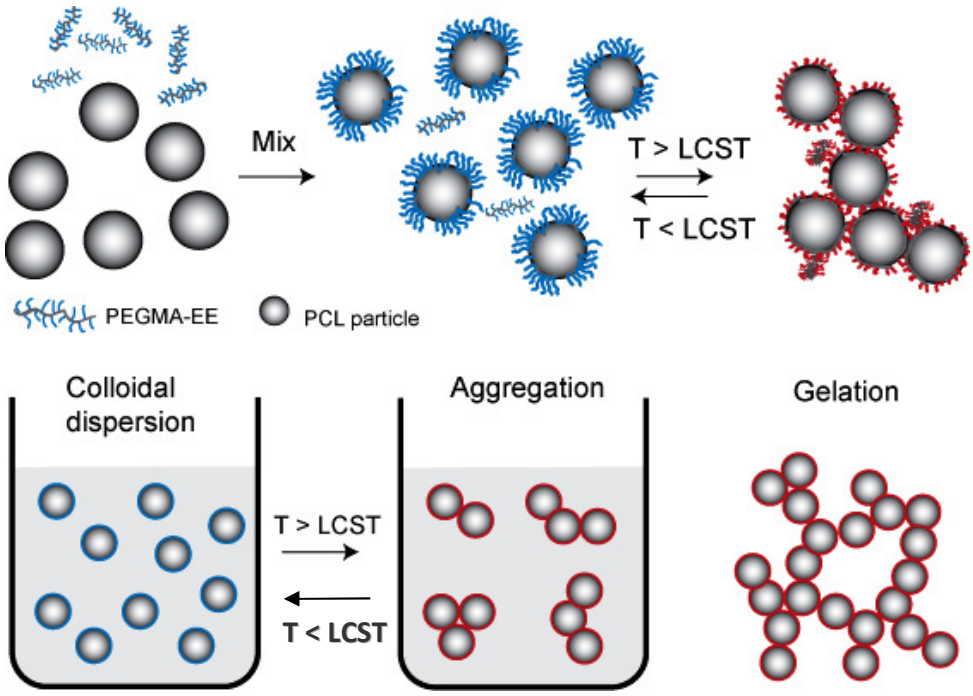

Figure 3.2: Schematic of the temperature triggered reversible aggregation of microparticles. Suspended microparticles, with the adsorbed polymer on their surface, are stable below a critical temperature (LCST). Particles aggregate above the LCST, and if they are present at sufficient concentrations volume-spanning networks of particles form, giving rise to a gel. Reduction of temperature disaggregates the particles, re-forming the dispersion.

3.4.1 The preparation of thermoresponsive PCL particles suspensions

3.4.1.A The microparticles

I. Preparation

The colloidal components of the suspensions, the microparticles, were made of polycaprolactone (PCL) , a biodegradable polymer established for use in drug delivery and tissue engineering, and FDA approved for certain biomedical applications (Sinha et al., 2004).

PCL microparticles, were prepared by the single emulsion solvent evaporation method (ODonnell and McGinity, 1997, Rosca et al., 2004). This method yields dispersed solid particles, from an emulsion of an organic solvent (in which PCL is dissolved) in water. The emulsion is made through the mechanical dispersion of the oil phase (containing the polymer) in the water phase which contains a surfactant (polyvinyl alcohol) that lowers the interfacial tension, and therefore aids the dispersion process and stabilises the final emulsion. The surface tension at the interface between the two immiscible liquids forces the dispersed droplets to adopt a spherical shape (Rosca et al., 2004). With time, the organic solvent evaporates from these droplets under stirring and the PCL precipitates into spherical solid particles.

The concentration of polyvinyl alcohol (PVA) in the aqueous phase was kept to the lowest possible ($0.3\%_{w/v}$) to stabilise the emulsion with minimum particle surface coverage, for a minimum influence on the surface chemistry of the resulting microparticles (Shakesheff et al., 1997).

The targeted particle size was 2 to 10µm to prevent potential internalisation of the particles when used with cells if they were too small (Rejman et al., 2004), while still keeping the microparticles in the colloidal range (Hughes, 2010). After a series of optimisation steps, the concentration of PCL in the oil phase (DCM) was found to be the most influential factor on

particle size, which falls in agreement with previous reports regarding polyester microparticle fabrication (Mao et al., 2007).

Using a concentration of 0.3%$_{w/v}$ of PCL in DCM and a high homogenisation speed of 24000 rpm when preparing the emulsion, predominantly spherical PCL particles were obtained , with a mean diameter of 3.6µm (SD=2.9µm, for particle samples from 5 different batches) (figures 3.3A and 3.4). The particles were polydisperse as expected for a dispersion prepared from an emulsion (ODonnell and McGinity, 1997). The particle preparation yield was 63 ±3.78 % (mean ± SD, from n=5 different batches).

II. Surface treatment

Various strategies have been employed to optimise the surface properties of polyester polymeric materials for applications in tissue engineering, including surface plasma polymerisation, chemical attachment of biomolecules, and surface hydrolysis (Jiao and Cui, 2007). Being inexpensive and simple to perform, the latter method was selected to improve the surface properties of the PCL microparticles to suit their intended application as cell culture scaffolds (see chapter 4).

This was achieved by incubating the particles in an ethanolic NaOH solution. While, this had no major effect on the particle size as shown by light scattering and SEM (figures 3.3A and 3.4), it led to changes in particle surface chemistry and topography.

Zeta potential measurements of PCL particles, before and after treatment, indicated that the NaOH treated particles had a net negative surface charge compared to the untreated particles (figure 3.3B). This can be attributed to ester group hydrolysis by NaOH, and the generation of free carboxylic acid groups at the particle surface.

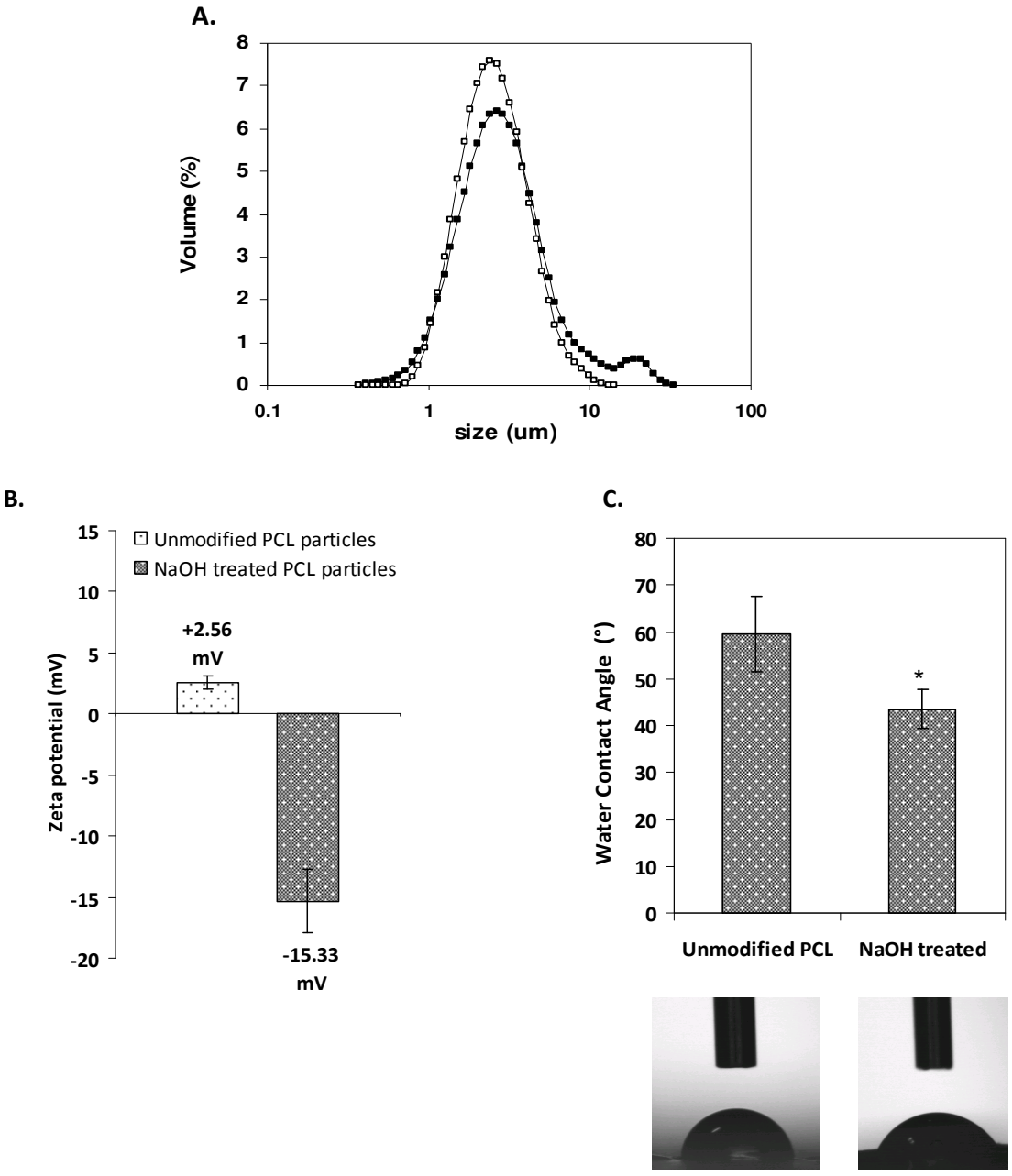

Figure 3.3: The effects of NaOH treatment on PCL particles.

A. The size distribution (volume %) of the PCL particles before (closed symbols) and after (open symbols) NaOH treatment (average of measurements made on 5 different batches). **B.** Zeta potential of unmodified and NaOH treated particles (average of values from 3 different batches) measured in PBS. **C.** WCA of PCL particle films before and after NaOH treatment (error bars represent SD from N=3 samples). Student t-test indicated statistical significance of the difference in the WCA before and after treatment ($p<0.05$).

Unmodified PCL particles

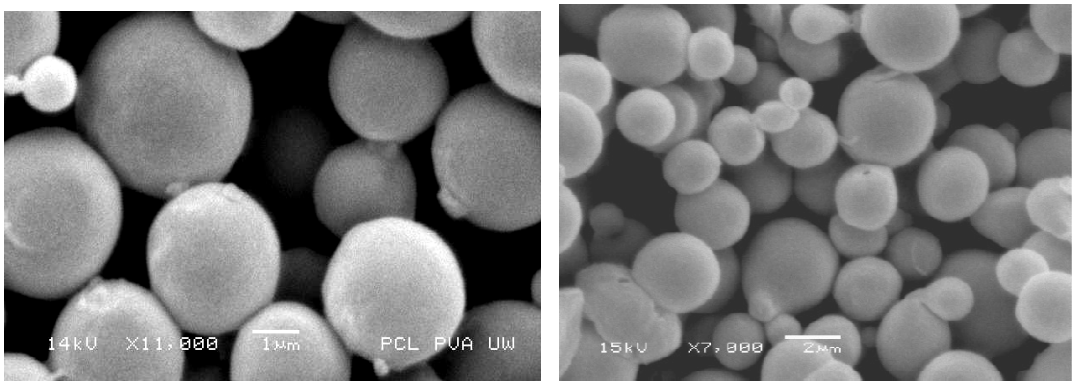

NaOH-treated PCL particles

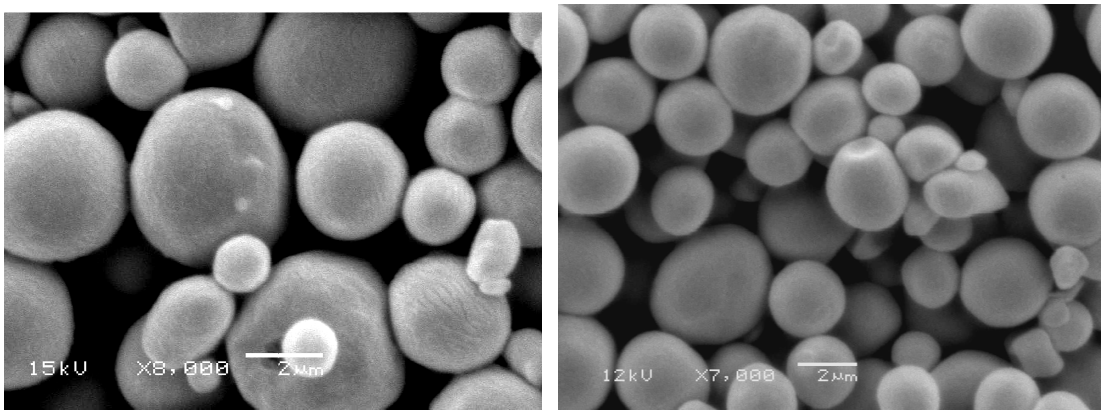

Figure 3.4: PCL microparticles as they appear by SEM before (top) and after (bottom) NaOH treatment.

To further confirm the effects of the surface treatment, the water contact angles (WCA) of solvent-cast films made from dissolved PCL particles were measured before and after NaOH/ethanol-treatment, for qualitative information on the chemical nature of these surfaces. WCAs were significantly lower after the NaOH/ethanol (WCA=59.4± 8.1 mean± SD, n=3) for PCL films without NaOH treatment and WCA=43.4±4.23, mean± SD, n=3) for PCL films after NaOH treatment) (figure 3.3C), indicating superior wetting of the films post-treatment.

Taken together, the NaOH treatment resulted in changes in surface charge, topography and wettability of the particles surface, factors that significantly improved the cellular response to the particles as shall be discussed in chapter 4. ***All PCL particles used in what follows were NaOH/ethanol surface treated.***

3.4.1.B The thermoresponsive component of the suspensions

An adsorbing polymer, with temperature dependent solubility in water, was required to act as steric stabiliser for the PCL particles under one set of temperature conditions, and as flocculent under another. The PEGMA based polymers were selected, as they combine the advantageous properties of poly (ethylene glycol) (non-toxicity, non-immunogenicity) and thermosensitivity in a single macromolecule (Lutz et al., 2006). Avni *et al* have previously reported the use of PEG grafted polymethacrylates as emulsifiers for water in oil emulsions, where the PMMA backbone was the anchoring moiety, while PEG was the stabilising moiety (Garti et al., 1993).

Also, Koh and Saunders have previously shown that a thermoresponsive polymer could be used as a stabiliser for oil in water emulsions, and gelation could be triggered in those emulsions by changes in temperature (Koh and Saunders, 2000).

I. Polymer Synthesis

High molecular weight polyPEGMA (>10KDa) polymers were needed to achieve sufficient particle surface coverage, and so effective steric stabilisation, in good solvency conditions (Napper, 1983b).

Two polyPEGMA thermoresponsive polymers were synthesised by conventional free radical methods using a thiol as a chain transfer agent to control molar mass. Thiols have been employed as efficient chain transfer agents due to the weakness of the S–H bond and the high reactivity of the thiyl radicals (Henrı´quez et al., 2003). 1-Dodecanethiol was chosen to produce a polymer terminus that would enhance the overall ampiphilicity of the polymer and promote its adsorption to hydrophobic substrates.

The homopolymer of poly(ethylene glycol) methacrylate ethyl ether (denoted as **polyPEGMA$_{246}$-EE**) was the main thermoresponsive polymer used in the PCL suspensions. A second co-polymer of PEGMA$_{246}$-EE and the more hydrophilic monomer poly(ethylene glycol) methacrylate methyl ether (PEGMA$_{475}$-ME), denoted as *poly(PEGMA$_{246}$-EE-co-PEGMA$_{475}$-ME)* was also synthesised, in order to study the effects of changing the thermoresponsive polymer on the properties of suspensions. The polymers were characterised by NMR spectroscopy and their structures are shown in figure 3.5.

II. The characterisation of the synthesised polymers

Thermoresponsive polymers undergo a coil-to-globule transition at the lower critical solution temperature (LCST) and become water insoluble (Liu et al., 2009). When the polymers are in the collapsed state their solution becomes turbid as a result of polymer chain aggregation. The solution turbidity starts at the cloud point temperature (Cpt) and this can be easily

determined experimentally by light transmission measurement. Cloud point temperatures were measured to determine the LCST for each polymer (Alava and Saunders, 2006).

The cloud points of the two PEGMA based polymers were measured in deionised water and in complete medium. The cloud points of the homo- and co-polymers are listed in table 3.2. As expected, these were lower in complete medium than in deionised water, owing to the presence of solutes and ions in the cell culture medium that were able to compete with the polymer chains for water molecules and facilitate polymer chain dehydration. Similar effects were reported for a number of thermosensitive polymers (Magnusson et al., 2008, Zhang et al., 2005, Cho et al., 2008).

The molar masses for the respective polymers quoted in table 3.2 are relative to linear PS standards. The differing solution properties of PEG-side-chain polymers compared to linear PS result in an error in absolute Mn values; however, based on prior work with related copolymers the differences in absolute values lie within 5–10% (Magnusson et al., 2008).

The polymers synthesised had a large polydispersity index, as expected for polymers prepared by free radical methods.

Free radical methods were used since they do not require the complex chemicals or metals, employed in controlled polymerisations that might be difficult to eliminate and could potentially present a source of toxicity when used with cells (Chen et al., 2006, Chang et al., 2009). In fact, the polymer's high polydispersity did not hinder the attainment of thermogelling suspensions but was probably beneficial as explained in **4.2.2.B**

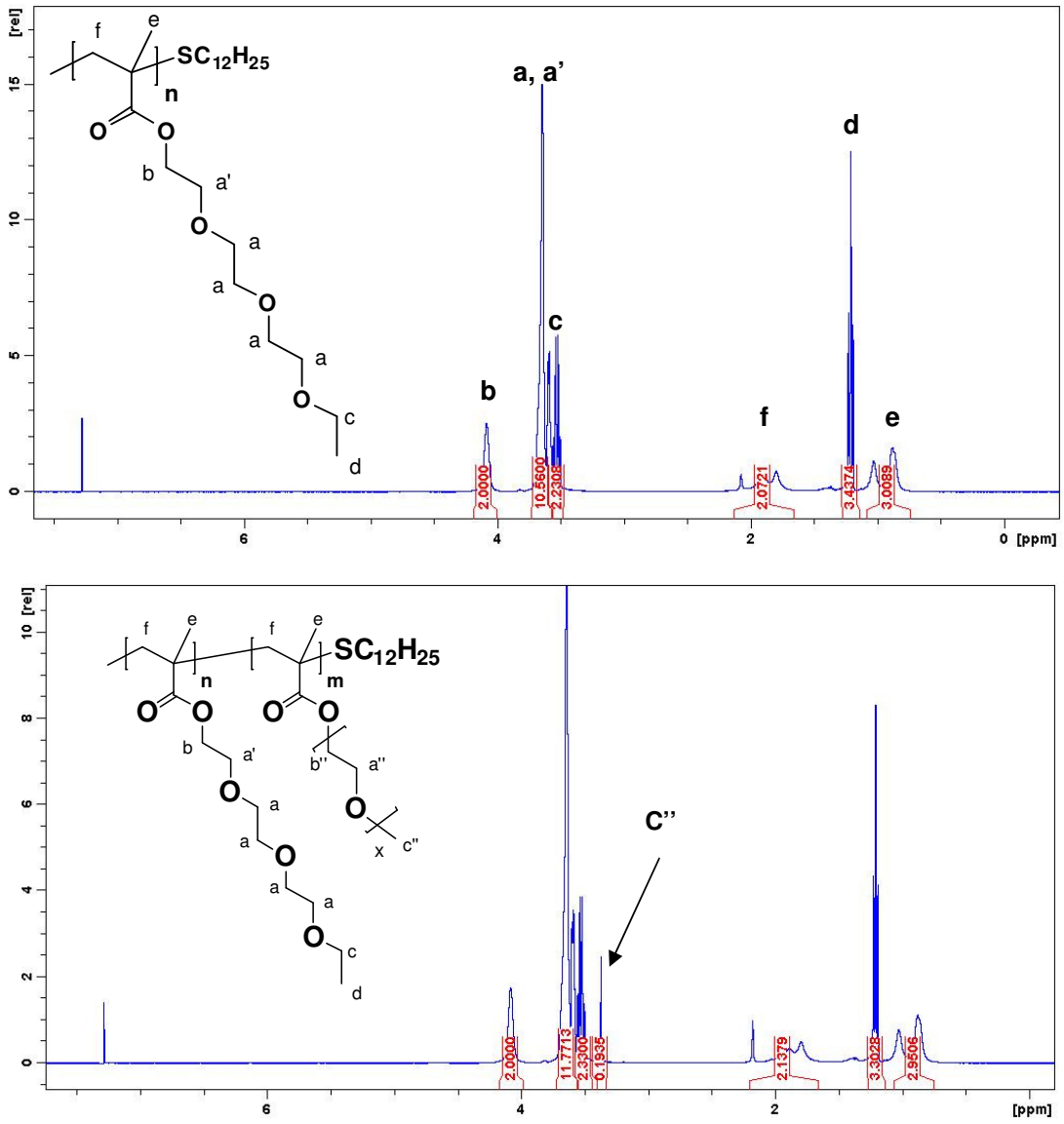

Figure 3.5: NMR spectra of polyPEGMA246-EE (top) and polyPEGMA246-EE-co-PEGMA475-ME (bottom) prepared by free radical polymerisation.

The integrals were used in the calculations to estimate the copolymer composition shown in table 3.2.

Monomer ratio	Mn (KDa)	PDI	T_{cpt}/°C (dH_2O)	T_{cpt}/°C (complete medium)
$PEGMA_{246}$- EE (100 %)	23.17±1.1	1.8 ± 0.05	21.66 ± 0.2	18.6± 0.2
$PEGMA_{246}$-EE co-$PEGMA_{475}$- ME (93.55: 6.45 %)*	22.02	1.7	25.7	22.6

Table3.2: The thermoresponsive polymers synthesised with their respective cloud point temperatures in deionised water and in complete medium. Values for polyPEGMA$_{246}$-EE are averages of 3 different batches of polymer (values are given as mean ± SD, N=3 polymer batches). * Monomer ratios calculated from the NMR integrals.

Mn is the number average molecular weight, PDI is the polydispersity index and Tcpt is the cloud point temperature.

3.4.2 The PCL particles/polyPEGMA$_{246}$-EE polymer suspensions

Thermoresponsive suspensions were obtained by mixing PCL microparticles with polyPEGMA$_{246}$-EE dissolved in an aqueous medium. Complete medium was selected as a diluent for the suspensions to suit the intended applications of these materials in tissue engineering. polyPEGMA$_{246}$-EE was used as a temperature dependent steric stabiliser for the PCL particles in suspension. Generally, the main conditions needed for effective steric stabilisation are (Duijneveldt, 2010):

1. High surface coverage, where the adsorbing polymer needs to be in the plateau region of the adsorption isotherm.
2. Strong polymer adsorption, to ensure high surface coverage.
3. Good solvency for the stabilising chains for effective repulsions.
4. Low free polymer concentration, to prevent depletion attractions.

Experiments were performed to determine whether these criteria were met by polyPEGMA$_{246}$-EE as described below.

3.4.3 The adsorption of polyPEGMA$_{246}$-EE onto PCL particles

Steric stabilisation can be achieved by polymers grafted to the particles (Shay et al., 2001), or adsorbed onto their surface upon mixing with the particles. For polymers added to colloidal systems two very different scenarios can occur depending on whether the added polymer adsorbs to the colloid surface or not. Particle destabilisation and flocculation can occur if the added polymer is non-adsorbing, in what is termed depletion flocculation (Napper, 1983a). By contrast particle stabilisation will ensue from polymer adsorption, and it acting as steric stabiliser.

Below its LCST, polyPEGMA$_{246}$-EE is water soluble with an amphiphilic character, due to its hydrophobic methacrylate backbone and hydrophilic pendant poly(ethylene glycol) side chains. This enables the adsorption of polymethacrylate chains (as well as the hydrocarbon tail on the polymer chains originating from the chain transfer agent) to the rather hydrophobic polycaprolactone surfaces at the interface with the aqueous dispersant.

Being a homopolymer, its adsorption is more likely of a loop-like type, which leads to some segments abutting the interface (trains) together with both tails and loops (figure 3.6) (Napper, 1983b). At the interface, adsorbed loops and tails of polyPEGMA$_{246}$-EE provide a steric barrier that helps prevent particle aggregation, when soluble below the LCST.

polyPEGMA$_{246}$-EE adsorption to the particles surface was confirmed by comparing the zeta potential of bare PCL particles and those mixed with polyPEGMA$_{246}$-EE, a method used commonly to detect polymer adsorption on particles surface (Fraylich et al., 2008). The PCL particles carrying a negative charge (figure 3.7) became almost neutral when mixed with polyPEGMA$_{246}$-EE. The polymer adsorbed onto the slightly negatively charged PCL particles and extended tails and loops into the aqueous dispersant (figure 3.6), that screened the particle

surface charge and shifted the shear plane from the particle surface, dropping the zeta potential to near neutrality (figure 3.7).

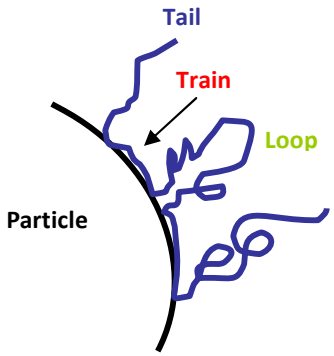

Figure 3.6: **A schematic of the predicted conformation adopted by polyPEGMA$_{246}$-EE chains when adsorbed onto PCL particles.**

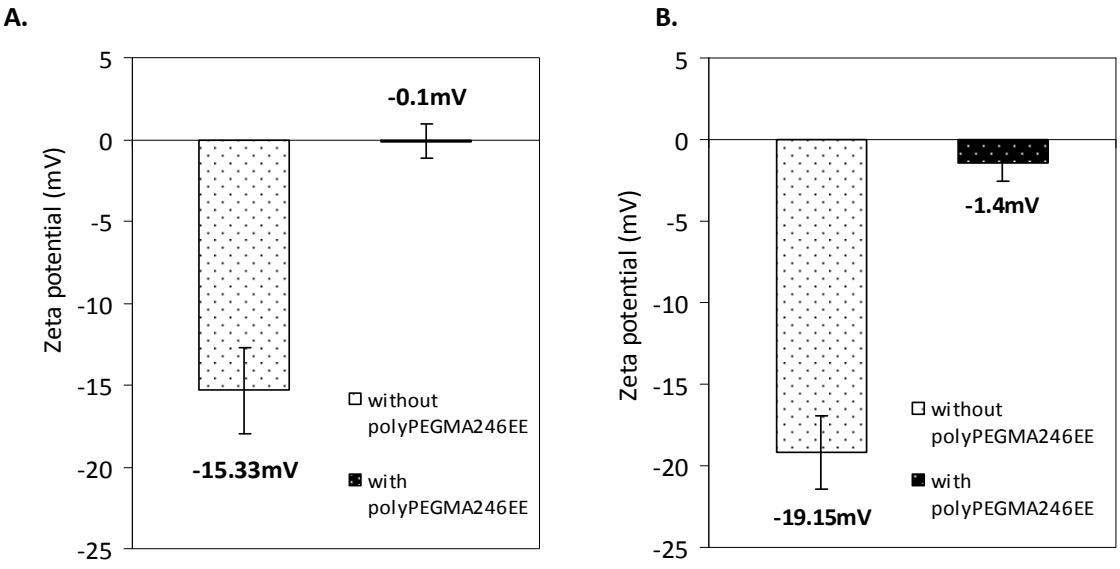

Figure 3.7: Effect of the adsorption of polyPEGMA$_{246}$-EE on the zeta potential of PCL particles. Zeta potential of PCL particles from suspensions containing polyPEGMA$_{246}$-EE compared to PCL particles from suspensions not containing polyPEGMA$_{246}$-EE. The suspensions were made in **A.** deionised water or in **B.** complete medium. The charge screening effect of polyPEGMA$_{246}$-EE confirms its adsorption to the particles surface in both aqueous media used. Error bars represent SD from N=3 different particle batches.

3.4.4 Quantification of polyPEGMA$_{246}$-EE adsorption onto PCL particles

Generally, the concentration of polymer required to impart stability depends on the ability of the particles to adsorb it.

Polymer *adsorption isotherms* give the amount of adsorbed polymer on the particles surface (weight/surface area) as a function of polymer concentration in the dispersant at a specific temperature. The adsorption isotherm can take a variety of forms, an ideal one was proposed by Langmuir where the adsorbed amount increases as the concentration in solution is increased until the surface "saturates" and the amount adsorbed reaches a constant value.

The experimental methods used for construction of adsorption isotherms may be direct or indirect (Tadros, 2009):

- Indirect methods usually involve some spectroscopic techniques such as ultraviolet-visible (UV), nuclear magnetic resonance or infra red (FTIR) techniques to measure the concentration of polymer in the solvent before and after adsorption to some surface.
- Direct methods usually involve techniques such as neutron- or optical reflectometry, ellipsometry, quartz crystal microbalance (QCM) or surface enhanced Raman scattering which measures the concentration of polymer at the surface.

Although direct methods are more accurate, as they measure an absolute quantity, UV spectroscopy was used to measure the amount of polyPEGMA$_{246}$-EE adsorbing to PCL particles and construct an adsorption isotherm, as it is simpler to perform.

3.4.4.A polyPEGMA$_{246}$-EE synthesis by RAFT

One way to accurately measure the concentration of solutes is through UV/VIS spectroscopy. UV/VIS spectroscopy can be used with conjugated compounds which absorb UV/VIS light in proportion to their concentration, following the Beer Lambert Law:

$$\mathbf{A = \varepsilon\, b\, c}$$

where **A** is absorbance, **ε** is molar absorbtivity or extinction coefficient, **c** is the concentration and **b** is the path length (cm).

This method was chosen to determine the amount of polyPEGMA$_{246}$-EE in solution before and after adsorption to PCL particles. However, since polyPEGMA$_{246}$EE synthesised by FRP does not absorb in the UV/VIS region, the reversible addition fragmentation transfer (RAFT) polymerisation was used to introduce a chromophore into the polymer chains, since when the RAFT polymerisation is complete (or stopped), most of chains retain the thiocarbonyl thiol-end group and can be isolated as stable materials (Moad et al., 2005).

This was the RAFT chain transfer agent 4-cyanopentanoic acid dithiobenzoate (CPADB), shown in figure 3.8A, which becomes attached to the polyPEGMA$_{246}$-EE chains during the RAFT polymerisation. This molecule is highly conjugated and absorbs strongly at 300nm.

The synthesised polymer, polyPEGMA$_{246}$-EE, was extensively purified by precipitation and dialysis, with purity confirmed with NMR (figure 3.8). Similar molecular weight to that of polyPEGMA$_{246}$-EE synthesised by FRP was targeted. Characterisation by GPC gave the following:

Mn= 35543, Mw= 40772, PDI= 1.147

The PDI was much lower than that obtained with polyPEGMA$_{246}$-EE synthesised by FRP, as would be expected from a controlled living radical polymerisation (Thang et al., 1999).

The purified polymer absorbed strongly at 300nm (since bound to the RAFT agent), with a linear correlation to the polymer concentration as shown in figure 3.9. This standard curve was used to calculate the solution concentrations of polyPEGMA$_{246}$-EE.

A.

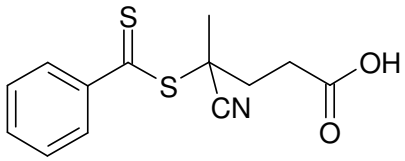

B.

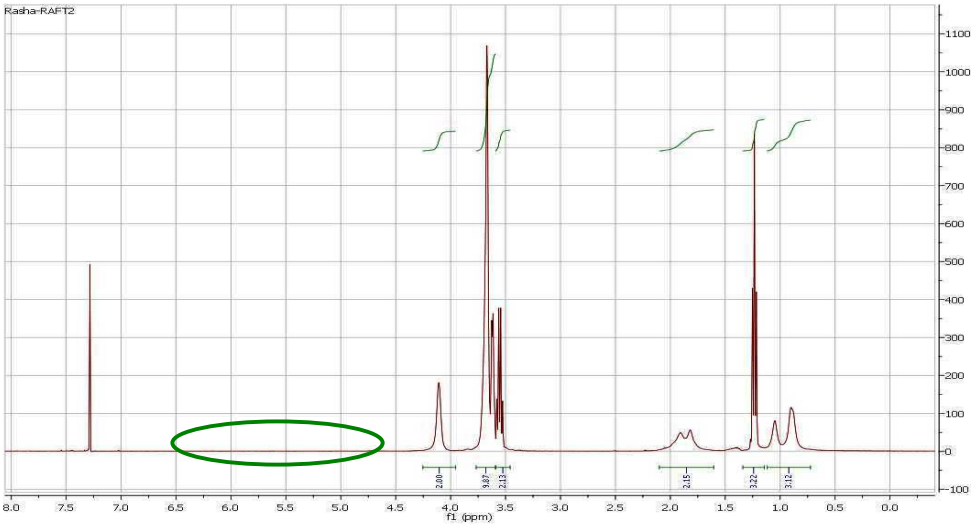

Figure 3.8: **A. Chemical structure of the RAFT agent 4-cyanopentanoic acid dithiobenzoate (CPADB) B. NMR spectrum of polyPEGMA$_{246}$-EE prepared by RAFT polymerisation and used in the adsorption isotherm studies.**

The absence of monomer peaks (circled region) confirms the complete removal of monomer.

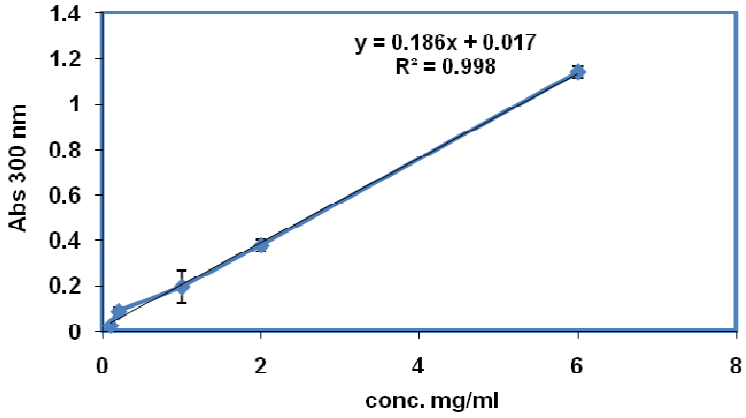

Figure 3.9: Standard curve for the concentration of polyPEGMA$_{246}$-EE (prepared by RAFT) versus its absorption at 300nm.

The corrected Abs300nm values are plotted against the polymer concentration in deionised water. Error bars represent SD from measurements on N=3, samples.

3.4.4.B The adsorption isotherm of polyPEGMA$_{246}$-EE onto PCL particles

Accurate calculations of the PCL particle surface area were not possible due to their size polydispersity. Therefore, the amount of polymer adsorbed per weight of PCL particles was plotted against the total concentration of polyPEGMA$_{246}$-EE in the suspensions, in order to produce the "adsorption isotherm" shown in figure 3.10. This graph quantifies the adsorption of polyPEGMA$_{246}$-EE, synthesised by RAFT, in its soluble state to PCL particles .i.e. below the LCST. Above the LCST, the adsorption is expected to increase without bounds, as would be expected for polymers in theta solvents (Cosgrove, 2010). Hence the isotherm in figure 3.10 only describes the adsorption of polyPEGMA$_{246}$-EE chains to PCL particles below its LCST, while above the LCST total adsorption from solution would be expected.

Polymer adsorption is also molecular weight dependent, with the shorter chains having a lower affinity isotherm, compared to longer chains. Hence, polymer polydispersity can lead to rounded isotherms and effective irreversible adsorption (Cosgrove, 2010), a note that is specifically applicable to polyPEGMA$_{246}$-EE (synthesised by FRP) which has a high polydispersity index. Accordingly, the generated adsorption isotherm for polyPEGMA$_{246}$-EE synthesised by RAFT serves only as an estimate for the adsorption of the same polymer synthesised by FRP. This is due to their different polydispersities and also their different end groups, where the more hydrophobic chain transfer agent 1-dodecanethiol used in FRP is expected to enhance the adsorption of polyPEGMA$_{246}$-EE to the PCL particle surface.

One might expect, based on these differences, that polyPEGMA$_{246}$-EE synthesised by FRP would have a higher affinity adsorption isotherm than that measured for polyPEGMA$_{246}$-EE made by RAFT and shown in figure 3.10, although this could not have been confirmed experimentally due to the lack of UV-active moieties in polyPEGMA$_{246}$-EE chains synthesised by FRP.

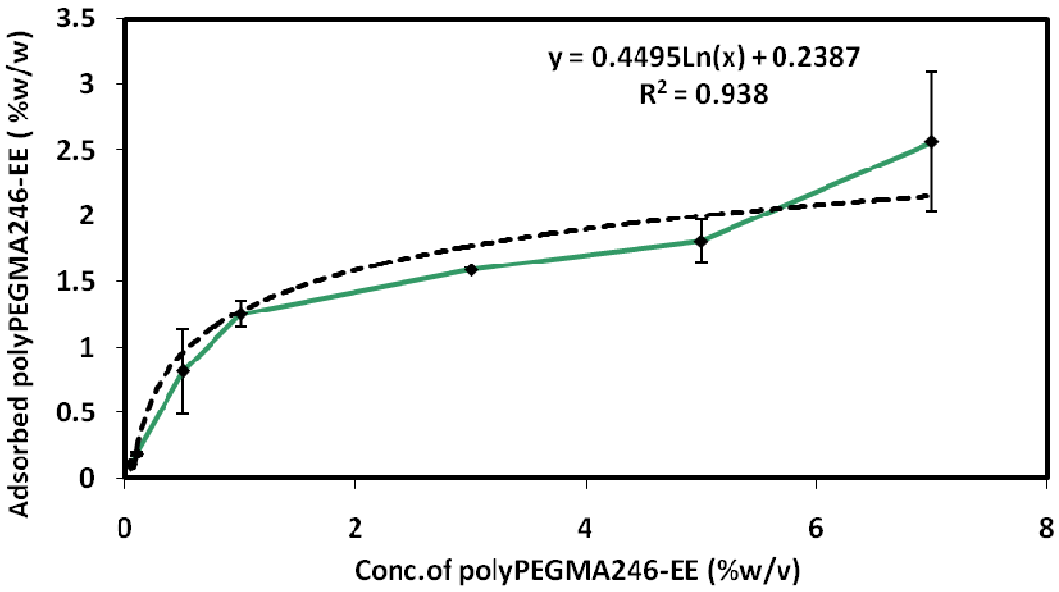

Figure 3.10: Adsorption isotherms of polyPEGMA$_{246}$-EE on PCL particles.

The amount of adsorbed polyPEGMA$_{246}$-EE per 100mg of PCL particles (plotted as $\%_{w/w}$) is plotted against the total concentration of polyPEGMA$_{246}$-EE in complete medium ($\%_{w/v}$) added to the PCL particles to make up the PCL/polyPEGMA$_{246}$-EE suspensions. Error bars represent SD of N=3 measurements from 3 different adsorption experiments.

3.4.5 The effects of polyPEGMA$_{246}$-EE on the flow properties of PCL particle suspensions

The rheology of suspensions is affected by various parameters including interparticle interactions (Tadros, 1992, Van Vliet and Lyklema, 2005). Hence, polyPEGMA$_{246}$-EE adsorption to PCL particles is expected to have a major impact on the aggregation state, and therefore the flow (rheological) properties of PCL particle suspensions.

In steady shear testing, a non-interacting suspension displays a Newtonian flow, where steady shear viscosity is independent of shear rate. Unstable flocculated suspensions, on the other hand, exhibit shear-thinning behaviour (SHAY et al., 2000).

By comparing the flow curves obtained for a suspension of PCL particles in complete medium with or without polyPEGMA$_{246}$-EE (below its LCST) suspensions containing polyPEGMA$_{246}$-EE had lower viscosities. Moreover, while PCL particle dispersions in complete medium showed a strong shear thinning behaviour, those containing polyPEGMA$_{246}$-EE had rather a Newtonian profile where viscosity was independent of shear.

Without polyPEGMA$_{246}$-EE, the attractive van der Waals forces between the PCL particles were not shielded, allowing for particle clusters or flocs to form and impede flow, in spite of the particles' net negative charge which was not sufficient for electrostatic stabilisation in the high ionic strength aqueous dispersant used (complete medium). The observed shear-thinning behaviour resulted from the destruction of those particle flocs under shear and release of trapped solvent (figure 3.11). By contrast polyPEGMA$_{246}$-EE prevented particle flocculation (below the LCST), as the adsorbed layers gave rise to steep repulsions between the particles that counteracted the van der Waals attractions.

A. 25%$_{w/v}$ PCL

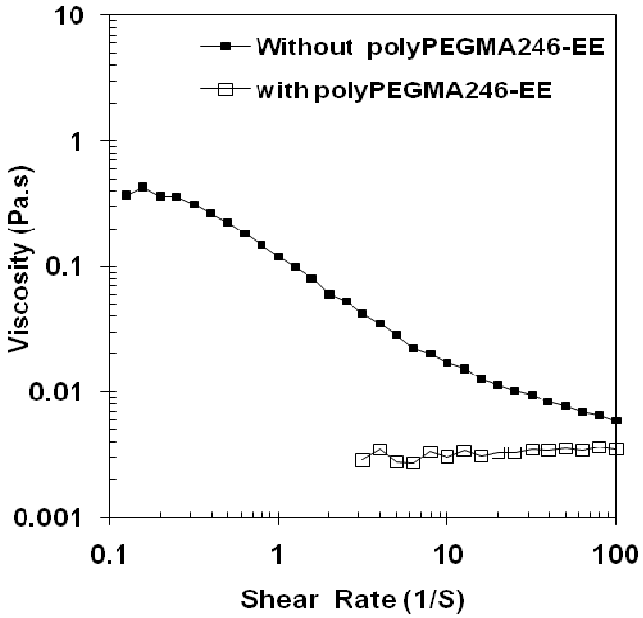

B. 33%$_{w/v}$ PCL

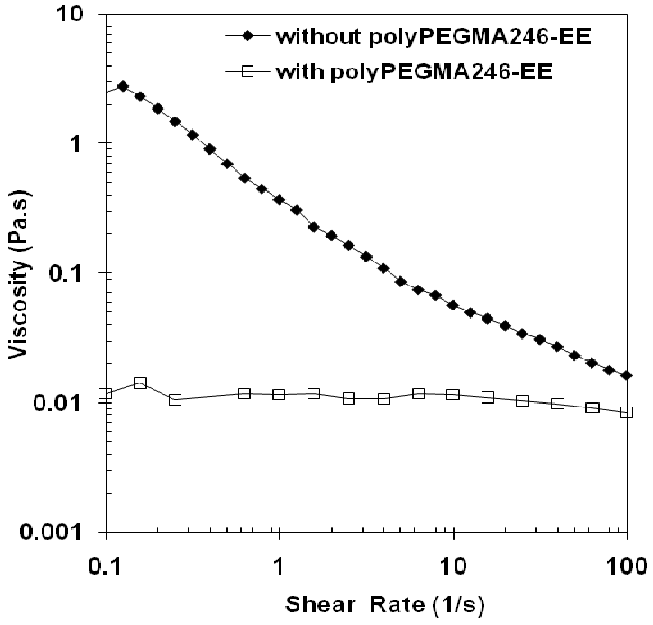

Figure 3.11: Flow curves for PCL/polyPEGMA$_{246}$-EE suspensions measured at 10°C (below the LCST).

A. 25%$_{w/v}$ PCL and **B.** 33t%$_{w/v}$ PCL with or without 2%$_{w/v}$ polyPEGMA$_{246}$-EE in complete medium. Note the shear thinning behaviour observed only in suspensions not containing polyPEGMA$_{246}$-EE and the higher viscosity values of suspensions a containing higher solid content.

3.4.6 The effects of temperature on PCL/polyPEGMA$_{246}$–EE suspensions

3.4.6.A Particles flocculation

Solvent quality is of a vital importance for steric stabilisation, which is expected to break down around the θ temperature (Van Duijneveldt, 2010) leading to *incipient flocculation* (Napper, 1983b, Yanez et al., 1999).

Since the solvent quality for the steric stabiliser polyPEGMA$_{246}$-EE is largely dependent on temperature, altering the temperature over the range at which polyPEGMA$_{246}$-EE exhibited coil-to-globule transition resulted in marked changes in the associative behaviour of the PCL particles in suspension. Above the LCST, particle flocculation was observed (figure 3.12).

According to the segmental attraction hypothesis, the incipient flocculation mechanism is driven by the switch in polymer chain interactions from being repulsive to being attractive at the flocculation temperature (Napper, 1983b).

Polymer chain interactions depend on the polymer chain-solvent interactions, described by the Flory-Huggins interaction parameter **χ.** In good solvency condition **χ > ½,** while in poor solvency conditions **χ < ½.** This parameter determines whether the particles interaction is attractive or repulsive, since for sterically stabilised particles the energy of mixing (**G_{mix}**) of the adsorbed polymer chains on close particles contact is given as follows:

$$G_{mix} = kT\, V_2^2\, v_2/V1 \left(\frac{1}{2} - x\right)(3a + 2\delta + \frac{h}{2})\left(\delta - \frac{h}{2}\right)^2$$

Where V_2 and V_1 are the molar volumes of the polymer and solvent respectively, v_2 is the number of chains per unit area, **δ** is the polymer layer thickness, **h** is the inter-particle separation, k is the Boltzmann constant, a is the particle radius.

G_{mix} is positive (repulsive) if $\chi > ½$ in good solvency conditions, and negative (attractive) if $\chi > ½$ in poor solvency conditions (Tadros, 1996).

Accordingly, in the PCL/polyPEGMA$_{246}$-EE suspension, when water is a good solvent for polyPEGMA$_{246}$-EE (i.e. below the LCST) contacts with solvent molecules are enthalpically favoured which causes the polymer chains to swell and repel each other. However, these polymeric segments undergo a dimensional collapse, or a coil-to-globule transition, when water becomes a poor solvent (i.e. above the LCST) and become mutually attractive. These mutual intermolecular attractions lead to *inter*molecular aggregation and the build up of polymeric associations between the particles, giving rise to large 3D particle clusters. The particles retain their identities in the clusters (i.e. aggregation occurs without coalescence), and spontaneous particle re-dispersion occurs on making water a better solvent for the polyPEGMA$_{246}$-EE chains by reducing the temperature (figure 3.12).

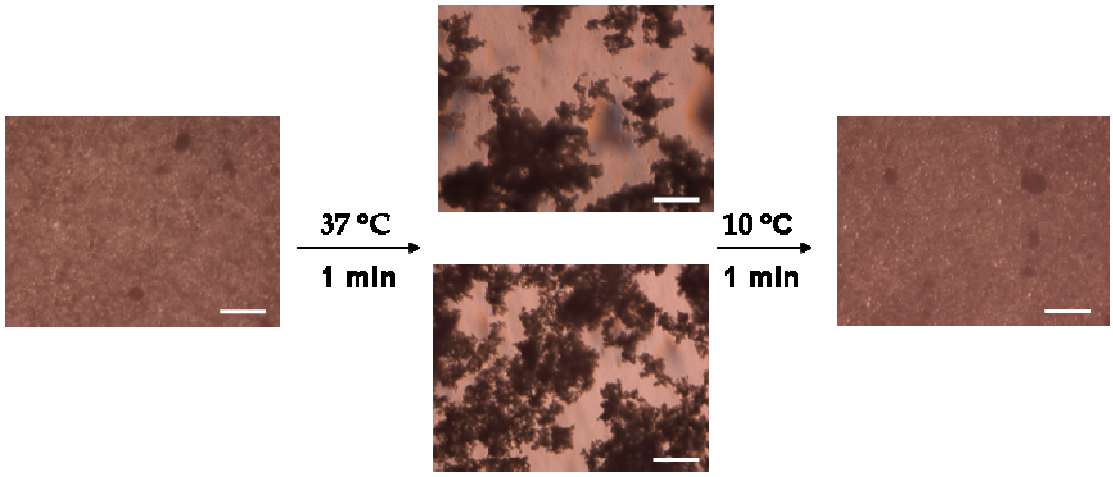

Figure 3.12: Optical microscope images of temperature triggered particle aggregation in a suspension of PCL microparticles (25%$_{w/v}$) and polyPEGMA$_{246}$-EE (2%$_{w/v}$) in complete medium. Scale bar 100µm.

3.4.6.B Effects of temperature on the flow properties of PCL/polyPEGMA$_{246}$-EE suspensions

Particle flocculation above the LCST resulted in marked changes in the suspension flow properties. In steady shear testing a non-interacting suspension displays a Newtonian flow, where steady shear viscosity is independent of shear rate, while unstable flocculated suspensions exhibit shear-thinning behaviour (SHAY et al., 2000).

The PCL particle dispersions (sterically stabilised with polyPEGMA$_{246}$-EE) were non-interacting below the LCST. Above the LCST, both the viscosity and the degree of shear thinning increased significantly as a result of structural build up from the aggregating particle networks (figure 3.13).

The particle clusters immobilise some of the aqueous medium, and with increasing shear the clusters are broken down to smaller and smaller units releasing the immobilised liquid, and so the viscosity drops.

The temperature induced flocculation was strong, since although the shear forces could break the particle network into smaller units, these could withstand the shear forces and continue to contribute to the viscosity, which was higher by orders of magnitude (even at the high shear rate range) than the viscosity below the LCST, with this being more significant at 37°C than at 20°C. This suggests that the higher the temperature (above the LCST) the stronger the inter-particle attractions.

In the absence of polyPEGMA$_{246}$-EE, the PCL dispersions had higher viscosities with shear thinning behaviour irrespective of temperature (figure 3.13). This is expected from concentrated suspensions, where the absence of effective stabilisation led to particle flocculation.

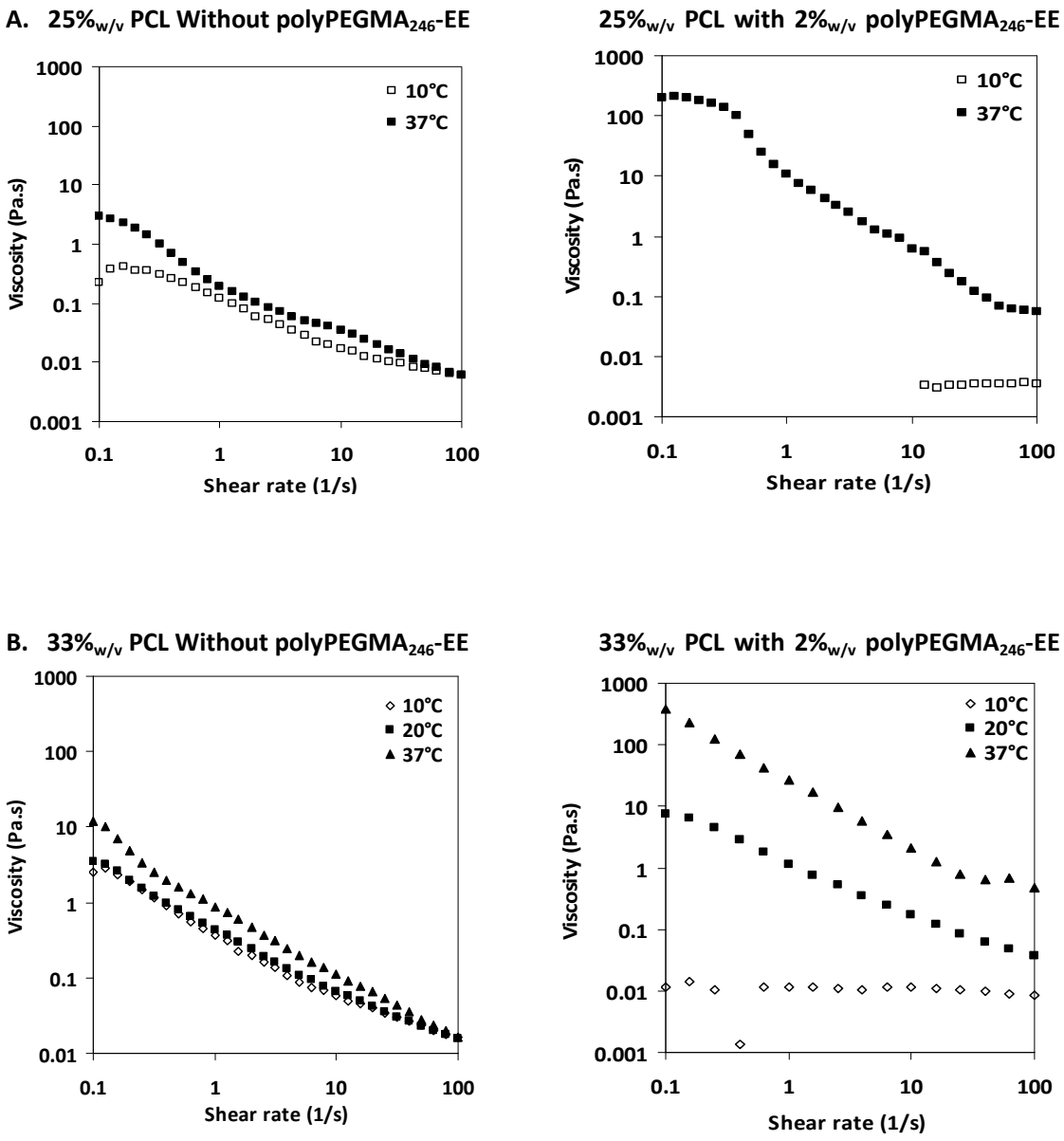

Figure 3.13: Effects of temperature on the flow properties of PCL suspensions.

Representative flow curves of PCL suspensions containing **A.** 25%$_{w/v}$ PCL and **B.** 33%$_{w/v}$ PCL with/without polyPEGMA$_{246}$-EE (2%$_{w/v}$) at different temperatures. Note the shear-thinning behaviour of the suspensions not containing polyPEGMA$_{246}$-EE irrespective of temperature, while those containing polyPEGMA$_{246}$-EE only became shear-thinning at temperatures above the LCST.

3.4.6.C Temperature driven gelation of PCL/polyPEGMA$_{246}$-EE suspensions

Particle aggregation can lead to suspension gelation. Sufficiently high volume fraction of particles and strong inter-particle attractions are required, to obtain space-filling networks of particle flocs of sufficient strength and number to give rise to space filling particle gels (Yanez et al., 1999, Larson, 1999).

An experiment was conducted to determine the concentrations of PCL and polyPEGMA$_{246}$-EE required to obtain space-filling gels, particularly at 37°C since the gels would ultimately be used at this temperature.

Different weight combinations of polyPEGMA$_{246}$-EE and PCL particles were tested using the tube inversion assay. Although this method is selective for strong gels that could resist gravitational shear forces, it is a simple way for determining the compositions that would give strong "practical" gels at a given temperature. From the adsorption isotherm (figure 3.10), in PCL/polyPEGMA$_{246}$-EE suspensions, the maximal amount of adsorbed polyPEGMA$_{246}$-EE was 2-2.5%$_{w/v}$ relative to the mass of PCL particles. This was sufficient to saturate the surface and maintain strong repulsions in good solvency conditions. This maximal adsorption was achieved when polyPEGMA$_{246}$-EE was added to a final concentration of 2-6%$_{w/v}$ in the suspensions.

Accordingly, the concentration of polyPEGMA$_{246}$-EE in the suspensions tested was varied between 0.1-6.5%$_{w/v}$ to determine the relative lowest concentration of PCL particles (the critical particles concentration-ϕ_g) required to obtain gels at 37°C.

Gels were considered space-filling if they maintained their weight without syneresis upon tube inversion (figure 3.14A). Gels were only obtained above a critical PCL concentration ϕ_g of 19%$_{w/v}$ combined with 6.5%$_{w/v}$ polyPEGMA$_{246}$-EE at 37°C, while at PCL concentrations below 19%$_{w/v}$ only particle aggregates were formed. When the PCL content was increased to above the ϕ_g (19%$_{w/v}$),

the amount of polyPEGMA$_{246}$-EE required for gelation decreased reaching as little as 0.1%$_{w/w}$ with 40%$_{w/w}$ PCL (figure 3.14B).

Aggregates tend to separate faster than individual particles, unless they form space filling or percolating (connected) structures that are stable against sedimentation at particle concentrations above ϕ_g. Above this threshold, increasing particle concentration will increase the number of particles contributing to the network structure (Yanez et al., 1999).

Cryo-SEM images of frozen "wet particle gels" sections revealed the continuous space-filling particle networks (figure 3.15A). Similar observations were obtained from SEM of freeze dried gels (figure 3.15B). The images also revealed the microporosity of the gels with most pores being between 5-20µm in size.

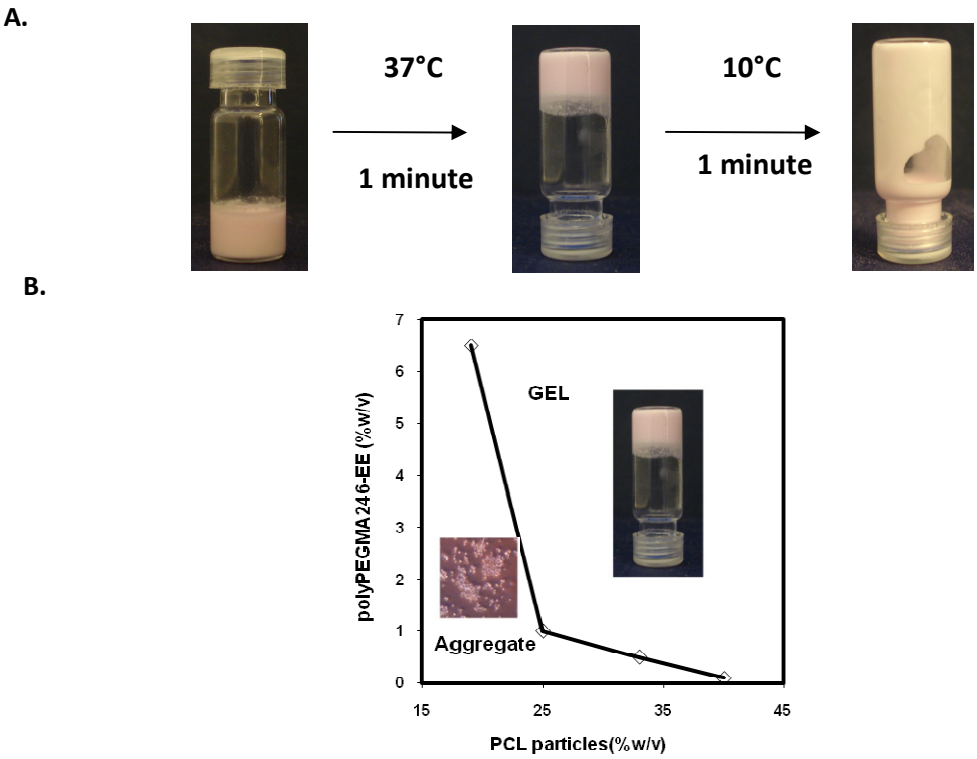

Figure 3.14: A. Reversible temperature induced gelation and flow of PCL/polyPEGMA$_{246}$–EE (25-2 %$_{w/v}$) suspension in complete medium. B. Gel–fluid phase diagram for two-component PCL/polyPEGMA$_{246}$-EE suspensions at 37°C, as determined by the tube inversion assay.

A.

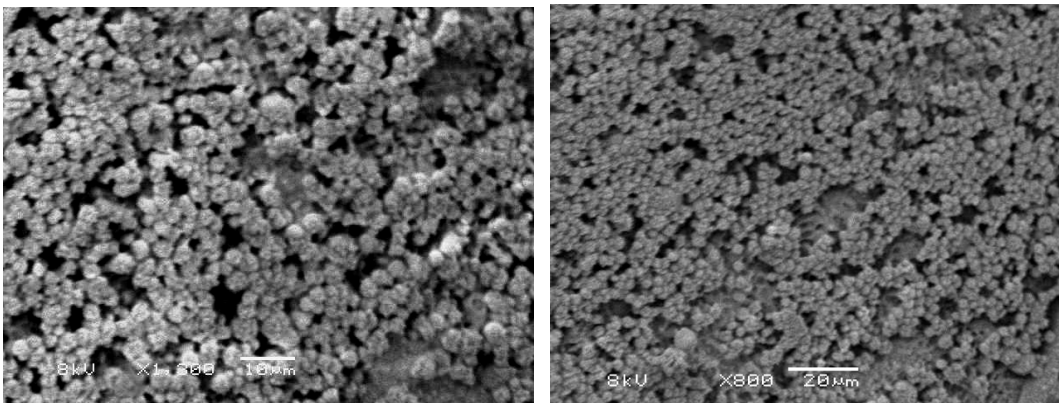

B.

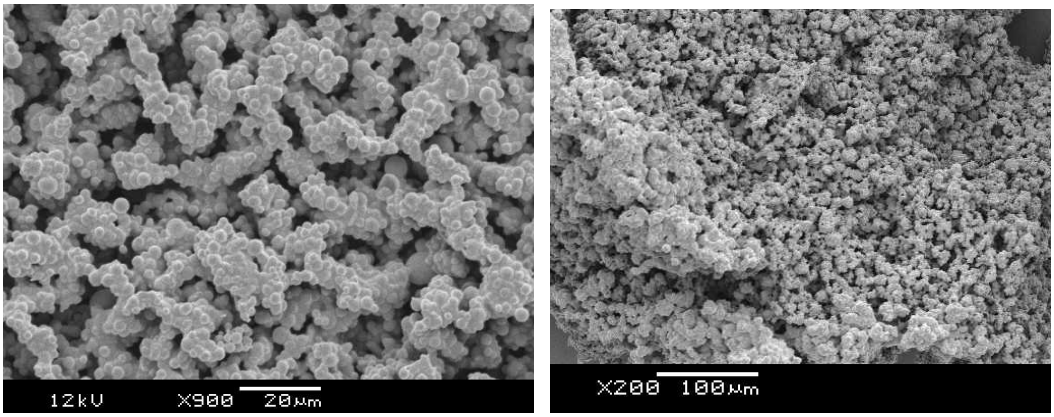

Figure 3.15: Sections showing the internal structure of a gel consisting of 33%$_{w/v}$ PCL and 6.5%$_{w/v}$ polyPEGMA$_{246}$-EE.

A. Representative CRYO-SEM images of particle gel sections **B.** Representative SEM images of freeze dried particle gels at different magnification.

3.4.7 Characterisation of the temperature driven gelation by rheology

Particle gels are viscoelastic materials, i.e. they show both viscous (flow) and elastic responses to an applied force (Tadros, 1996, Kwon et al., 2000), therefore rheology was used to study their physical properties. Rheology can be defined as "the study of the relations between forces exerted on a material and the ensuing deformation as a function of time" (Van Vliet and Lyklema, 2005).

Although the technique has proved very useful for the characterisation of viscoelastic materials (Mezger, 2006, Larson, 1999), the rheological characterisation of particulate gels can be faced with many difficulties including: poor reproducibility, sensitivity to gel preparation, sensitivity to shear history, limited range of viscoelastic response and slip (Larson, 1999). Attempts to eliminate these difficulties included similar sample preparation procedures and the use of roughened rheometer tools.

3.4.7.A Amplitude sweeps

In an amplitude sweep the elastic (G') and viscous (G'') moduli are plotted against the deformation. These tests were performed first, to determine the linear viscoelastic (LVE) range, which is the range of deformation (strain) the gels can take before their structure breaks and flow occurs. Over the LVE, G' and G'' are constant until a critical strain at which the sample structure is changed irreversibly and broken down under the applied shear. The critical strain is usually taken as the strain at which a G', G'' crossover occurs.

Typical amplitude sweeps for sample PCL/polyPEGMA$_{246}$-EE suspensions gelled at 37°C, are shown in figure 3.16. The gels were highly elastic suggesting they were strongly flocculated. For suspensions containing the same concentration of PCL particles (25%$_{w/v}$), those not containing polyPEGMA$_{246}$-EE did not show any significant elastic behaviour at 37°C (figure 3.16

A). This confirms that gelation is a result of temperature induced incipient flocculation in the PCL/polyPEGMA$_{246}$-EE suspensions.

The gels showed a small LVE, with critical strain values of around 1%. Since particles are less deformable than polymer molecules and the strands of aggregated particles are much less curved and flexible, particle gels tend to be more brittle than macromolecular gels and critical strain values less than 1% are common (Fraylich et al., 2009, Kwon et al., 2000).

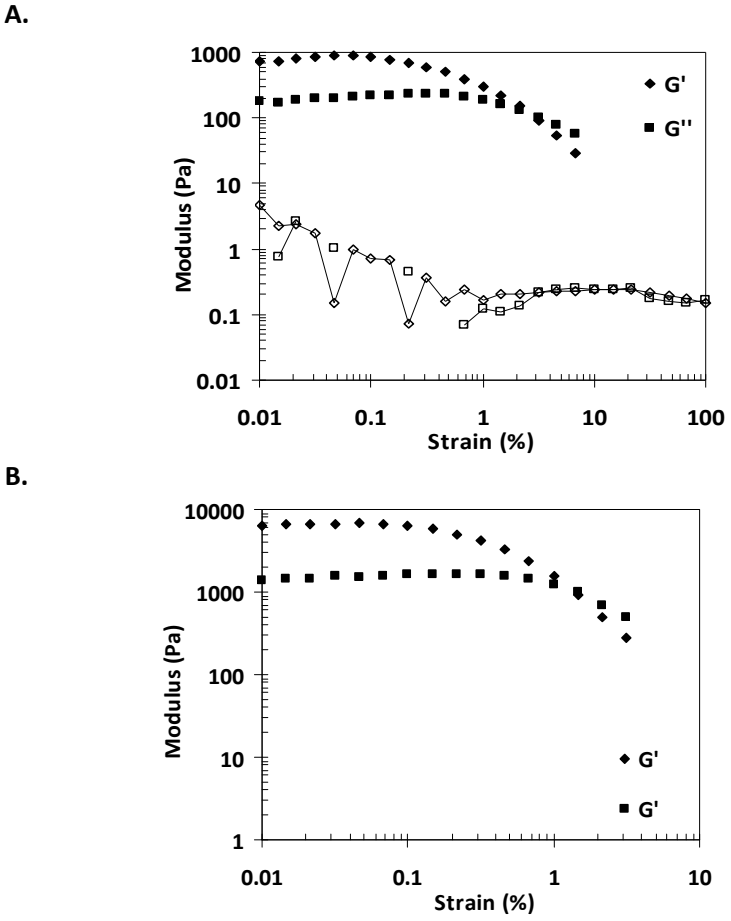

Figure 3.16: **Plots of G' and G'' versus strain amplitude for suspensions containing: A. 25%$_{w/v}$ PCL particles with (closed symbols) or without (open symbols) polyPEGMA$_{246}$-EE (2%$_{w/v}$) at 37°C B. 40%$_{w/v}$ PCL particles with polyPEGMA$_{246}$-EE (2%$_{w/v}$) at 37°C.**

3.4.7.B Thermo-reversibility of the PCL/polyPEGMA$_{246}$-EE suspensions gelation

The suspensions were subjected to heating and cooling ramps while following the evolution of their storage and loss moduli by rheological oscillatory tests.

A graph for a sample suspension containing 40%$_{w/v}$ PCL and 2%$_{w/v}$ polyPEGMA$_{246}$-EE is shown in figure 3.17. The critical flocculation temperature (CFPT) of a suspension, is the point at which flocculation is first detected on decreasing the solvency of the dispersion medium for the stabilising moieties (Napper, 1970). From figure 3.17 the CFPT coincided with the LCST of polyPEGMA-EE$_{246}$ (19°C). At the LCST the particles aggregated forming space filling networks transforming the suspension into gel as indicated by the G'/G" crossover.

Below the LCST the suspension behaved as a viscoelastic fluid with G">G'. Cooling the suspensions back to below the LCST (after heating) dropped G' and G'' with significant hysteresis but did not lead to a G'/G'' crossover.

In another test, taking the suspensions through multiple consecutive heating/cooling cycles confirmed their temperature sensitivity (figure 3.18).

Gelation occurred immediately on heating to 37°C, with gels being obtained in less than 30 seconds. On cooling back to 10°C both G' and G'' dropped but not to their initial values. Full gelation reversibility i.e. G' becoming smaller than G'' did not occur over the time scale of the experiment, although the gel-fluid transition (reversibility of gelation) was easily observed in the tube inversion assay over very short time scales (see figure 3.14).

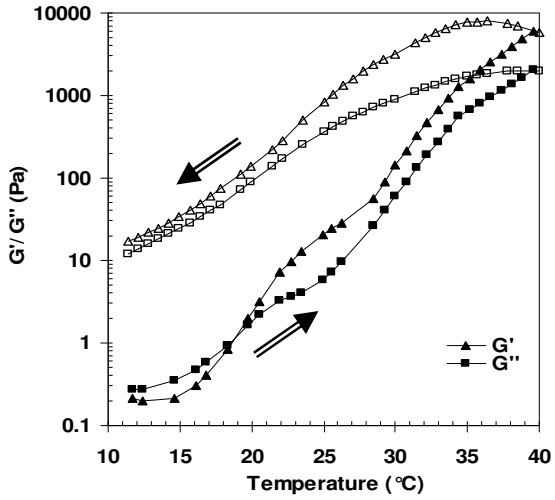

Figure 3.17: Variation of G'/G'' with temperature for a suspension containing PCL (40%$_{w/v}$) /polyPEGMA-EE$_{246}$ (2%$_{w/v}$) dispersions. Cooling the suspensions dropped the G' and G'' moduli but did not show a G'/G'' cross over.

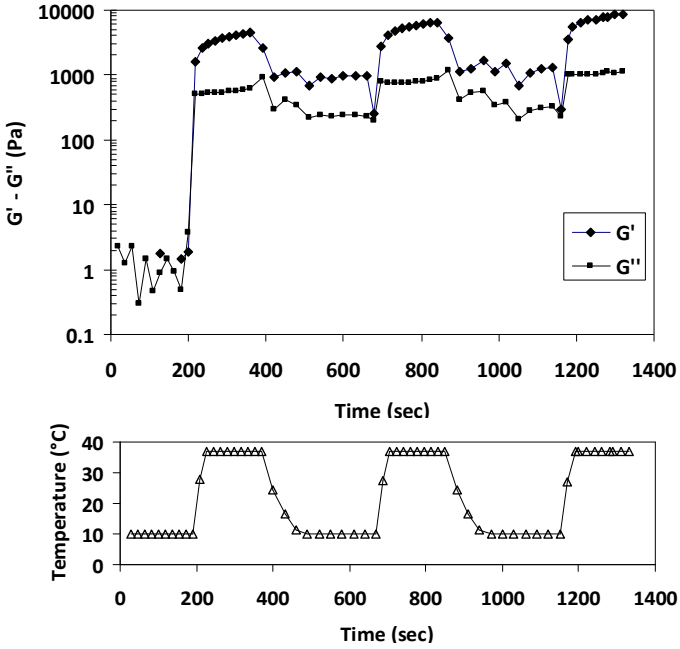

Figure 3.18: Temperature driven Sol-Gel-Sol behaviour of suspensions composed of 33%$_{w/v}$ PCL and 3%$_{w/v}$ polyPEGMA$_{246}$-EE. Although cooling the suspensions dropped G' and G'', full gelation reversibility i.e. a G'/G'' crossover was not observed over the time scale of the experiment.

Upon heating the polymer chains, adsorbed or free in solution, are precipitated on the particles surface. The observed hysteresis and the absence of a G'/G'' crossover on cooling could be a result of physical entanglements of the polymer chains (adsorbed to the particles surface) following their strong hydrophobic interactions that occurred on heating to above the LCST (Duijneveldt, 2010), which makes the re-dispersion process on cooling slower. A similar observation has been reported for aqueous Fe_2O_3 dispersions stabilised with thermoresponsive poly(vinyl ether) block copolymers in a study by De Laat *et al* (De Laat and Schoo, 1997). Following observation by hot-stage microscopy, they explained the unobserved gelation reversibility by the slower particles re-dispersion process compared to flocculation.

The weak physical nature of polymer entanglements remaining after cooling was confirmed by an experiment involving the application of a small brief shear force ($50s^{-1}$ for 12 sec) on suspensions cooled to below the LCST. As shown in figures 3.19 and 3.20, G' and G'' dropped to their initial magnitudes post-shear, in both the temperature ramp and the multiple heating-cooling cycles tests, as the shear helped disentangle the polyPEGMA$_{246}$-EE chains. On the contrary, the application of the same shear force to the suspension in its "gelled state", i.e. above the LCST, lead to an increase in the magnitudes of G' and G'' (figure 3.20-B).
Hence polymer chain entanglements remaining below the LCST, are weak and totally different from their strong hydrophobic interactions above the LCST.

Taken together, the temperature driven gelation of the PCL/polyPEGMA$_{246}$-EE suspensions is reversible, although this could be masked by polymer chain entanglement that remains after cooling, necessitating a small shear force to disrupt it. Full gelation reversibility was easily and rapidly observed on cooling in the tube inversion assay (figure 3.14A), because the gravity shear forces helped disentangle the polymer chains.

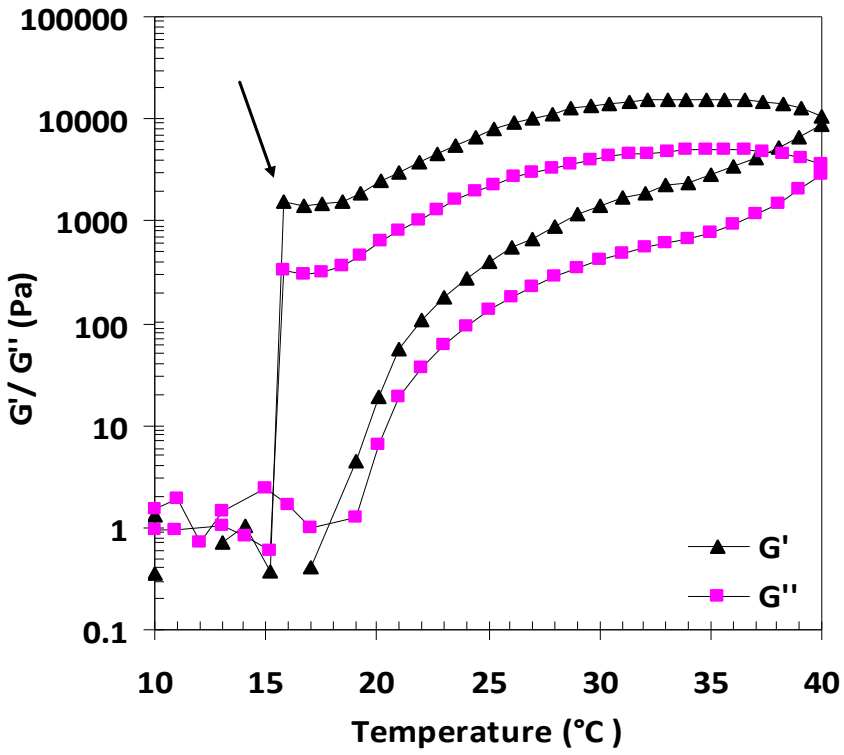

Figure 3.19: **Variation of G'/G'' with temperature for a suspension containing PCL (40%$_{w/v}$) /polyPEGMA$_{246}$-EE (2%$_{w/v}$).**

Cooling the suspensions to below the LCST dropped the G' and G'' moduli but a G'/G'' cross over was only observed following the application of a brief shear (50s^{-1} for 12 seconds) indicated by the arrow.

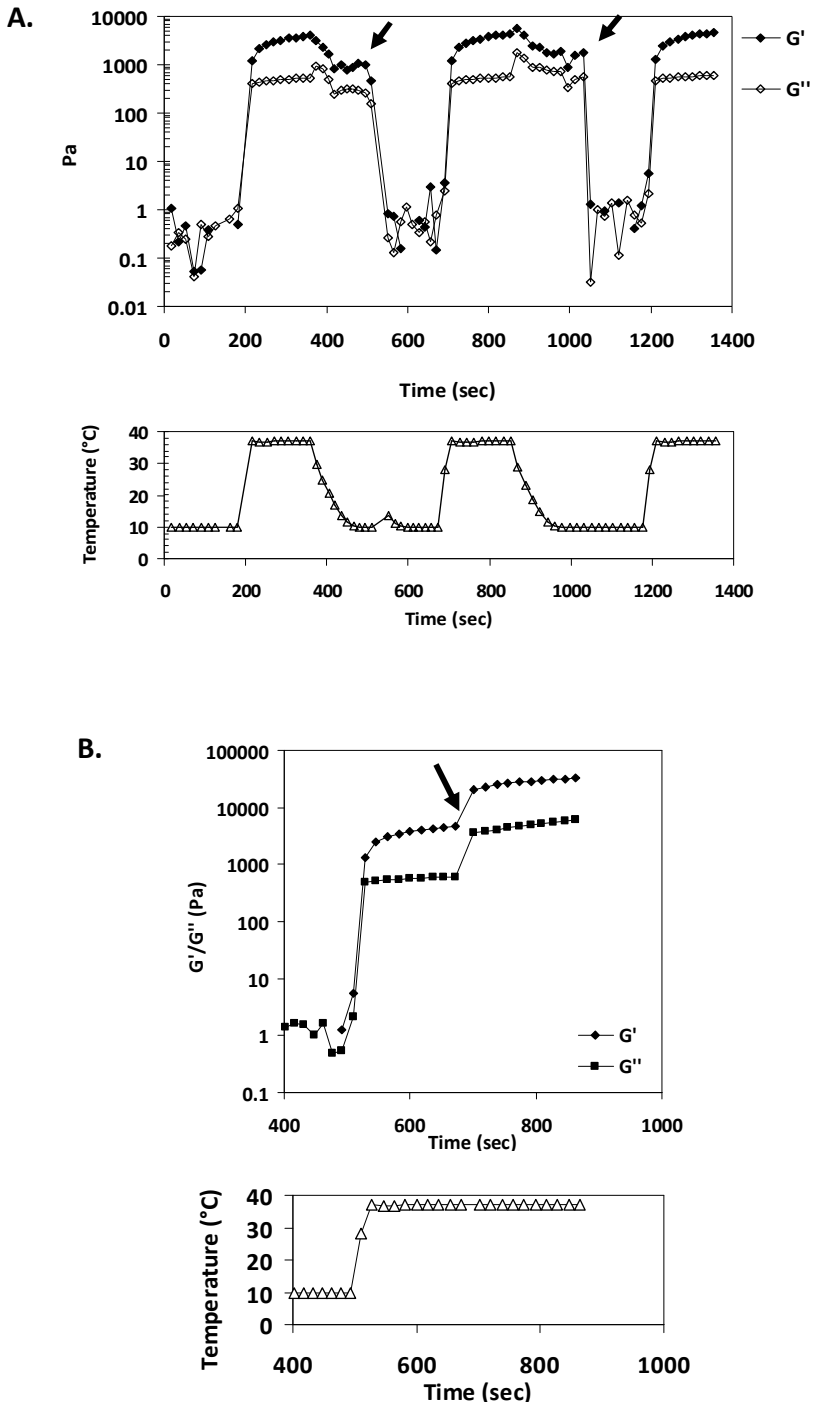

Figure 3.20: Multiple heating-cooling cycles of a suspension containing 33%$_{w/v}$ PCL particles and 3%$_{w/v}$ polyPEGMA$_{246}$-EE. The arrows indicate the application of shear (shear rate, $\dot{\gamma}$=50s^{-1}) for 12 seconds below the LCST **(A)** and above the LCST **(B).**

3.4.8 Characterisation of the mechanical properties of the particle gels

Frequency sweeps are oscillatory tests performed at variable frequencies, keeping the deformation amplitude and temperature constant to generate a mechanical spectrum. These aim to investigate the time-dependent shear behaviour since the frequency is the inverse of time.

In practical systems, G' values recorded at an angular frequency ω= 0.1 rad/sec (or even ω= 0.01 rad/sec) are used to evaluate long term stability at rest, where the G' value at this low frequency is taken as the gel strength at rest (Mezger, 2006).

Typical mechanical spectra for particle gels of different compositions performed at 37°C are shown in figure 3.21. G' was mostly independent of frequency and much larger than G'' indicating the presence of a gel structure with space spanning networks of particles (figure 3.21). Towards the lower frequencies, G' started to show a slight slope and a G'/G'' cross over occurred at very low frequencies (<0.1rad.sec). Hence, the particle gels show a flexible structure that tends to relax at longer timescales. This is expected for systems that form through physical crosslinks, such as polymer gels, which behave as solids (gels) at high frequencies with relaxation at low frequencies.

This relaxation gives the gels flexibility that would be beneficial should these gels be used for cell culture (see chapter 5).

The tan delta values for the particle gels were ≥ 0.1. Such tan delta values indicate a flexible and deformable gel structure that helps resist potential densification or syneresis with time (Mezger, 2006).

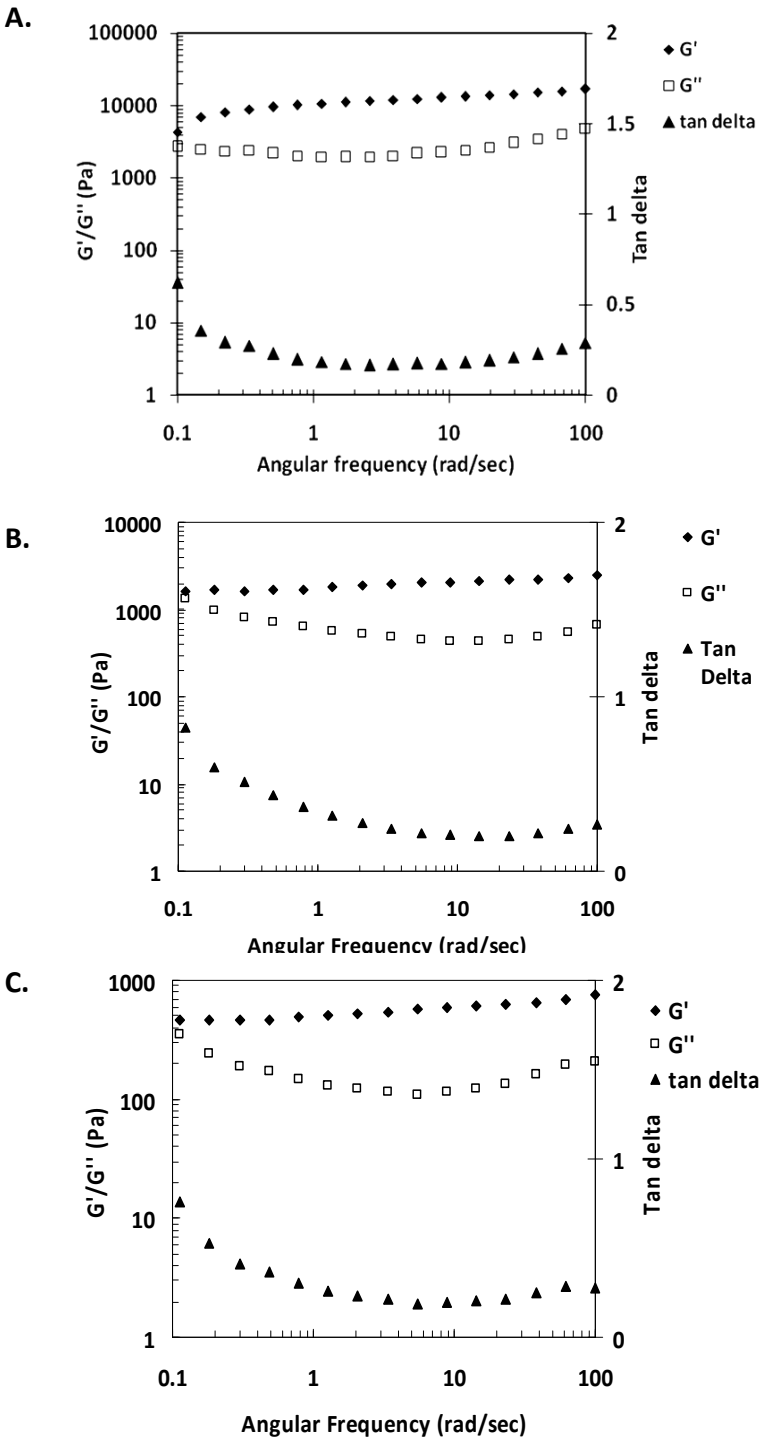

Figure 3.21: The dynamic moduli (G' and G'') and tan delta (G'/G'') plotted versus angular frequency (ω) of sample particle gels A. PCL (40%$_{w/v}$) and 2%$_{w/v}$ polyPEGMA$_{246}$-EE and **B.** PCL (33%$_{w/v}$) and 3%$_{w/v}$ polyPEGMA$_{246}$-EE **C.** PCL (25%$_{w/v}$) and 3%$_{w/v}$ polyPEGMA$_{246}$-EE. All measurements were taken in the linear viscoelastic region.

3.4.9 Factors affecting the mechanical properties of PCL/polyPEGMA$_{246}$-EE particle gels

3.4.9.A The effect of the particle cohesiveness on the gels elasticity

The frequency spectra of the elastic (G') and viscous (G") moduli for the suspensions were obtained at various temperatures. Figure 3.22 shows the dependence of G' on frequency for PCL/polyPEGMA$_{246}$-EE suspensions at two different compositions.

For the sample suspensions studied, below the LCST, G' was strongly dependent on frequency indicating a sol state. G' became independent of temperature at 25°C and above, signifying gel formation, with higher G' magnitudes being detected at higher temperatures across the whole frequency range.

Since dynamic measurements do not disrupt microstructure, the dynamic moduli, measured as a function of frequency, are a direct reflection of the interparticle forces (Tadros, 1996). Particle gel elasticity depends on how strong the particles interconnections are (Fraylich et al., 2009). Therefore, the increase in G' with temperature indicates that inter-particle attraction also increases with temperature. Increased dehydration of the adsorbed polyPEGMA$_{246}$-EE layers with increasing temperatures resulted in stronger hydrophobic interactions, and so interparticle associations.

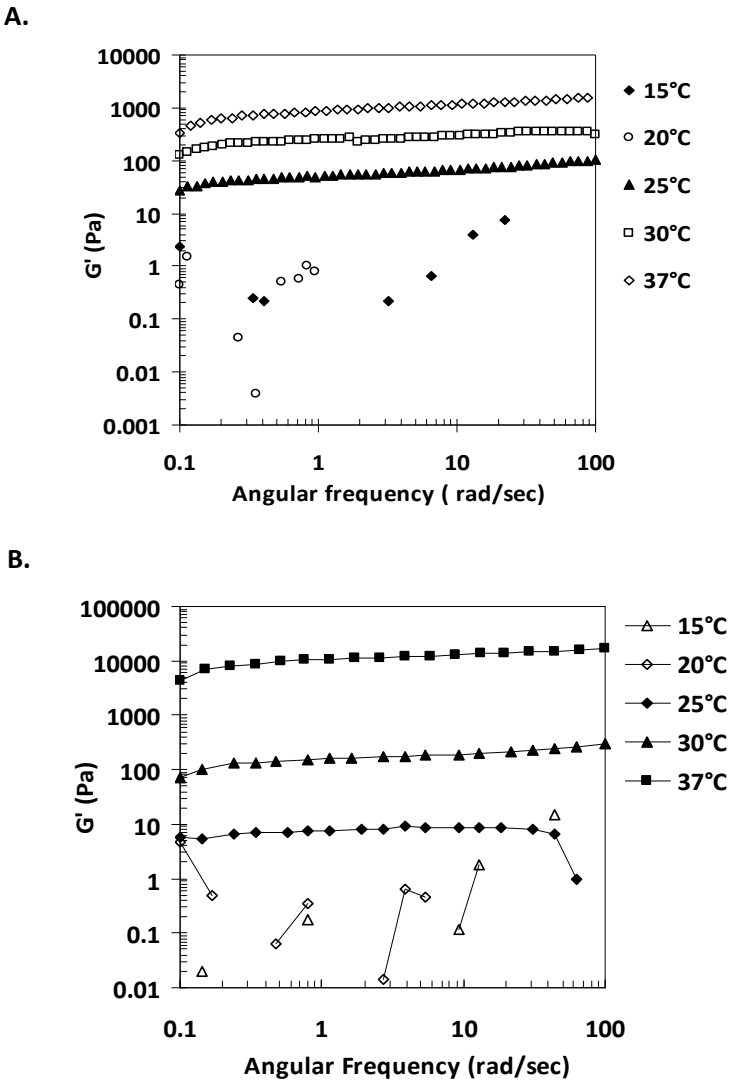

Figure 3. 22: The dynamic elastic modulus (G') of sample particle gels containing (A) 25%$_{w/v}$ PCL (B) 40%$_{w/v}$ PCL, and 2%$_{w/v}$ polyPEGMA$_{246}$-EE measured at different temperatures, and plotted versus angular frequency (ω).

3.4.9.B The effect of the number of elastically effective chains on the particle gels elasticity

Irrespective of thermoresponsive polymer concentration, increasing the PCL concentration yielded more elastic gels (figure 3.23), with trend dependence of G' on solids concentration, a feature widely reported for particle gels (Yanez et al., 1999). The increase of G' with particle volume fraction has been explained in different studies based on different models of the gel microstructure.

According to the fractal model, the particle networks consist of close packed fractal flocs (Yanez et al., 1999), and as a result mechanical properties (G') are expected to have a power law dependence on particle volume fraction:

$$G' = G_0 \phi^p$$

with ϕ being the volume fraction of the particles and G_0 and p are constants for a particular dispersion (Chen and Russel, 1991) and the power law exponent p being a function of the gel's fractal dimension. According to this model there is no lower threshold for the onset of elasticity i.e. $\phi_g = 0$.

Various studies , however, have shown the existence of a well defined critical volume fraction in practice, $\phi_g > 0$, because of disturbances by flow or sedimentation (Van Vliet and Lyklema, 2005). This led to another model based on percolation concepts to describe the mechanical properties of particle gels (Yanez et al., 1999). Percolation of clusters allows stress to be transmitted through the network and, as a result, is a necessary condition for measurable elasticity in low volume fraction, flocculated systems. Therefore, a threshold volume fraction ϕ_g representing the minimum volume fraction is necessary for a sample to form an infinite cluster, and this is used to describe the relative distance from the gel point. Percolation models predict the elastic modulus (G') to scale in the form:

$$G' = G_0 (\phi - \phi_g)^s$$

where the exponent, s, relates to the microstructure of the network. The particle gels in this study, appear to follow this trend, since a minimum particles concentration was required for gelation to be observed.

Particle gels elasticity was also influenced by the concentration of polyPEGMA$_{246}$-EE. Increasing the concentration of the responsive polymer from 0.1 to 1 %$_{w/v}$ led to an order of magnitude increase in G'. This was likely due to the extent of surface coverage by the responsive polymer with higher amounts of polyPEGMA$_{246}$-EE being required to ''glue'' the particles and increase the elastic modulus.

These rheological measurements correlate well to the tube inversion experiments used to construct the phase diagram shown in figure 3.14.

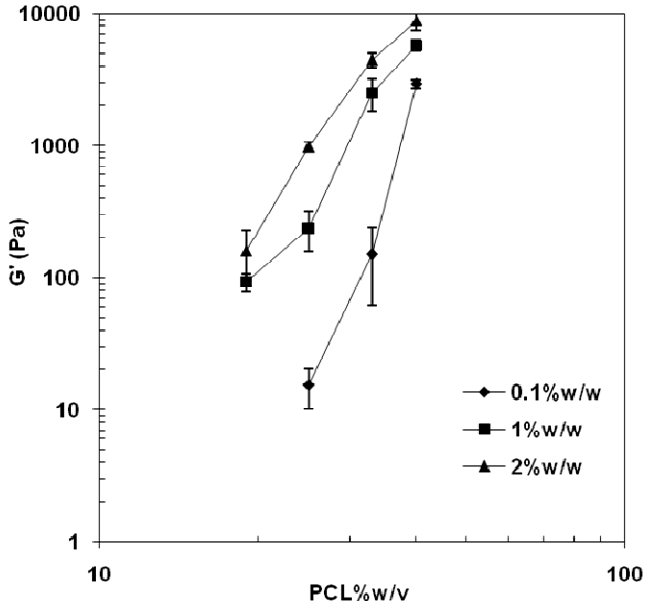

Figure 3.23: Elasticity of PCL/polyPEGMA$_{246}$-EE particle gels as a function of PCL particle concentration.

The elastic modulus (G') of particle gels containing 0.1, 1 or 2 %$_{w/v}$ polyPEGMA$_{246}$-EE, is plotted against their PCL particle concentration. G' was measured at 37°C at ω= 10 rad/s. Error bars represent SEM for measurements on N=3 different particle gel batches.

3.4.9.C The effect of particle concentration on the brittleness of PCL/polyPEGMA$_{246}$-EE particle gels

Particle gels containing higher concentrations of PCL particles were found to be more elastic but also slightly more brittle as shown in figure 3.24. In this figure, the strain at which the gel structure stated to rupture (the critical strain) was smaller at higher particle concentration. Higher numbers of elastic particle networks were present at higher concentrations. These networks of flocculated particles are not flexible and hence affected the overall flexibility of the gels (Van Vliet and Lyklema, 2005, Yanez et al., 1999).

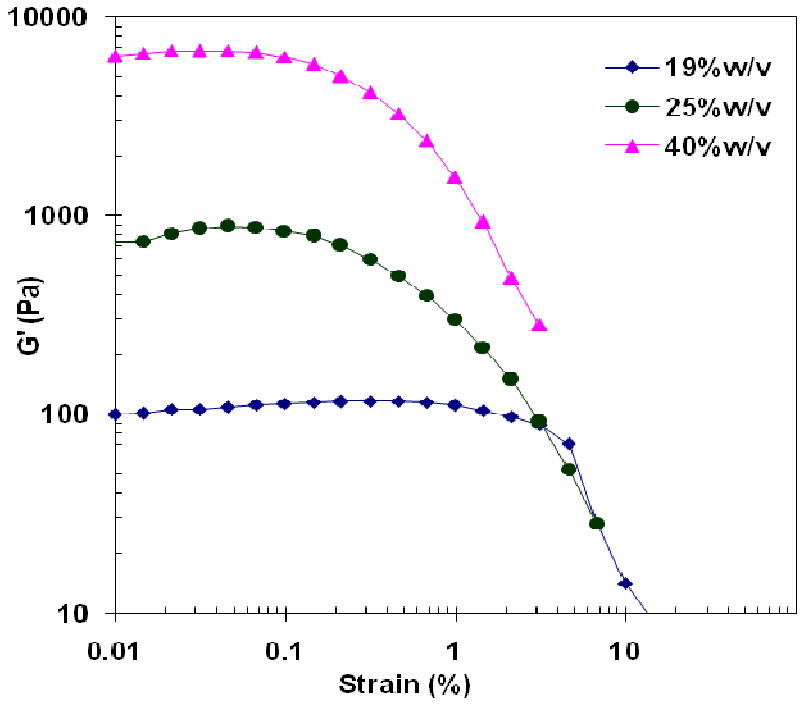

Figure 3.24: Effect of PCL particle concentration on the brittleness of PCL/polyPEGMA$_{246}$-EE particle gels.

All particle gels contained 2%$_{w/v}$ polyPEGMA$_{246}$-EE in complete medium. Note the narrower LVE region for the gels at higher concentration of PCL.

3.4.9.D The effect of thermoresponsive polymer on the thermogelling properties of the PCL particle gels

As shown in figure 3.25, by using a thermoresponsive polymer with a different LCST, the temperature at which the suspension elasticity started to increase was altered. This finding confirms the gelation mechanism and offers a way of tuning the responsiveness of the gels.

In addition to modifying the gelation temperature, using the thermoresponsive polymer polyPEGMA$_{246}$-EE-co-PEGMA$_{475}$-ME, which has a higher LCST than polyPEGMA$_{246}$-EE, had a significant impact on the mechanical properties of the resulting PCL particle gels at 37°C.

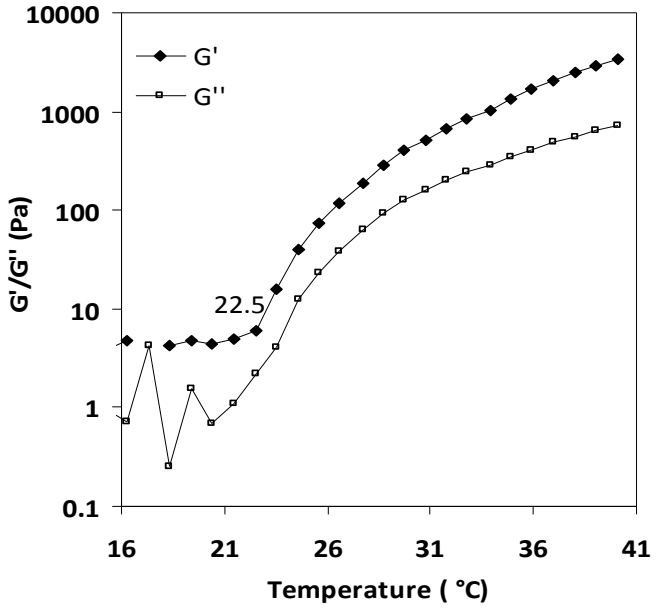

Figure 3.25: Variation of G'/G'' with temperature for a suspension containing PCL (40%$_{w/v}$) / polyPEGMA$_{246}$-EE-co-PEGMA$_{475}$-ME (2 %$_{w/v}$).

At 22.5°C the (LCST of poly PEGMA$_{246}$- EE -co-PEGMA$_{475}$- ME) marked increases in G' and G'' are recorded.

For equivalent composition ratios, gels containing polyPEGMA$_{246}$-EE were stronger (more elastic) than those containing polyPEGMA$_{246}$-EE-co-PEGMA$_{475}$-ME, over the whole range of compositions tested at **37°C** (figure 3.26). This is since the higher the temperature from the LCST the stronger the inter-particle attractions, as was shown in section 3.4.9.A. Therefore, at a given temperature, above the LCST, the inter-particle attractions are stronger in suspensions containing polyPEGMA$_{246}$-EE than in those containing polyPEGMA-EE$_{246}$-co-PEGMA$_{475}$ due to the 4°C difference in their respective LCSTs.

Phase diagrams for PCL particle gels containing 2%$_{w/v}$ polyPEGMA$_{246}$-EE or polyPEGMA$_{246}$-EE-co-PEGMA$_{475}$-ME are shown in figure 3.26. The minimum particle concentrations required to form space-filling gels at a given temperature were plotted.
Lower concentrations of PCL particles were required to obtain space-filling gels in suspensions containing polyPEGMA$_{246}$-EE compared to those containing polyPEGMA$_{246}$-EE-co-PEGMA$_{475}$-ME.

Also, for both polymers, the higher the temperature the lower the particle concentration required for gelation. The stronger inter-particle attractions at higher temperatures led to the formation of stronger particle networks, which although less dense, formed strong gels that sustained their weights in a tube inversion assay. However, when the inter-particle attraction is weaker at temperatures just above the LCST, more particles are required to form denser networks of sufficient elastic strength. This falls in agreement with numerous studies on thermo-aggregating suspensions (Shay et al., 2001, Yanez et al., 1999, Ramakrishnan and Zukoski, 2006)

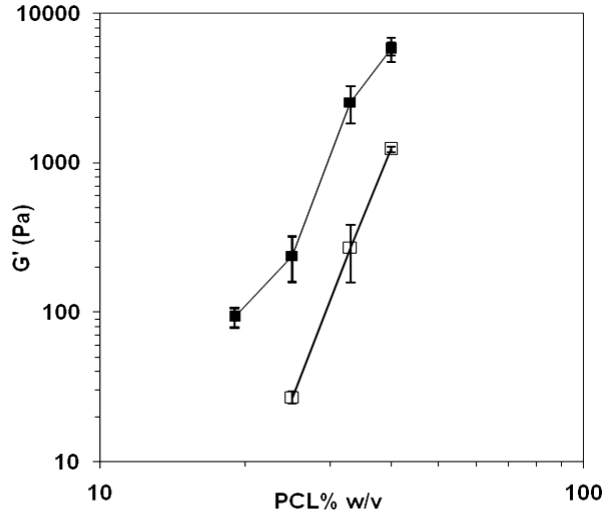

Figure 3.26: Variation of G' with PCL particle concentration for suspensions containing 1 $\%_{w/v}$ of polyPEGMA$_{246}$-EE (closed symbols) or polyPEGMA$_{246}$-EE-co-PEGMA$_{475}$-ME (open symbols).

Note the difference in G' values due to the 4°C difference in the LCSTs of the thermoresponsive polymers used. The plotted G' values were measured at 37°C at 10 rad/sec within the LVE region. The error bars represent SEM of measurements on N=3 different particle gel batches.

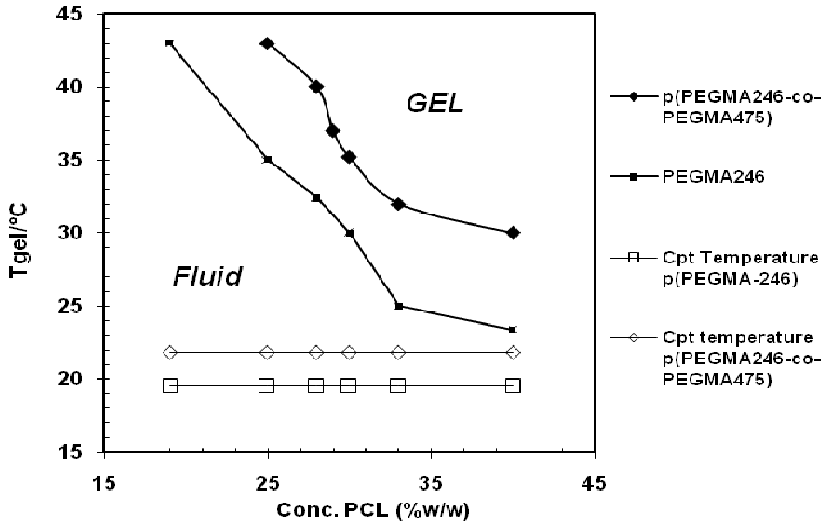

Figure 3.27: Fluid to gel phase diagrams for PCL suspensions containing 2$\%_{w/v}$ polyPEGMA$_{246}$-EE or polyPEGMA$_{246}$-EE-co-PEGMA$_{475}$-ME

Temperature is plotted against the minimum PCL particle concentration required for gelation at that specific temperature as determined using the tube inversion assay.

3.5 Discussion

The initial work to prepare thermoresponsive particulate suspensions involved the preparation of microparticles with surface entrapped thermoresponsive polymer (see the article attached at the back of the thesis). The method employed however led to the plasticisation of the microparticles and their irreversible aggregation on heating (Wang et al., 2009).

Here, the preparation of a new variant of thermoresponsive particulate suspensions is described. An adsorbing thermoresponsive polymer is used to coat suspended biodegradable particles and incur thermosensitivity on them, with the particles and polymer being prepared in two discrete stages. This methodology has several advantages over the previous system:

- The thermoresponsive polymer can, in principle, be adsorbed to any pre-existing micro- or nanoparticles as long as they have a relatively hydrophobic surface, without the need for surface entrapment or plasticisation.

- Also, importantly, the system described here allows the *reversible* assembly and disassembly of particles under a mild temperature stimulus.

Simple methods were employed for the preparation of the individual components needed in the responsive suspensions. This makes them easily scalable, especially that the used materials were of a low cost.

The single emulsion solvent evaporation method used for particle preparation yielded polydisperse particles. Although this did not seem to hinder the gelation, a tighter particle size distribution might be desirable to allow for a more accurate prediction of the material's

characteristics. This can be achieved through other particle preparation techniques such as spray drying (Vehring, 2008). The same holds true for the thermoresponsive polymer, although commonly used polymeric stabilisers are often polydisperse (Yanez et al., 1999, Napper, 1983b).

Suspensions containing PCL particles and polyPEGMA$_{246}$-EE were the main suspensions studied. Upon mixing the two components, polyPEGMA$_{246}$-EE adsorbs to the PCL particles surface. This leads to an entropic loss as the adsorbed polymer chains lose their spherical symmetry adopted when free in solution, but this is compensated for by the gain in entropy on displacing the solvent from the interface.

Below the LCST, effective steric stabilisation was incurred by polyPEGMA$_{246}$-EE. Various theories have been put forward to explain steric stability incurred on suspensions by polymers (Napper, 1983b, Van Duijneveldt, 2010). When two particles approach, the polymer layers at the surface will touch as soon as the separation becomes less than double the polymer layer thickness. The polymer layers can then either:

- Interpenetrate, doubling the local polymer concentration and the osmotic pressure forces solvent into the local region pushing the particles apart. Moreover, chain segments interpenetration is associated with a change in the free energy associated with the partial demixing of chain segments and solvent as the stabilising layers overlap. This contribution is repulsive in good solvency conditions but become attractive in poor solvency conditions.
- Compress, resulting in a loss of configurational freedom which is entropically unfavourable. This is referred to as the volume restriction or elastic interaction effect.

Both scenarios would result in steep repulsion between the particles and stabilise the suspension against aggregation.

However, on increasing the temperature to above the LCST, the polyPEGMA$_{246}$-EE chains shrunk into a globular conformation and their hydrophobic nature dominated the inter-particle interactions. The strong hydrophobic attractions between the collapsed layers drove the system into a gelled state.

The gels obtained were strong but brittle, and their elasticity and microstructure could be tuned with composition. In addition to being a strong function of temperature, gels elasticity was highly dependent on PCL particle concentration, and also the thermoresponsive properties of the steric stabiliser employed i.e. its LCST. The gels could be easily liquefied by dropping the temperature below the LCST followed by gentle shear required to disentangle the polymer chains.

In the developed suspensions, subtle control over the particle interaction potential was possible, which offered a way for a systematic investigation of the gelation properties. The combination of particle concentration, temperature, thermoresponsive polymer represents a powerful way to tune the gelation behaviour and the resulting properties of the particle gels in hand. Such properties of thermogelling suspensions have made them of a particular academic and industrial importance for probing the rheology of particle gels as a function of inter-particle bond strength, as reported in various published studies (Larson, 1999, Yanez et al., 1999).

In principle, it is be possible to obtain a thermogelling suspension of a variety of thermoresponsive polymers (of different LCSTs) and particles provided they are of a suitable size and sufficient hydrophobicity to allow for polymer adsorption. For example gels were obtained when 2µm polystyrene microparticles were used instead of the PCL particles (data not shown). Although using a thermoresponsive polymer with an LCST closer to physiological temperature would have been possible, it was important to select a gel with appropriate mechanical properties for cell culture and manipulation. For this reason, polyPEGMA$_{246}$-EE (which has a low LCST) was selected in order to obtain gels of a suitable elasticity to withstand the manipulations when applied as cell culture scaffolds at 37°C, as shall be discussed in more detail in chapter 5. To further illustrate this, when using the thermoresponsive polymer polyPEGMA$_{246}$-EE-co-PEGMA4$_{75}$-ME weaker gels were obtained, at a given temperature above the LCST, compared to polyPEGMA$_{246}$-EE. Hence the rest of thesis is solely concerned with use of the thermoresponsive polymer polyPEGMA$_{246}$-EE in the particle gels developed in this study.

Reversible temperature induced destabilisation of a sterically stabilised suspension has already been applied as a novel method to form ceramic green bodies (Bergström and Sjöström, 1999) and in various other industrial latexes. The suspensions described in this chapter are, however, novel with respect to their design, compositions, the temperature range over which they exhibit sensitivity and also their potential application as biomaterials, examples of which are discussed in more details in chapters 4 and 5.

3.6 Conclusions

Novel thermogelling suspensions were developed based on the incipient flocculation mechanism. Although suspensions exhibiting similar behaviour have been widely used for industrial applications, the current ones were prepared of biologically relevant components, and designed to show easily reversible thermal gelation at temperatures of biological relevance.

The suspensions gave strong but brittle gels on heating above the LCST of the steric stabiliser employed (polyPEGMA$_{246}$-EE). In addition to temperature, the gel elasticity and microstructure could be tuned by varying its composition; with PCL particle concentration being the most influential factor, as well as the thermoresponsive properties of the steric stabiliser employed i.e. its LCST.

These novel gels were investigated for use as cell culture scaffolds as discussed in the following chapters.

CHAPTER 4

The study and optimisation of the cytocompatibility of PCL/polyPEGMA$_{246}$-EE particle gels

4.1 Introduction

Biomaterials have found application in tissue engineering as scaffolds to support cells *in vitro* and *in vivo*, in addition to their use as space filling agents and carriers of bioactive molecules.

Different types of polymeric materials have been used as scaffolds including fibres (Ashammakhi et al., 2008, Sill and von Recum, 2008), hydrogels (Brandl et al., 2007, Drury and Mooney, 2003), foams (Day et al., 2004, Mooney et al., 1996) and various others. Particle gels, on the other hand, have not been applied in tissue engineering to any large extent, with a limited number of studies investigating their use as scaffolds (Wang et al., 2008).

PCL/polyPEGMA$_{246}$-EE thermoresponsive particle gels were developed to be ultimately used as cell scaffolds (see chapter3). Various requirements are needed in a candidate material to be suitable as tissue scaffold. These are generally: non-toxicity, biodegradability, porosity as well as mechanical integrity.

The constituting materials of thermoresponsive particle gels were carefully selected to suit their intended application. Polycaprolactone (PCL), the major constituent of these gels, is a biodegradable polymer considered to be non-toxic, and is approved by the FDA for use in

biomedical devices (Sinha et al., 2004), and has been widely used in tissue engineering scaffolds (Hoque et al., 2009, Hutmacher et al., 2001). The second component, the thermoresponsive polymer, is a PEG-based methacrylate polymer also reported to be biocompatible, being rich in PEG (Lutz et al., 2006, Lutz, 2008, Wischerhoff et al., 2008).

On detailed physical characterisation, the prepared PCL/polyPEGMA$_{246}$-EE thermoresponsive particle gels were found to be 60-75% porous, with tuneable elasticity ranging between 0.1-10 KPa (see chapter 3). Their microporosity and elasticity suggest that they would be relevant for soft tissue engineering applications (Discher et al., 2009).

Although, PCL/polyPEGMA$_{246}$-EE particle gels are likely to meet the non-toxicity and mechanical properties criteria, there are further requirements needed in scaffolds. For example, surface properties, namely chemistry and topography, are key determinants of the cellular response to biomaterial, as they have a major influence on cell adhesion.

Cell adhesion is central to biomaterial cytocompatibility, since it precedes and dictates other cell behaviours such as cell spreading, cell migration and often differentiated cell function (Hynes, 1999). Lack of adhesion can also lead to anoikis in anchorage dependent cells (Frisch and Screaton, 2001).

Generally, cell adhesion to a material is mediated by the proteins adsorbed to its surfaces from the surrounding environment (extracellular fluid *in vivo* or cell nutrient medium *in vitro*). Surface-adsorbed proteins provide binding ligands to the integrin receptors on the cell surface, initiating cell adhesion. When bound, these transmembrane receptors activate a cascade of intracellular signalling pathways, leading to changes in gene expression that affect most aspects of cell behaviour including differentiation, proliferation, the further expression of ECM proteins, activation of growth factors, and the maintenance of survival signals to prevent apoptosis

(Giancotti and Ruoslahti, 1999). A widely studied ligand for the integrin receptors is the RGD (arginine-glycine-aspartic acid) peptide sequence found in various proteins such as fibronectin, vitronectin, osteopontin, bone sialoproteins and the collagens, which are part of the natural extracellular matrix. Cell nutrient media used *in vitro* are normally supplemented with such proteins.

Protein adsorption to the surface of biomaterials occurs through non-covalent interactions such as hydrophobic, electrostatic, hydrogen bonding and van der Waals forces. The amount, type and conformation of bound proteins is mainly determined by the material's surface chemistry (Scotchford, 2009) and topography (Ranella et al., 2010). *In vivo*, this layer of adsorbed proteins translate the foreign surface into a biological signal which can either stimulate a positive cellular response favouring wound repair or tissue regeneration, or a negative cellular response leading to inflammation and rejection (Wilson et al., 2005).

As part of evaluating the PCL/polyPEGMA$_{246}$-EE particle gels for use as tissue engineering scaffolds, their cytocompatibility was initially assessed with respect to two main criteria: cytotoxicity and cell adhesion, followed by prolonged culture of cells on their surface while observing the adopted cellular morphology and cell proliferation pattern. A murine fibroblastic cell line was selected for these studies, and *in vitro* methods were used, which although might not give fully conclusive information on the response the material would induce *in vivo*, they still provide information on how well the cells respond to the material, and indications for its suitability to act as *in vitro* scaffold in the first place (Gurav, 2009), and its use *in vivo* eventually .

4.2 Aim and objectives

The aim of the work described in this chapter was "To assess and optimise the cellular response to PCL/pPEGMA$_{246}$-EE particle gels intended for use as cell scaffolds".

This was achieved through the following objectives:

1. The study of polyPEGMA$_{246}$-EE for any cytotoxicity.
2. The study of the cells ability to adhere to the individual components of the particle gels.
3. The optimisation of cell adhesion to the particle gels.
4. The culture of cells on top of pre-formed particle gels, and assessing their viability, proliferation and morphology over time.

4.3 Materials and Methods

Mouse fibroblasts 3T3 cell line, of either the NIH3T3 or Swiss Albino strains, were used in the following experiments. Cells were used within n+20 passages (from the initial passage at the cryopreservation).

4.3.1 The study of the effects of polyPEGMA$_{246}$-EE on cells

Two experiments were performed using two different metabolic assays to determine whether polyPEGMA$_{246}$-EE induced cell toxicity.

4.3.1.A Influence of polyPEGMA$_{246}$-EE on cell viability

NIH 3T3 cells (10^5) were seeded in 48 well plates and left to attach in a humidified incubator at 37°C for 3 hours, after which the media in each well was replaced by 1 ml of fresh media containing increasing amounts of polyPEGMA$_{246}$-EE (Mn=23.7KDa , PDI= 1.9): 0, 3, 5, 10, 15, 20 and 30mg respectively. PolyPEGMA$_{246}$-EE was synthesised by FRP as described in chapter 3 (section 3.3.1).

The cells were incubated at 37°C for 24 hours with the added polymer. After removing the added polymer by washing with PBS, cell morphology was examined using a Nikon Eclipse TS100 microscope (Nikon, UK). MTS cellular metabolic assay was then performed. MTS assay is based on the use of a *tetrazolium* salt that is cleaved into a coloured water-soluble *formazan product* by metabolically active cells. The rate at which the tetrazolium salt is reduced is an indicator for the extent of the cells metabolic activity which can be related to the number of viable cells using a standard curve. An increase in the detected mitochondrial activity over time can indicate cell proliferation, while a decrease could indicate cell death from the toxic effects of an added compound/agent, or as a result of suboptimal culture conditions (Barltrop et al., 1991).

The assay was carried out by adding 20µl of MTS reagent (Promega, UK) and 100µl of complete medium to each well, and incubating at 37°C for 60 minutes. Aliquots (100µl) of the test solution were transferred into a Costar-96 well plate (flat bottom, transparent), and their absorbance was measured at 492nm in an Infinite M200 Tecan plate reader.

The relative cell viability was calculated from the ratio of MTS readings from the test wells to those from the negative control wells (without polyPEGMA$_{246}$-EE).

4.3.1.B Influence of polyPEGMA$_{246}$-EE on cell proliferation

Alamar blue metabolic assay (Invitrogen, UK) was used to determine the effects of polyPEGMA$_{246}$-EE on cell viability and proliferation. The active ingredient of Alamar Blue® (resazurin) is a nontoxic, cell permeable compound that is blue in colour and virtually non-fluorescent. Upon entering cells, *resazurin* is reduced by the mitochondrial enzymes to *resorufin*, which is fluorescent. Viable cells continuously reduce resazurin to resorufin, thereby generating a quantitative measure of viability (Nociari et al., 1998).

Briefly, NIH 3T3 cells were seeded in 12 well plates (5000 cells/ well) and left to attach for 3 hours. polyPEGMA$_{246}$-EE was added to the wells at: 0, 5, 15 or 30 mg/well. The metabolic activity of the cells was measured using Alamar blue after 4, 24, 48 hours to assess the cell viability and proliferation. Alamar blue working solution (10%$_{v/v}$ stock solution in HBSS buffer) (500µl) was added to each well and incubated at 37°C for 90 minutes. Thereafter, 100µl X3 aliquots were transferred to a Costar-96-well plate (flat bottom, black), and the fluorescence was measured in MFX-300 Microplate reader at excitation 530nm and emission 590nm. Although Alamar Blue is not a terminal assay, separate samples were tested at each time point and the experiment was performed in triplicates.

4.3.2 Cell adhesion to polyPEGMA$_{246}$-EE

A total of 20mg of polyPEGMA$_{246}$-EE dissolved in 200µl of media was added to 48 well-plates and placed at 37°C for 15 minutes. This led to the precipitation of polyPEGMA$_{246}$-EE at the bottom of the wells. The supernatant was removed and the plates containing the precipitated polyPEGMA$_{246}$-EE were gently shaken, to form a homogenous layer of precipitated polyPEGMA$_{246}$-EE. NIH 3T3 cells (2.5 X10^3) pre-labelled with cell tracker orange were seeded on top of the polyPEGMA$_{246}$-EE layer. Nikon eclipse TS100 microscope with epi-fluorescence attachement was used for cell imaging at different time-points during culture.

4.3.3 Polycaprolactone particles surface treatment

PCL microparticles were subjected to NaOH/ethanol surface treatment, before they were used to prepare the suspensions, as was described in chapter 3, section 3.3.5.

4.3.4 Cell labelling with fluorescent dyes

3T3 cells were cultured as described in chapter 2. At 80% confluence the cells were incubated for 30 minutes with 10 ml of nutrient medium (complete medium) to which 50µg of cell-tracker® (orange or green, Molecular Probes-Invitrogen) dissolved in 10µl DMSO was added. The cells were then incubated with 10ml of fresh complete medium for 45 minutes. Single cells suspension was obtained by trypsinisation, and a cell count was determined using a haemocytometer (see chapter 2, see section 2.2.1).

4.3.5 Cell adhesion to the PCL films

PCL films were prepared by liquid sintering. The PCL particles were suspended in deionised water at 33%$_{w/v}$. The suspension (300µl) was placed in 48 well plates and incubated at 60°C for 1 hour for the water to evaporate leaving behind the melted PCL particles as a

continuous film. Some of the films were then subjected to NaOH surface treatment following the protocol given in 3.3.5. NIH 3T3 cells ($5X10^4$cells) (pre-labelled with the cell-tracker orange) were seeded on top of the films in 0.5 ml of media. Nikon eclipse TS100 fluorescence microscope was used for cell imaging at different time-points (days 1 and 5) during culture.

4.3.6 Sterilisation

PCL particles and films were sterilised through exposure to UV light at a wavelength of 280nm for 60 minutes, in a class II microbiological safety cabinet (Class II MST walker safety cabinets, Glossop, Derbyshire). PCL particles (500mg) were contained in glass vials and placed on a rotatory shaker during sterilisation to ensure maximal exposure of all particles to the UV light. PolyPEGMA$_{246}$-EE solutions were filter- sterilised using a Minisart® 0.2µm filter.

4.3.7 Cell culture on top of the particle gels

The particle gels used in the cell experiments consisted of 33%$_{w/v}$ PCL and 6.5%$_{w/v}$ polyPEGMA$_{246}$-EE prepared as described in chapter 3 (section 3.3.2). Typically, 200µl of the PCL/polyPEGMA$_{246}$-EE suspension (kept at 4°C) was added to each well in a 48 well-plate, and transformed into gels by incubating at 37°C for 5 minutes. NIH3T3 cells ($5x10^4$), labelled with cell tracker orange® or Swiss albino 3T3 cells labelled with cell tracker green, dispersed in 200µl of media were seeded on top of the gels and maintained in humidified incubator at 37°C. The cell nutrient medium (300µl complete medium) was changed every other day. Cell viability and proliferation was assessed using the Alamar blue assay (Invitrogen,UK) as described above in 4.1.3.B.

4.3.8 Cell imaging

Various labelling and imaging techniques were used to study the 3T3 cell morphology, spreading and proliferation following their culture on the PCL/polyPEGMA$_{246}$-EE particle gels.

4.3.8.A Scanning electron microscopy (SEM)

Cells cultured on particle gels were incubated in 5%$_{w/v}$ glutaraldehyde in PBS solution (TAAB laboratories, Reading-UK) overnight. The samples were then washed three times with PBS, each wash performed over 5 minutes. For further fixation and dehydration, the samples were incubated with 1%$_{v/v}$ osmium tetroxide solution (TAAB laboratories, England-UK) for 2 hours. The osmium solution was removed and the samples were left to air dry overnight. SEM imaging was as described in chapter 2 (section 2.2.3).

4.3.8.B Fluorescence microscopy

Cell tracker orange labelled cells cultured on top of the particle gels were imaged by fluorescence microscopy using a Nikon SMZ1500 microscope with Epi-fluorescence attachment linked to a digital camera (Nikon digital sight). Excitation wavelength for TRITC was 450-490nm, while that for FITC was 544/572nm.

4.3.8.C Cell cytoskeletal F-Actin staining

Cells cultured on tissue culture plastic (control) or on the PCL/polypEGMA$_{246}$-EE particle gels were fixed with 4%$_{w/v}$ paraformaldehyde (PFA, Sigma-Aldrich) for 15 minutes at room temperature in a laminar air-flow cabinet (externally vented class I MSC); then permealised with 0.1%$_{v/v}$ Triton-X 100 (Sigma, UK) for 10 minutes at room temperature. After washing with PBS, the cells were incubated with 1µg/ml TRITC-Phalloidin (P1951, Sigma-USA) in PBS for 1hour at room temperature to stain F-actin (fibrous actin polymerised in the form of a double helix). Following multiple washes with warmed PBS, the samples were mounted with SlowFade® Gold antifade reagent with DAPI (P36931, Invitrogen-UK). Cell Images were taken using the stereoscopic microscope Nikon SMZ1500 with Epi-fluorescence Attachment linked to a Nikon digital camera (Nikon digital sight).

4.3.9 Collagen I immunostaining

NIH3T3 cells cultured on top of the particle gels were rinsed with warm PBS and fixed with 3.7 $\%_{w/v}$ paraformaldehyde (PFA) in PBS for 30 minutes, followed by a wash with warm PBS for 5 minutes. The cells were then permealised using warm 0.1$\%_{w/v}$ triton-X 100 (Sigma, UK) for 30 minutes. Non specific binding sites were blocked by incubation in 4$\%_{v/v}$ normal goat serum (G9023, Sigma-UK) in PBS for 1 hour.

The primary antibody was rabbit polyclonal Collagen I antibody (ab292, Abcam) which reacts with most mammalian type I collagens. The cells were incubated in Collagen I primary antibody diluted in 1$\%_{w/v}$ BSA (in PBS, 1:200) for 2 hours at room temperature, followed by three washes with PBS supplemented with 0.05$\%_{w/v}$ Tween-20 (10 minutes each). The secondary antibody, rabbit IgG-FITC antibody produced in goat (T6778, Sigma-UK), diluted in 1$\%_{w/v}$ bovine serum albumin (BSA) in PBS (1:200) was then added for 2 hours, followed by three washes with PBS supplemented with 0.05$\%_{w/v}$ Tween-20 (10 minutes each). The cells were mounted in SlowFade® Gold antifade reagent with 4',6-diamidino-2-phenylindole nuclear stain DAPI (P36931, Invitrogen-UK) to preserve the fluorescence and stain the cell nuclei. Nikon SMZ1500 stereoscopic microscope with Epi-fluorescence attachment linked to a Nikon digital camera (Nikon digital sight), was used for cell and collagen-I imaging.

4.4 Results

The thermoresponsive polymer, polyPEGMA$_{246}$-EE, was combined with PCL microparticles to prepare gels with temperature responsive behaviour, for tissue engineering related applications.

This chapter comprises the initial investigations of the ability of these particle gels to promote positive cellular responses with regards to cell adhesion, viability and proliferation. Murine 3T3 fibroblasts were used as a model cell line being easily cultivated, adhesion dependent, and widely used as a model cell in biocompatibility studies of polymeric scaffolds (Bashura et al., 2006, Zhua et al., 2006).

4.4.1 Effects of polyPEGMA$_{246}$-EE on cell viability and proliferation

CellTiter 96 assay (MTS) was used to measure the cellular mitochondrial REDOX activity, as an indicator for cell viability, since only viable cells are metabolically active

The percentage of viable NIH3T3 cells relative to the control group, when incubated with increasing amounts of polyPEGMA$_{246}$-EE is shown in figure 4.1.

No significant toxicity was seen with up to 20mg of added polyPEGMA$_{246}$-EE. Even with 30mg, the number of viable cells relative to the control, was 80% after 24 hours. Optical microscope images of the cells, following 24 hours incubation, showed that they maintained their normal morphology as observed for the control group (figure 4.2).

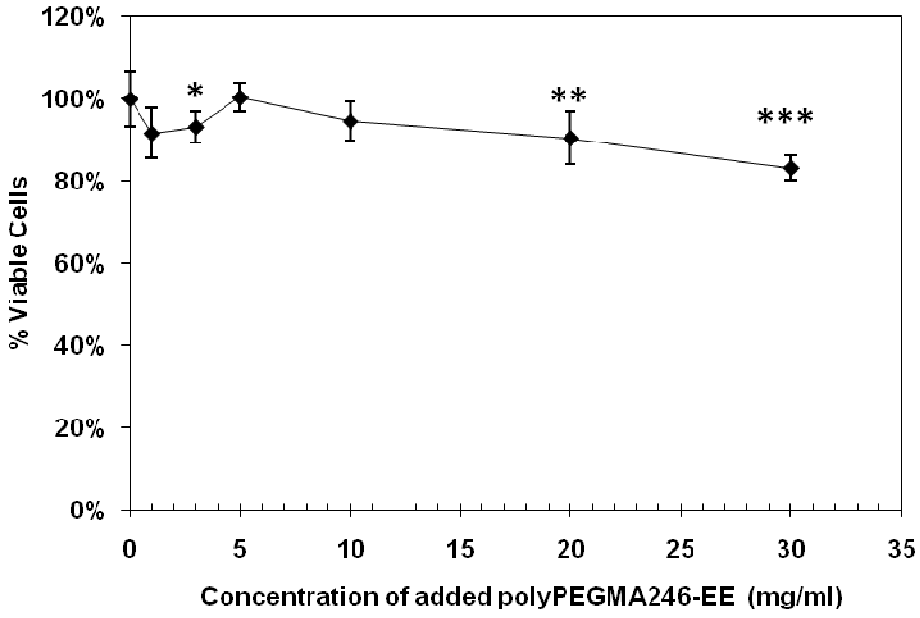

Figure 4.1: The percentage of viable NIH 3T3 cells, relative to the control, after 24 hours incubation with increasing quantities of polyPEGMA$_{246}$-EE.

The percentage of viable cells was calculated from the ratio of MTS readings of the test cells to that of the control (cells with no added polyPEGMA$_{246}$-EE).). Error bars representing standard deviation for N=3 samples. Statistical significance was calculated using the statistical test ANOVA with Dunnet multiple comparison post-test between the test and the control (no polyPEGMA$_{246}$-EE added) is denoted as * ($p < 0.05$), ** ($p<0.01$) and *** ($p < 0.001$).

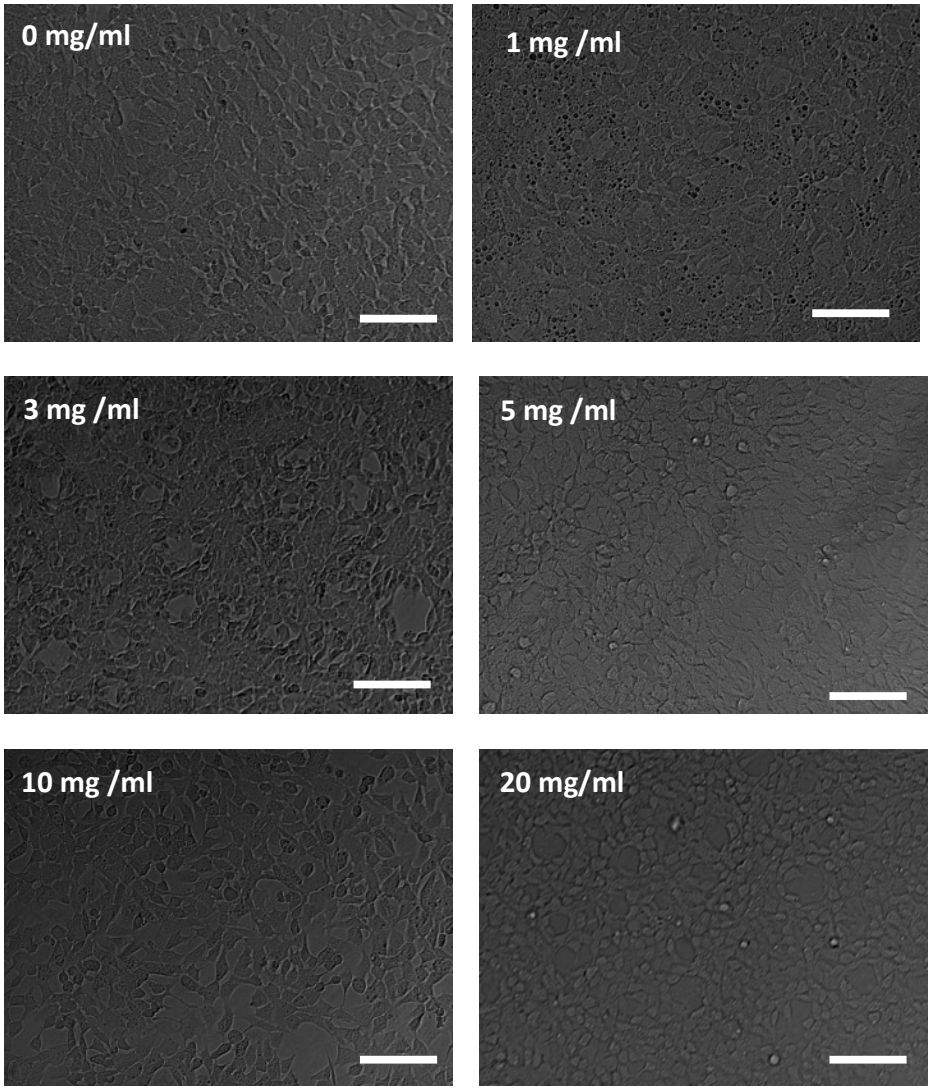

Figure 4.2: Representative light microscopy images illustrating NIH 3T3 cell morphology following 24-hours incubation with increasing concentrations of polyPEGMA$_{246}$-EE (indicated on the left corner of each picture). Scale bar represents 100µm.

These results were confirmed with a second experiment using a different metabolic assay, Alamar blue, to probe the effects of polyPEGMA$_{246}$-EE on the cells ability to proliferate.

As shown in figure 4.3, Alamar blue reduction by the cells incubated with 15mg and 30mg polyPEGMA$_{246}$-EE for 4 hours was smaller compared to the control. This can be indicative of polyPEGMA$_{246}$-EE inducing cell toxicity and thus reducing the number of viable cells. No statistically significant difference was found between the cells incubated with smaller amounts of polyPEGMA$_{246}$-EE and the control, which suggested a concentration dependent impact of polyPEGMA$_{246}$-EE on the cells.

Nevertheless, the cells incubated with polyPEGMA$_{246}$-EE at all the concentrations used were able to proliferate normally, with no further expansion of the difference in Alamar blue reduction between the control and the test wells over the 48 hours. This suggested that no further toxicity took place, after that observed 4 hours following the addition of polyPEGMA$_{246}$-EE.

Therefore, the drop in cell viability with higher amounts of added polyPEGMA$_{246}$-EE was likely to be due to physical effects (osmotic damage) when polyPEGMA$_{246}$-EE precipitated out of solution on addition to the wells maintained at 37°C (higher than its LCST).

Taken together, it appears that polyPEGMA$_{246}$-EE up to 15mg had negligible toxicity on the cells. This finding was taken into consideration when deciding the amount of polyPEGMA$_{246}$-EE to be included in the particle gels to be used for cell culture (see 4.4.2).

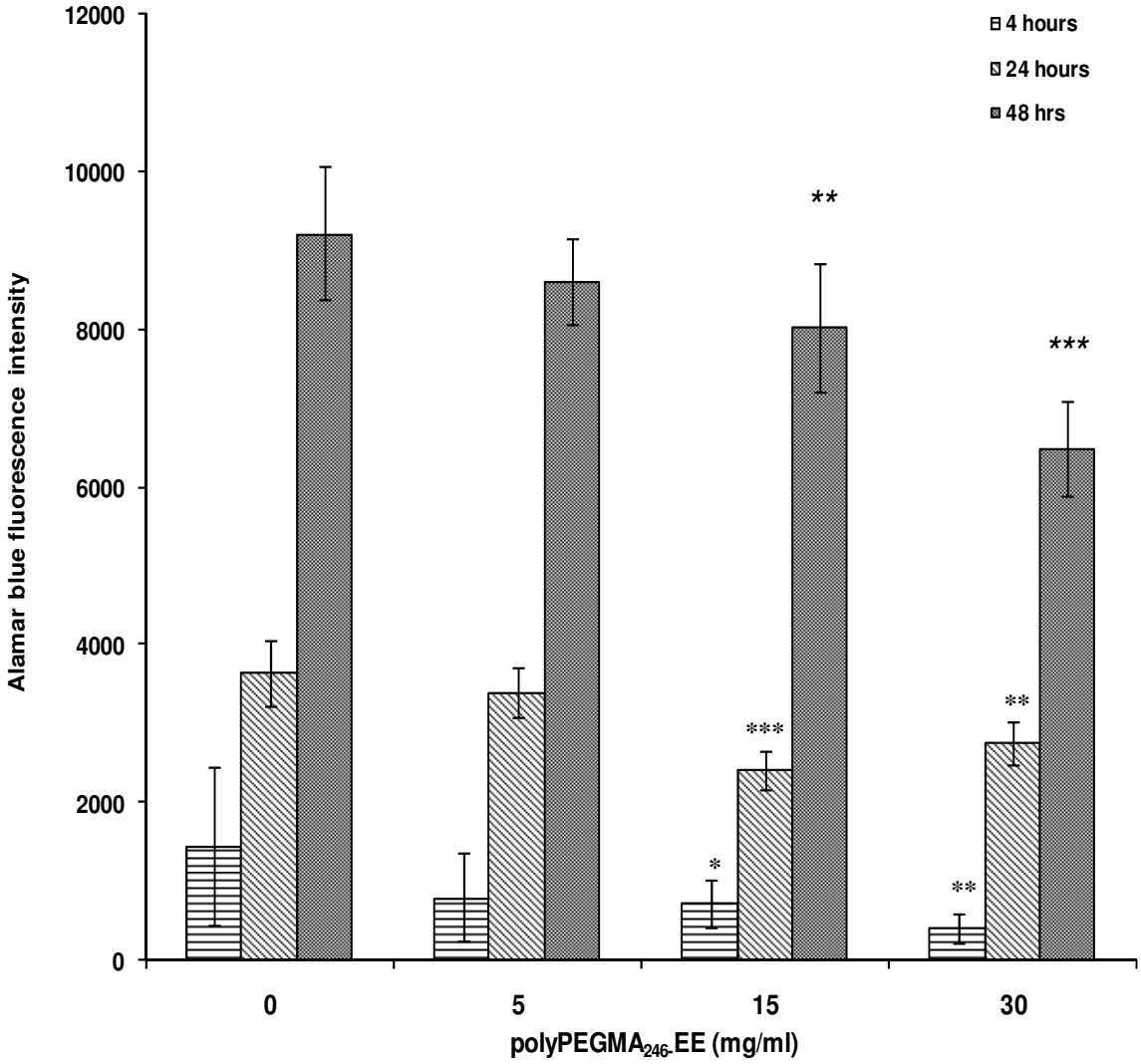

Figure 4.3: Effect of polyPEGMA$_{246}$-EE on the viability and proliferation of NIH 3T3 fibroblasts.
Alamar blue fluorescence units are plotted against the amount of polyPEGMA$_{246}$-EE added to the cells. Error bars represent SD from N=3 different samples for each time point. Note the increase in Alamar blue reduction with time indicating cell proliferation. A t-test was performed between the control (cells without polyPGEMA$_{246}$-EE) and the test samples at each time point, and statistical significance was denoted as: * $p<0.05$, ** $p<0.01$, ***$p<0.001$).

4.4.2 Cell adhesion to the components of the particle gels

As part of assessing the use of PCL/polyPEGMA$_{246}$-EE particle gels as tissue engineering scaffolds, the ability of cells to adhere to their two main constituents was studied.

4.4.2.A Cell adhesion to polyPEGMA$_{246}$-EE

Fluorescently labelled NIH3T3 cells were seeded on thin films of temperature-precipitated polyPEGMA$_{246}$-EE. After 24 hours, the cells did not adhere nor spread but were rounded and clustered (figure 4.4). After 5 days similar cell clusters were still observed with no difference in size, which suggested that the cells did not proliferate. These results indicate that polyPEGMA$_{246}$-EE does not promote cell adhesion. This would be expected from poly(ethylene glycol) (PEG) rich structures and falls in agreement with previous reports on poly PEG-methacrylates (Ma et al., 2005, Ma et al., 2004b).

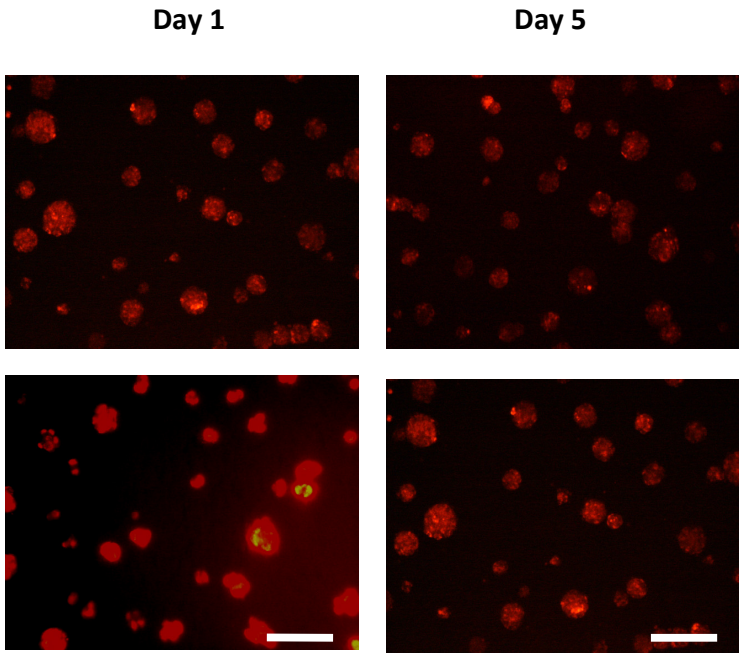

Figure 4.4: Representative fluorescence microscopy images of NIH3T3 Cells seeded on a layer of polyPEGMA$_{246}$-EE after 1 and 5 days of culture. Scale bar 200µm

4.4.2.B Cell adhesive properties of polycaprolactone microparticles

With regards to cell adhesion to PCL/polyPEGMA$_{246}$-EE particle gels, it was important that an optimum platform for cell adhesion was to be provided by PCL microparticles, to compensate for the minimal cell-adhesion to polyPEGMA$_{246}$-EE.

- **Cell adhesion to PCL particle films**

The thermoresponsive particle gels consisted mainly of PCL particles. Hence, studying cell adhesion to these particles was key to the evaluation of the particle gels as cell scaffolds.
In order to study the ability of cells to adhere to PCL particles, these were melted into continuous films, on which NIH 3T3 cells were seeded and incubated at 37 °C. This was done to facilitate the experimental setup and analysis.

As shown in figure 4.5, the cells did not adhere nor spread on the films but were clustered in large aggregates, on days 1, 2 and 5 of culture. These results suggest that PCL microparticles did not promote cell adhesion.

In an attempt to improve cell adhesion, and since cell adhesion to biomaterials is mainly protein-mediated (Wilson et al., 2005), the PCL particle films were soaked in pure foetal bovine serum (rich in fibronectin and other proteins), or pure fibronectin (1μg/ml) solution overnight prior to cell seeding. No improvement in cell adhesion was observed (data not shown), indicating that the surface properties of the PCL particle films did not promote protein adsorption in a way that is recognisable to the cells. This can be attributed to the poor hydrophilicity of polycaprolactone and the lack of natural recognition sites, or surface chemical groups that could participate in protein binding.

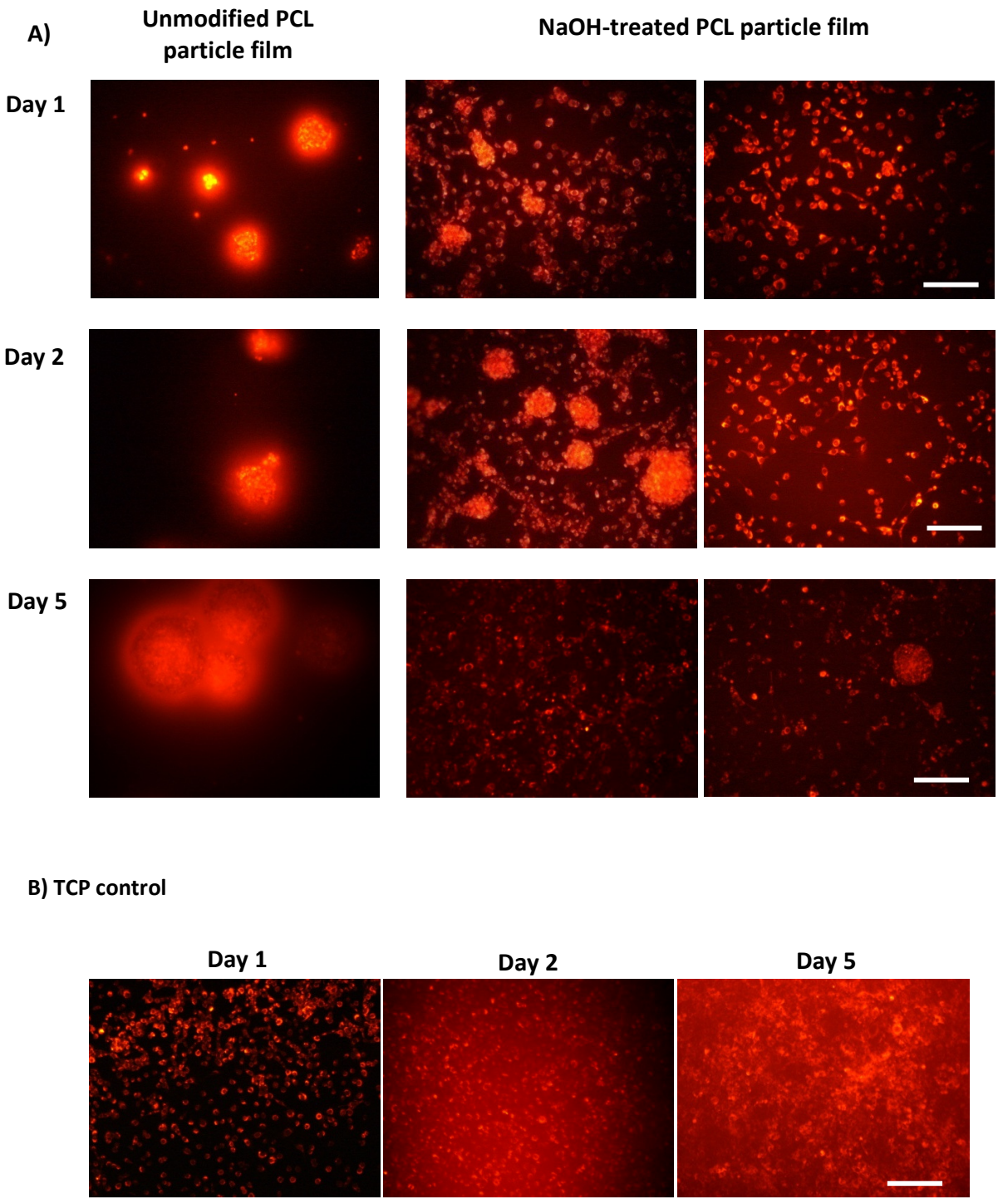

Figure 4.5: Effect of NaOH-surface treatment on cell adhesion to PCL particles films.

Representative fluorescence microscopy Images are for NIH 3T3 cells (labelled with cell-tracker orange) on **A.** PCL films unmodified or after NaOH treatment **B.** on tissue culture treated plastic.

Various surface modification strategies have been employed to improve the surface properties of polyester scaffolds and therefore their cytocompatibility (Jiao and Cui, 2007). These include:

- Morphological modifications which alter the surface porosity, roughness and structure of the material.
- Chemical modifications that alter the surface composition using different methods. These include plasma polymerisation of functional polymers to promote proteins and cell attachment (Shen et al., 2007, Lopez-Perez et al., 2010) and plasma treatment with reactive gases to create new functional groups on the polymer surface.

  Wet chemical methods have been reported to generate hydrophilic and rough surfaces that promote cell adhesion. Base hydrolysis, in particular, was found to significantly improve cell adhesion to polyesters (Serrano et al., 2005, Gao et al., 1998, Park et al., 2005, Pattison et al., 2005). Other reported chemical/biological modifications include grafting or immobilising bio-molecules such as RGD and poly-L-lysine which promote cell adhesion to polymer surfaces (Zhu et al., 2002, Quirk et al., 2001).

- **Cell adhesion to NaOH/ethanol treated PCL particle films**

The modification of PCL particles surface properties was required to improve cell adhesion. Out of the possible surface modification techniques listed above, alkaline hydrolysis was selected, being simple to perform as not requiring complex equipments or chemical reactions.

Following NaOH treatment of PCL particle films, significant improvement in cell distribution and spreading was observed (figure 4.5). One day after seeding, the cells were distributed all over the PCL particle film's surface, with the majority showing good spreading. Some cells were clumped in small groups, which has been previously observed for fibroblasts cultured on PCL films (Serrano et al., 2004), and also for keratinocytes on PCL films where these clumps of cells were described

as cellular differentiation zones (Khor et al., 2002). By day 5 of culture, there were visibly more cells present on the films surface, suggesting cell proliferation had taken place.

All the PCL particles used subsequently in the gels throughout the thesis were NaOH/Ethanol treated (unless stated otherwise).

4.4.3 The culture of NIH 3T3 cells on the surface of PCL/polyPEGMA$_{246}$-EE gels

Following the optimisation of the surface properties of PCL microparticles, PCL/polyPEGMA$_{246}$-EE particle gels were investigated for their ability to support cell adhesion and proliferation, by culturing cells on their surface.

The gels selected consisted of 33%$_{w/v}$ PCL particles and 6.5%$_{w/v}$ polyPEGMA$_{246}$-EE suspended in complete medium. At this composition, the gels had sufficient mechanical strength to sustain the manipulations during cell culture, while their total content of polyPEGMA$_{246}$-EE (13mg) was lower than the amount found to cause cell damage (see section 4.4.1 and figure 4.1).

4.4.3.A Characterisation of the particle gels surface

For any biomaterial, the surface structure in addition to composition, can influence cell adhesion and proliferation (Jiao and Cui, 2007).

Using SEM, the gels appeared to have a topographically featured surface from the random organisation of the particle networks, resulting in a surface with significant “micro-islands and micro-pores” of random distribution. In other words, the particle gels possessed a *“3D structured surface”* (figure 4.6).

Numerous studies reported on how the nano- and micro-structure of different surfaces influenced various aspects of cell behaviours such as cell adhesion, migration, morphology, proliferation, osteogenesis and others (Curtis and Dalby, 2009).

This was taken into consideration when studying the cellular response to the particle gels.

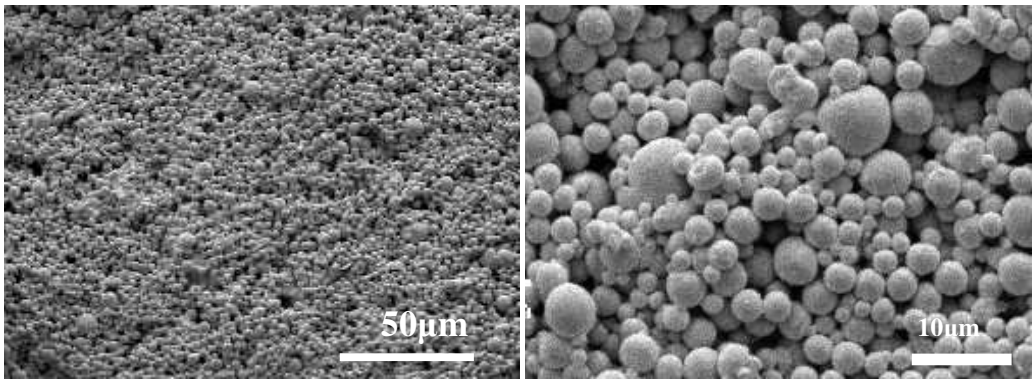

Figure 4. 6: Representative SEM images of PCL/polyPEGMA$_{246}$-EE particle gels surface. Note the non-planar nature of the surface with connected micro-islands and pores in between.

4.4.3.B Characterisation of cell adhesion and growth by fluorescence microscopy

The opacity of the particle gels limited the range of imaging techniques that could be used to visualise the cells. Labelling the cells with a fluorescent dye was therefore required to use fluorescence microscopy for this purpose.

NIH3T3 cells cultured on the particle gels are shown in figure 4.8. After 1 day of seeding, single cells adhered to the gel surface, but with little spreading. By day 5, the cells were well spread, and appeared to have proliferated in distinct cellular zones or islands. Note the improvement observed in cell distribution, spreading and growth on the gels constituting of *NaOH-treated* PCL particles (figure 4.8) compared to those constituting of *unmodified PCL* particles (figure 4.7).

This confirms that surface modification of PCL particles using NaOH/ethanol resulted in a significant improvement in the ability of cells to attach and spread on the PCL/polyPEGMA$_{246}$-EE particle gels. More well spread single cells were seen on the films (figure 4.5), while the cells on the surface of PCL/polyPEGMA$_{246}$-EE particle gels were mainly distributed in groups that became larger on longer culture. This could be attributed to the surface topography of the gels, in

addition to their content of polyPEGMA$_{246}$-EE, which was found to be non- promoting of cell adhesion, and could therefore have interfered with the extent of cell spreading and coverage of some parts of the gel surface.

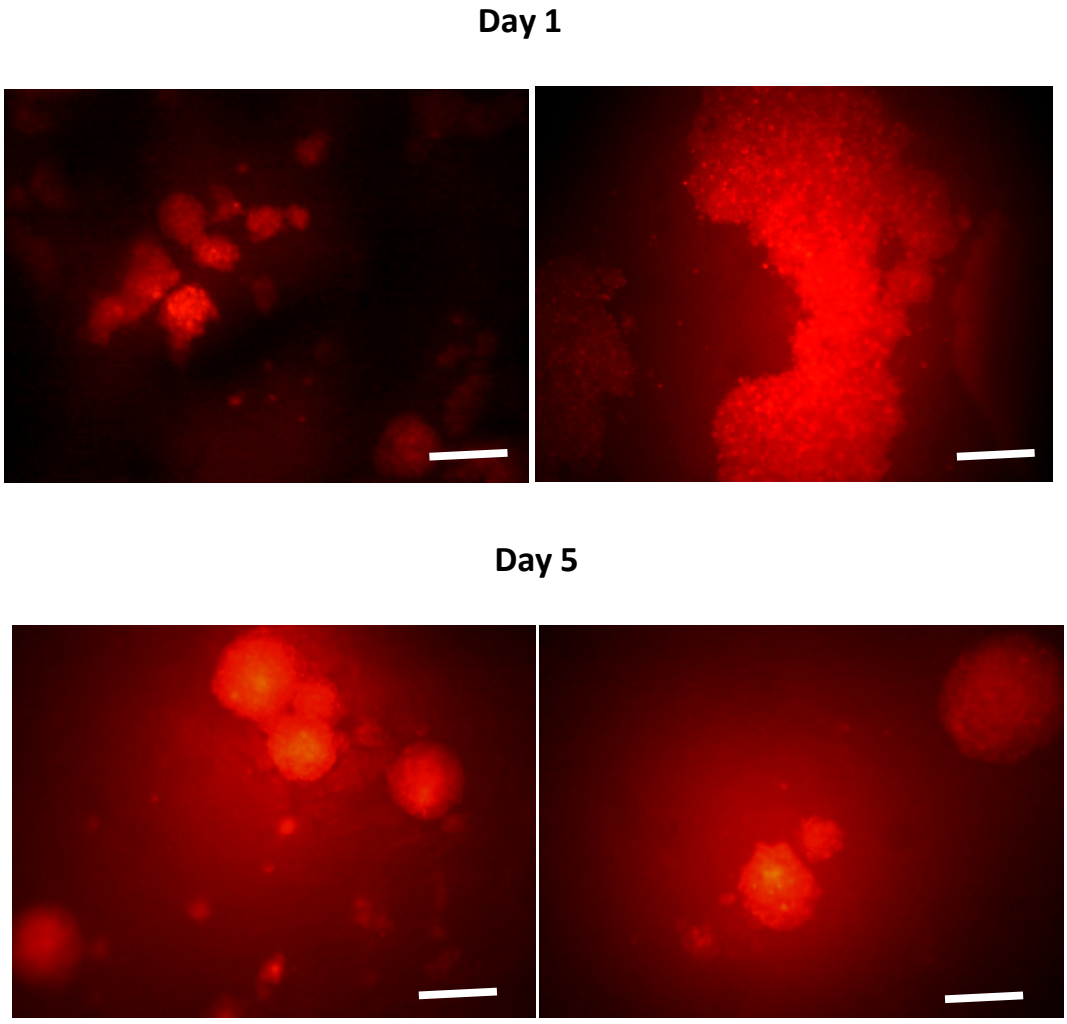

Figure 4.7: Representative fluorescence microscopy images of NIH3T3 cells cultured on the surface of PCL/polyPEGMA$_{246}$-EE particle gels made of unmodified PCL particles over 8 days.
The gels were made of 33%$_{w/v}$ unmodified (i.e. Not subjected to the NaOH treatment) PCL particles and 6.5%$_{w/v}$ polyPEGMA$_{246}$-EE. Scale bar: 100µm

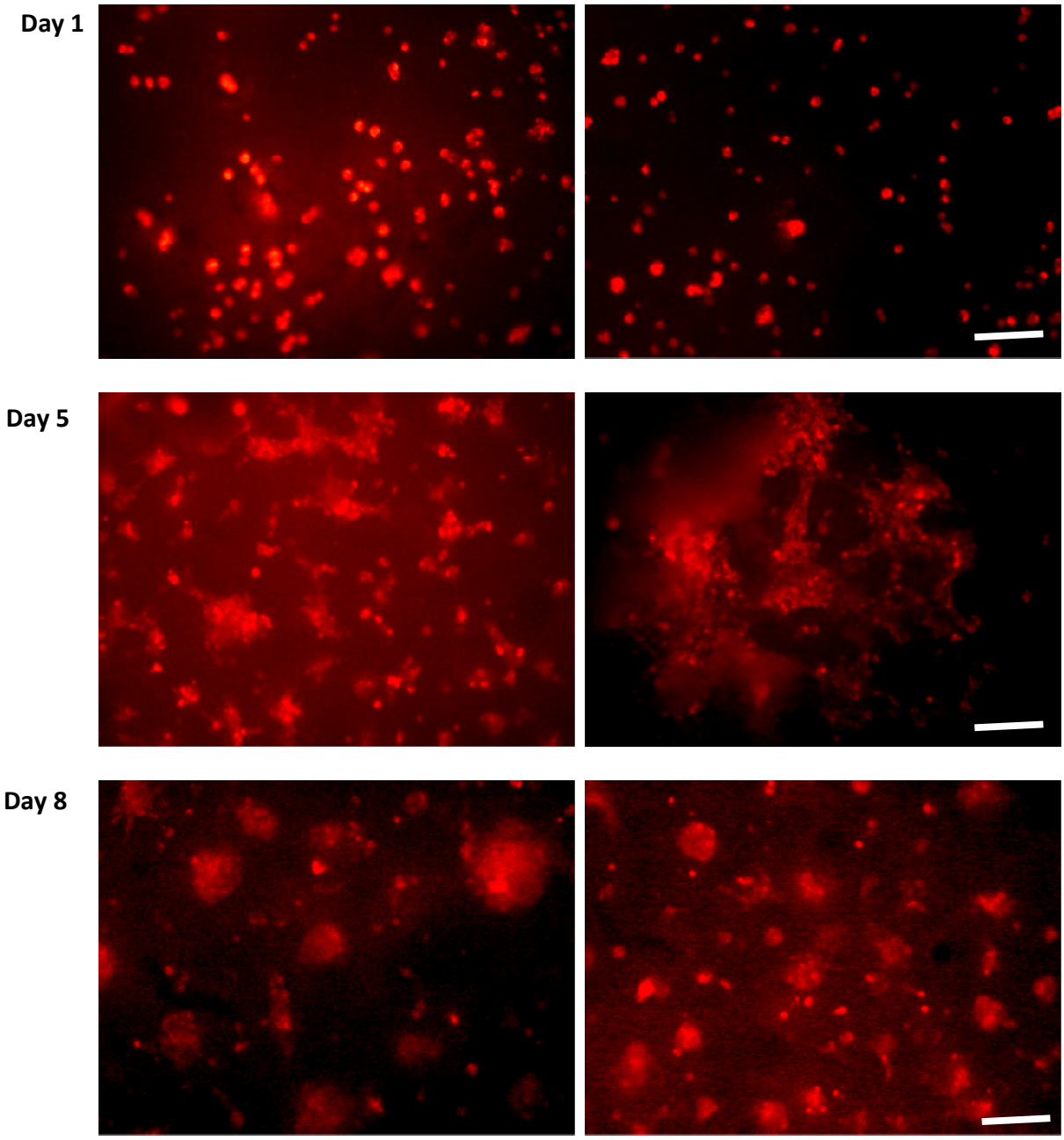

Figure 4.8: Representative fluorescence microscopy images of NIH3T3 cells cultured on the surface of PCL/polyPEGMA$_{246}$-EE particle gels over 8 days.

The gels were made of 33%$_{w/v}$ *NaOH-modified* PCL particles and 6.5%$_{w/v}$ polyPEGMA$_{246}$-EE. Images are representative fluorescence microscopy images of cell-tracker orange labelled 3T3 cells. Note the significant cell spreading and proliferation by day 5 of culture. Scale bar: 100µm

Hence, fluorescence microscopy images indicated cell spreading and proliferation on longer culture. This was confirmed using the Alamar blue assay as described below.

4.4.3.C Quantification of cell viability and proliferation

The viability and proliferation of NIH3T3 cells cultured on the particle gels surface were quantified using the Alamar blue assay (figure 4.9A). The increase in cell metabolic activity with longer culture, suggested that the cells were viable and proliferating.

Cell proliferation was slower on the particle gels than it was on tissue culture plastic used as a control (figure 4.9B). This can be attributed to the large differences in the surface properties between these two substrates. Tissue culture plastic presented a planar surface, with which the cells were interacting mainly in 2D, compared to the micro-structured particle gel's surface which could allow for 3D cell-surface interactions. Cell culture in 3D is known to result in a different cell growth pattern compared to that in 2D, with cell proliferation being generally slower in 3D culture systems (Cukierman et al., 2002).

Moreover, it has been commonly observed that on surfaces with higher roughness and disorder, cell differentiation and/or extracellular matrix synthesis increase with a corresponding reduction in cell proliferation (Wilson et al., 2005), providing a further explanation for the slower cell proliferation on the particle gels.

A.

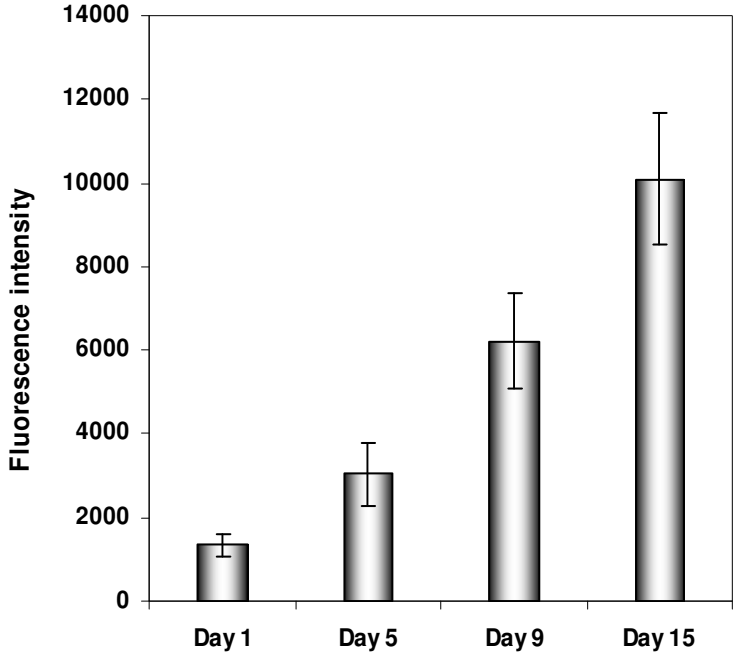

B.

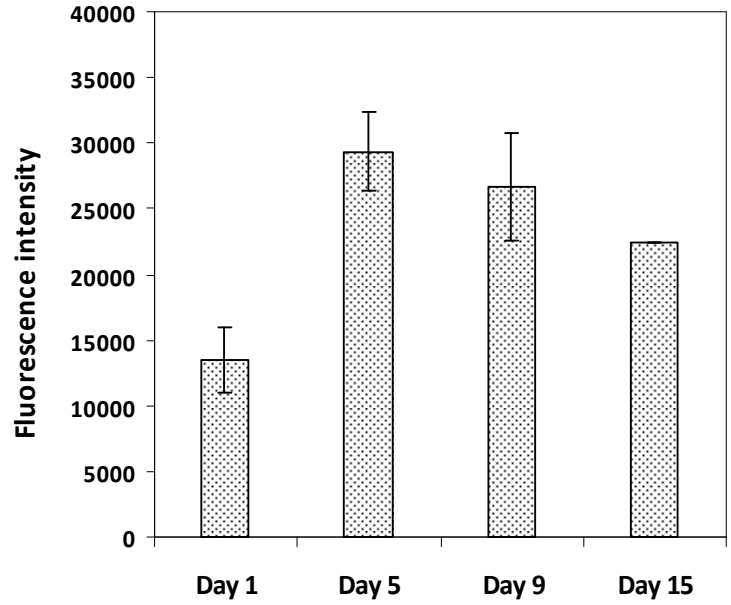

Figure 4.9: Viability and proliferation of NIH3T3 cells when cultured on PCL/polyPGEMA$_{246}$-EE particle gels over 15 days.

Alamar blue assay was used to quantify the cells metabolic activity when cultured on **A.** particle gels and **B.** tissue culture plastic (control). Error bars representing SD; N=5 samples for each time point from 2 experiments.

4.4.4 Imaging of the cellular cytoskeletal F-Actin

The initial phase of cell-matrix interaction is characterised by the binding of **integrin** receptors to ECM molecules and the lateral aggregation of receptors at these contact sites forming *focal adhesions* (figure 4.10). Various proteins are involved in the formation of the focal adhesions, which play a role in cell signalling and impacting on various aspects of cell behaviour. The integrins are attached by their cytoplasmic domains to actin microfilaments (F-actin), linking the cellular cytoskeleton to the external environment.

Hence, the distribution of the focal adhesion sites dictates the cellular morphology, through the intracellular tension and the contractile forces generated inside the cell and exerted onto the substratum by the F-actin anchored to these focal adhesions (Hynes, 1999) (see figure 4.9). Accordingly, cytoskeletal F-actin staining was performed to study the morphology of NIH 3T3 cells, and their spreading when cultured of PCL/polyPEGMA$_{246}$-EE particle gel.

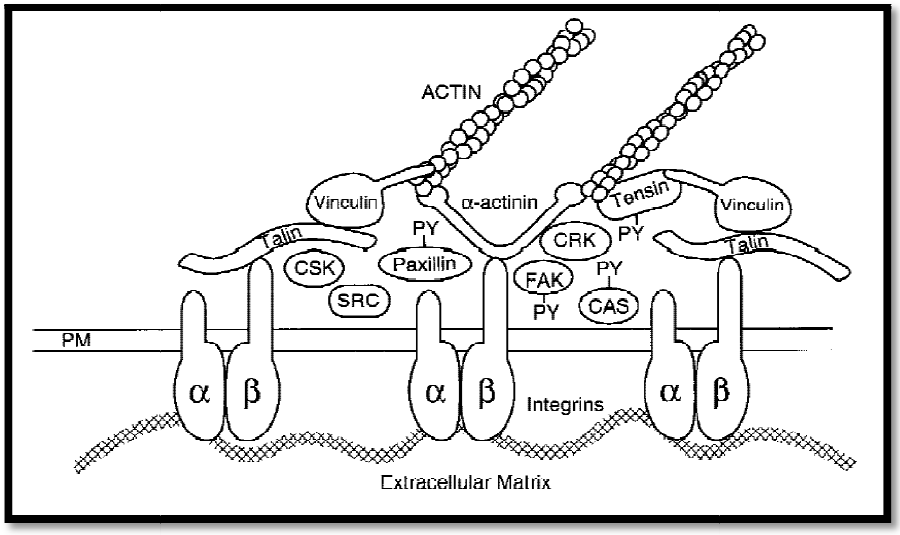

Figure 4.10: The focal adhesions formed between the cells and the ECM.

The cytoplasmic domains of the integrin receptors (α and β subunits) link the intracellular actin filaments to the extracellular matrix. Various other proteins are involved in the formation of focal adhesions (taken from (Vuori, 1998)).

Phalloidin can stabilise the cellular actin microfilaments. Hence, phalloidin conjugated to the fluorescent tag, tetramethyl rhodamine isothiocyonate (TRITC-Phalloidin), was used to stain the cytosekeleton of cells cultured on the particle gels.

After 2 days of culture, most cells were in small clusters of 3-4 cells, with few cells adopting a more spindle-like morphology (figures 4.11 A and B). By contrast, cells cultured on TCP had a much larger cytoplasmic and stress fibres spreading (figures 4.11 C and D).

Polygonal cell spreading is indicative of extensive interaction between the surface and the cells, whereas less extensive cell-surface interaction results in cell clustering (Ranella et al., 2010). Accordingly, NIH 3T3 cells interacted more strongly with tissue culture plastic with extensive spreading compared to the particle gels surface.

However, this did not seem to impact on cell proliferation, as confirmed by F-actin staining of cells cultured for 14 days on the particle gels (figure 4.10E-H). On longer culture, more cells showed larger polygonal cytoplasmic spread, and the small cell clusters observed at the beginning of culture became much larger, with single cells radiating out and spreading in between (figure 4.11 E- H). This indicated that cells were proliferating actively in these distinct groups, which falls in agreement with the Alamar blue results. The morphology of the cellular clusters suggests that the cells were interacting in 3D, with tight intercellular junctions.

The patchy cell adhesion observed on the particle gel surface, could have been attributed to their content of polyPEGMA$_{246}$-EE. This suggestion was tested by repeating the culture of NIH3T3 on gels containing less polyPEGMA$_{246}$-EE (3%$_{w/v}$). A similar initial pattern of cell adhesion and spreading was observed on these gels compared to those containing double the amount of polyPEGMA$_{246}$-EE (figures 4.12A and B). Nevertheless, differences in cell spreading and proliferation became more apparent at the end of the 15 days of culture.

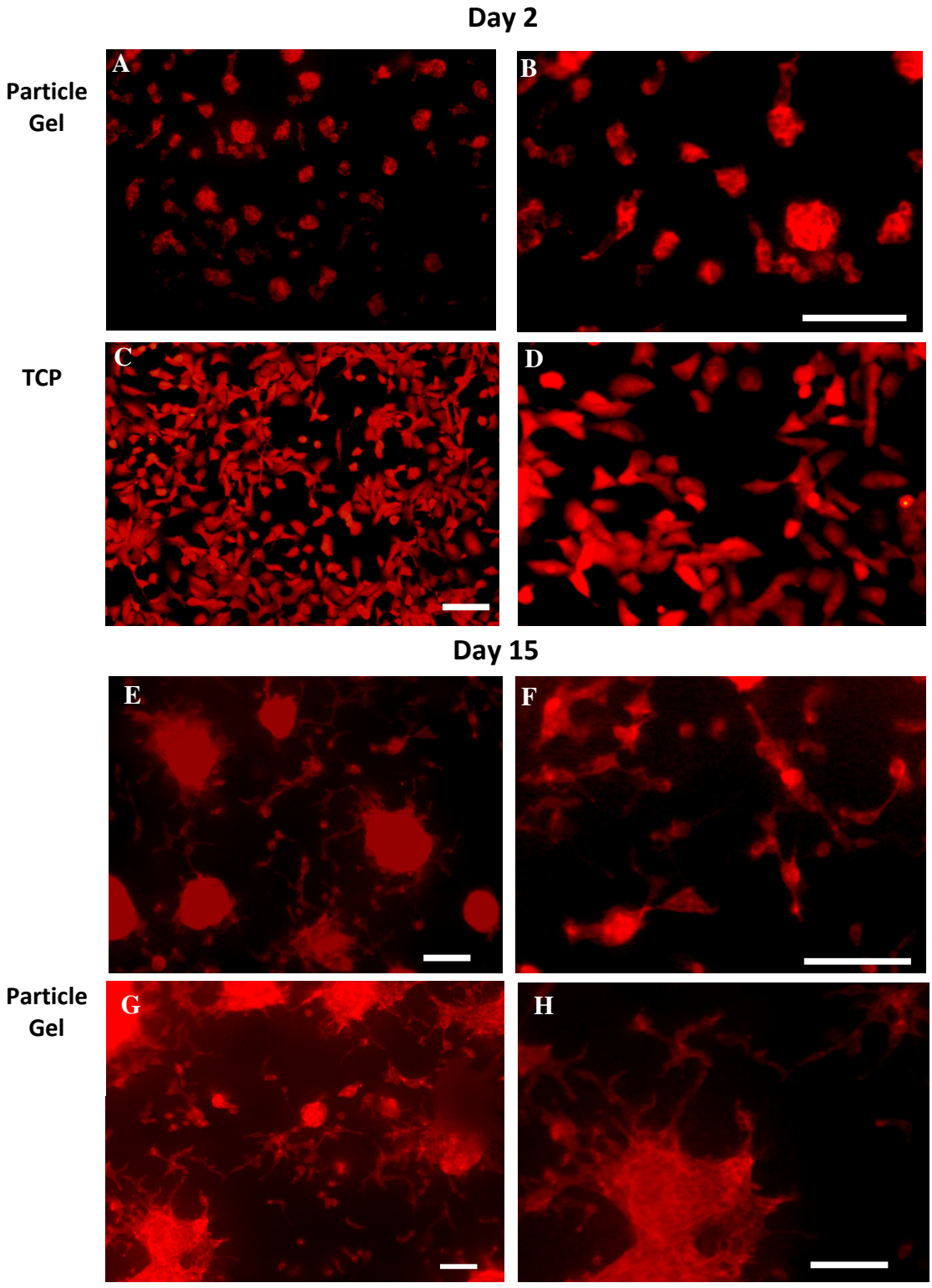

Figure 4.11: Representative fluorescence microscopy images of Cytoskeletal F-Actin stained NIH 3T3 cells cultured on particles gel (33%$_{w/v}$ PCL particles and 6.5%$_{w/v}$ polyPEGMA$_{246}$-EE) for 2 days (top) and day 15 (bottom). The control cells cultured on TCP are shown after 2 days of culture for comparison (in C and D). Scale bar: 100µm

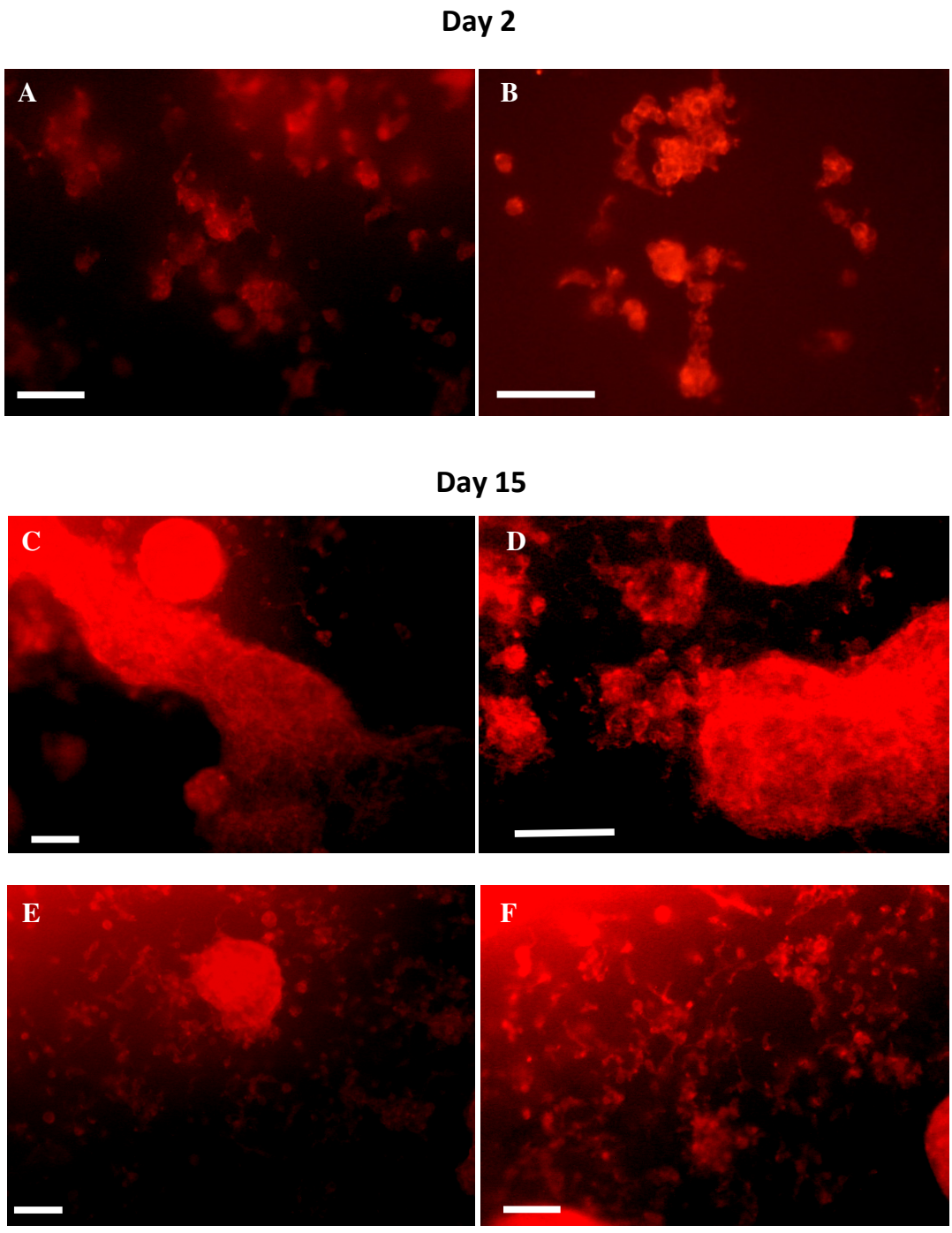

Figure 4.12: Representative fluorescence microscopy images of cytoskeletal F-Actin stained NIH 3T3 cells, cultured for 2 and 14 days on the surface of particles gel containing 33%$_{w/v}$ PCL particles and 3 %$_{w/v}$ polyPEGMA$_{246}$-EE.

Scale bars represent 100µm.

Larger areas on the surface were covered by single well spread cells as opposed to the gels containing higher concentration of polyPEGMA$_{246}$-EE (figures 4.12 E and F). Cells were also proliferating within groups, forming large multicellular assemblies by the end of culture, in what seemed to be a merger between distinct proliferating cell groups.

Overall, decreasing polyPEGMA$_{246}$-EE concentration in the particle gels might improve cell adhesion and spreading.

4.4.5 Scanning Electron Microscopy imaging (SEM)

The majority of biocompatibility tests described in the literature involve morphological assessment of cells on materials usually by light scattering or electron microscopy which allows for cells imaging with high resolution (Gurav, 2009). Thus, the latter technique was employed to provide further details on NIH3T3 cells interaction with the PCL/polyPEGMA$_{246}$-EE gels, and with each other while cultured on top of these gels. The cells were fixed to lock in their morphology, and were imaged at different time points during a 1 month culture on the particle gels surface. Listed below are the main observations from the SEM images of the NIH3T3 cells on the particle gels surface:

- The particle gels had a *"3D micro-structured surface"* that appeared to be malleable by the cells growing on top reflecting the flexible nature of the particle gels (figures 4.13A, 4.13B).

- Cells were attached to the surface individually or in small groups (figures 4.13A and B). Although some cells appeared rounded, others showed good spreading with focal adhesions formed at the particles (arrows in figures 4.13C*).*

- Filopedia and other cell appendages could be seen in multiple planes (figures 4.13C and D, 4.14E, 4.14E). These were indicative of 3D cell-interactions with the particle gels surface.

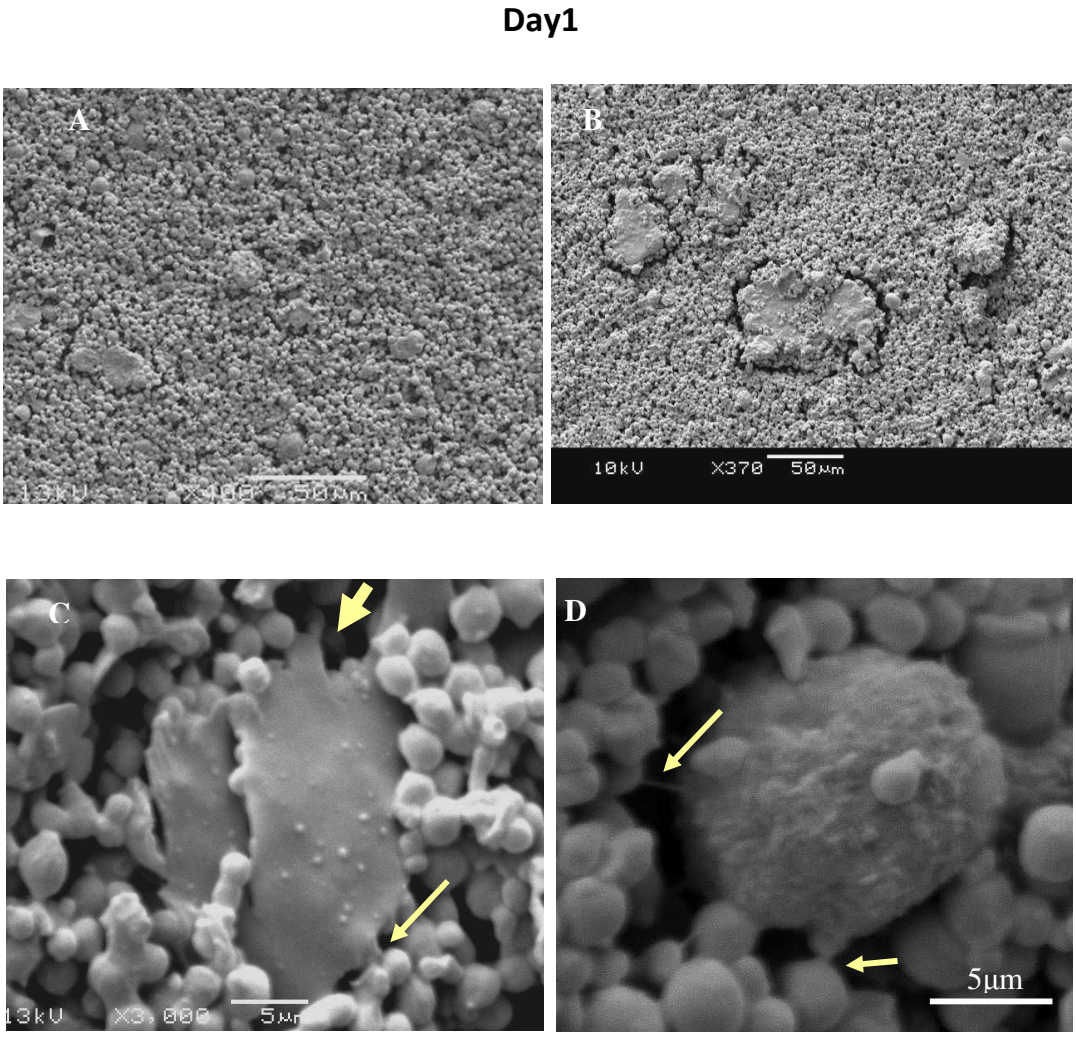

Figure 4.13: Representative SEM images of NIH 3T3 cells cultured on top of PCL/polyPEGMA$_{246}$-EE particle gels for 24 hours.

Cell appendages are indicated by the arrows: **C.** Focal adhesions, **D.** Cellular filopedia and

Day 7

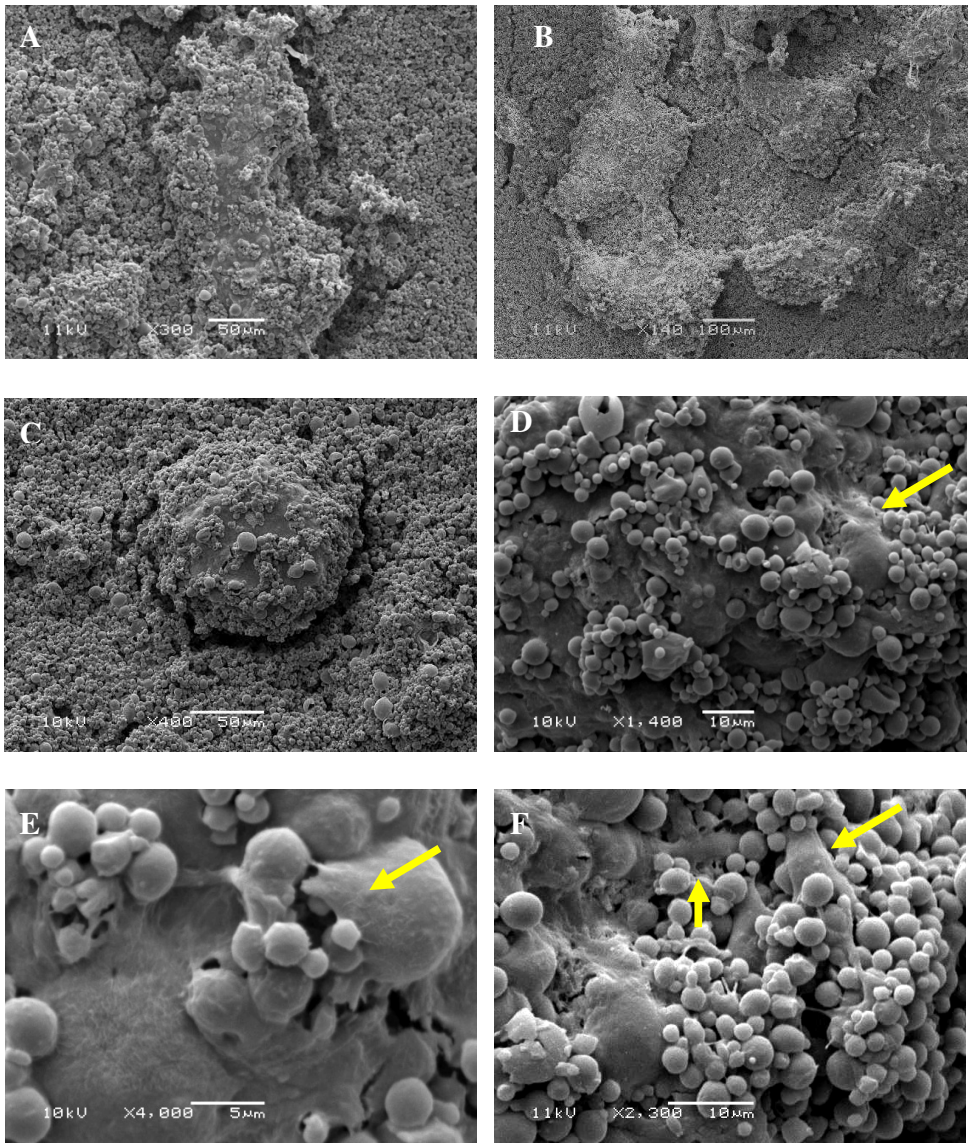

Figure 4.14: Representative SEM images of NIH 3T3 cultured on top of PCL/polyPEGMA$_{246}$-EE particle gels for 7 days.

A, B and **C** show the proliferating cell groups while **D, E** and **F** are the higher magnification images showing the individual cells interacting with the PCL particles (arrows).

Day 14

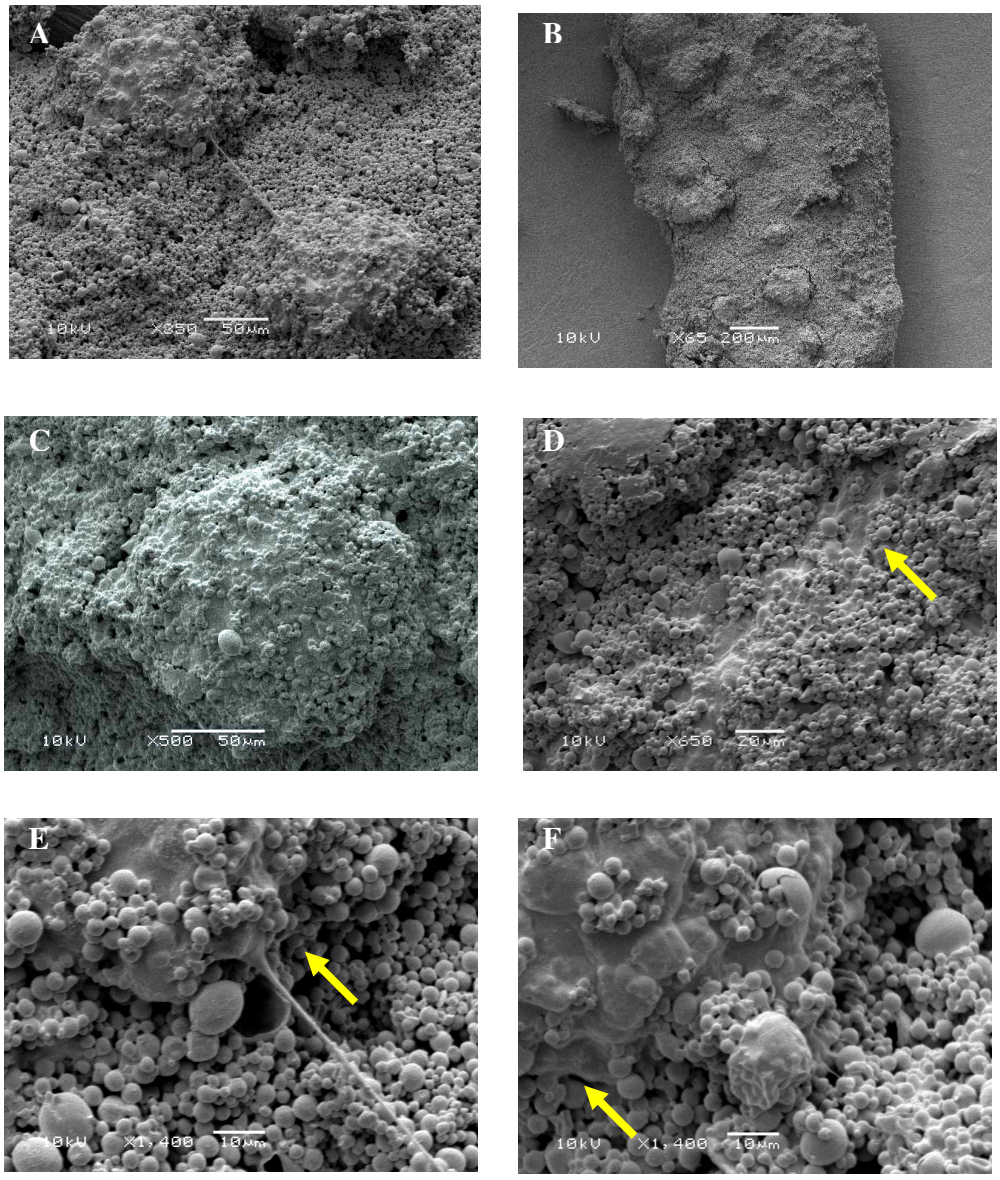

Figure 4.15: Representative SEM images of NIH 3T3 cultured on PCL/polyPEGMA$_{246}$-EE particle gels for 14 days.

A, B and **C** show the proliferating cell groups while **D, E** and **F** are the higher magnification images showing the individual cells interacting with the PCL particles (arrows).

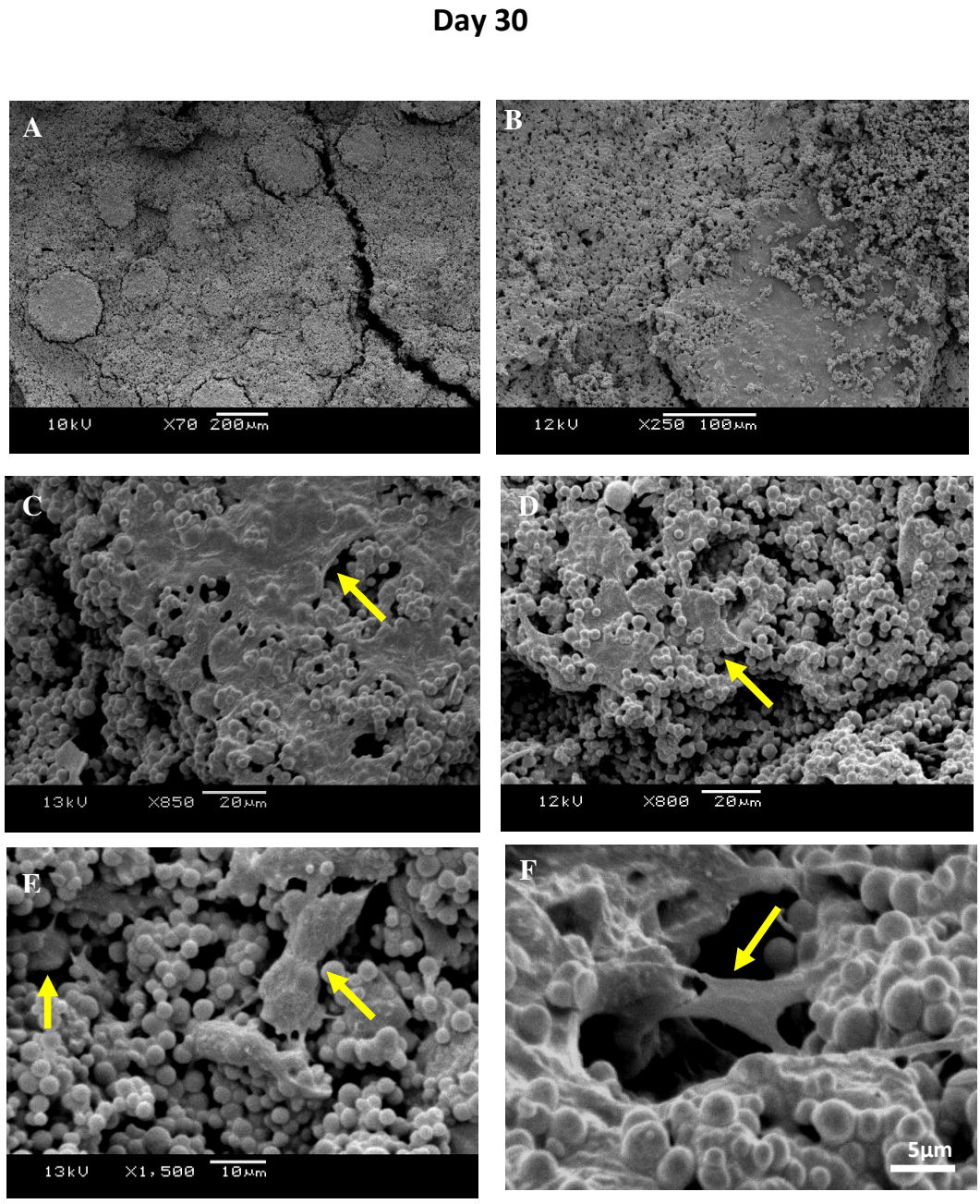

Figure 4.16: Representative SEM images of NIH 3T3 cells cultured on the PCL/polyPEGMA$_{246}$-EE gels for 1 month.

A and B show the proliferating cell groups while C, D, E and F are the higher magnification images showing the individual cells interacting with the PCL particles (arrows).

- After 7 days of culture, larger groups of cells were seen on the gel surface (figure 4.14) in accordance with observations from fluorescence microscopy (section 4.4.3). The cells were actively proliferating with a 3D growth pattern in these cell groups, forming larger cellular clusters with time (figures 4.15 and 4.16). Other areas of the surface were covered by individual cells spreading and interacting with the gel surface (figures 4.14D and 4.15C and D).
- Numerous cellular processes were developed between the cells and the scaffold (arrow in figure 4.13D and figure 4.14 E). Fibrous ECM protein secretions were also observed (figures 4.15.A and 4.16.F), likely to be collagenous fibres.

4.4.6 ECM proteins secretion

The extracellular matrix (ECM) is a proteinaceous structure that consists of various macromolecules, with collagen being one of its main components. There are many types of collagen, depending on the tissue tyoe and function, with type I collagen being the most abundant. One of the functions of fibroblasts is the synthesis and secretion of collagen, mainly of type I. Immunofluorescent staining of collagen type-I was performed to confirm the ability of NIH3T3 cells to perform their normal secretory roles when cultured on the particle gels.

After 7 days of culture, the particle gels stained positive for collagen type I (figure 4.17 C). Collagen type-I was detected peri-cellularly with some para-cellular localisation.

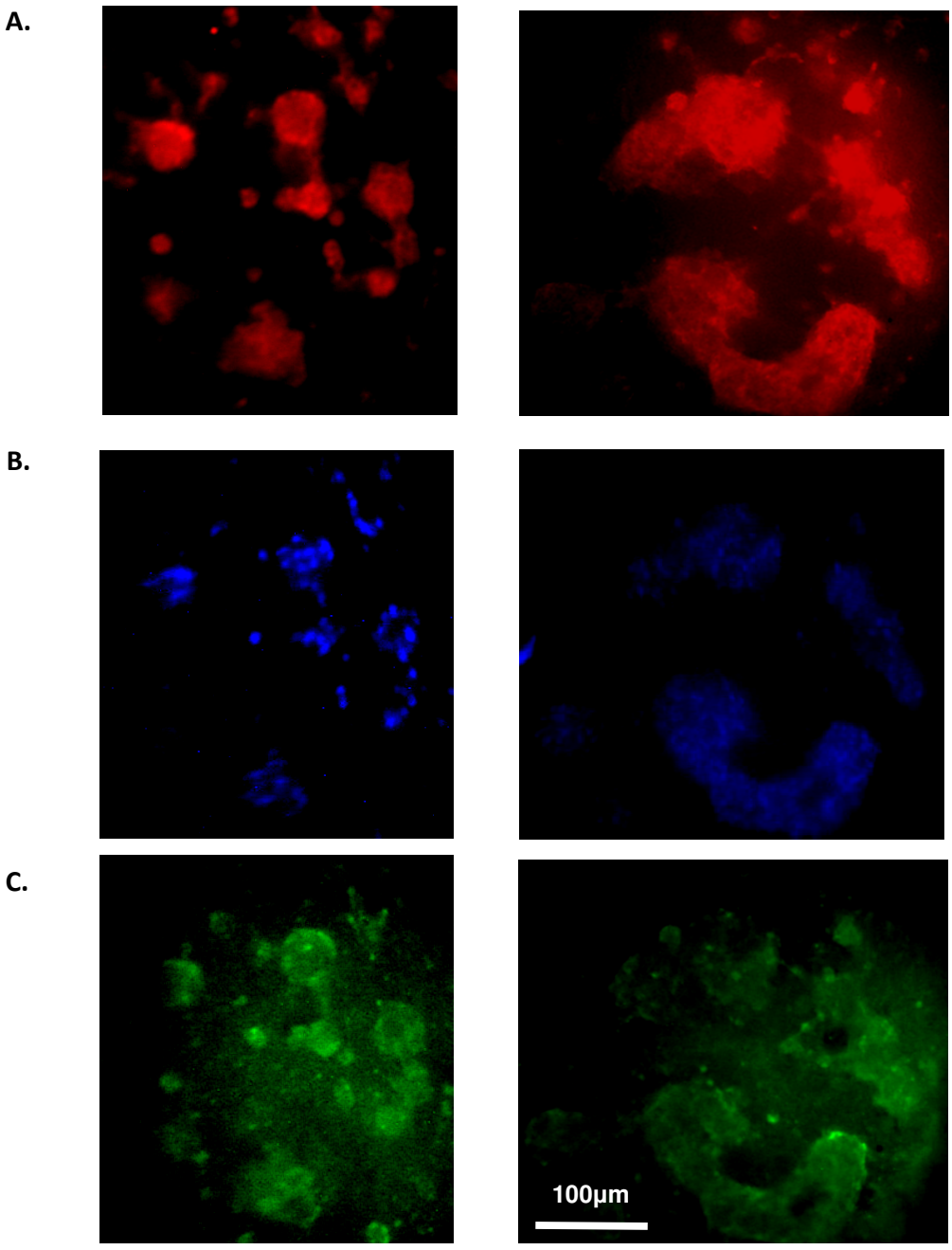

Figure 4.17: Fluorescence Immunostaining of collagen I secreted by NIH 3T3 cultured on PCL/ polyPEGMA$_{246}$-EE gels.

Two different areas from the gels surface were imaged. Three types of cell staining were performed : **A.** TRITC-Phalloidin staining of F-actin **B.** Cell nuclei staining with DAPI **C.** Immunostaining of collagen I secreted by NIH 3T3 cultured on top of the gels

4.4.7 The culture of Swiss 3T3 cells on the particle gels

A different strain of mouse fibroblasts, Swiss albino 3T3, was also cultured on PCL/polyPEGMA$_{246}$-EE particle gels, to further study their ability to support cell growth. Fluorescence (figure 4.18) and electronic microscopy images (figure 4.19) showed a similar pattern of cell adhesion and spreading to that observed with NIH 3T3 cells. The cells proliferated in clusters which grew larger with longer culture in a 3D fashion. The SEM images indicate that the cells interacted favourably with the particle gels surface (figures 4.19-4.21) with good spreading and extensive fibrous ECM protein secretions (figure 4.21).

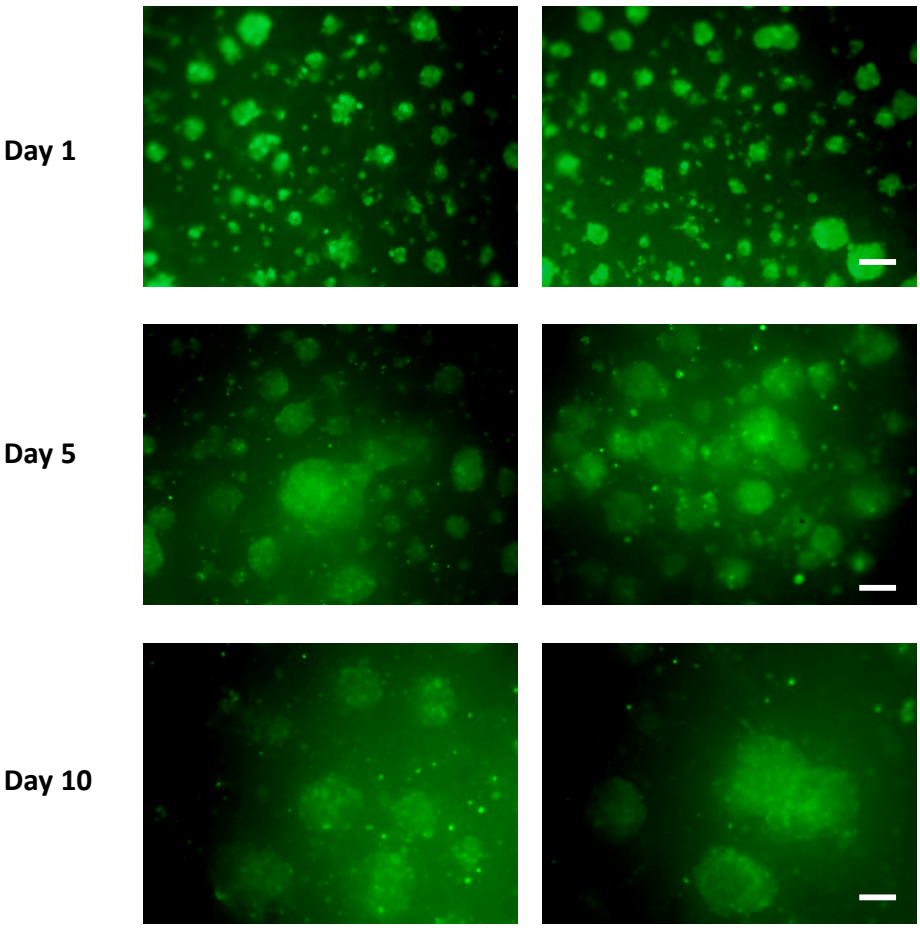

Figure 4.18: Representative fluorescence microscopy images of cell tracker-green labelled Swiss 3T3 cells cultured on the PCL/polyPEGMA$_{246}$-EE gels. Scale bar 100µm.

Day 1

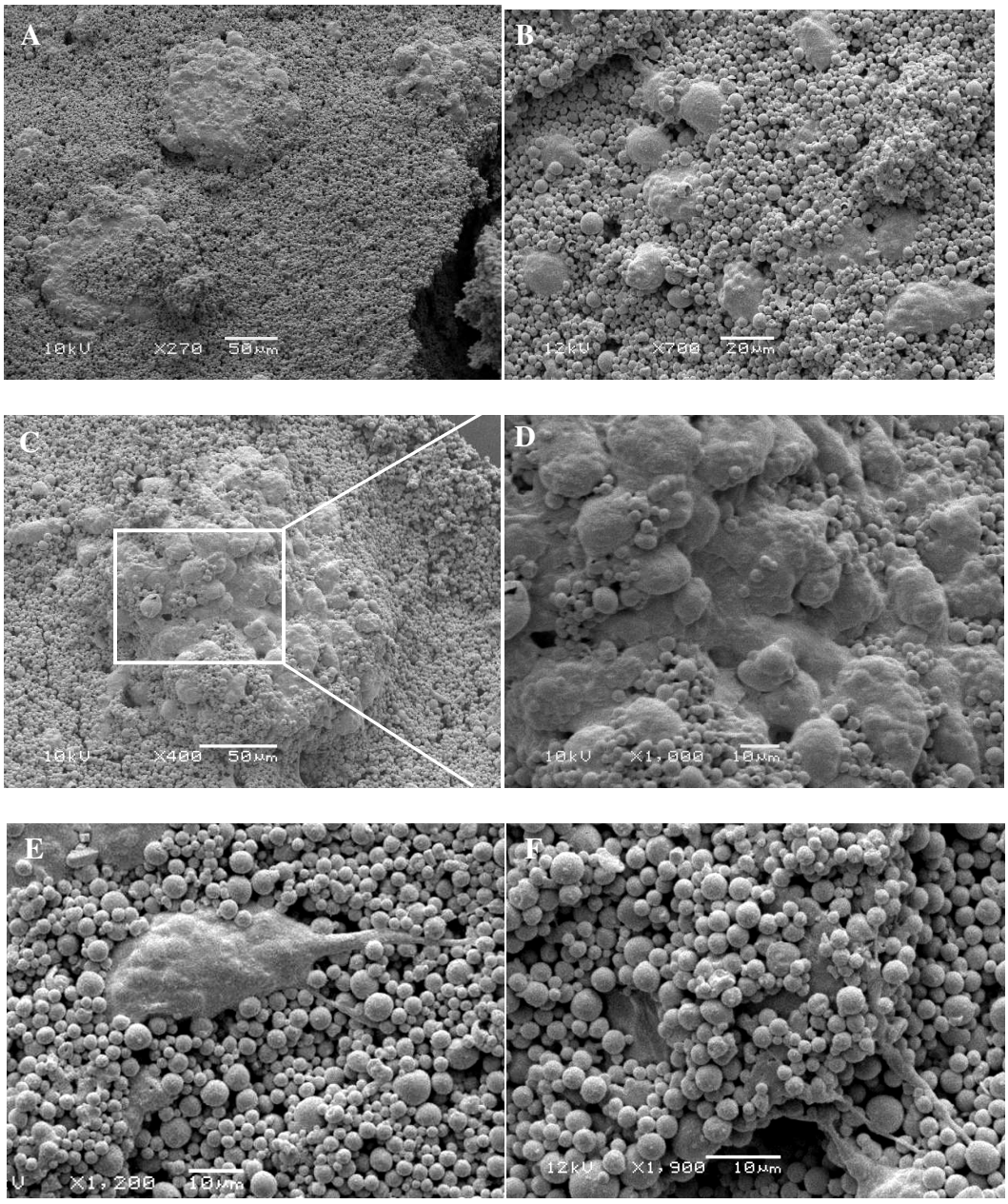

Figure 4.19: Representative SEM image of Swiss 3T3 cells after 24 hours culture on PCL / polyPEGMA$_{246}$-EE gels.

A, B, C and **D** show cells adhered in groups or individually. **E** and **F** are higher magnification images showing the individual cell interacting with the PCL particles.

Day 5

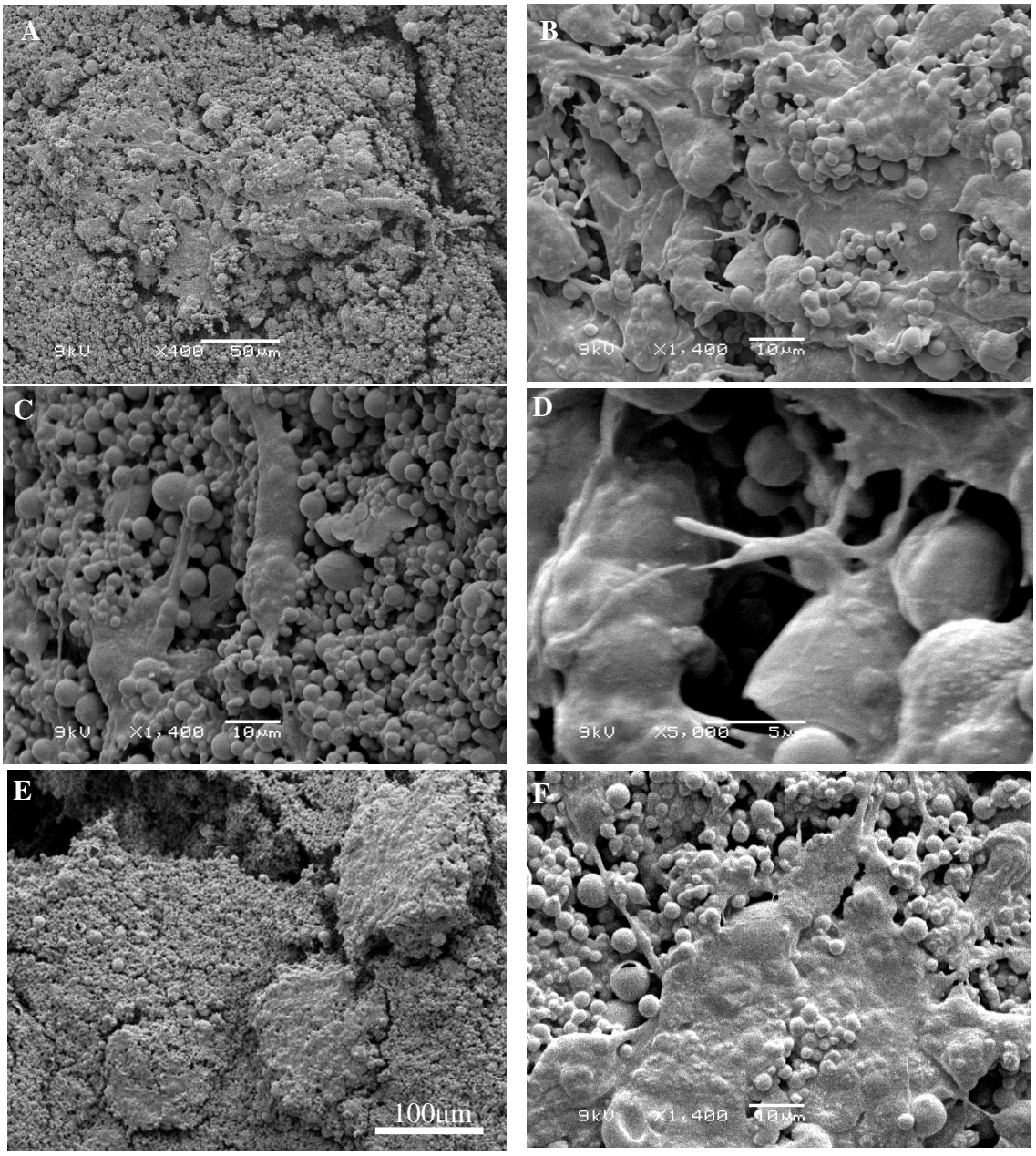

Figure 4.20: Representative SEM images of Swiss 3T3 cells after 5 days of culture on PCL / polyPEGMA$_{246}$-EE gels.

Note the cell appendages and the extensive interaction of cells with the PCL particles.

Day 10

A.

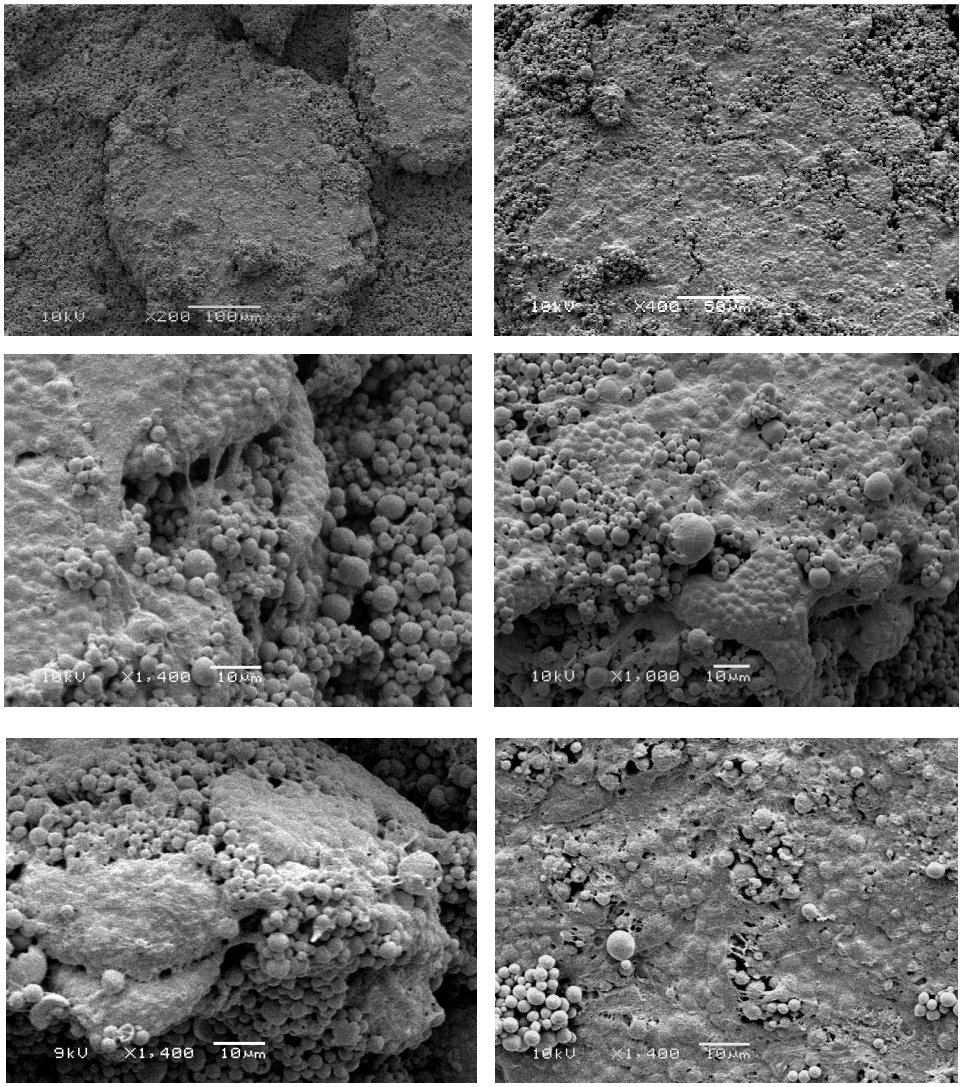

B.

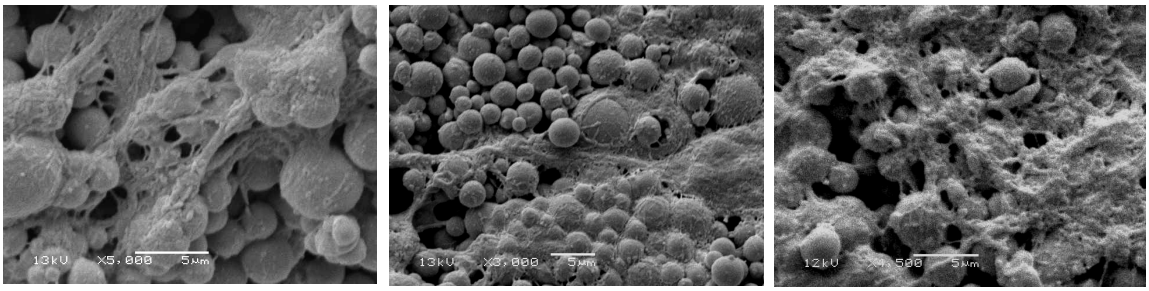

Figure 4.21: A. Representative SEM images of Swiss albino 3T3 cells cultured on PCL/polyPEGMA$_{246}$-EE gels for 10 days. B. Higher magnification images of ECM fibrous secretions by the cultured cells.

Note the well spread cell morphology, cells migration on the surface and size of the cell groups

4.5 Discussion

The overall aim of this chapter was to study the cellular response to PCL/polyPEGMA$_{246}$-EE particle gels, as an initial evaluation of the use of these gels in tissue engineering as cell scaffolds.

Cell adhesion to the thermoresponsive polymer, polyPEGMA$_{246}$-EE, used in these gels was found to be poor. Although PEG-methacrylates have been reported to possess antifouling properties by various groups (Hucknall et al., 2009, Ma et al., 2004a, Li et al., 2005), our results come in disagreement with the recent report of employing a thermoresponsive PEG-based methacrylate polymer in cell sheet engineering. Lutz *et al* grafted gold surfaces with a random copolymer of 2-(2-methoxyethoxy) ethyl methacrylate (MEO_2MA) and oligo(ethylene glycol)methacrylate (OEGMA). They were able to switch the resultant surfaces from being cell-repellent to cell-adhesive with temperature, based on the responsive behaviour of the polymer employed (Wischerhoff et al., 2008). The difference between the results reported herein and those reported in that study could possibly be related to the different conformation of the polymer chains used in each case. While the polymer films used in the experiment assessing the cell-adhesiveness of polyPEGMA$_{246}$-EE were of a sufficient thickness to mask the underlying surface, the brush configuration of the polymer chains grafted to the gold surface in the study by Lutz *et al* could have exposed some areas of the underlying surface when the polymer chains were collapsed above their LCST. In that case, the cells would probably be adhering to the underlying surface rather than to the collapsed polymer chains. This point was not addressed in the study by Lutz *et al*, and further investigations are needed with this regard.

It is worth noting that the experiment carried out to study cell response to polyPEGMA$_{246}$-EE (see 4.3.2) does not totally and accurately mirror the cell response to polyPEGMA$_{246}$-EE within

the particle gels. The conformation and thickness of collapsed polyPEGMA$_{246}$-EE chains within the gel are likely to be different than the polyPEGMA$_{246}$-EE layers tested in this experiment.
Overall, the experiment suggested that polyPEGMA$_{246}$-EE is likely not to participate in cell adhesion to the PCL/polyPEGMA$_{246}$-EE gels.

Next, the ability of PCL particles to support cell adhesion was studied. NIH3T3 cells were not able to adhere to the as-made PCL particles and a surface modification step was required to improve their surface properties. Three factors are commonly accepted to be the most influential on cell adhesion to solid substrata, these being: surface chemistry, wettability and roughness/topography (Ranella et al., 2010, Jiao and Cui, 2007). With respect to these factors, the observed improvement in the cell adhesion following the alkaline hydrolysis of PCL particles can be explained as follows:

1. The alkaline hydrolysis introduced surface charge and chemical functionalities through the cleavage of PCL ester bonds, and the generation of carboxylic acid and hydroxyl groups at the newly exposed chain ends, which could participate in higher adsorption of biomolecules. This was confirmed by zeta potential measurements of PCL microparticles, which were found to carry a more negative charge post-hydrolysis (see chapter 3).
2. NaOH/ethanol treatment of the PCL films changed their surface wettability, and reduced their water contact angle to an intermediate value (see chapter 3), found in various studies to achieve optimum protein adsorption and cell adhesion (Bacakova et al., 2004). A 15° difference in the water contact angle was found to result in a ten-fold increase in cell adhesion or spreading area (von Recum and van Kooten, 1995). The higher wettability can also facilitate cell migration, as was observed with PLA and PLGA foams wetted with ethanol possibly through facilitating water entry into air-filled pores (Mikos et al., 1994).

3. Finally, the alkaline hydrolysis of PCL modulated the particle surface topography by generating surface roughness (see chapter 3) which generally increases cell adhesion, migration and the production of ECM (Pattison et al., 2005). Although, this was only based on qualitative observations (SEM) in this study, various other studies where alkaline hydrolysis was found to significantly improve cell adhesion and spreading to polyesters, have confirmed such an effect using surface characterisation techniques such as Atomic Force Microscopy (AFM) (Thapa et al., 2003). The exact mechanism for the benefits seen with this change in topography remains largely unknown. Some possible mechanisms may be related to receptor regulation (clustering, density, and ligand-binding affinity) and the conformation of adhered proteins for cellular recognition sites (Wilson et al., 2005).

Accordingly, the NaOH/ethanol surface treatment was adopted as part of the preparation stages of PCL particles to be used in the gels (see chapter 3).

NIH 3T3 cells were found to adhere, spread and proliferate on the PCL/polyPEGMA$_{246}$-EE particle gels made of surface modified PCL particles. The patterns of cell spreading and proliferation on the gels were different from those observed on the control planar tissue culture plastic. This could be attributed to the particle gels surface structure. Surface topography both at the nano- and micro-scales has been widely reported to influence cell adhesion and spreading as well as proliferation, migration and differentiation. This has been observed with many cell types including cardiomyocytes (Desai, 2000), fibroblasts (Dalby et al., 2004) and various others (Curtis and Dalby, 2009). Specific features on the surface can force the cells into specific adhesion and spreading patterns, this being referred to as *contact guidance* (Curtis and Dalby, 2009).

The particle gel surface showed randomly distributed micro-islands (figure 4.6). Similar topographical features have been associated with a less diffuse cell spreading compared to planar surfaces. In a study by Dalby *et al* (Dalby et al., 2004), human fibroblasts were smaller, thicker and less well spread when grown on surfaces with nano-columns than when cultured on planar controls. In another study by (Gentile et al., 2010) observation of stained actin filaments clearly revealed the different cell morphologies for cells cultured on rough silicone surfaces compared to the planar controls. The particle gels were also different because of their 3D structured surface; the NIH 3T3 cells cultured on the particle gels were therefore interacting with their surroundings in a 3D fashion which might explain the formation of the multicellular clusters observed.

In addition to surface topography and composition, the rigidity of the substrate was found to have a significant influence on cell behaviour. Cells were found to exhibit more *in vivo* like morphological and functional features, when cultured on flexible substrates of a similar rigidity to that of the particular tissue from which they were derived (Levental et al., 2007). In other studies, cells on flexible substrates showed reduced spreading and increased rates of motility or lamellipodial activity (migration), compared to those on rigid substrates (Schwarz, 2007, Robert et al., 1997).

When NIH3T3 mouse fibroblasts were cultured on PCL/polyPEGMA$_{246}$-EE particle gels, they could synthesise and secrete Collagen I. The deposited cell-secreted collagen I could have participated in the larger cell spread on the gel surface observed on longer cultures. Indeed, while the scaffold properties at the onset of *in vitro* seeding will provide the set of environmental conditions that dictate the initial cellular responses, such as cell adhesion, these properties will evolve over time in response to passive and active interactions with the culture environment and cells respectively. This was exemplified in this study by cell deposition of their own ECM

components. However, it must be noted that the cells' ability to condition their environment differs between cell types, so while fibroblasts, which are naturally responsible for ECM molecules production, are efficient with this regard; other cell types such as embryonic stem cells may not possess the same ability and further optimisation of the particle gels might be required (see chapter 7).

Very similar results were seen with Swiss 3T3 cells with regards to cell adhesion, spreading and morphology when cultured on the particle gels to those obtained using NIH3T3. SEM provided evidence for secretions of ECM fibrils by these cells.

4.6 Conclusions

The particle gels studied were made of biocompatible materials and did not, therefore, induce significant cell toxicity. Surface etching using NaOH/ethanol was required to improve cell adhesion to the PCL microparticles, the major component of the particle gels. This surface modification had a substantial influence on the ability of the cells to adhere to the gels. Once adhered, the cells were actively proliferating on the particle gels surface as confirmed by Alamar Blue assay and microscopy. The gel surface with its 3D microstructure supported a 3D pattern of cell growth, and formation of proliferating multicellular assemblies.

Overall, the particle gels were found to support the different cellular functions of adhesion, migration, secretary roles and cell-cell interactions. The data presented in this chapter provides a preliminary evidence for the ability of PCL/polyPEGMA$_{246}$-EE particle gels to be used as cell-scaffolds, and this shall be further studied in the following chapter.

CHAPTER 5

The 3D culture of 3T3 cells in PCL/polyPEGMA$_{246}$-EE particle gels and their enzyme free subculture

5.1 Introduction

In the body, cell populations are organised in the extracellular matrix through the arrangement of biological polymers in all three dimensions (Freshney et al., 2007). Both synthetic and natural polymers have been used to construct cell niches (scaffolds) that can provide an environment that mimics the natural extracellular matrix, and promote a "natural" cell survival and function.

The relationship between the cells and their culture environment is by no means a passive one, but it is rather dynamic and strongly influential on cellular behaviour. The cells constantly receive *mechanical* (Discher et al., 2009, Schindler et al., 2006) *temporal* and *spatial cues* from their environment, the combination of which determine their fate. In tissue engineering and regenerative medicine, designing scaffolds and cell culture substrates that present these cues in the appropriate balance is of paramount importance.

Since the spatial arrangement of cells and the mechanical cues from their culture environment are now recognised to be key factors affecting cells behaviour, this being particularly important for stem cells, a key paradigm shift to be witnessed in tissue engineering

within the coming years is the dominance of 3D cell culture practice over the routine practice of cell culture on 2D planar rigid substrates (Lee et al., 2008, Lutolf et al., 2009, Lutolf and Blau, 2009).

Accordingly, there is a large demand for biomaterials that would allow for the successful and scalable 3D culture of cells. This would require the use of materials in innovative ways to build cell culture matrices that present the relevant cues for cells, while allowing for simple *in vitro* processing of expanding cell populations or forming tissues.

Thanks to their semi-solid morphology and high water content, which resembles native tissues, hydrogels have been largely studied as substrates for the 3D culture of cells. Examples include gels made of self-assembling peptides (Webber et al., 2010, Hartgerink et al., 2002, Zhou et al., 2009, Mart et al., 2006) polymeric hydrogels, nanocomposite and biological gels.
These are highly promising in many individual aspects (Drury and Mooney, 2003), yet most of them to date have not demonstrated the full complement of features required for repeated cell culture. This is specifically the ability to be assembled and disassembled rapidly and reversibly in an easily tuneable manner to allow for multiple cycles of cell growth in 3D, and the facile manipulation and processing of the cell-material constructs.

Traditionally, proteolytic enzyme treatment (e.g. with trypsin), which digests the cell-surface proteins responsible for cell adhesion, has been used to free the cells from the culture substrate and allow for their transfer to another culture vessel for further cycles of cell growth. This practice, however, is thought to affect the cells ability to adhere to further substrates, and

their long term quality. It also leads to the proteolytic damage of the extra-cellular matrix (ECM) proteins secreted by the cells (Steinberg et al., 1973, Huang et al., 2010).

Thermoresponsive polymers have enabled the culture of cells and the subsequent recovery of cell sheets from the culture substrates by a small temperature drop of the medium, eliminating by that the need for enzymes. This preserved the cells deposited extra-cellular matrix (ECM) and the critical cell surface proteins such as ion channels, growth factor receptors and cell-to-cell junction proteins (AI et al., 1999).

A novel way by which thermoresponsive polymers were employed to construct particle gels with thermoresponsive properties was described in chapter 3. In this chapter, the application of these particle gels as cell scaffolds for the 3D culture of cells, which allow for the enzyme-free subculture and processing of the cultured cells, is described.

5.2 Aim and objectives

The aim of this chapter was: "To investigate the use of PCL/polyPEGMA$_{246}$-EE particle gels as 3D cell scaffolds, that allow for enzyme-free processing of expanding cell populations".

This was achieved through the realisation of the following objectives:

1. The encapsulation of cells within PCL/polyPEGMA$_{246}$-EE particle gels.
2. The measurement of cell viability, proliferation and their distribution, following culture within the particle gels using reliable assays.
3. The evaluation of enzyme-free temperature-mediated processing of cells cultured within the particle gels.

5.3 Materials and methods

NIH3T3 cells of (n+10) passages were used in all the cell experiments listed below. PCL microparticles used in all gels were surface modified by NaOH/ethanol treatment (see chapters 3 and 4).

5.3.1 Cell encapsulation and culture within the particle gels

Aliquots of suspensions (150µl) containing 30%$_{w/v}$ PCL particles and 3%$_{w/v}$ polyPEGMA$_{246}$-EE in complete medium were added to 48-well culture plates. While still fluid, complete medium (20µl) containing approximately 10^5 cells were mixed in. The plate was placed at 37°C for 10 minutes to obtain individual gels within which the cells were encapsulated. Further complete medium (500µl) was added on top of the gelled suspensions and the plate was incubated at 37°C (see figure 5.1). The cell nutrient medium was changed every day. Cell viability and proliferation were assessed using the CellTiter 96® Aqueous One Solution Cell Proliferation Assay (MTS) (Promega, UK) (see 5.3.2), and cell proliferation was confirmed by total cellular DNA quantification (see 5.3.3).

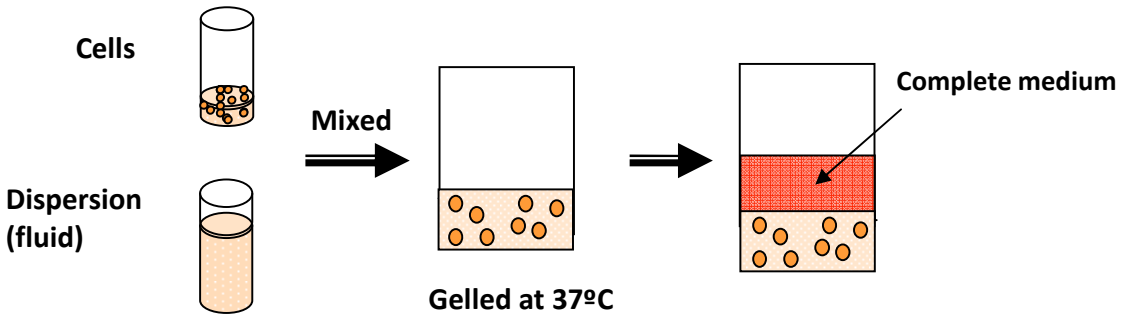

Figure 5.1: A Schematic of the steps followed for cell encapsulation within PCL/polyPEGMA$_{246}$-EE particle gels

5.3.2 MTS assay on cells encapsulated within PCL/polyPEGMA$_{246}$-EE particle gels

Particle gels (150µl) were liquefied at 4°C for 4 minutes. Complete medium (100µl) was then added to each gel along with 44µl of MTS solution, while the gels were still in the fluid state. The overall volume ratio of MTS: complete medium selected was 1:6, taking into account complete medium already contained within the gels. The liquefied gels, with the added MTS reagent, were put back into the incubator at 37°C for 60 minutes. Following the incubation period, the gels were liquefied at 4˚C for 4 minutes, and transferred into 0.5ml plastic eppendorf-tubes, and centrifuged at 14000rpm for 5 minutes. The supernatant was collected. Aliquots (100µl) of the supernatant were transferred into a Costar-96 well plate (flat bottom transparent), and their absorbance was measured at 492nm in an Infinite M200 Tecan plate reader.

5.3.2.A MTS Assay validation

The MTS protocol described above was validated by comparing the MTS readings from NIH3T3 cells encapsulated within the particle gels, to those obtained from the same numbers of cells seeded onto tissue culture plastic.

NIH3T3 cells were encapsulated in the particle gels at the following densities: 0, 1, 2.5, 5, 10, 20, 30, 50 or 100 X 10^4 cells. Immediately, following gelation, MTS assay was performed on these gels as per the protocol in 5.3.2. The same numbers of free cells in suspension were added to 48-well plates, and incubated with 220µl of complete medium and 44µl of MTS solution at 37°C for 60 minutes. The MTS readings obtained from this experiment were used to construct standard curves, for both encapsulated and free cells.

5.3.3 DNA quantification assay for cells encapsulated within PCL/polyPEGMA$_{246}$-EE gels

Particle gels, within which cells were encapsulated and cultured, were liquefied at 4°C for 4 minutes, and subsequently diluted with 1 ml of cold PBS and transferred into 1 ml plastic eppendorf-tubes. These were centrifuged at $10^3 xg$ for 5 minutes. The supernatant was discarded and the collected pellet of particles and cells was treated following the tissue protocol for the QIAmp DNA mini kit (tissue protocol) (QIAGEN, West Sussex, UK). The amount of the isolated DNA from each sample was determined by UV-spectroscopy, by measuring the absorbance of the collected aqueous solutions at 260 nm, using a Nanodrop spectrophotometer (ND-1000 spectrophotometer and the associated software ND-1000 3.3). Cell numbers could be estimated from a linear standard curve, obtained by measuring the amounts of isolated DNA from increasing cell densities.

5.3.3.A DNA assay validation

The DNA protocol described above was validated by comparing the amounts of DNA isolated from increasing numbers of NIH3T3 cells, when encapsulated within the particle gels or free in suspensions.

NIH3T3 cells were encapsulated in the particle gels at the following densities: 0, 5, 10, 20, 40, 60, 100 or 150 X 10^4 cells. Immediately following gelation, the DNA assay was performed on these gels as per the protocol above (5.3.3), while cells free in suspension were collected by centrifugation and the cell pellet was used for DNA extraction as per the steps described in 5.3.3. The data obtained from this experiment was used to construct standard curves, of the amount of DNA versus cell numbers for both encapsulated and free cells.

5.3.4 Trypsin-free subculture of cells cultured within PCL/polyPEGMA$_{246}$-EE particle gels

NIH 3T3 cells (2 X 10^5) encapsulated in the particle gels were cultured for 7 days. The gels were then disassembled (liquefied) by cooling at 4°C for 4 minutes, and the obtained suspension was split (while still fluid) into approximately equal halves using a positive displacement micropipette (Microman® M250, Anachem, UK) . An equal volume of fresh particle suspension (of the same composition: 30%$_{w/v}$ PCL and 3%$_{w/v}$ poyPEGMA$_{246}$-EE) was added to each half, then the mixtures were each heated to 37°C, to produce two new diluted gels (referred to as daughter gels) each containing approximately half the number of cells in the 'parent gel'. The new gels were cultured for 7 more days, after which an MTS assay was performed.

At day 14 of culture, the splitting process was repeated on a set of gels already split on day 7, and the culture was continued till day 20, at which point an MTS assay was performed.

Total cellular DNA quantification was also performed on the split and the non-split gels, at days 7, 14 and 21 of culture. The experimental steps are schematically described in figure 5.2.

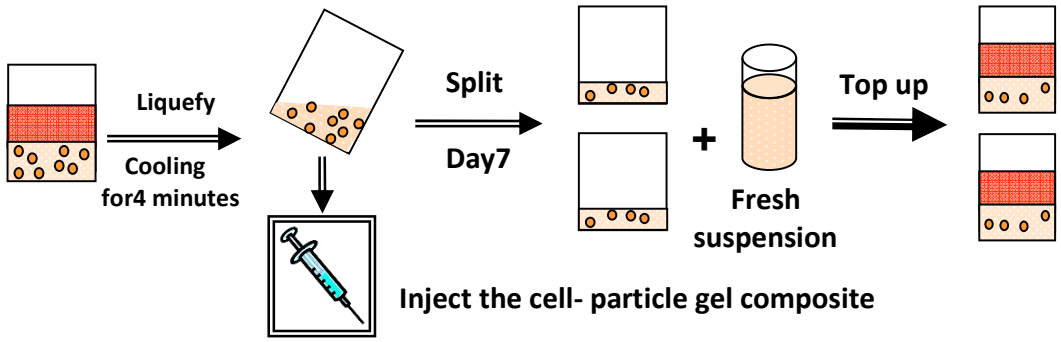

Figure 5.2: Schematic of the particle gels liquefaction and the subculture process. Following liquefaction the suspension can otherwise be used as an injectable scaffold.

5.3.5 Scanning electron microscopy (SEM)

The preparation of particle gels encapsulating cells for SEM was carried out as described in chapter 4, section 4.3.9. Random sections from the gels were imaged by SEM following the protocol given in chapter 2 (2.2.3).

5.3.6 Micro-Computed Tomography (micro-CT)

Gels encapsulating cells, contained within plastic inserts, were treated following the SEM sample preparation protocol (see 5.3.5).

Micro-computed tomography (micro-CT) was performed on the particle gels using a high resolution 1174 Skyscan system (Skyscan, Belgium), with assistance from Susan Dodson and Dr. Lisa White (Tissue Engineering Group, University of Nottingham).

Sample scanning was performed at 11.8µm voxel resolution and with the system running at a voltage of 55kV and current of 800µA. The accompanying *Skyscan® software packages* were used to process the transmission images obtained from the Micro-CT scans. Firstly, transmission images were converted into reconstructed 2D cross-sections using the *Nrecon* programme, and these were saved as 16 bit images in the tagged image file format (tiff). Image analysis was then performed using the *CTAn* software package, with manual thresholding to exclude voids and distinguish between the polymeric material and the NIH3T3 cells. Noise was reduced by removing white and black speckles of less than 100 voxels. The 3D Models were built using the *CTVol* programme. Two models were built for each gel, where the polymeric material was set to high and low opacities respectively, for a clearer visualisation of the cell distribution within the gels.

Particle gels, without any encapsulated cells, were used as controls to account for potential artefacts.

5.4 Results

PCL/polyPEGMA$_{246}$-EE particle gels were developed for use as scaffolds in tissue engineering, and were found cytocompatible as described in chapter 4. They were designed to possess reversible thermogelling behaviour, and to be used for culturing cells in 3D environments that can be reversibly constructed/deconstructed. The study described in this chapter, aimed mainly at investigating the ability of PCL/polyPEGMA$_{246}$-EE particle gels to encapsulate and support the culture of NIH3T3 cells, and whether their temperature responsiveness could be harnessed for simpler processing of the cell-gel constructs.

5.4.1 Validation of the biochemical assay protocols used with the PCL/poly PEGMA$_{246}$-EE particle gels

As part of evaluating the use of PCL/ polyPEGMA$_{246}$-EE particle gels as 3D cell scaffolds, reliable cell viability and proliferation assays were needed for quantitative information on the behaviour of encapsulated cells. While there are numerous reports detailing the use of these assays with cells in 2D culture, these protocols were not found to accurately extrapolate to 3D settings (Ng et al., 2005). Prudent selection and validation of the assays to be used in this study were therefore required.

5.4.1.A Cell viability

Alamar blue® metabolic activity assay was initially selected to assess the viability and proliferation of NIH3T3 cells within the particle gels (see section 4.4.1 for details on the assay). The results obtained were vastly variable (data not shown). Intense pink patches were visible in the gels while the supernatant remained blue. This suggested a failure of a high proportion of the reduced substrate to diffuse out of the intact gels incubated with Alamar blue reagent. The same limitation was encountered by Ng *et al* (Ng et al., 2005).

Accordingly, the gels were liquefied before adding the assay reagent and also at the end of the incubation period, to allow for a more uniform exposure of the encapsulated cells to the reagent, and its efficient release and diffusion into the supernatant to be assayed. Since Alamar blue® is affected by serum proteins present within the particle gels, CellTiter 96 assay (MTS) was used instead (see section 4.4.1 for details on the assay).

The MTS protocol used with cells encapsulated within particle gels was validated against that used with cells on 2D substrates. The MTS readings from encapsulated cells were attenuated by 13%, (figure 5.3A), but generated a linear standard curve, up to a cell density of $3X10^5$ (figure 5.3C).

Therefore, the MTS assay was used in this study for information on cell viability, but not cell numbers, especially for cell populations above $3X10^5$ cells when assay saturation was observed (figure 5.3B).

5.4.1.B Cell proliferation

The most prominent parameter for analysing cell proliferation is the measurement of DNA synthesis as a specific marker for replication. In the study by Ng *et al*, which evaluated the use of different metabolic and other assays to quantify cell numbers and proliferation in 3D culture, DNA quantification assay was found to be the most accurate in portraying cell proliferation (Ng et al., 2005).

Generally, fluorescence based assays are used to quantify the amount of DNA within cell lysates. These are based on specific nucleic acid stains, such as Picogreen or Hoechst, which specifically bind the DNA molecules and exhibit significant fluorescence enhancement. However, due to problems related to autofluorescence and inadequate cell lysis encountered with these assays (data not shown), the DNA mini kit (QIAGEN,UK) was used to isolate purified DNA from the cells within the particle gels, and subsequently quantify it by UV spectroscopy.

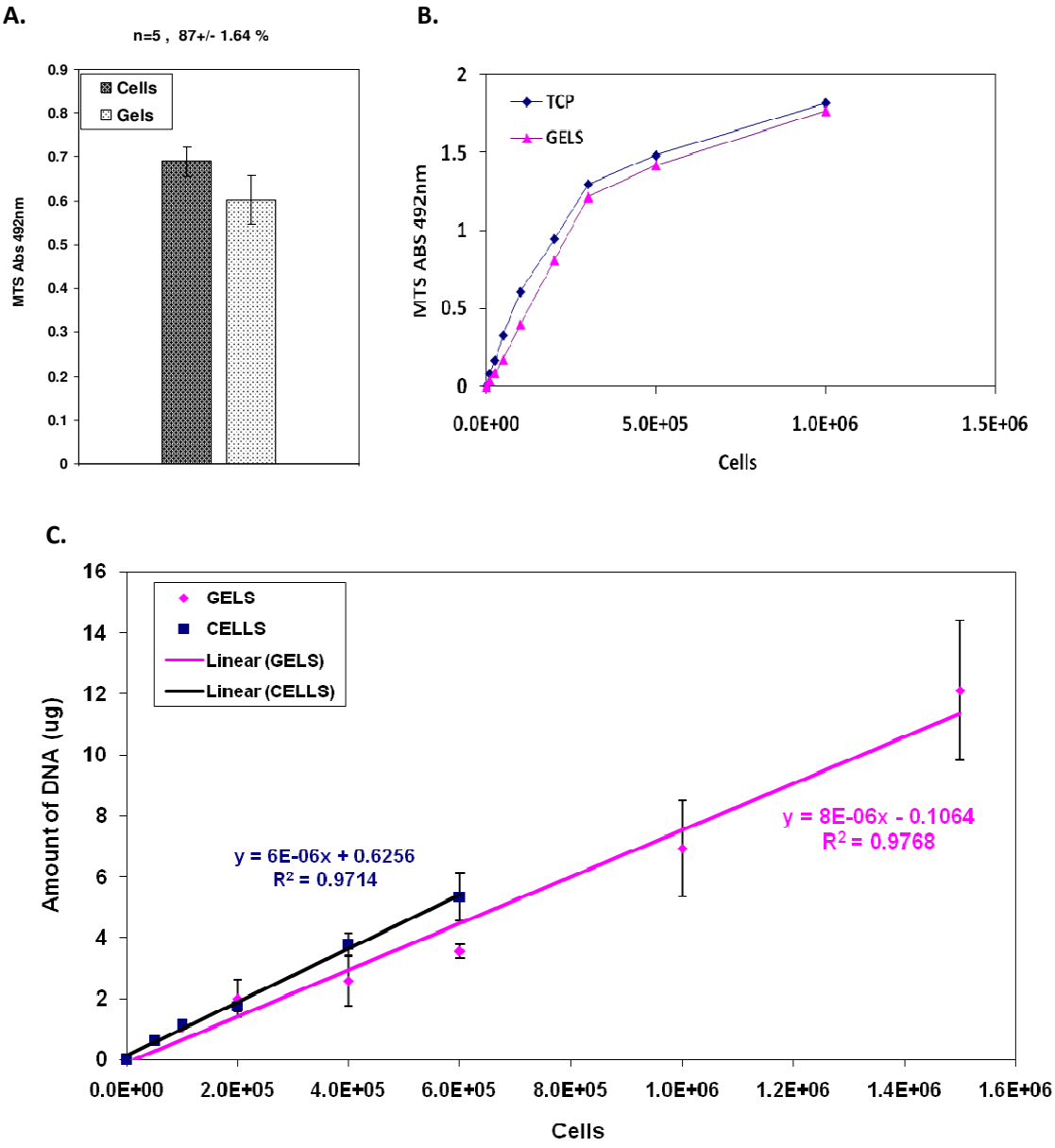

Figure 5.3: Validation of the MTS assay protocol used with cells encapsulated within particle gels.

A. The difference in MTS readings when the assay was performed on 1.5X10^5 NIH 3T3 cells attached to TCP or encapsulated within the particle gels. **B**. MTS readings versus the number of cells encapsulated within gels (pink) or attached to TCP (blue). The assay showed saturation starting from 3X10^5 cells**. C.** The linear region of the MTS Abs $_{492nm}$ versus cell number used as a standard curve for estimation of the number of viable cells.

Error bars represent standard deviation; N=3 samples.

The use of the kit in this study was different to its common use in the isolation of DNA for PCR (polymerase chain reaction) and blotting procedures (QIAGEN, 2010).

The developed protocol for DNA purification and quantification was validated by preparing a standard curve for the amount of DNA isolated using the kit from increasing number of cells freely suspended or encapsulated within the particle gels. Linear standard curves were obtained in both cases (figure 5.4).

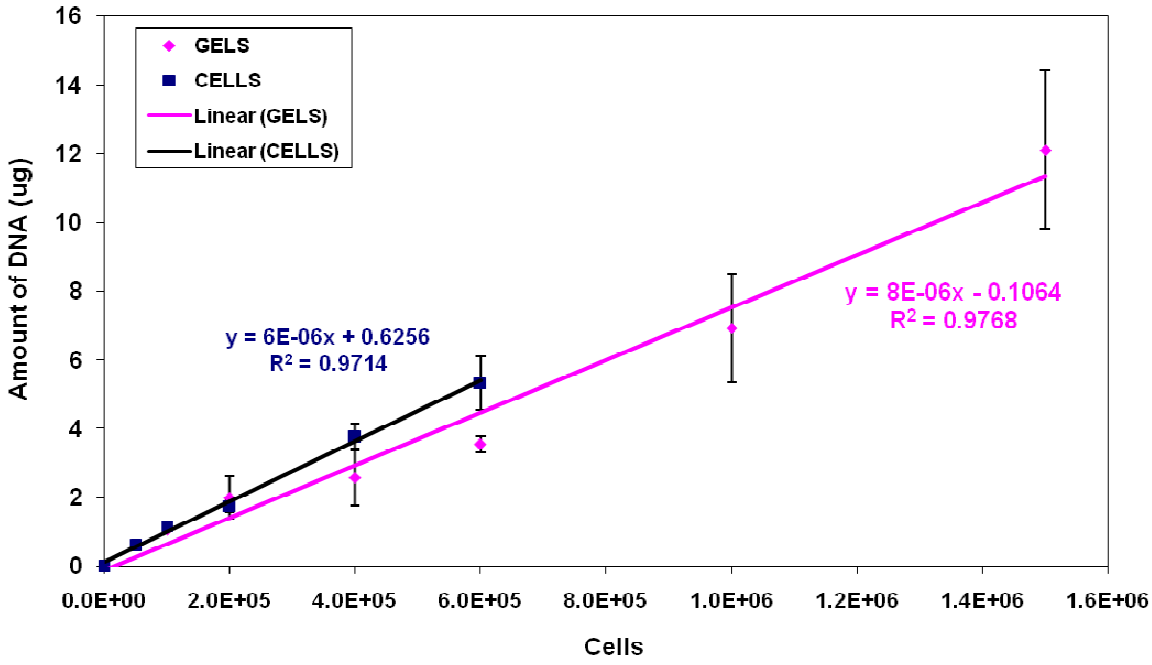

Figure 5.4: **Validation of the DNA quantification assay for estimation of cell numbers**.
The pink and blue lines represent the amount of DNA isolated from cells encapsulated within particle gels or free cells in suspension respectively. The former was used for the estimation of cell numbers in the following experiments. Error bars representing standard deviation; N=6 samples from 2 different experiments.

5.4.2 The encapsulation and culture of NIH 3T3 cells in the particles gels (3D)

The particle gels used as 3D scaffolds in this study contained 30%$_{w/v}$ PCL and 3%$_{w/v}$ polyPEGMA$_{246}$-EE, a composition selected such that the gels were sufficiently porous (~70%) for nutrients ingress, while retaining sufficient strength to allow for manipulation during multiple cycles of cell growth, gel disassembly and splitting. Each gel was made of 150µl of suspension, giving a gel thickness of about 2mm (in 48-well culture plates).

The temperature dependent fluid-to-gel transition of the PCL/polyPEGMA$_{246}$-EE suspensions allowed for cell seeding by mixing the cells with the suspensions in their fluid state. Upon warming to 37°C, the rapid gelation locked the cells within the gel matrix, providing them with a 3D culture environment. This compares to preformed PCL scaffolds (Park et al., 2009), where an initial homogenous cell seeding is more difficult as it relies on the ability of the cells to colonise the inner parts of the scaffold.

The overall cell number remaining in the gels after 24 hours was 81± 19.5% (mean ± SD, n=8 samples), at two cell seeding densities (1 and 2 x 10^5 cells/gel). This was calculated from the ratio of the number of cells seeded to those present in the gels after 24 hours of encapsulation, as determined by the DNA quantification assay.

5.4.3 Quantification of cell viability and proliferation in the particle gels

A scaffold must maintain the viability of the encapsulated cells and support their proliferation and interaction to allow for neo-tissue formation. Cells at high density were seeded within the particle gels, to maintain sufficient cell interactions and communications.

The encapsulated cells were viable over 14 days of culture, with evidence of proliferation from both MTS and DNA quantification assays (figure 5.5).

The MTS readings increased significantly at days 3 and 7, suggesting that more cells were present. No further increase in MTS was detected at day 14 (figure 5.5A) which could be suggestive of a cease in cell proliferation. However, this is more likely to be due to limited MTS reagent diffusion into and out of the large cell clusters formed on longer cultures. This suggestion was borne out by the DNA quantification assay findings, which showed a continued cell proliferation over the 14 days of culture (figure 5.5B).

This again, came in agreement to what was reported by Ng *et al*, who found that while the MTS assay indicated a drop in the number of cells cultured in 3D scaffolds, DNA quantification assay showed the opposite (Ng et al., 2005).

5.4.4 Cell distribution within the particle gels

The assays described in the previous section are quantitative, but do not provide information on cell distribution within the gels. The opacity of the particle gels limited the range of imaging techniques that can be used to image the encapsulated cells. The common methods for imaging cells within 3D scaffolds include fluorescence or confocal microscopy, but these require a certain degree of porosity in the scaffolding material. Sectioning followed by histological staining can also provide information on the scaffolds interior, but it is tedious and destructive.

Micro-computed tomography (micro-CT) is an imaging technique that can penetrate deep into the scaffold interior and is non-destructive (Dorsey et al., 2009). Micro-CT combines X-rays with tomographical reconstruction to create 2D consecutive images (slices) of the internal structure of materials. From the 2D slices, images of the material in 3D can be reconstructed and information on its internal structure can be obtained. This technique was selected to image cells cultured within the particle gels.

A.

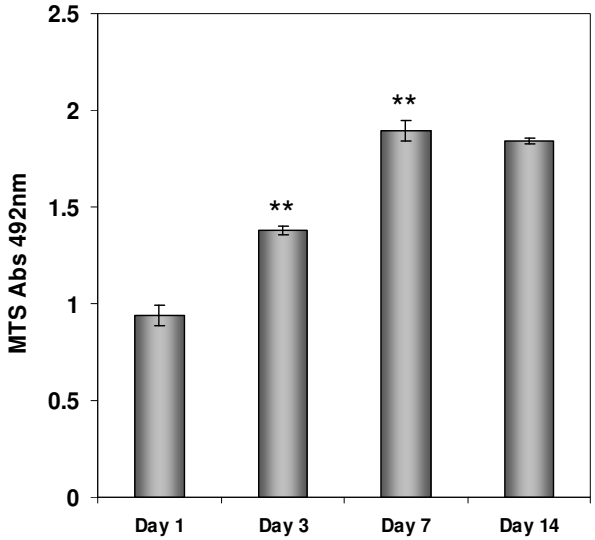

B.

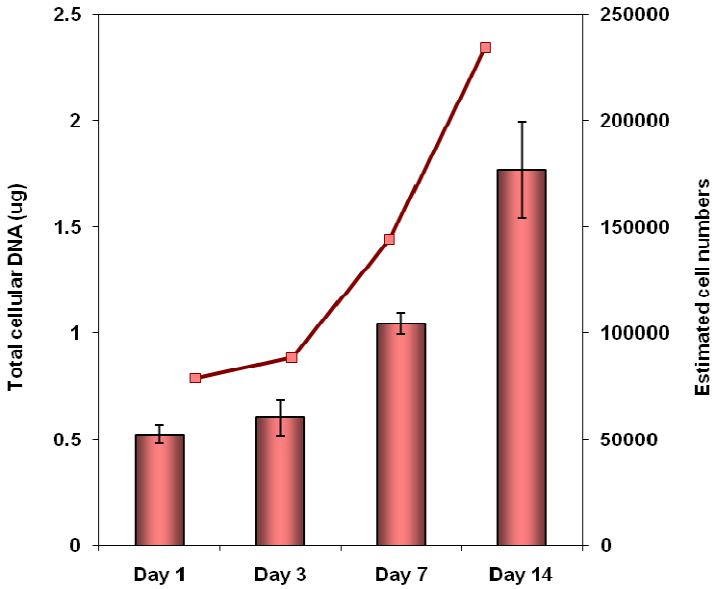

Figure 5.5: **NIH3T3 cell viability and proliferation when cultured within the particle gels for 14 days**

A. MTS assay performed on NIH3T3 cells cultured within PCL/polyPEGMA$_{246}$-EE particle gels. Error bars representing SEM for N=3 samples for each time point. Statistical significance between the readings at the different time points compared to that at day 1 was calculated using a student t-test and was denoted as : * $p < 0.05$, ** $p<0.01$.

B. Total DNA quantification for NIH 3T3 cells cultured within the particle gels over 14 days, with the line graph showing the estimated cell numbers. Error bars representing SEM for N=5 samples for each time point.

Prior to micro-CT scans, the gels were treated with osmium tetroxide, a heavy metal that stains cell membranes, to enhance their X-ray contrast. The obtained transmission images of the particle gel slices were processed and used to construct 3D models for the gels. Figure 5.6 reveals the distribution pattern of cells at different time points during culture. The cells were growing in clusters, which substantially increased in size with time. This is commonly observed with cells cultured in gels, where they tend to reform multicellular structures that are reminiscent of tissue architecture(Saltzman and Kyriakides, 2007).

An important observation from the micro-CT analysis was the tendency of the cellular proliferation to occur at the top region of the gels. While, at the beginning of culture, cells were detected throughout the gel depth, the cells were mainly located at the gels periphery at the end of culture (day 20).

One explanation for the observed pattern of cell distribution is cell death at the central regions of the gel and cell proliferation at the periphery. Sectioning and histology would provide more information on whether necrosis occurred in deeper regions of the gels. The biochemical assays (MTS and DNA quantification), however, were not suggestive of cell loss during culture but rather of continuous cell proliferation. Another explanation is that most encapsulated cells migrated towards the top regions of the gels, where molecular transport was maximal due to their proximity to the nutrient medium. More homogenous distribution of proliferating cells would have been probably obtained if the gels were exposed to nutrient media from the top and bottom, if contained in filter well-inserts for example.

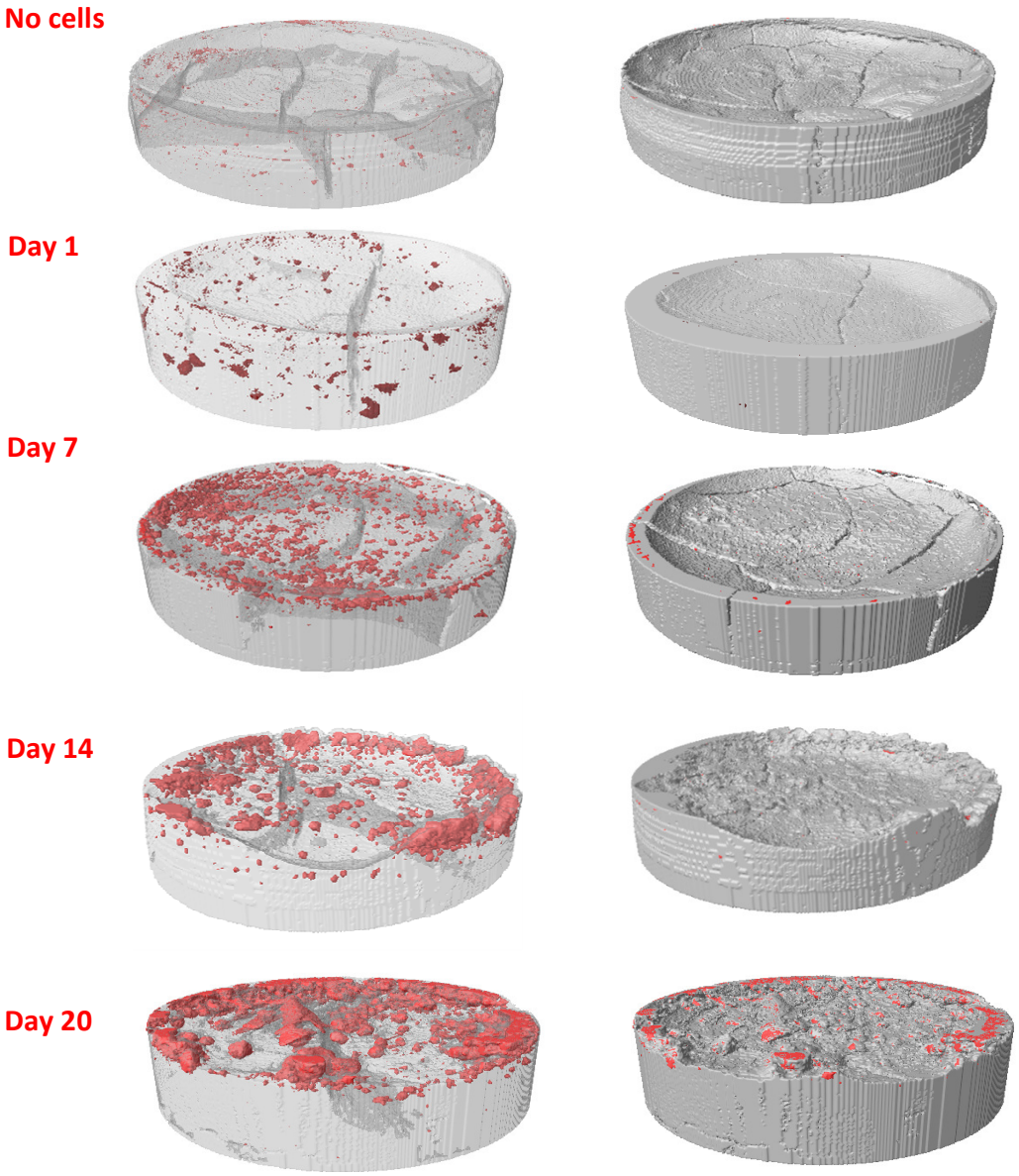

Figure 5.6: Micro-CT reconstructed 3D models of representative particle gels with encapsulated NIH 3T3 cells (red) at different time points over the 20 days culture.

Images on the left show the reconstructed particle gel models where the gel material was chosen to be merely 20% opaque to reveal the interior of the gels, while the images on the right are for the same gels but the opacity of the gel material was set to 100%. The combination of both models for each gel confirmed that NIH3T3 cells were embedded in the gel matrix.

5.4.5 Scanning electron microscopy study of encapsulated cell morphology

Following the micro-CT characterisation of cell distribution and proliferation patterns, higher resolution imaging of the individual cell clusters was obtained by SEM.

Images at early culture (figure 5.8) showed cells with spread morphology, mostly in groups. At day 7 of culture fibrous ECM secretions were seen (figure 5.9C). Figure 5.7 shows representative SEM images of gels within which no cells were encapsulated for comparison.

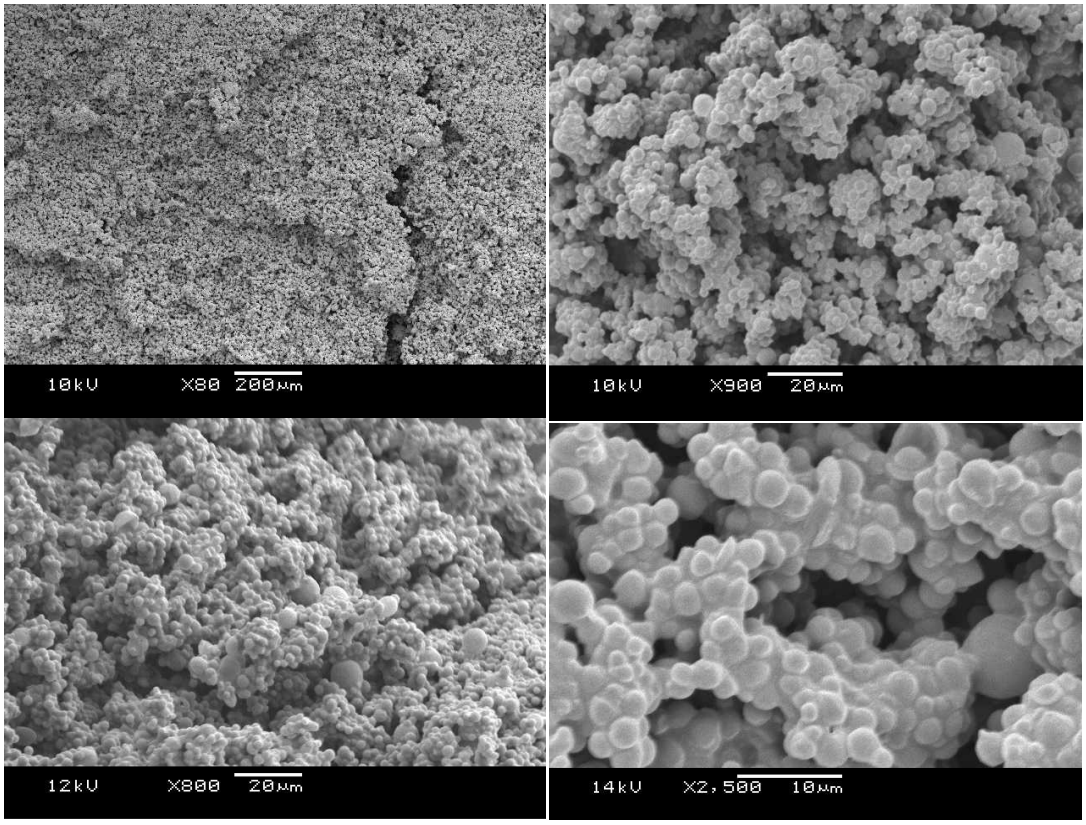

Figure 5. 7: Representative SEM images showing sections from PCL/polyPEGMA$_{246}$-EE gels NOT containing cells.

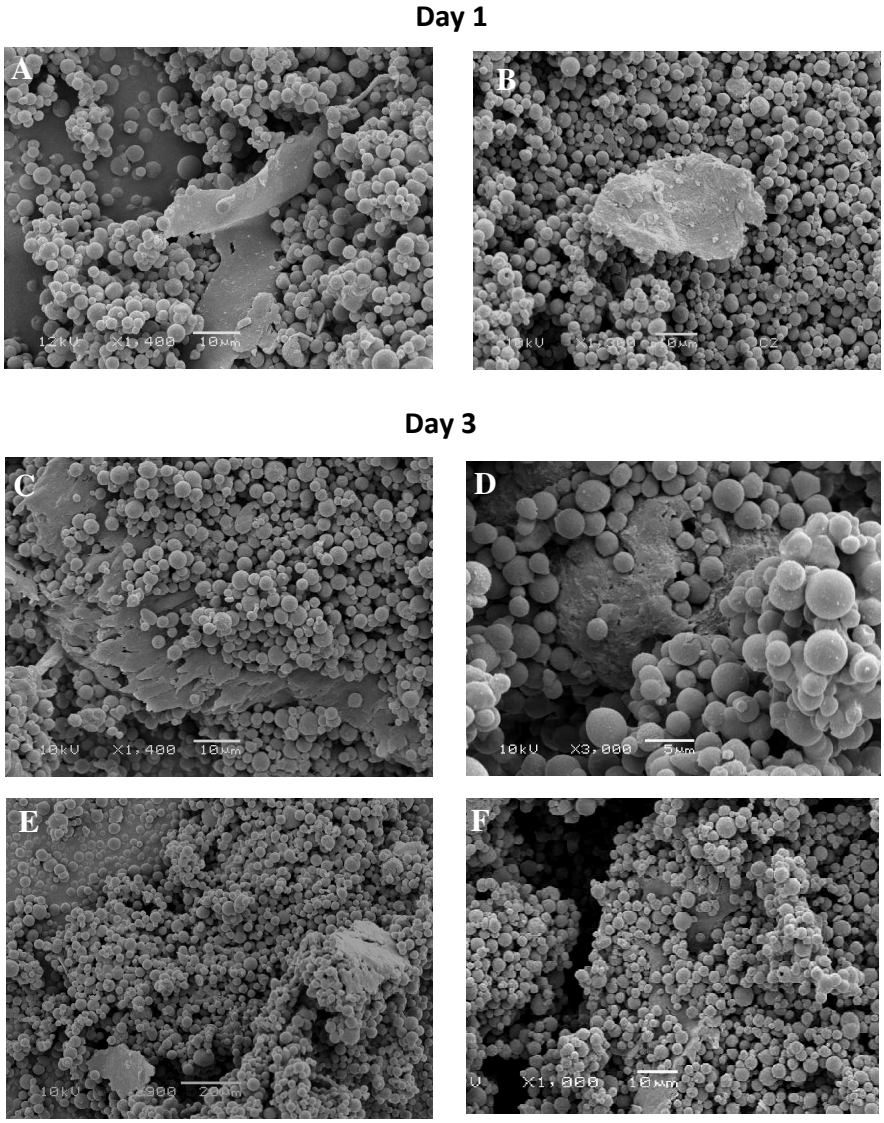

Figure 5.8: Representative SEM images of gel sections containing encapsulated NIH 3T3 cells after 1 and 3 days of culture.

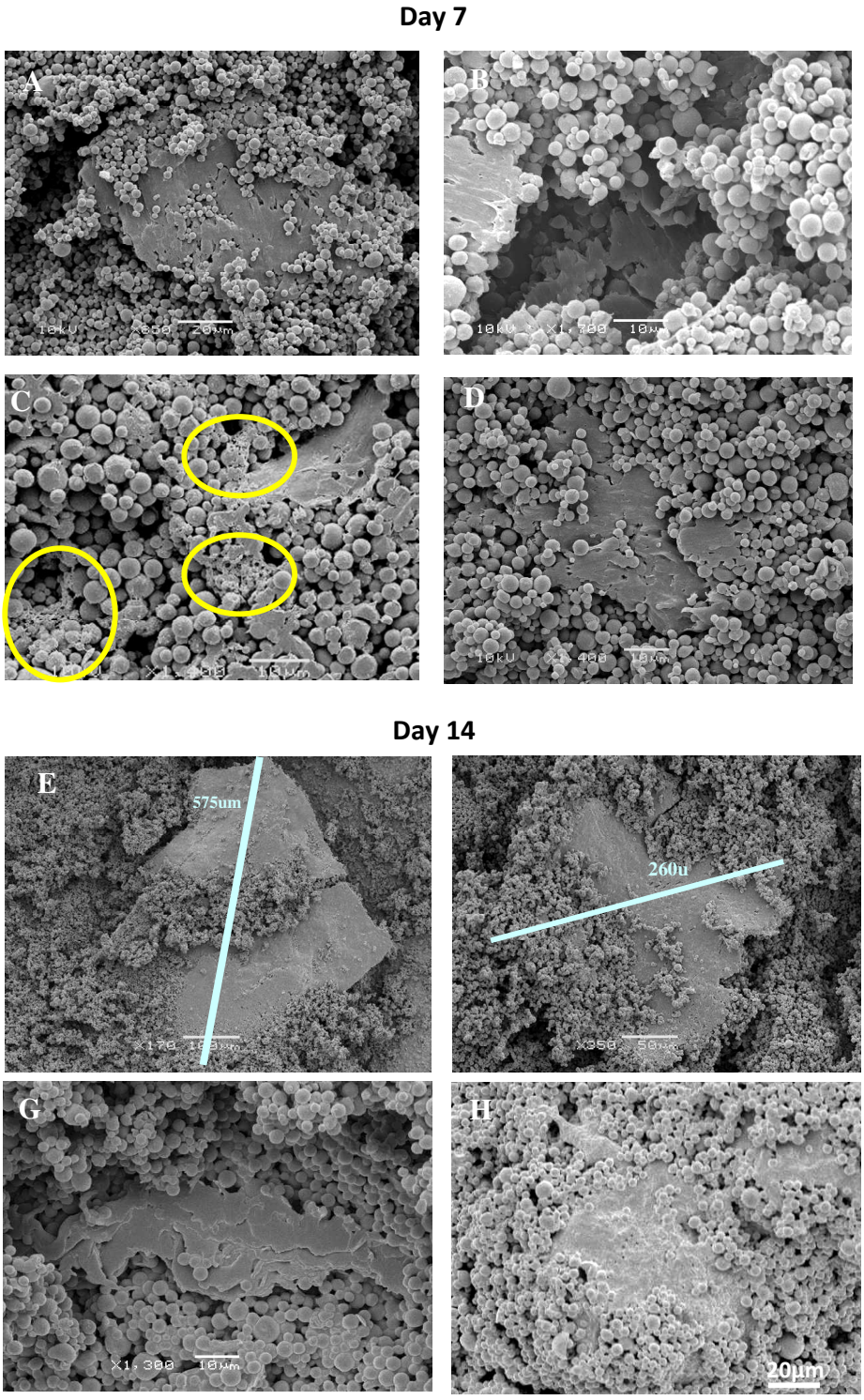

Figure 5.9: Representative SEM images of gel sections showing encapsulated NIH 3T3 cells after 7 and 14 days of culture within PCL/polyPEGMA$_{246}$-EE gels.

Note the circled fibrous ECM secretions in **C.** In **H** the image is for a group of cells located at the surface of the gel

On longer culture (figure 5.9), the cell clusters became significantly larger, suggesting the cells were actively proliferating. Some of these were as large as 0.5 mm by day 14 (figure 5.8E). Cells within the clusters had indistinct boundaries with tight intercellular junctions, which is considered a prerequisite for the successful proliferation of cells inside polymeric materials (Hesse et al., 2010). Higher magnification images revealed a multilayered tissue like structure of the cellular clusters (figure 5.10B and D) confirming the 3D pattern of cell growth.

The cells were actively interacting with their surrounding, through exploratory filopedia (figure 5.10A and D) and migratory lamelopedia as indicated by the arrows in figures 5.8H, 5.9A and 5.9D.

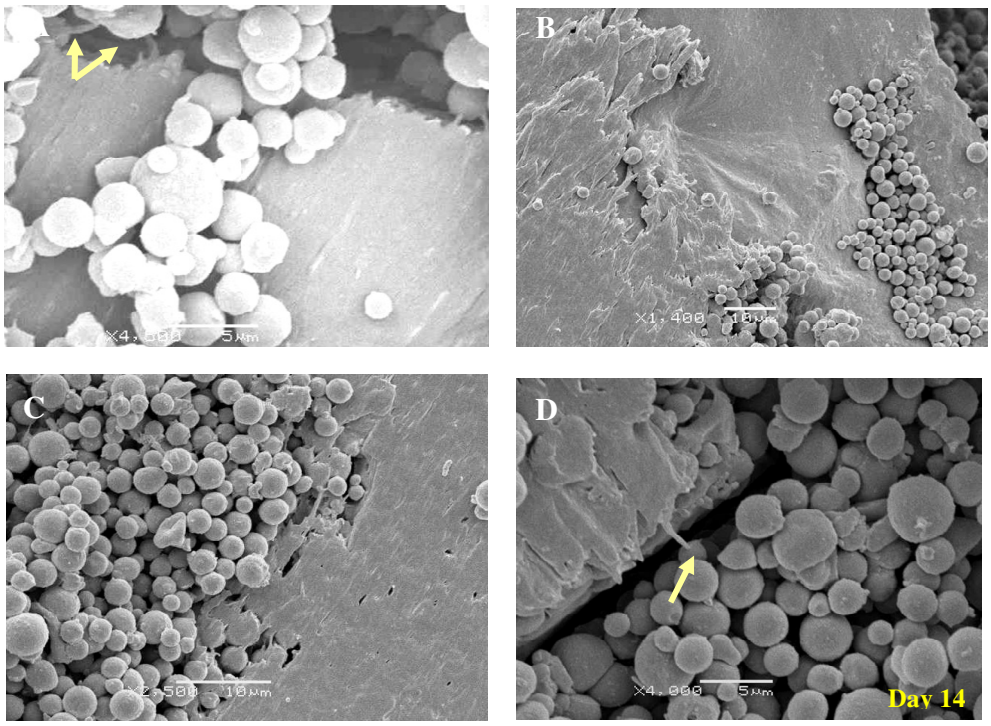

Figure 5.10: Representative higher magnification images of the NIH 3T3 cell clusters (figure 5.8E and F) after 14 days of culture within the particle gels.

The arrows in **A** and **D** point to a cell filopaedia.

5.4.6 Temperature mediated subculture for cells cultured within PCL/polyPEGMA$_{246}$-EE particle gels

A routine practice in cell culture is *cell subculture*. When the cultured cells occupy the entire available surface for growth, or those grown in suspension exhaust the medium, the culture may be transferred to a fresh culture vessel or *subcultured* (Freshney et al., 2007). If the cultured cells are adherent they must be first dislodged, usually using proteolytic enzymes, such as trypsin, which degrade the cell-ECM bonds. However, the continuous/repeated used of such enzymes might affect the long term quality of the cultured cells, especially those sensitive or undifferentiated (Steinberg et al., 1973, Huang et al., 2010). Moreover, many enzymes employed in these processes are derived from animal sources, further complicating the use of the enzymatic reagents for cell expansion and recovery for applications in human cell therapy.

Experiments detailing how the thermally triggered fluid-to-gel-to-fluid properties of the PCL/polyPEGMA$_{246}$-EE particle gels could be harnessed for enzyme free cell-subculture are given below. The experiments show how multiple cell growth cycles and processing of the cell-gel constructs was simplified by exploiting the thermoresponsiveness of the gels.

5.4.6.A Validation of the temperature – driven subculture

The efficiency of particle gels disassembly (liquefaction) and the transfer of the resulting suspension into new culture dishes was investigated. A set of gels encapsulating cells were liquefied and transferred into new wells. An MTS assay was performed on the transferred gels and non- liquefied gels were used as the control. The results, as shown in figure 5.11, indicated that about 85% of viable cells were successfully transferred, with the rest remaining in the original wells. This was likely to be due to limitations in transferring the whole suspension using the positive displacement pipettes, and possibly effects of shear forces on the cells.

Overall, the transfer process appears not to have any major detrimental effects on the cells.

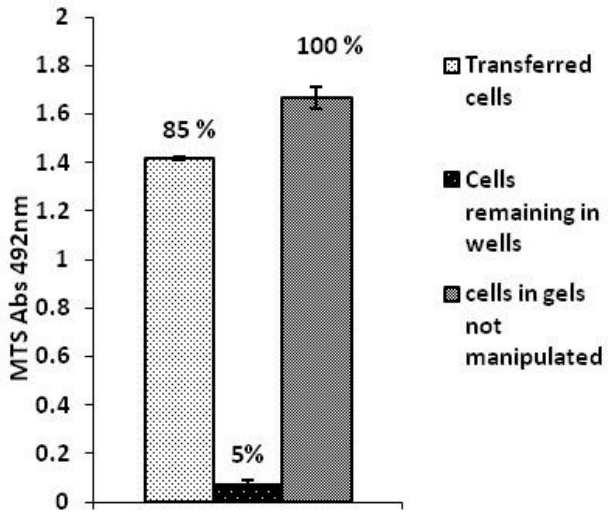

Figure 5.11: Efficiency of the transfer method of a whole gel (within which NIH 3T3 cells were encapsulated) into a new well, using a positive displacement pipette.

The control used was cells within gels not subjected to any manipulations. The percentages represent the ratio of the MTS readings of the test sample to that of the control. Error bars represent SEM for N=3 samples.

5.4.6.B The effect of subculture on the long term culture of NIH/3T3 cells in the particle gels

Temperature-driven splitting of gels within which cells were encapsulated and cultured was suggested as an alternative for trypsin-mediated cell subculture. An experiment was performed where gels with encapsulated cells, were temperature-manipulated twice during a 20-day culture. Cells at a higher density ($2X10^5$) were cultured in the gels. After a week of culture, the gels were liquefied and split into two halves. These were diluted with an equal volume of fresh suspension and then re-gelled giving two "daughter gels".

As shown in figure 5.12 the splitting (subculture) process, performed on day 7 and repeated on day 14, did not adversely affect cell viability or ability to proliferate in the diluted gels. The relative amounts of MTS product and DNA measured in the "daughter gels" were higher than those measured in the non-split gels, suggesting that the subculture process stimulated cell proliferation and growth.

A.

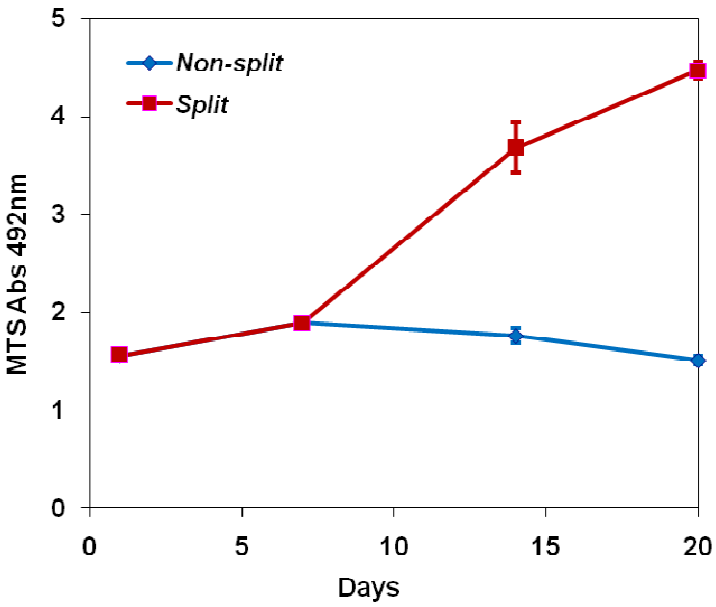

B.

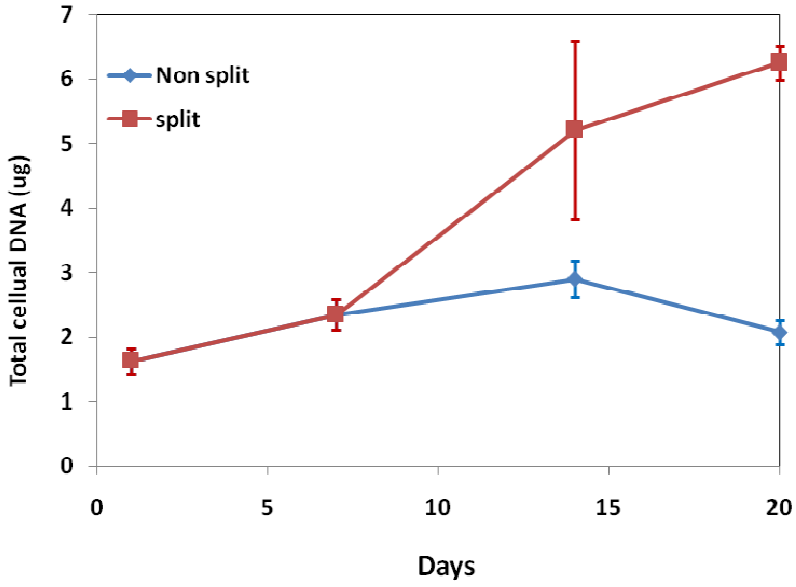

Figure 5.12: Prolonged cell culture of NIH 3T3 cells within PCL/polyPEGMA$_{246}$-EE particle gels with or without subculture.

A. MTS readings from NIH 3T3 cells cultured within the particle gels over 20 days with/without subculture (splitting). Error bars represent SEM from N=5 samples for each time point. **B.** Total cellular DNA of NIH 3T3 cells cultured within the particle gels over 20 days with/without subculture (splitting). Error bars represent SEM for N=15 samples from 3 different experiments (except for time point day 1 N= 11 samples and time point day 20 (non split) N=10 samples).

There was a small drop in cell numbers in the non-split gels after 20 days of culture, which was likely due to cell migration outside the gels. This comes in agreement with the micro-CT observations, where most of the cells were actively proliferating and getting closer to the surface with longer culture (see the gel model at day 20 in figure 5.7).

In some gels it was observed that the cells migrating towards the walls of the culture vessel, eventually formed a contractile fibre structure indicated by the arrows in figure 5.13, which is an observation that was previously reported for fibroblasts (James and Taylor, 1969).

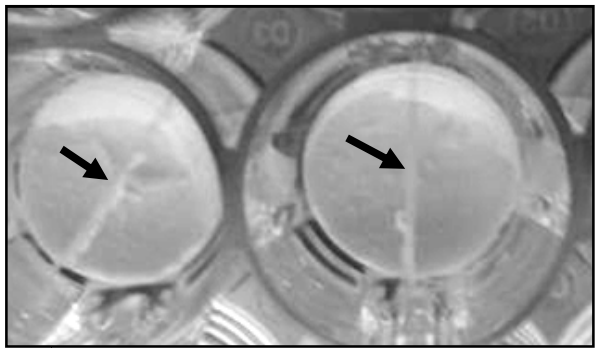

Figure 5.13: The contracted cell sheet which migrated from the gel surface on prolonged culture (day 20).

5.4.6.C The distribution of cells in the split gels

One limitation of the temperature-driven subculture process was the difficulty of dividing the original group of cells equally between the new gels, since the original suspension was randomly split into two halves (figure 5.14). However, metabolically active (viable) cells were present in all split gels (figure 5.14A and B), which confirms the efficiency of the subculture process to distribute the cells, although not equally, to all the new gels following subculture (figure 5.14 C and D).

The random cell distribution was also portrayed in the micro-CT reconstructed 3D models of the "daughter gels" shortly after subculture. Although both gels contained cells, one had less cells than the other (figure 5.15).

Additionally, micro-CT revealed smaller cell clusters distributed throughout the gel depth shortly after subculture, compared to the parent gel containing larger cell clusters mainly at the top (figure 5.16).

Larger cell clusters were detected in the gels after 7 days following subculture (figure 5.16), which constituted a qualitative evidence for cell proliferation in the daughter gels, as well as in the parent gel.

Again the cell clusters were mostly located near the gel periphery for superior access to oxygen and nutrients.

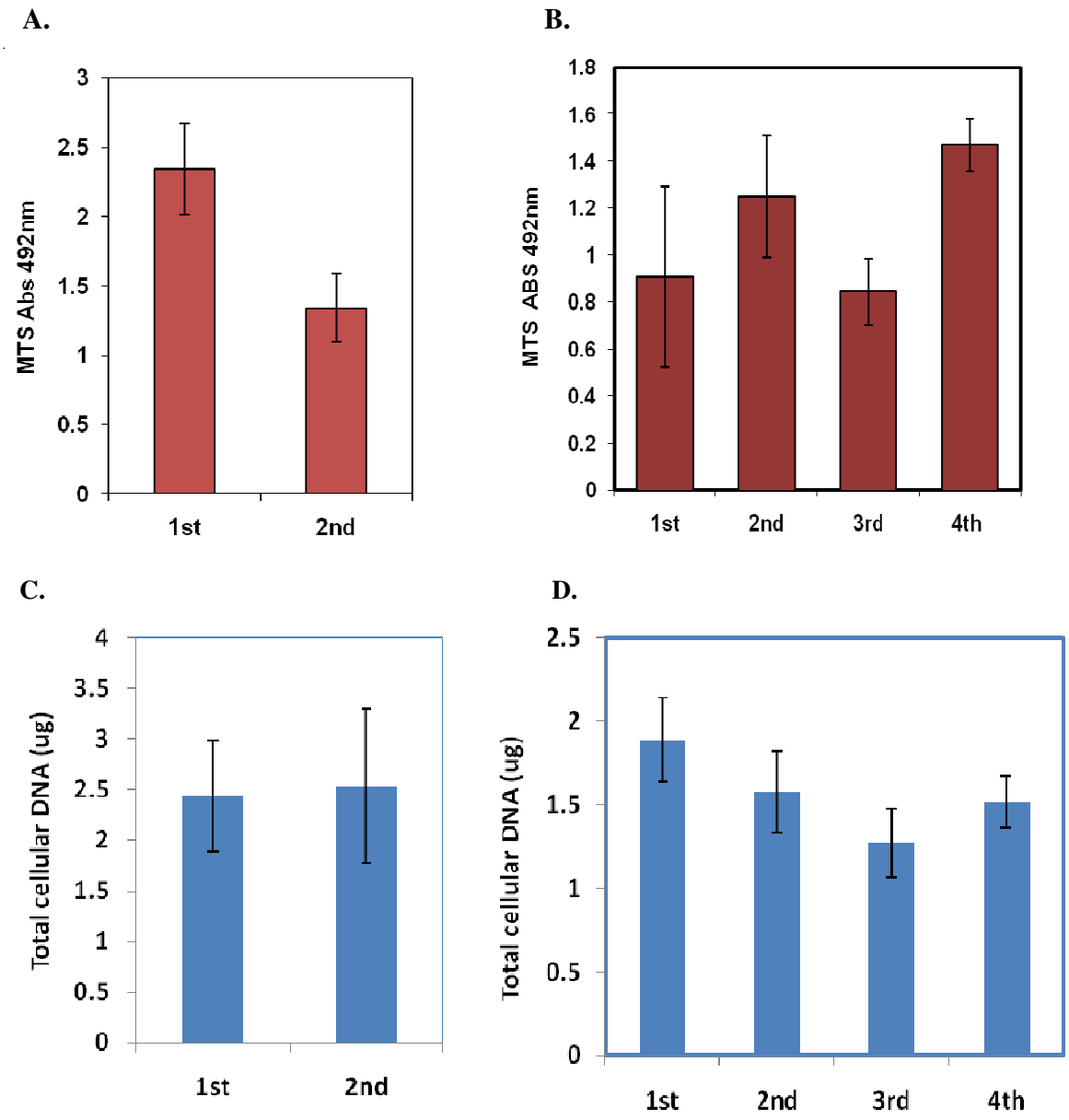

Figure 5.14: The efficiency of the temperature subculture process.

A and B: NIH3T3 cell viability, as measured by the MTS assay, in the two (**A, labelled 1st and 2nd**) and four (**B, labelled 1st, 2nd, 3rd, 4th**) daughter PCL/polyPEGMA$_{246}$-EE particle gels after 14 and 20 days of culture respectively. The initial "parent" gel was split on day 7 of culture and splitting was repeated on day 14. Error bars are SEM for N=5 samples.

C and D: DNA quantification as an estimate for NIH3T3 cell number in the two (**C**) and four (**D**) daughter gels after 14 and 20 days of culture respectively. The initial "parent" gel was split on day 7 of culture and splitting was repeated on day 14. Error bars represent SEM for N=15 samples from 3 different experiments.

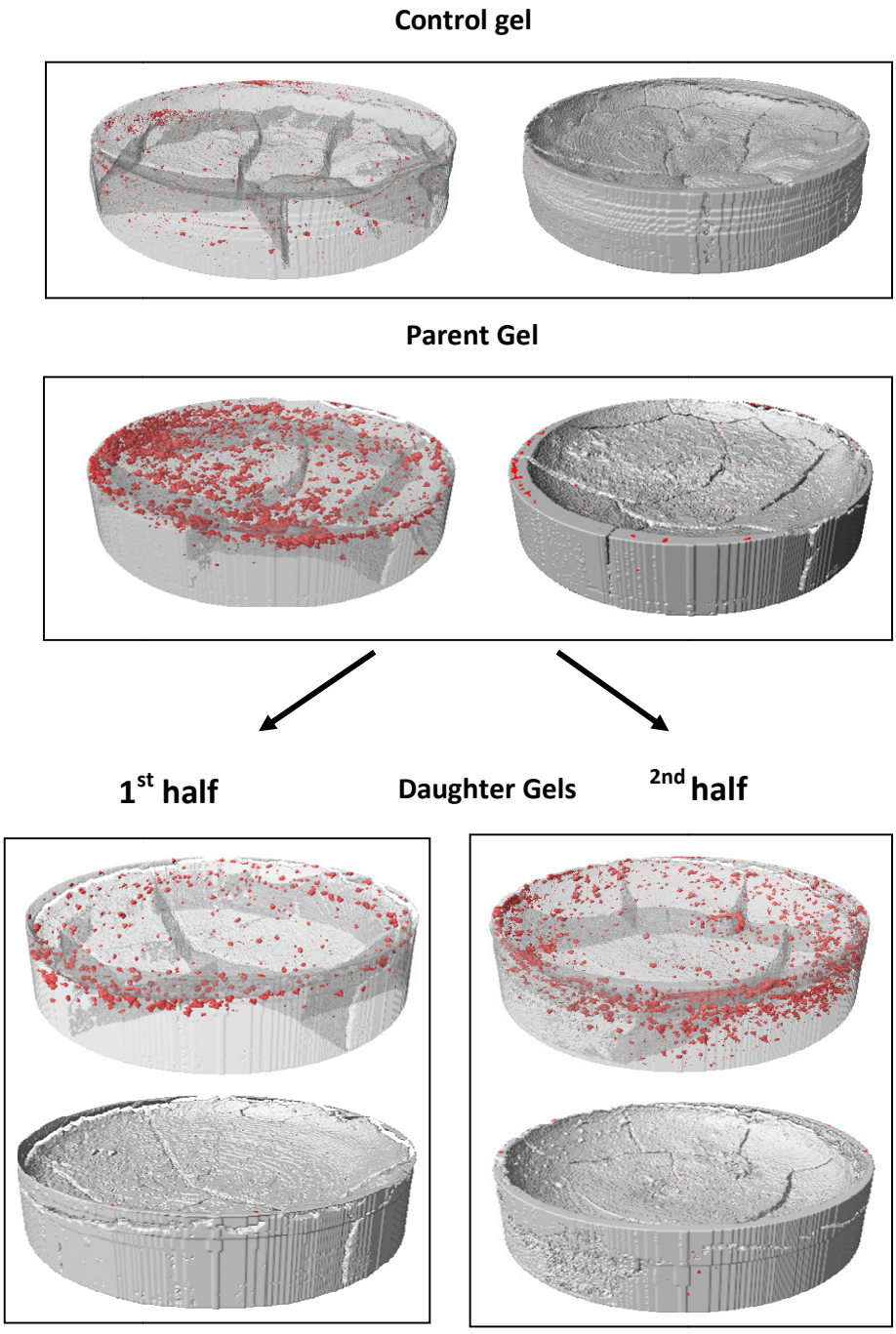

Figure 5.15: Micro-CT reconstructed 3D images of gels (with encapsulated cells) which were split after 7 days of culture. The images are of the gels shortly after subculture.

Images show the reconstructed particle gel models where the gel material was chosen to be merely 20% opaque to reveal the interior of the gels, or 100% opaque. The combination of both models for each gel (placed within the same box) confirmed that NIH3T3 cells were embedded in the gel matrix.

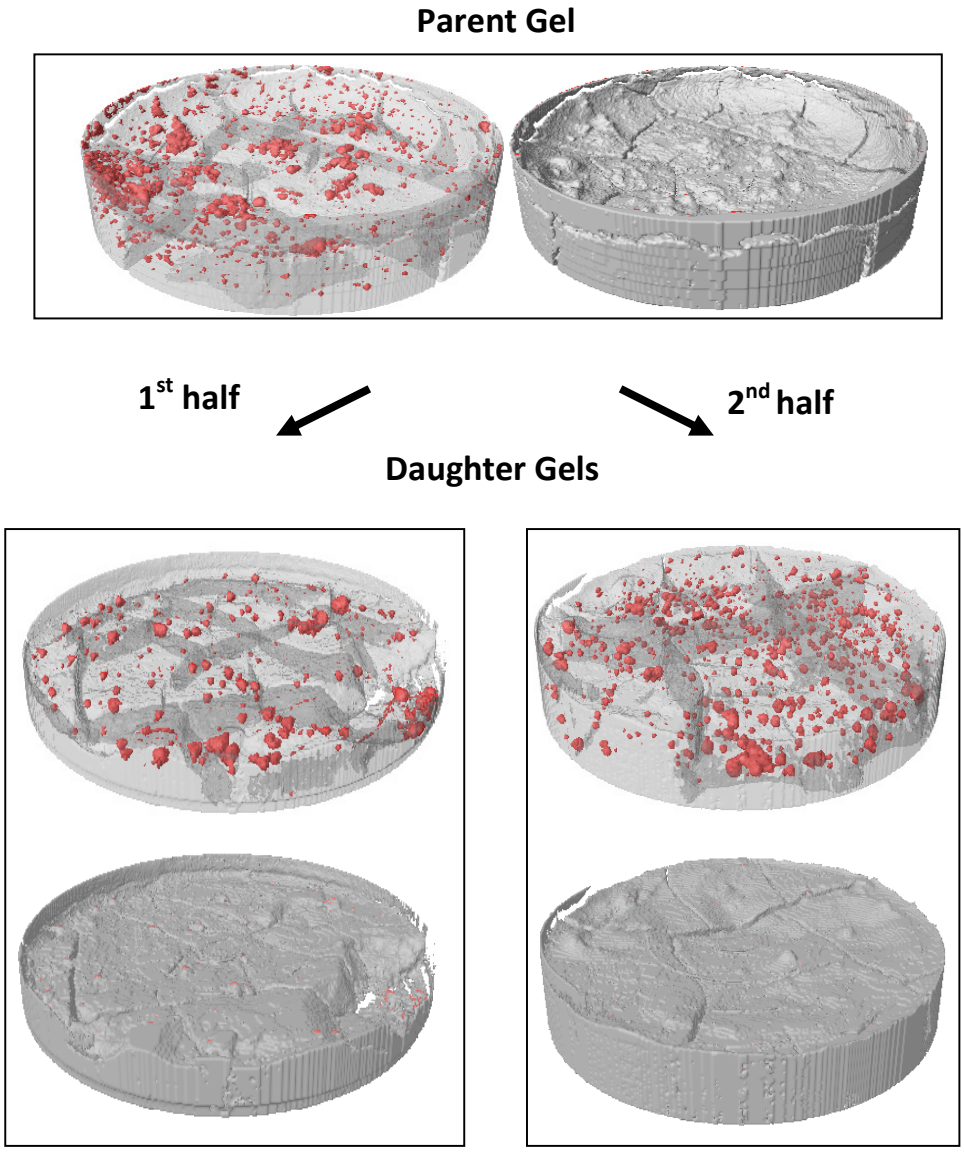

Figure 5.16: Micro-CT reconstructed 3D images of gels after 14 days of culture.

The daughter gels were obtained on day 7 of culture and were cultured for 7 further days after which the micro-CT analysis was performed. Images show the reconstructed particle gel models where the gel material was chosen to be merely 20% opaque to reveal the interior of the gels, or 100% opaque. The combination of both models for each gel (placed within the same box) confirmed that NIH3T3 cells were embedded in the gel matrix.

5.4.7 Injectability of PCL/polyPEGMA$_{246}$-EE Particle Gels

Thermoresponsive particle gels could ultimately be applied as injectable scaffolds. Because they can gel reversibly, the cells can be grown within the particle gels *in vitro*, and then the conditioned gel–cell construct can be liquefied and injected.

Due to time limitations, experiments to exemplify such applications were not conducted. However, a proof of concept preliminary demonstration, shown in figure 5.17, would support such a suggestion.

A chilled (10°C) PCL/pPEGMA$_{246}$-EE suspension was injected using a 23G needle into a warm PBS bath (37°C). The suspension became more viscous on injection forming "gelled precipitates".

The injected suspension was monitored over the following 25 days. The gels pink colour was quickly lost (2hours after) as a result of the rapid diffusion of its content of phenol-red into the water bath. Hence, there existed active diffusion between the precipitates and their environment.

The precipitates maintained their structure and shape over at least 25 days without disintegration in the aqueous medium. This was a crude demonstration of the shape matching capability of these suspensions, if they were to be injected into a cavity at a site of interest *in vivo.*

A.

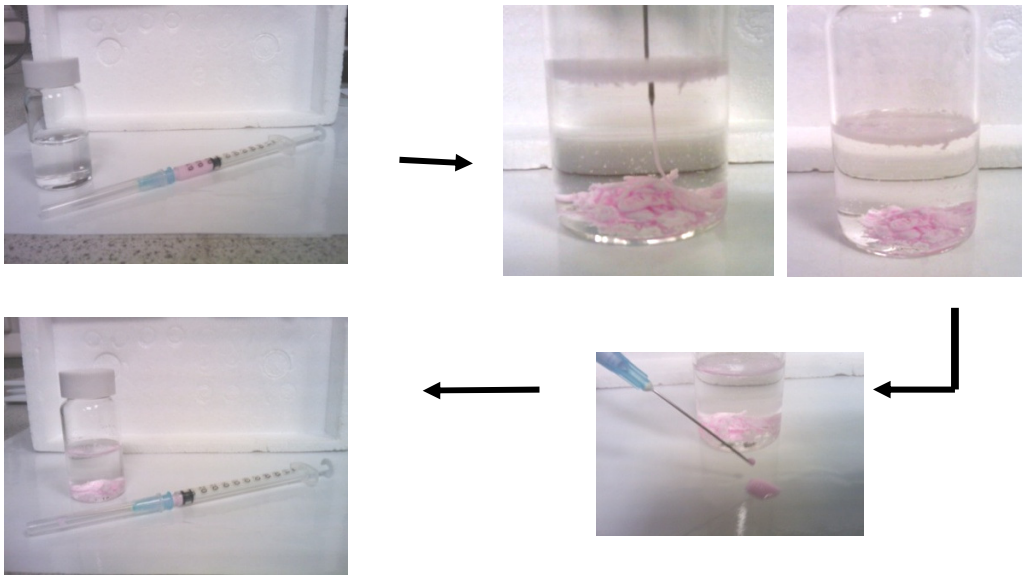

B. After:

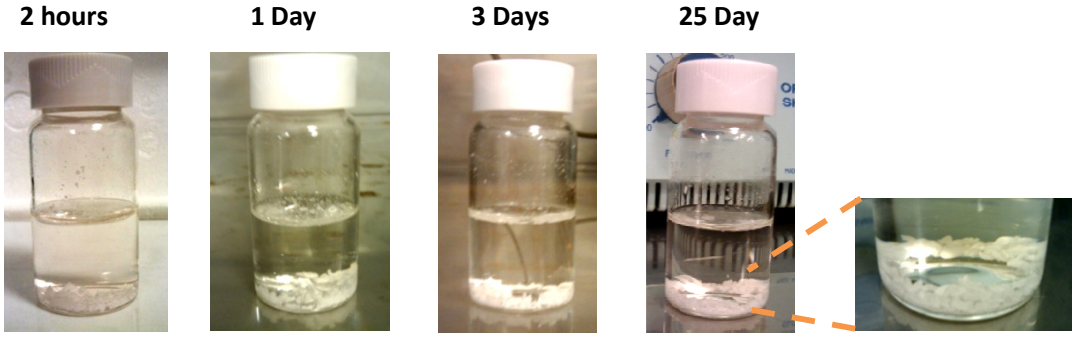

Figure 5.17: A. Injectability of PCL/polyPEGMA$_{246}$-EE suspension (25%$_{w/v}$-2%$_{w/v}$) into a 37°C PBS bath using a 23G needle. B. The injected suspension (flocs) up to 25 days following injection into the warm PBS bath.

5.5 Discussion

The main aim of the work described in this chapter was to explore the use of thermoresponsive particle gels, a class of material not previously applied in tissue engineering, as cell scaffolds. Following on from the study on the cytocompatibility of PCL/polyPEGMA$_{246}$-EE particle gels described in chapter 4, cell encapsulation and their subsequent distribution, viability and proliferation were the main criteria selected to evaluate the ability of particle gels to support the 3D culture of NIH3T3 fibroblasts, used as a model mammalian cell line.

MTS and DNA quantification assays, with optimised protocols for the 3D culture settings, were used to quantify cell viability and proliferation respectively. The MTS assay findings confirmed the maintenance of cell viability following cell encapsulation and culture for at least 20 days within the particle gels. This was supported by the DNA quantification assay findings, which showed that the cells were proliferating continuously while in 3D culture, although at a slower rate than that recorded for NIH3T3 cells when cultured on tissue culture plastic. Micro-CT observations confirmed cellular proliferation during culture, where the cells were distributed and growing in clusters, which is typical of cell behaviour when cultured in 3D. Higher magnification images of these cell clusters, obtained by SEM, confirmed their multicellular nature, and indicated favourable cell interactions with the scaffold through exploratory filopedia and migratory lamellopedia.

The cells were well distributed within the particle gels shortly after encapsulation, but cell migration towards the top region of the gels became more apparent with time, as observed by micro-CT. This cell localisation pattern was probably driven by the highest availability of nutrients and oxygen at the regions of the gels most proximal to the nutrient media. In the deeper regions, the limited diffusion restricted the exchange of nutrients, metabolic wastes and molecular signalling, with oxygen being generally the main factor affecting cell survival and

tissue growth due to its low solubility, slow diffusion and high consumption rate. Moreover, as the density of cells in the peripheral regions of the gels increased, the distribution and availability of nutrients to cells within the scaffold interior was more likely to be further limited (Luo et al., 2007). On the other hand, the observed cell migration and redistribution in the gels reflected the flexible nature of the particle gels with their physical crosslinks, which would allow for cell remodelling of their culture environment.

Indeed, molecular transport is a key issue in tissue culture. In engineered tissue constructs cultured under static conditions without medium perfusion (which was the case with the particle gels), neo-tissue formation is generally limited to the peripheral 100-200μm of the scaffold due to diffusion limitations. This compares to the situation *in vivo* where most cells reside within 100μm of a capillary (Luo et al., 2007). Various strategies have been attempted to improve molecular diffusion within tissue scaffolds through the introduction of larger and denser pores in the scaffold structure (Hollister, 2006). A higher degree of porosity can be built into the particle gels by incorporating gelatin microparticles that can be degraded by cells, or by decreasing the solids concentration in these gels if smaller particles are used.

Overall, the results confirmed the ability of the thermoresponsive PCL/polyPEGMA$_{246}$-EE particle gels to support prolonged 3D culture of NIH3T3 cells.

In addition to being able to control their mechanical properties by varying their composition, these gels have the unique advantage of assembling and disassembling rapidly and reversibly in response to a mild temperature change. This property was harnessed for the non-enzymatic subculture of encapsulated cells. Gels in which cells were encapsulated and cultured were liquefied, split into two halves, and then gelled again giving two new gels, with the original

cell population split between them. This subculture process, performed twice during a 20 day culture, was found to maintain cell viability and proliferation as confirmed by MTS and DNA assays. Micro-CT confirmed the presence of cells in the new diluted gels, and the continued cell growth.

These reversible thermo-gelling properties would also allow for the injection of cell-gel constructs pre-conditioned *in vitro*, and their re-solidification *in vivo* driven by the temperature change. The cells with their secreted ECM, or even tissues formed *in vitro*, would be easily transferred to the target tissues by injecting the liquefied constructs. This would be expected to aid their integration with the host tissue and facilitate tissue regeneration.

Using PCL/polyPEGMA$_{246}$-EE particle gels as cell scaffolds offers another level of control on the cells cultured within through the incorporation of growth factors or other biomolecules within the particles. A common method for controlling the release from a scaffold involved the pre-fabrication of biofactor loaded particles and embedding them into a scaffold matrix. This method takes advantage of established systems (Freiberg and Zhu, 2004), but involves double matrices, which influence the release profile. Although no experimental data were presented in this chapter to support this proposition, building on the established technology of microparticle-based protein delivery, the particles in the PCL/polyPEGMA$_{246}$-EE gels can be designed to encapsulate various biomolecules and growth factors, which can be released at different rates. The particles would then serve the spatial role of supporting cellular adhesion, as well as the temporal role of delivering growth factors or other therapeutic factors. This has already been reported for PCL scaffolds made from heat-sintered PCL microparticles encapsulating growth factors (Luciani et al., 2008). However, the added advantage of the PCL/polyPEGMA$_{246}$-EE particle gels is that scaffold formation (gelation) occurs around the physiological temperature,

while high temperatures are required for particle sintering which can be detrimental to the encapsulated bio-actives.

5.6 Conclusions

Extended cell culture experiments with NIH 3T3 fibroblasts, as a model cell line, indicated cell viability was maintained and that cells proliferated within the PCL/polyPEGMA$_{246}$-EE gels.

Taken together, the experiments described in this chapter showed the materials exhibited key characteristics advantageous for the 3D culture of cells:

(a) Ability to assemble around the cells at temperatures above the LCST of polyPEGMA$_{246}$-EE and provide a supportive scaffold with appropriate mechanical properties for growth.

(b) Good cytocompatibility enabling cell spreading and proliferation over extended culture times.

(c) Rapid return to a flowable state on cooling enabling suspension transfer for cell subculture and harvesting, and also for injectable delivery of cell-gel constructs for therapeutic applications.

While scaffolds made of sintered microparticles have been reported, constructing scaffolds from microparticles through physical crosslinks solely has not been reported previously. The ability to construct and deconstruct PCL scaffolds on demand, with simple change in temperature shall open up many avenues for novel applications of these materials in cell culture and injectable cell delivery.

CHAPTER 6

Thermoresponsive magnetic-particle gels as cell scaffolds

6.1 Introduction

Stimuli responsive materials offer many advantages for biomedical applications (De Las Heras Alarcon et al., 2005). Various stimuli, such as temperature, light, pH or magnetism could be employed to induce significant changes in the mechanical and physical properties of such materials. Such changes could be harnessed for various applications in drug delivery and tissue engineering (Chaterji et al., 2007).

Magnetic materials have found a variety of applications in cell separation, drug delivery and hyperthermia of biological tissues (Gupta and Gupta, 2005). Magnetically responsive microspheres can be used *in*-vitro to remove specific bound cells and molecules, and also *in*-vivo to target and hold the magnetic carriers at specific sites (Dobson, 2010). The latter is an innovative approach capable of effective drug targeting, where upon intravenous administration, the magnetic carriers can be accumulated within an area to which a magnetic field is applied.

In the previous chapters, the development of particle gels based on polycaprolactone microparticles (PCL) and the thermoresponsive polymer polyPEGMA$_{246}$-EE was described. The

particle gels supported the 3D culture of mouse fibroblasts, and their thermoreversible gelling behaviour allowed for simpler processing of the cell-loaded gels.

The PCL/polyPEGMA$_{246}$-EE particle gels are well suited for the traditional tissue engineering paradigm of using the therapeutic combination of cells, scaffold and biomolecules as an injectable or implantable construct (Langer and Vacanti, 1993).These particle gels can also be used for the expansion of cells *in*-vitro, although the difficulty in doing so lies in recovering the cultured cells or formed tissues from the gel matrix at the end of culture if a scaffold-free outcome is desired.

Recovering pure cell suspensions from the liquefied gels (suspensions) is challenging, since the particles are of a comparable size to many eukaryotic cells, which hinders their separation by size filtration.

Other cell separation techniques that could be used include magnetic cell separation, which has been widely employed for the recovery of cells from mixtures or crude samples such as blood, tissue homogenates and stools (Safarik and Safarikova, 1999).

The magnetic separation technique is based on the contrast of magnetic susceptibility between the separand (magnetic) and medium (containing other non-magnetic materials). Most cells, with the exception of erythrocytes and magnetotactic bacteria, have to be labelled to become susceptible to the magnet exposure.

Magnetic particles are commonly used to label cells, where some ligands (antibodies, strepatvidin...etc) recognisable by the target cells are immobilised on their surface. Upon incubation with the sample, the target cells bind these ligands and the complex formed can be separated in a magnetic separator.

A number of particulate magnetic labels are commercially available, such as the monosized polymer particles marketed as *Dynabeads* (Dynal, Oslo, Norway). These consist of an iron-containing core surrounded by a polystyrene shell to which biomolecules, such as antibodies, may be adsorbed. The diameter of magnetic particles used is typically 1–5μm, and the technique is usually referred to as immunomagnetic cell separation when antibodies are used (see figure 6.1).

Magnetic cell separation can be achieved through the negative or positive selection of cells. In the former, the target cells are purified by removing all other cell types from the sample by magnetic separation, while in the latter the target cells themselves are separated out. The positively selected cells may, in many cases, be analysed with the particles attached on them. In some cases, it is necessary to remove the particles from the cells after their isolation. This can be achieved via the application of shear (repeated pipetting through a narrow tipped pipette) or the use of proteolytic enzymes. The released magnetic particles can then be removed from the purified cell suspension using a magnetic separator (Dynal, 1996).

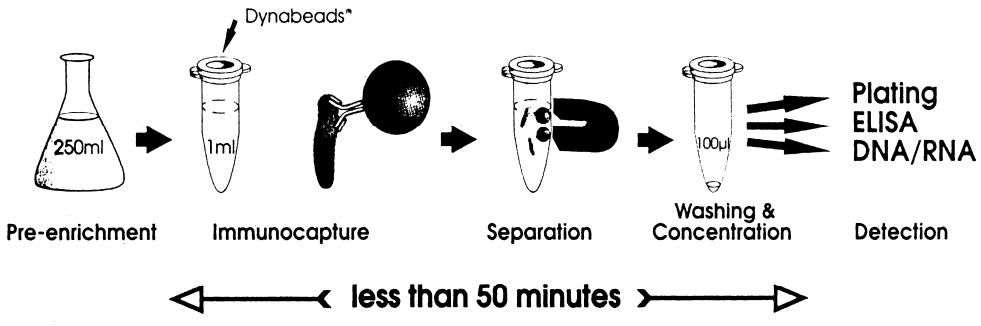

Figure 6.1: The principle of immune-magnetic separation of target microorganism using Dynabeads.

Taken from (Dynal, 1996).

Most particles used in magnetic cell separation are super-paramagnetic, that is they only exhibit magnetic properties in the presence of an external magnetic field. The particles are, therefore, not attracted to each other and can be easily suspended into a homogeneous mixture in the absence of an external magnetic field, and removed from suspension in a simple magnetic separator (Safarik and Safarikova, 1999)

Inspired by the use of magnetic particles for cell separation as described above, magnetism was considered as a means to separate particles from cells, in a magnetic separator, for cells cultured within particle gels used as scaffolds. Hence, in this chapter is discussed the development of thermoresponsive magnetic particle gels, and the added advantages such materials can offer if used as cell scaffolds particularly with regards to cell recovery.

6.2 Aim and objectives

The work in this chapter aims to: “Demonstrate the recovery of cells encapsulated within thermoresponsive magnetic particle gels”. This was achieved through the following objectives:

1. The preparation of thermoresponsive magnetic particle gels.
2. The characterisation of the rheological properties and the temperature responsiveness of the magnetic particle gels developed.
3. The recovery of viable cells from a suspension of magnetic particles in a magnetic separator.
4. The recovery of cells encapsulated within magnetic particle gels by magnetic separation with maintenance of cell viability.

6.3 Materials and Methods

6.3.1 Magnetic microparticles

Magnetic microparticles (Fluka, UK), of 5µm size, based on polystyrene (PS) and containing 20%$_{w/v}$ iron oxide were purchased from Sigma-Aldrich (Poole, UK).

The purchased magnetic PS particles suspensions were diluted and taken through multiple centrifugation/re-dispersion washes with deionised water to remove any potential contaminants (e.g. surfactants). The particles were then lyophylised and characterised by SEM as described in chapter 2 (2.2.3).

6.3.1A Surface modification of the magnetic particles

A surface modification step was required to render the purchased magnetic particles sufficiently hydrophobic to build thermoresponsive particle gels.

The magnetic PS particles were subjected to plasma polymerised hexane (ppHEX) deposition, carried out with the help of Dr. Lloyd Hamilton (Tissue Engineering Group, University of Nottingham). The details of the plasma process were given in (Alexander and Duc, 1998), and a brief description of the process is given below.

The plasma reactor used consisted of a cylindrical borosilicated glass T-piece closed with stainless steel end plates sealed with Viton O-rings. A radiofrequency generator (13.56 MHz) was capacitively coupled to two external inductively coupled copper band electrodes, used to initiate the plasma. The power was matched manually such that the reflected power was <1W. The gas pressure was monitored via a Pirani gauge and controlled by needle valves.

The hexane monomer was degassed by at least three freeze–thaw cycle prior to use. The flow of hexane vapour and oxygen into the glass chamber was adjusted using manual needle

valves (BOC Edwards). Liquid nitrogen and alumina traps were used to prevent contamination of the rotary pump with condensable plasma products and the plasma reactor by pump oil (Fomblin) respectively.

The particles were thinly spread in petri dishes, and frequently shaken during the plasma polymerisation process to ensure homogenous surface modification.

First, the particles were subjected to three 5 minute cycles of oxygen etching at the settings shown in table 6.1A. These were followed by 5 cycles of hexane plasma polymerisation (to a ppHEX cumulative thickness > 4 kA°), the settings of which are shown in table 6.1B. Following plasma polymerisation, the ppHex- modified particles were washed to remove any excess monomer or other residual contaminants. This was achieved by initially re-dispersing the particles in polyPEGMA$_{246}$-EE solution (0.2%$_{w/v}$) at 50mg/ml, followed by 3 cycles of centrifugation/re-dispersion washes with deionised water, all performed at 10°C.

A.

Power	Time	Incident	Reflected	Base pressure	Working pressure
20W	5 minutes	20.3	0.5	9mtor	340mtor

B.

Power (W)	Rate (A°/S)	Total Thickness (KA°)	Incident	Reflected	Base pressure	Working pressure
20	2.1	4.166	20.5	0.2	9mtor	330mtor

Table 6.1: Details of the plasma polymerisation experiment parameters (power, thickness, time, incident, reflected, base pressure and working pressure).

A. Parameters during the oxygen etching cycles. **B.** Parameters during the ppHEX deposition cycles.

6.3.2 Confirmation of magnetic particles surface modification

For a relative confirmation of the particles surface modification and ppHEX deposition, WCA measurements were taken for PS magnetic particles derived films, subjected to the same plasma process, as was described in section 6.3.2. PS particles (100mg) were added to 2 ml of dichloromethane to dissolve the PS fraction leaving a fine suspension of iron oxide. The dissolved fraction, with the suspended iron oxide, was cast onto glass slides and left to air dry at room temperature in order to form films. The WCA values of the films measured before and after plasma-treatment were compared.

6.3.3 Preparation of the thermoresponsive magnetic particle suspensions/gels

The gels were prepared from suspensions of ppHex-modified polystyrene magnetic particles (33%$_{w/v}$) and polyPEGMA$_{246}$-EE (2-3%$_{w/v}$) in complete medium.

6.3.4 Synthesis of polyPEGMA$_{246}$-EE

The thermoresponsive polymer polyPEGMA$_{246}$-EE was synthesised by free radical polymerisation as described in chapter 3. The polymer had a number average molecular weight of Mn=33KDa with PDI=1.9 (based on polystyrene standards), as determined by GPC performed as described in chapter 3 but using chloroform as a solvent at 30°C. The LCST of the polymer was 19°C in complete medium.

6.3.5 Characterisation of the magnetic particle gels

Sample gels containing 33%$_{w/v}$ magnetic PS particles and 3%$_{w/v}$ polyPEGMA$_{246}$-EE were characterised by rheology. The tests were performed in an Anton Paar Physica MCR 301 rheometer, with a 25mm diameter serrated parallel plate at 0.6mm gap (see chapter 3, section 3.3.13, for a further description on the rheological tests). To minimise solvent evaporation a

solvent trap was used and the external chamber was filled with water. The gels were characterised using the following two oscillatory tests:

- **Strain amplitude sweep:** This was performed between 1 and 100% strain amplitude (at an angular frequency ω of 10 rad/sec) to determine the linear viscoelastic region of the gel at 37°C.
- **Heating-cooling cycles:** An oscillatory rheology test was conducted on a sample magnetic particle gel to determine the effects of temperature on the rheological properties of these materials. The gel was subjected to 3 cycles of consecutive heating to 37° C followed by cooling to 10°C, under an oscillatory strain of 0.01% applied at an angular frequency ω of 10 rad/sec, while the G' (storage) and G''(loss) moduli for the gels were being recorded.

6.3.6 Cell recovery by magnetic separation

NIH 3T3 cells maintained as described in chapter 2, were used in the following experiments. The cells were of passages 15-17. All experiments were carried out in triplicate.

6.3.6A Recovery of cells from cell/magnetic particles suspensions

Magnetic particles (as purchased) were suspended in cell nutrient media (complete medium) at 33%$_{w/v}$. In a 1ml eppendorf, 100µl of this suspension was mixed with 20µl of cell suspension containing 2X10^5 cells. The mixture was diluted with 1ml of complete medium, and then exposed to the MACS® magnetic separator (Multinye Biotec, Germany) (Miltenyi et al., 1990) for 1 minute. The magnetic PS particles sedimented while the cells remained suspended (figure 6.2). The cell suspension was collected and seeded onto tissue culture plastic. The process was repeated twice by redispersing the particles and re-aggregating them, collecting the suspended cells each time, to maximise cell recovery.

6.3.6B Recovery of cells encapsulated within magnetic particle gels by magnetic separation

In a 1-ml eppendorf tube 100µl of a suspension, containing ppHex-modified magnetic particles 33%$_{w/v}$ and 2%$_{w/v}$ polyPEGMA$_{246}$-EE, was mixed with 20µl of cell suspension containing 2x10^5 cells. The mixture was gelled at 37°C for 2 minutes, and then liquefied by cooling at 4°C for 2 minutes. The obtained suspension was diluted with 1 ml of chilled PBS, and this was centrifuged at 180Xg for 5 minutes.

The wash/centrifugation step was introduced to remove excess polyPEGMA$_{246}$-EE, which was expected to interfere with the particles aggregation/re-dispersion during the magnetic separation process performed at room temperature. Following centrifugation, the particles/cells were re-suspended in 1 ml of complete medium, and exposed to the MACS® magnetic separator (Multinye Biotec, Germany) for 1 minute (see figure 6.2).

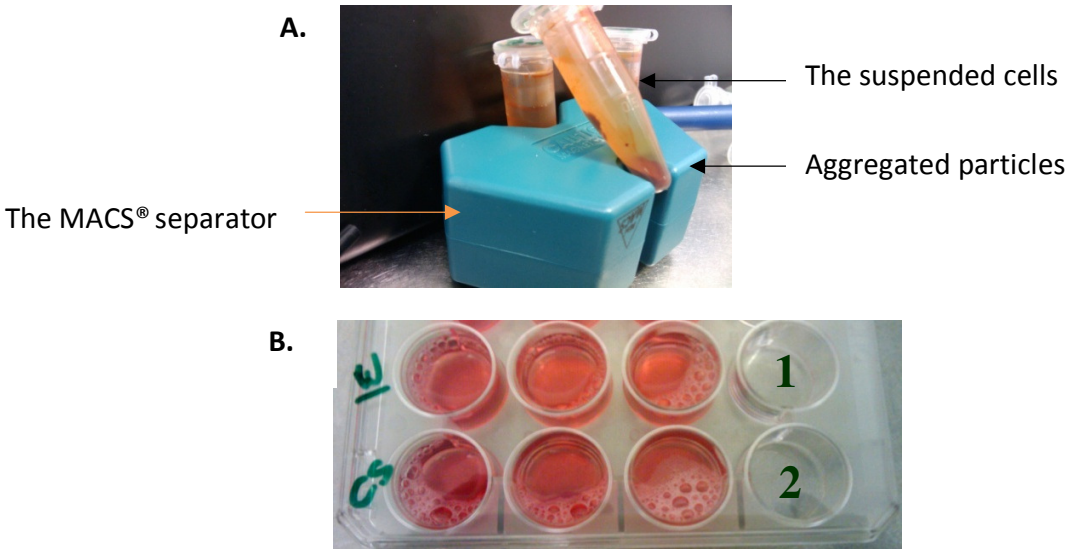

Figure 6.2 : Cell recovery by magnetic separation.

A. The MACS® Magnetic separator used to separate the particles from the cells. **B.** The recovered cell suspensions from (**1**) mixtures of cells and particles after 3 separation cycles and (**2**) the control wells containing pure cell suspensions.

This lead to the aggregation of particles while the cells remained suspended. The collection step was repeated 3x times by re-dispersing the particles in 1ml of complete medium, re-aggregating them and collecting the cell suspension each time. The collected cells were seeded on tissue culture plates and left to attach for 3 hours. The recovered cells were imaged using a Nikon Eclipse TS100 microscope (Nikon, UK) attached to a digital camera to assess their morphology.

The MTS assay (Invitrogen, UK) was performed on these cells, and data was compared with a control of pure cell suspension ($2X10^5$cells) seeded on tissue culture plastic without pre-manipulations. To each well 220µl of complete medium and 44µl MTS reagent were added and incubated at 37°C for 60 minutes. Following the incubation, 100µl aliquots of the test solution were transferred into Costar-96 well plate (flat bottom transparent), and their absorbance was measured at 492nm using an Infinite M200 Tecan plate reader. The percentage of recovered cells was calculated from the ratio of MTS signal obtained from recovered cells to that obtained from control cells.

6.3.6C Potential factors affecting the efficiency of cell recovery

The magnetic cell recovery protocol followed was analysed to identify the potential contributing factors affecting the efficiency of cell recovery from particle gels. NIH3T3 cells (2x 10^5) were suspended in 100µl of:

- $2\%_{w/v}$ polyPEGMA$_{246}$-EE solution in complete medium.
- Pure cell nutrient media (complete medium)

The obtained cell suspensions, not containing any particles, were taken through the process of magnetic cell recovery used with cells encapsulated within the magnetic gels (section 6.3.6B). Briefly, the suspensions were put at 37°C for 2 minutes, and then at 4°C for 2 minutes. 1 ml of cold PBS (4°C) was added to the cell suspensions and these were centrifuged at 180*xg* for 5

minutes. The supernatant was discarded and the cell pellet was re-suspended in 1 ml of complete medium. The cell suspension was exposed to the MACS® magnetic separator for 1 minute (x3 times) and then seeded on TCP in 24 well plates.

The cells were left to attach to TCP (for approximately 2-3 hours) and then MTS assay was performed as described in **2.4.2.** The percentage of recovered cells was calculated from the ratio of MTS signal obtained from recovered cells to that obtained from control of cells ($2X10^5$ seeded directly on TCP without pre-manipulations).

6.4 Results

6.4.1 Preparing the thermoresponsive magnetic particle gels

Sterically stabilised suspensions can be gelled through incipient flocculation as described in chapter 3. In this chapter, the preparation of magnetic suspensions that are also thermogelling is described. These thermoresponsive magnetic gels were designed around the same concept as the PCL/polyPEGMA$_{246}$-EE particle gels, and therefore the same parameters found necessary for space-filling gels formation were expected to apply. These included, as detailed in chapter 3:

1. Particle size of 2 to 10μm.
2. Particle surface, of suitable properties, to allow for the adsorption of polyPEGMA$_{246}$-EE.
3. The concentration of particles and polyPEGMA$_{246}$-EE in suspension need to be above a certain critical concentration, before space-filling gels could be obtained.

6.4.2 The magnetic microparticles

Model magnetic particles based on polystyrene were used for the preliminary study of thermoresponsive particle gels which are also magnetic. The polystyrene (PS) microparticles contained encapsulated iron oxide which has been widely used for biomedical applications due to its biocompatibility (Weissleder et al., 1989).

As apparent in figure 6.4 (SEM image of the magnetic PS microparticles after freeze-drying) the particles were of ~ 5μm of diameter, a size comparable to that of the previously studied polycaprolactone particles (chapter 3). These particles did not give thermogelling suspensions when mixed with polyPEGMA$_{246}$-EE, most likely due to their high surface polarity. This was confirmed by the very low WCA of solvent-cast films derived from these particles (the absolute WCA could not be accurately measured as no settling drop was obtained) (figure 6.4B).

Plasma polymerisation was used to modify the particles, through the deposition of a hydrophobic polyalkyl layer on their surface, to allow for the adsorption of polyPEGMA$_{246}$-EE. Plasma polymerisation is a technique widely used to fabricate thin polymer films (100 Å - 1µm) from a variety of organic and organometallic starting materials. The plasma polymerised films are highly cross-linked and therefore insoluble, thermally stable and chemically inert. These films are highly coherent and adherent to a variety of substrates including conventional polymer, glass and metal surfaces (Arefi et al., 1992) which made the plasma polymerisation technique widely applicable to protective coatings and biomedical materials (Chu et al., 2002).

Accordingly, the polystyrene magnetic particles were rendered hydrophobic through the surface deposition of plasma polymerised hexane (ppHEX). The WCA of solvent-cast films, derived from the magnetic particles, and similarly ppHEX modified was higher than 90°C (see figure 6.4), a WCA value consistent with previous reports of ppHEX modified surfaces (Zelzer et al., 2008).

Also, while the unmodified particles re-dispersed readily in water, the ppHEX surface modified particles did not (figure 6.3), which confirmed their hydrophobisation. Re-dispersion was only possible in the presence of a surfactant, such as polyPEGMA$_{246}$-EE (below its LCST). While the surface properties were drastically changed by the ppHEX surface modification, the particles morphology and size were not affected as indicated by SEM (figure 6.3).

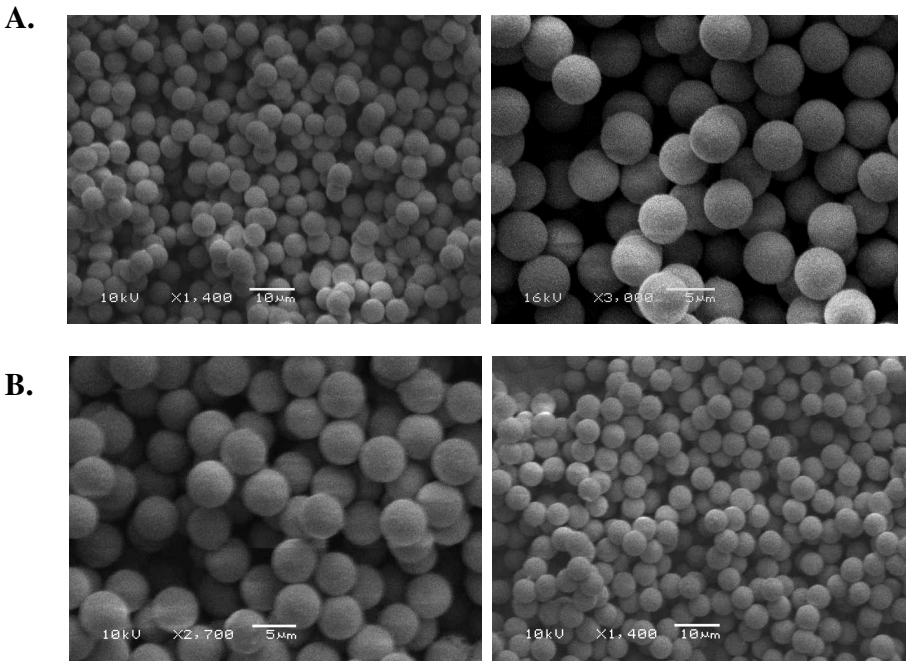

Figure 6.3: A. Representative SEM images of: A .Magnetic polystyrene particles after freeze drying. B. Magnetic polystyrene particles following plasma polymerisation of hexane on their surface.

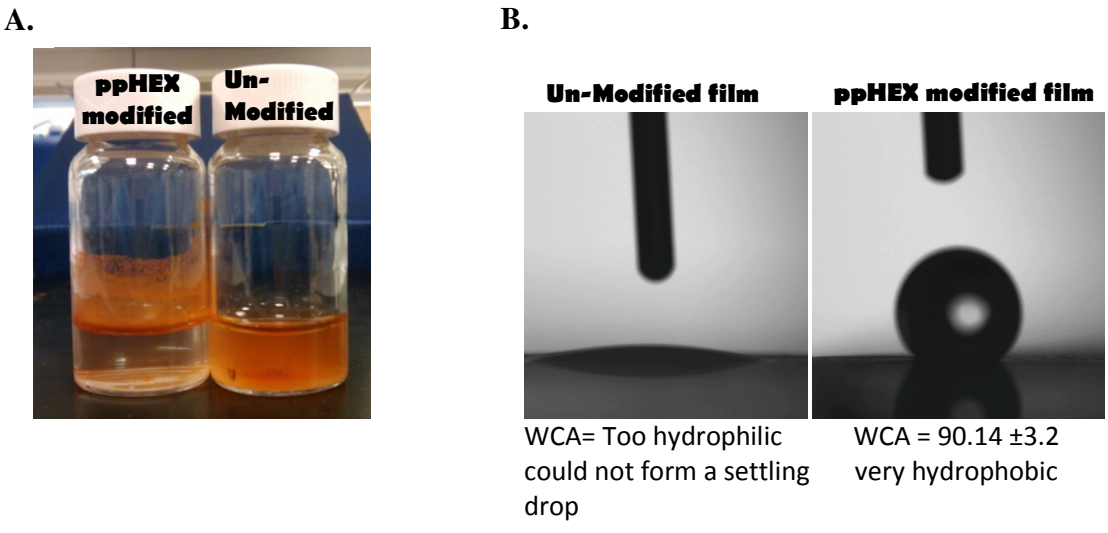

Figure 6.4: Effect of hexane plasma polymerisation on the wettability of magnetic particles.

A. Magnetic polystyrene particles suspendibility in water before and after ppHEX modification. **B.** WCA values recorded for films derived from magnetic polystyrene particles, before and after ppHEX surface modification. Values are given as mean ± SD for N=3 samples.

6.4.3 The thermoresponsive magnetic particle gels

Particle gels could be obtained from particulate suspensions, sterically stabilised with polyPEGMA$_{246}$-EE, on heating to above the LCST of polyPEGMA$_{246}$-EE (see chapters 3 and 5). The suspensions of as-purchased polystyrene magnetic particles, with added polyPEGMA$_{246}$-EE, did not show such a response on heating. This was attributed to the lack of surface adsorption of polyPEGMA$_{246}$-EE, necessitating the surface hydrophobisation of those particles by plasma polymerised hexane (ppHEX) surface deposition described above.

Suspensions containing ppHEX surface modified magnetic PS particles (33%$_{w/v}$) and polyPEGMA$_{246}$-EE (2-3%$_{w/v}$) in complete medium gelled on heating to 37°C without syneresis (figure 6.5). The gelation was quickly reversed by cooling to below the LCST (~19°C).

The temperature induced gelation of magnetic particle gels was confirmed by rheology, where an oscillatory strain amplitude sweep on a sample gel (33%$_{w/v}$ magnetic PS particles and 3%$_{w/v}$ polyPEGMA$_{246}$-EE) showed that G'(the storage modulus) was higher than G'' (loss modulus) at 37°C (figure 6.6). The plot indicated a narrow linear viscoelastic region, a known property for particle gels (Mezger, 2006).

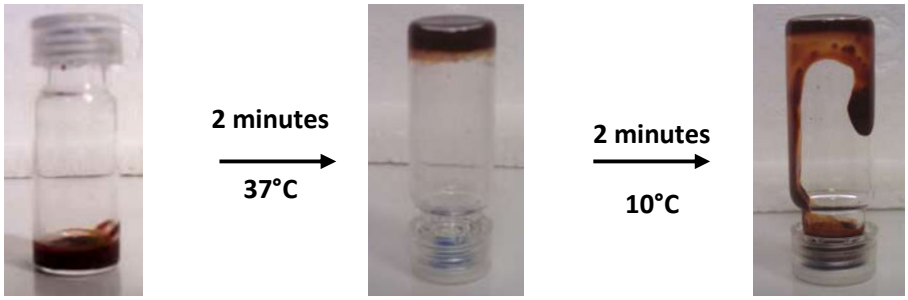

Figure 6.5: Tube inversion assay showing the temperature induced fluid to gel to fluid transition of a suspension consisting of 33%$_{w/v}$ magnetic PS particles (ppHEX modified) and 3%$_{w/v}$ polyPEGMA$_{246}$-EE.

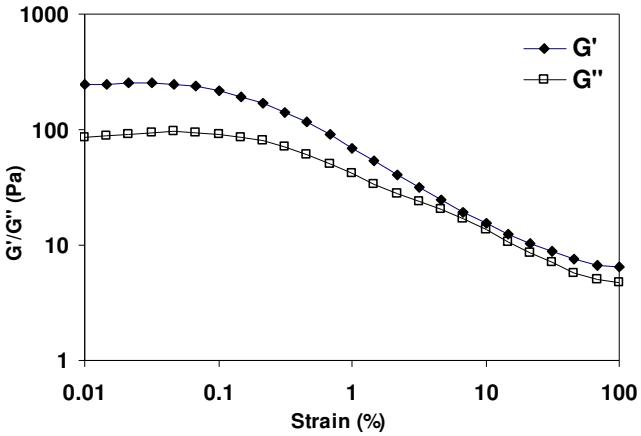

Figure 6.6 : Plots of G' and G'' versus strain amplitude for suspensions containing magnetic PS particles -ppHEX modified- (33%$_{w/v}$) and polyPEGMA$_{246}$-EE (3%$_{w/v}$) at 37°C.

6.4.4 Temperature dependent rheological properties of the magnetic particle gels

The reversible temperature dependent fluid-gel transition of the magnetic particle gels was confirmed by rheology. As shown in figure 6.7, at 10°C the material behaved as a viscoelastic fluid with G'<G''. However, G' and G'' increased rapidly when the temperature was raised to 37°C. At this temperature, the aggregated particles formed continuous elastic networks, giving a space-filling gel with G' becoming higher than G". Lowering the temperature back to 10°C, led to a significant drop in G' and G'' back to their initial values after cooling. G'' became eventually higher than G', indicating full reversibility of gelation into a liquid state. The heating-cooling cycle was repeated, and a similar dependence of the moduli on temperature was observed.

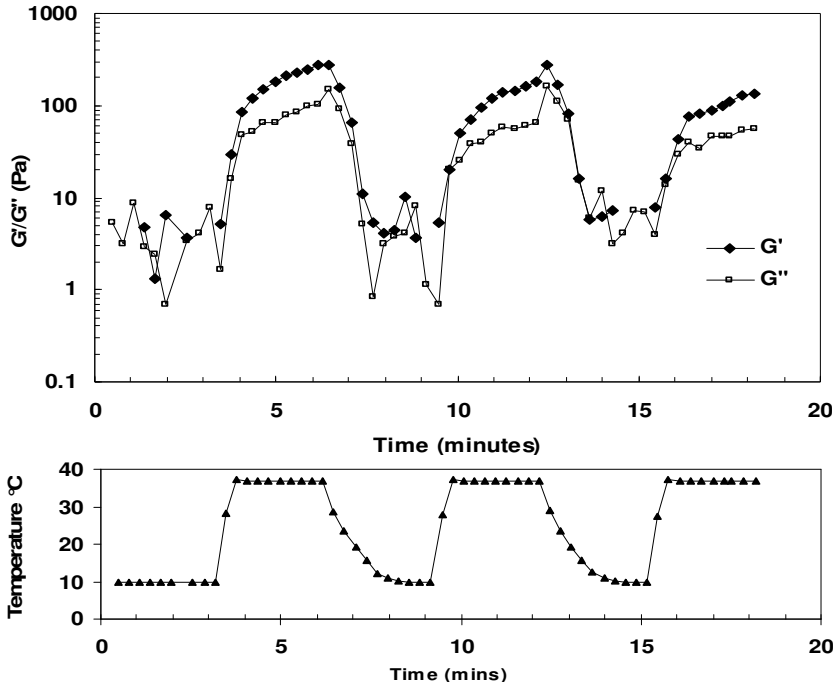

Figure 6.7: Multiple heating-cooling cycles of a suspension containing 33%$_{w/v}$ magnetic polystyrene particles (ppHEX modified) and 3%$_{w/v}$ polyPEGMA$_{246}$-EE at 37°C.

6.4.5 Magnetic particle separation for cell recovery

Proof of principle experiments were performed to demonstrate the feasibility of cell recovery from suspensions of magnetic particles, and from thermoresponsive magnetic gels thereafter, should these gels be used for the 3D culture of cells.

6.4.5A Recovery of cells mixed with magnetic particles

NIH3T3 cells were added to magnetic PS particles suspended in nutrient complete medium. Most cells (98%) were successfully recovered as quantified by MTS assay (figure 6.8). Optical microscope images of recovered cells showed they maintained their characteristic morphology (figure 6.9). Very few particles were collected with the cells, as observed under the microscope (indicated by the arrows in figure 6.9). This particle carry-over was likely due to human experimental/human error during manipulations of the magnet and cell mixtures. Although these particles could be easily washed off, such contamination might be avoided if an automated, *specifically designed* magnetic separation system, where the eppendorfs are fully aligned with the magnet, was to be developed.

The magnetic separation procedure followed allowed for near complete cell recovery (99%), from mixtures of PS magnetic particles and cells, with maintenance of cell viability.

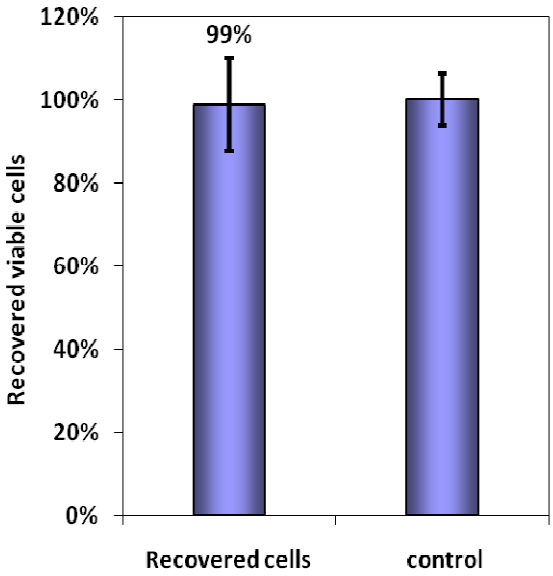

Figure 6. 8: The magnetic separation efficiency for cell recovery. Nearly all the cells could be recovered. Error bars represent SD for N=3 samples.

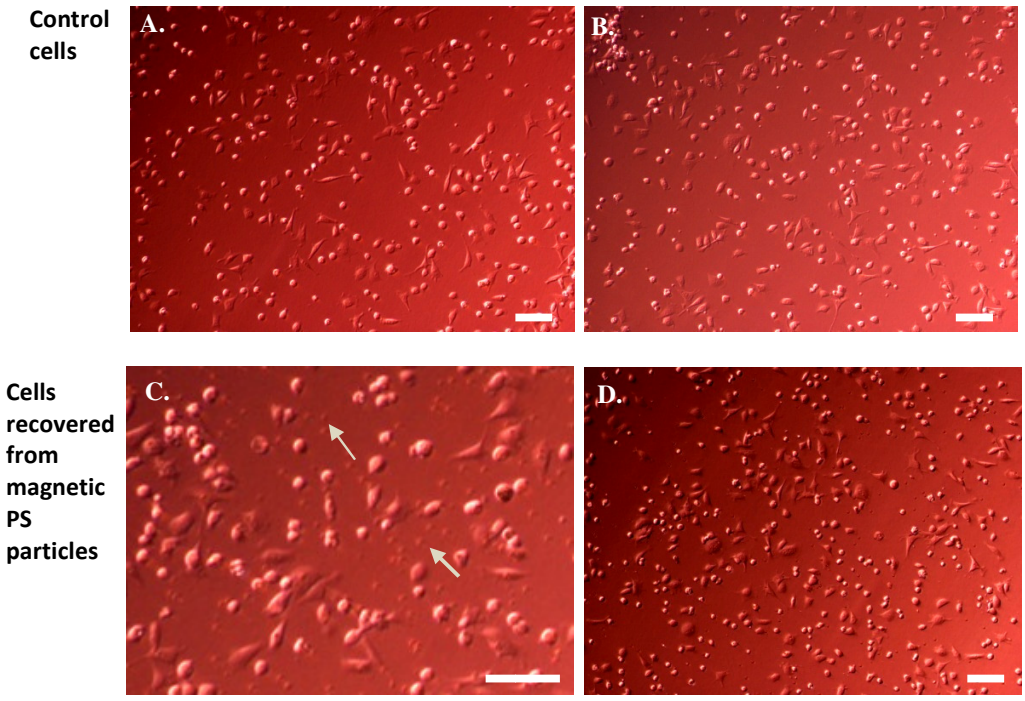

Figure 6.9: Representative light microscopy images of NIH3T3 cells recovered from the cell/particles mixture after 3 hours of seeding onto tissue culture plastic. Few magnetic particles were collected with the cells as indicated by the arrow in C and D. Scale bar 100µm.

6.4.5B Recovery of cells encapsulated within thermoresponsive magnetic-particle gels

After establishing that the magnetic particles separation allowed for the recovery of cells from suspensions of particles, this was used for the recovery of cells encapsulated within magnetic- particle gels.

NIH3T3 cells were encapsulated within thermoresponsive magnetic-particle gels consisting of ppHEX-modified magnetic PS particles ($33\%_{w/v}$) and polyPEGMA$_{246}$-EE ($2\%_{w/v}$). Following a brief (2 minutes) cell encapsulation at 37°C, the gels were liquefied and diluted. The cells were recovered from the obtained suspensions using the MACS separator®. In total, 84±3.25% (mean ± s.d, N=3 samples) of the encapsulated cells were successfully recovered (figure 6.10), with maintenance of viability and normal characteristic morphology (figure 6.11).

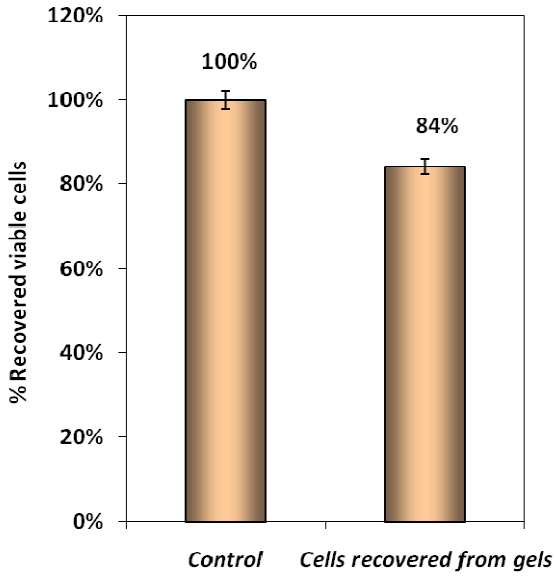

Figure 6.10: Cell recovery from thermoresponsive magnetic particle gels by magnetic separation.

Error bars represent SD, for the ratio of MTS signal from recovered cells to that of the control cells, from N=3 samples.

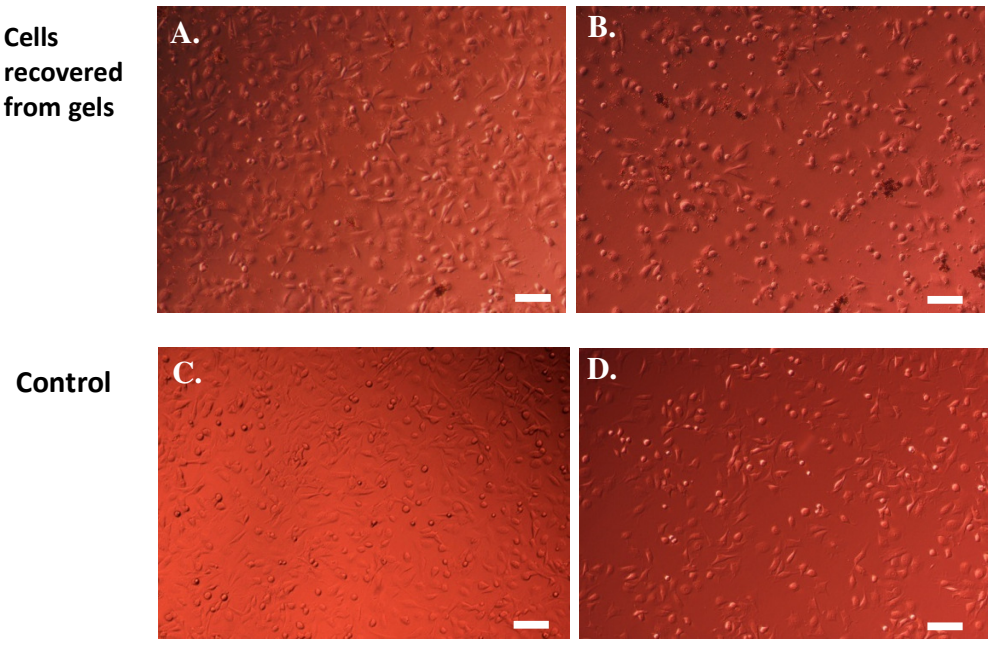

Figure 6.11: Representative light microscopy images of NIH3T3 cells recovered from the thermoresponsive magnetic particle gels/suspensions (A&B) and the control cells (C&D).
Scale bar 100μm

The incomplete cell recovery in this case was unlikely to be due to the magnet exposure, since near complete cell recovery was achieved in 6.4.5A.

In order to determine whether certain manipulations during the cell recovery procedure compromised its efficiency, an experiment was done where cells suspended in complete medium, or in 2%$_{w/v}$ polyPEGMA$_{246}$-EE solution were subjected to solely the heating/cooling and washing steps of the magnetic cell recovery process. In this experiment, any influence from the magnet or the particles on cells was eliminated.

As shown in the graph in figure 6.12, total cell recovery was not achieved in both the control (cell suspensions in pure complete medium) and the polyPEGMA$_{246}$-EE containing suspensions. PolyPEGMA$_{246}$-EE did not appear to be the factor responsible for cell loss since

there was no statistically significant difference between the percentage of cells recovered from pure nutrient medium and from that containing the thermoresponsive polymer.

Taken together certain steps during the cell recovery procedure, specifically the heating/cooling or the wash/centrifugation steps are likely to have contributed to the reduced efficiency of cell recovery from magnetic thermoresponsive particle gels. The magnetic particles separation step *per se* did not appear to cause cell damage or loss as concluded from 6.6.5A.

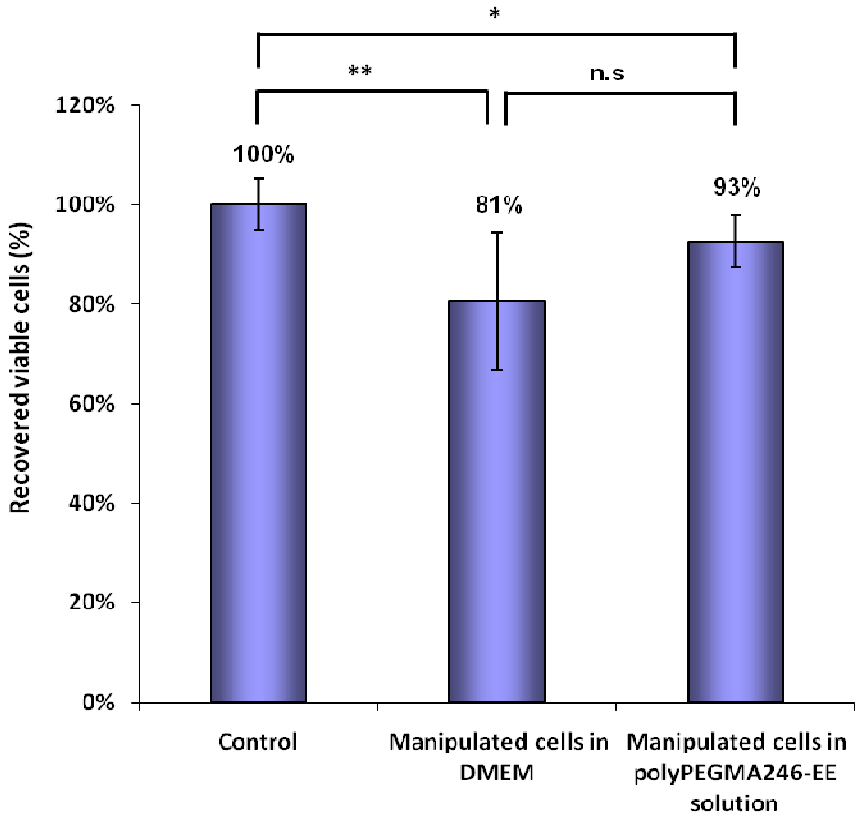

Figure 6.12: The effect of manipulations (heating/cooling and wash steps) on the efficiency of cell recovery by magnetic-particle separation. Error bars represent SD of N=3 samples. Statistical significance was calculated from t-test between the different groups. A t-test was performed between the control and the test samples, and statistical significance was denoted as: * $p<0.05$, ** $p<0.01$, ***$p<0.001$).

6.5 Discussion

When cells are cultured in collagen or other ECM derived gels, they are usually recovered through the enzymatic digestion of the gel material. However, using animal-derived proteases or glycosidases affects cell quality and carries risks of infections.

Particle gels, exemplified by the PCL/polyPEGMA$_{246}$-EE gels, could be successfully used to encapsulate and culture mammalian cells in 3D (chapter 5). However, these particle gels did not allow for a simple recovery of the expanded cell populations. Therefore, introducing a distinctive property to the constituent particles was required to allow for their separation from the cultured cells when needed. Inspired by the use of monosized superparamagnetic particles, such as Dynabeads, in cell separation and recovery, it was considered that the use of magnetic particles would allow for their facile separation from cells.

The previously developed thermoresponsive particle gels consisted of polycaprolactone with polyPEGMA$_{246}$-EE. The encapsulation of magnetite within the PCL particles would incur on these gels the additional property of magnetic field sensitivity. Different methods have been developed to encapsulate magnetite within polyester particles for various applications (Liua et al., 2007, Yang et al., 2006). However, in this proof of principle study, polystyrene magnetic microparticles (5μm) were purchased and used as model magnetic particles that can make up thermoresponsive particle gels. These particles encapsulated iron oxide and were super-paramagnetic i.e. exhibited magnetic properties solely within a magnetic field and could be easily dispersed otherwise. The purchased particles were modified by surface deposition of plasma polymerised hexane (ppHEX) films to make their surface sufficiently hydrophobic for polyPEGMA$_{246}$-EE to adsorb and act as a steric stabiliser below the LCST and as a flocculent above the LCST.

Below the LCST, polyPEGMA$_{246}$-EE facilitated the dispersion of the ppHEX modified magnetic particles in the aqueous medium, after they became too hydrophobic to be wetted post-plasma modification.

Above the LCST, thermoresponsive particle gels were obtained. The magnetic particle gels obtained at 37°C were less elastic than their PCL particles counterparts, at the same particles and polyPEGMA$_{246}$-EE composition (see chapter 3). This might be due to the higher density of the magnetic particles, and therefore their higher tendency to settle under gravity, which could have weakened the elasticity of the particle networks making the gel.

The developed magnetic particle suspensions could be taken through multiple cycles of fluid/gel states associated with consecutive heating/cooling cycles, and full reversibility between the two states was observed over very short timescales. Hence, the magnetic particle gels possessed the required properties to allow for their use as 3D cell culture scaffolds that would allow for the enzyme-free subculture and cell harvesting, as described previously for the PCL/polyPEGMA$_{246}$-EE particle gels in chapter 5.

In this study, NIH3T3 cells were encapsulated within the magnetic particle gels, but were not cultured within. This preliminary study mainly aimed at demonstrating the ability to recover cells encapsulated within the developed “model” magnetic particle gels, rather than studying their ability to support the culture of encapsulated cells.

Almost full recovery of NIH3T3 cells from suspensions of magnetic particles was achieved using the magnetic particle separation protocol developed. However, complete cell recovery

was not achieved with the NIH3T3 cells encapsulated within the magnetic particle gels, although the overall yield was higher than 80%, and the recovered cells maintained their viability and characteristic morphology.

Various factors could have contributed to the incomplete recovery of cells encapsulated within magnetic particle gels. These included:

1. **The exposure to the magnetic field**: although this is unlikely since full cell recovery was achieved from suspensions of particles and cells following the same magnetic separation protocol.
2. **Toxicity from polyPEGMA$_{246}$-EE**: this is also unlikely as the amount of polyPEGMA$_{246}$-EE in the gels was within the concentration range tolerated by the cells (see chapter 4).
3. **Toxic residues from particles**: Toxic residues from the plasma-modified particles might have caused some cell death. It was found that only 70 % of the encapsulated cells were recovered from particle gels prepared from ppHEX modified magnetic particle that had not been washed after plasma modification (data not shown). Accordingly, washing steps (with deionised water) following the plasma polymerisation were carried out. The use of organic solvent for the washing was hindered by the similar solubility profile of polystyrene and potential contaminants from the hexane plasma polymerisation process.
4. **The heating/cooling** of the suspensions to induce gelation and liquefaction.
5. **The centrifugation/re-dispersion wash steps**

The last three were the most likely contributing factors. The experiment where cell suspensions, not containing any magnetic particles, were taken through the cell recovery protocol used with cells encapsulated within gels, strongly suggested that the manipulations

during the process were responsible for the reduced efficiency of cell recovery. These problems appear to be surmountable, especially if a specifically designed magnetic separator and related equipment are made available for the application put forward in this study.
Although not performed in this study, due to time limitations, further purification and analysis of the particles would also be required, to eliminate any potential toxicity.

In addition to their use as scaffolds for the 3D culture of cells, thermoresponsive magnetic-particle gels, such as those described in this study, might find additional therapeutic applications. Le Renard *et al* attempted to develop injectable implants containing magnetic particles, to be used in tumour sites to induce particle-mediated local hyperthermia. The limitation they encountered was the restricted content of magnetic particles that could be incorporated in the hydrogel carriers they used. Higher contents of magnetic particles were required in the implants, but these interfered with the sol-gel transition and the mechanical properties of the carrier hydrogels used, leading to the instability of the implant (Le Renard et al., 2010).

The thermoresponsive magnetic particle gels would be relevant for this application, where the same particles making up the gel structure can induce the local hyperthermia. The thermoresponsive property of these gels would allow for their simple injection into the target tumour tissue, and their rapid gelation kinetics would help maintain the retention and mechanical stability of the implant.

6.6 Conclusions

Thermoresponsive particle gels were developed from magnetic polystyrene microparticles and the thermoresponsive polymer polyPEGMA$_{246}$-EE. Proof of principle experiments for the potential applications of these gels in tissue engineering showed how their reversible thermogelling behaviour allowed for cell encapsulation, while their magnetic sensitivity allowed for cell recovery through simple magnetic particle separation.

Surface modified magnetic polystyrene particles were used in this work. However the particles could be drawn from many biocompatible polymers, such as polycaprolactone encapsulating magnetite with suitable surface properties.

In summary, the proposed concept of scaffold deconstruction by temperature and cell recovery by magnetic separation was strongly supported by the experimental findings presented in this chapter. These newly developed materials offer a higher degree of control over their properties, and significantly add to the potential applications of magnetism in the biomedical field.

CHAPTER 7

General discussion and conclusions

Cell-cell and cell-matrix adhesion has a major impact on various aspects of cell behaviour (cell cytoskeletal arrangement, gene expression, cell viability and functionality), where the detachment of anchorage dependent cells from their native matrix can induce anoikis. Hence, the delivery of cells in a form that maintains cell-cell contact and cell-matrix interactions would enhance tissue engraftment and the outcome of cell therapy *in vivo*. This can be achieved by delivering cells in different forms of scaffolds such as gels or adhered to microspheres, or in the form of cell sheets.

In addition to their use as cell delivery vehicles, biomaterial scaffolds are important for the 3D culture of cells and the *in vitro* construction of tissue substitutes.

The work presented in this thesis describes the development of *stimuli-responsive particle gels*, and their use as scaffolds for tissue engineering. The particle gels were designed to possess easily reversible thermogelling behaviour, by employing the mechanism of "incipient flocculation" in particulate dispersions prepared from biocompatible materials. This involved preparing aqueous colloidal mixtures of microparticles and an adsorbing thermoresponsive polymer which acts as a steric stabiliser below its LCST, and as flocculent above its LCST.

The particle gels could be drawn from a wide range of materials. Pilot studies involved the preparation of thermogelling suspensions from poly(lactic-co-glycolic acid) PLGA microparticles with a surface entrapped thermoresponsive polymer, to obtain thermoresponsive particles (Wang et al., 2009). The combination of PLGA with the thermoresponsive polymer via surface entrapment led to the plasticisation of PLGA, leading to a drop in the Tg to below 37°C. This led to particle coalescence following their aggregation induced by a change in temperature, which made their aggregation irreversible and lead to formation of solid sintered scaffolds at 37°C. When PCL, a semi-crystalline polymer, was used instead of PLGA no plasticisation was observed, and particle gels could be obtained from concentrated suspensions above the polymer's LCST, with liquefaction on cooling (Wang et al., 2009). However, accurate characterisation and reproducibility in these gels was difficult to achieve, and the preparation of thermogelling suspensions from particles with surface-adsorbed as opposed to surface-entrapped thermoresponsive polymer was followed as a simpler, cheaper and a more reproducible method for the preparation of thermogelling suspensions.

The preparation of the main particle gels investigated in this thesis was described in chapter 3. Microparticles were prepared from polycaprolactone (PCL) using the single emulsion solvent evaporation method. This yielded polydisperse microparticles of mainly 2-6μm size range and these were characterised using SEM and sized with the Coulter Counter.

The thermoresponsive polymer selected was the ampiphilic homopolymer polyPEGMA$_{246}$-EE, with its hydrophobic methacrylate backbone and hydrophilic PEG pendant side chains. polyPEGMA$_{246}$-EE was synthesised by FRP, characterised using GPC, and its LCST was estimated using light transmission spectroscopy to be around 21°C in deionised water and ~19°C in complete medium.

A central theme in designing scaffolds is to understand the correlations between scaffold properties and biological functions. Following pilot experiments assessing the cellular response to the particle gels (chapter 4), a surface modification step was required to optimise the cellular response to the PCL particles. Particle surface hydrolysis, using NaOH/ethanol, generated surface charge (chapter 3) and improved cell adhesion to the particles as described in chapter 4.

Suspensions of PCL particles (subjected to the surface hydrolysis) and polyPEGMA$_{246}$-EE in complete cell nutrient medium possessed thermoresponsive properties, imparted by the smart polymer employed. Upon mixing, polyPEGMA$_{246}$-EE adsorbed to the particle surface and this was confirmed experimentally using zeta potential measurements and rheology.

In these suspensions, PCL particle aggregation occurred on increasing the temperature to above the LCST of polyPEGMA$_{246}$-EE, but could be reversed by cooling the suspensions back to below the LCST. On increasing the temperature to above the LCST, intermolecular attractions between the polymer chains, and the expulsion of water from the adsorbed polymer brush drove the particle aggregation. Space filling gels were obtained when the PCL particle concentration was 19%$_{w/v\ or}$ higher.

The particle gels' elasticity was found to increase with temperature. The higher the temperature, above the LCST, the stronger were the obtained particle gels. This was the reason for which a polymer with a low LCST was selected (i.e. polyPEGMA$_{246}$-EE as opposed to other polymers with higher LCST) in order to obtain sufficiently strong particles gels at 37°C, the temperature at which the gels were mainly intended for use.

A detailed characterisation of the particle gels with different compositions showed that their elasticity was also strongly dependent on the PCL particle concentration and to a lesser

extent on polyPEGMA$_{246}$-EE concentration. PCL/polyPEGMA$_{246}$-EE particle gels elasticity, at 37°C, ranged between 0.1-10KPa for gels containing 19-40%$_{w/v}$ PCL microparticles.

Although the application of this property was not explored in his thesis, it is an important feature since scaffold elasticity can be a key determinant for their successful application with certain cell types but not with others. For example, myoblasts were found to differentiate into a striated, contractile phenotype only in substrates within a very narrow range of muscle like stiffness (i.e. 8-11kPa) (Engler et al., 2004).

On further characterisation, the PCL/polyPEGMA$_{246}$-EE particle gels were found to be brittle with relaxation at rest. With regards to gelation reversibility on cooling, the physical entanglement of the large polymer chains meant that a small brief shear force might be required to allow for full and rapid liquefaction. polyPEGMA$_{246}$-EE chains entanglement was unlikely to be similar to the irreversible chain entanglement observed for polyNIPAM, as the PEG side chains can only act as H-bond acceptors, and therefore no inter-chain H-bonding is expected within the collapsed polyPEGMA chains upon loss of water above the LCST (Abulateefeh et al., 2009). During applications in cell culture gentle shaking by hand following cooling was sufficient for a quick liquefaction of the gelled suspensions.

In chapter 4, the developed particle gels were studied for cytocompatibility. PCL/polyPEGMA$_{246}$-EE gels supported the adhesion, proliferation and extracellular matrix production of mouse NIH3T3 fibroblasts cultured on their surface for at least 14 days. The particle gels surface had a considerable 3D microstructure, and the cultured cells were interacting with the gel-surface in all three dimensions.

Chapter 5 described the use of PCL/polyPEGMA$_{246}$-EE particle gels as scaffolds for the 3D culture of cells. Mouse 3T3 fibroblast cells, mixed with PCL/polyPEGMA$_{246}$-EE suspensions, were encapsulated within the particle gels obtained on heating to above the LCST of polyPEGMA$_{246}$-EE. Cell viability and proliferation over at least 20 days of culture was confirmed using MTS and DNA assays, and the 3D nature of cell growth and distribution was revealed by SEM and micro-CT. An important observation during this study was that with time most cells migrated to the top regions of the gels. Although this reflected the flexibility of the gels allowing for cell migration, this also indicated limited mass transfer in the deeper regions of the gels. Mass transfer is indeed a major challenge in tissue engineering scaffold design. One way that this can be tackled is through the incorporation of cell-degradable porogen, such as large gelatin microparticles, which can leave behind larger pores to allow for a more efficient molecular transfer (Luo et al., 2007).

Cells are traditionally recovered from scaffolds after expansion using proteases such as trypsin. However, cell dissociation from surfaces has been recognised as a contributing factor to cell death and poor cell adhesion and engraftment in cell therapy, in addition to the associated infection risk from using animal-derived enzymes for dissociation. Engineering and culturing cells in aggregates and using those for cell therapy is one approach which showed some promise for the maintenance of cell function and phenotypic characteristics during culture and cell delivery process (Bayoussef, 2009). Cell sheet engineering(Matsuda et al., 2007) and using microcarriers for cells (Martin et al., 2010) are other approaches developed to tackle this issue.

Implanting the cells within the same scaffolds used for their culture *in vitro* is another approach that can be applicable to the cells cultured within thermoresponsive particle gels. Indeed, the ability to construct and deconstruct cell culture environments on demand, by changing the

temperature, is one of the most significant strengths of the particle gels developed. In addition to simple cell encapsulation, this property allowed for the enzyme-free subculture of the cell population cultured within the gels, with maintenance of cell viability and ability to proliferate as confirmed by MTS and DNA assays. The micro-CT generated 3D images of the gels following subculture confirmed the cell population was split between the new "daughter gels".

The ability to construct and deconstruct these particle gel scaffolds also makes the particle gels, composed mainly of biodegradable materials, particularly interesting for the minimally invasive delivery of the cell-gel constructs *in vivo*. The suspensions could be mixed with cells and then injected into a defect site to form a mechanically functional scaffold upon implantation, or cells could be cultured within the particles gels and the conditioned *cell-gel* constructs can then be injected into the target tissue.

The potential that thermoresponsive particle gels, as a class of materials, carry and the versatility of the constituent materials, properties and applications for these gels was supported by the data presented in chapter 6. Further functionality was engineered onto these gels, by employing magnetic particles as the gel building blocks. These gels allowed for simple cell recovery by magnetic separation, a process that is particularly promising for applications that desire a scaffold-free outcome such as large scale cell expansion.

This particularly applies to the "large scale" expansion of stem cells for clinical applications, where the maintenance of their "stemness" is critically dependent on their culture niches, with three dimensionality being particularly important (Lutolf and Blau, 2009).

Future work and Conclusions

Through the work described in this thesis, thermoresponsive particle gels, a class of materials not previously explored for tissue engineering applications were introduced to the field. The superiority of these materials lies in the achievable level of control over their properties using mild stimuli such as temperature and/or magnetism, which opens up various avenues for applying these materials (see figure 7.1).

The thermoresponsive particle gels can be used for the *in vitro* construction of replacement tissues. Tissue formation can be initiated *in vitro* where it is possible to manipulate the culture environment and better control cell behaviour. The conditioned construct, containing the cells and their secreted ECM, can thereafter be injected to the site of interest, and better tissue engraftment and regeneration *in vivo* would then be expected. The superiority of these materials lies in the mild stimulus required for their liquefaction and injection into the site of interest, as well as their reversible gelling behaviour which allows for their transfer from the *in vitro* to the *in vivo* setting through a simple injection. This compares to injectable scaffolds requiring toxic chemicals (Van Tomme et al., 2008), or those systems where gelation or solidification is irreversible (Kretlow et al., 2007).

The particle gels can also be used for the *in vitro* construction of tissue models, as they offer an easily built three dimensional environment for cell culture. These tissues can be used in drug screening studies, as they provide a better representation of the cellular arrangement *in vivo* (Fischbach et al., 2007).

More complex three-dimensional scaffolds can be produced from thermoresponsive particle gels, if the latter are used as *inks* for bio-printing. In bio-printing, custom-designed inkjet printers deposit, ECM molecules cells and biomaterials in a controlled layer-by-layer fashion, on a micrometre scale and in three dimensions (Derby, 2008). The resulting scaffolds can be designed to contain biomolecules in a locally modular distribution. The thermoresponsive particle gels can be easily injected (printed) at low temperatures and rapidly solidify if deposited onto a warm environment. Therefore, these can be used as biocompatible inks which can encapsulate the mixed in cells without the need for potentially toxic chemicals or radiation to drive the solidification. Complex and more cell-instructive scaffolds can be obtained by printing gels composed of particles encapsulating different growth factors (Campbell and Weiss, 2007, Xie et al., 2006).

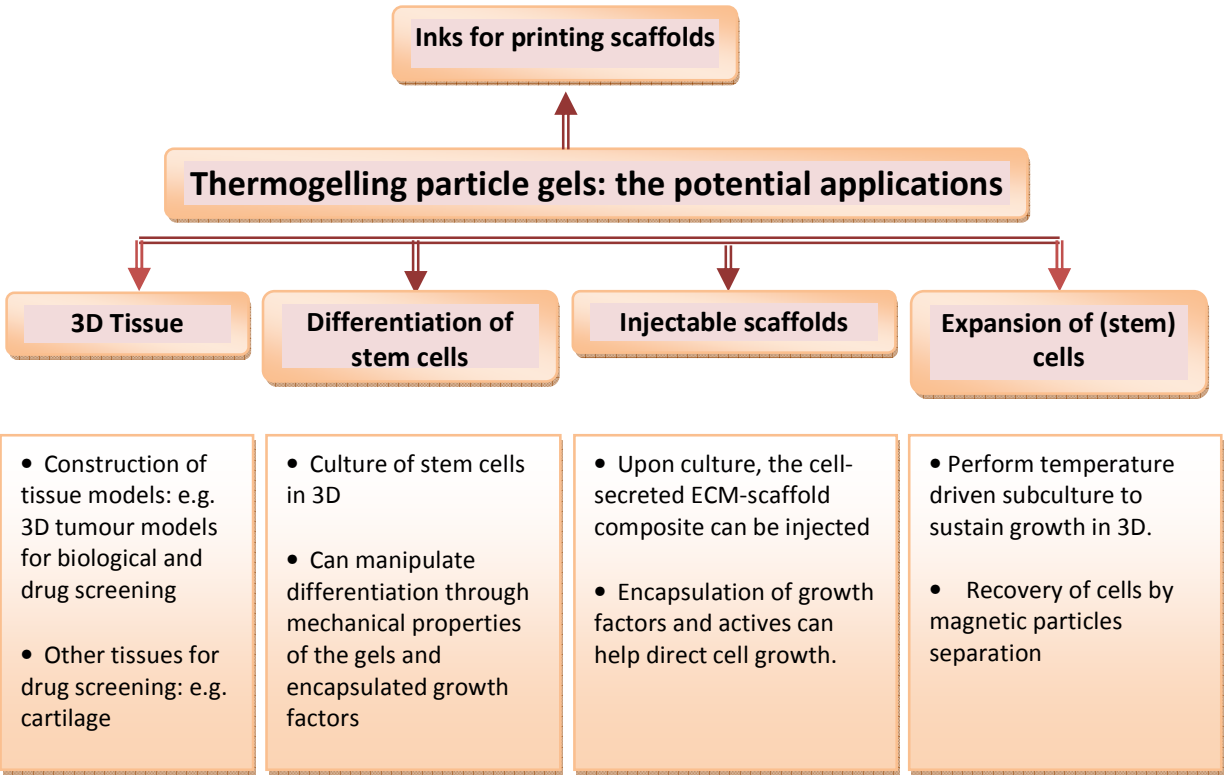

Figure 7.1: Flow chart summarising the potential applications of thermoresponsive particle gels in tissue engineering.

One of the other important potential applications for the developed particle gels is scalable cell culture for large scale production of therapeutic cells, thanks to their low cost, simple design, their 3D structure and physical associations. This is a challenging area of research particularly with regards to stem cells. (Azarin and Palecek, 2010). The use of microcarriers for this purpose has been reported (Alfred et al., 2011) but not the use of particle gels.

Cells can be grown within the particle gels and then recovered at the end of culture under mild environmental stimuli, which include temperature and magnetism, without the need for using enzymes that can impact on the quality of the cultured cells (Huang et al., 2010, Steinberg et al., 1973). One limitation to this is the observed pattern of cell growth within the particle gels which tends to occur in clusters. This might make the recovery of individual cell suspensions from the particle gels challenging without the use of enzymes. However, even if enzymatic treatment would be required, the number of enzymatic passages needed would be significantly reduced compared to current systems used for cell expansion. Subculture can be performed using temperature change and dilution with fresh particle gel as was described in chapter 5, and enzymatic treatment would be limited to the final stage of cell harvesting, only if individual cell suspensions are required rather than cells in clusters. On the other hand, cell growth in clusters might be desirable for the expansion of certain cell types like chondrocytes, or for the generation of embryoid bodies which can be easily recovered from the gel matrix without exposing them to any enzyme treatment.

Improving the ability of the particle gels to support superior cell spreading and attachment by building up their biological complexity (as described below see figure 7.2) would be expected to reduce the tendency of cell growth to occur in clusters, as it would promote superior interactions between the cells and the material, rather than the cells mainly interacting

with each other. Moreover, because the gels are formed through physical (non covalent links), and can be easily returned to a fluid state, they can be diluted with large volumes of fluid where the resulting shear forces of dilution would be expected to dislodge the cells without the need for enzymes, recovering individual cells in suspension.

In order to realise the full potential of the thermoresponsive particle gels, especially if used with stem cells, a higher level of bioactivity needs to be present in them. This is since for cells generally and for stem cells particularly, the cues presented within the culture environment are critical for deciding their proliferative and differentiation fates. Maintaining the "stemeness" of stem cells is highly dependent on many factors within their culture niches, a critical one of which is three-dimensionality (Lutolf and Blau, 2009) achievable in the developed particle gels.

The inclusion of bioactive compounds and cues is expected to significantly improve the cellular response and culture within the particle gels. This can be achieved through:

1. **The encapsulation of growth factors within the microparticles:** The incorporation of delivery systems in 3D scaffolds offers an indispensable platform for enabling temporal and spatial control in tissue constructs (Shen and Mooney, 2003). Different growth factors can be encapsulated and be released at different rates, through the careful selection and combination of encapsulating materials. The release of multiple growth factors with distinct release profiles can also help address the more complex tissue requirements such as vascularisation.
2. **The chemical conjugation of cell adhesion ligands to the thermoresponsive polymer backbone:** The thermoresponsive polymer chains can be functionalised with specific

cell-adhesion mediating peptides such as RGD. These can significantly enhance cell attachment and spreading within the gels. Such modification was reported to significantly improve cell response in alginate scaffolds, which are not normally cell adhesive. Alginate scaffolds containing short motifs of ECM adhesion proteins such as RGD encouraged mesenchymal stem cells to spread and attach to the matrix whereas on unmodified scaffolds only cell–cell interactions were seen (Re'em et al., 2010).

3. **The inclusion of small concentrations of water soluble macromolecules**

   The inclusion of purified ECM proteins such as collagens, hyaluronic acid or fibrin would provide sites for integrin-mediated cell attachment in scaffolds. For example, adding bovine gelatin to the particle gels to a concentration of 0.1_{wt}% was not found to affect their gelation (data not shown). Decellularized tissue powder can also introduce further bioactivity to the particle gels. Not only would these molecules be expected to improve and enhance the cellular response, but being large hydrophilic molecules, these can retain more water within the particle matrix. This might reduce the required solids concentrations within the gels improving mass transfer, and make them less brittle. Extensive physical and cellular characterisation tests would be needed to identify the optimum amount and combination of materials to be added to the gels without compromising the gelation behaviour.

4. **Microparticle surface modification through plasma polymerisation**. Modulating the cellular response by engineering nanotopography and specific chemistry onto particles surface can be achieved by plasma polymerisation (Bible et al., 2009).

Figure 7.2 summarises the different approaches to build up biological complexity within thermoresponsive particle gels, for optimal cell responses and tissue regeneration.

To conclude, in this thesis the preparation and application of first generation thermoresponsive particle gels in tissue engineering was described. We believe the materials developed and studied in this thesis represent a significant contribution to the fields of biomaterials, drug delivery and tissue engineering.

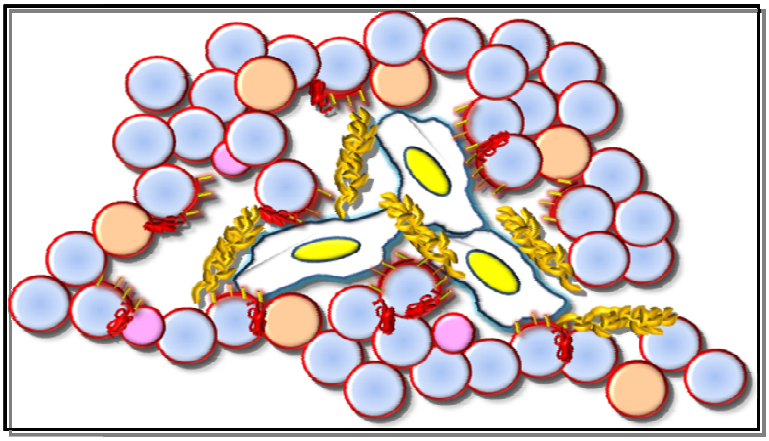

Particles encapsulating growth factor A

Particles encapsulating growth factor B

Scaffolding Particles

Biomolecules such as collagen, de-cellularised tissue powder

Engineered surface motifs (eg.RGD peptides) attached to the thermoresponsive polymer.

Figure 7.2: The various strategies and combinations of cell-instructive materials and cues to improve the bio-activity within thermoresponsive particle gels

REFERENCES

ABULATEEFEH, S. R., SAEED, A. O., AYLOTT, J. W., CHAN, W. C., GARNETT, M. C., SAUNDERS, B. R. & ALEXANDER, C. (2009) Facile synthesis of responsive nanoparticles with reversible, tunable and rapid thermal transitions from biocompatible constituents. Chemical Communications, 6068-6070.

AI, K., MASAYUKI, Y., CHIE, K., AKIHIKO, K.,, YASUHISA, S. & TERUO, O. (1999) Decrease in culture temperature releases monolayer endothelial cell sheets together with deposited fibronectin matrix from temperature-responsive culture surfaces. Journal of Biomedical Materials Research, 45, 355-362.

ALAVA, C. & SAUNDERS, B. R. (2006) Polymer stabilisers for temperature-induced dispersion gelation: versatility and control. J Colloid Interface Sci, 293, 93-100.

ALEXANDER, R. M. & DUC, M. T. (1998) The chemistry of deposits formed from acrylic acid plasmas. Journal of Materials Chemistry, 8, 937-943.

ALFRED, R., TAIANI, J. T., KRAWETZ, R. J., YAMASHITA, A., RANCOURT, D. E. & KALLOS, M. S. (2011) Large-scale production of murine embryonic stem cell-derived osteoblasts and chondrocytes on microcarriers in serum-free media. Biomaterials, 32, 6006-6016.

AREFI, F., ANDRE, V. M.-R., P. & AMOUROUX, J. (1992) Plasma polymerization and surface treatment of polymers. Pure & Appl. Chem., 64, 715-723.

ASHAMMAKHI, N., NDREU, A., NIKKOLA, L., WIMPENNY, I. & YANG, Y. (2008) Advancing tissue engineering by using electrospun nanofibers. Regen Med, 3, 547-74.

ATALA, A. (2007) Engineering tissues, organs and cells. J Tissue Eng Regen Med, 1, 83-96.

AZARIN, S. M. & PALECEK, S. P. (2010) Development of scalable culture systems for human embryonic stem cells. Biochemical Engineering Journal, 48, 378-384.

BABENSEE, J. E., MCINTIRE, L. V. & MIKOS, A. G. (2000) Growth Factor Delivery for Tissue Engineering. Pharmaceutical Research, 17, 497-504.

BACAKOVA, L., FILOVA, E., RYPACEK, F., SVORCIK, V. & STARY, V. (2004) Cell adhesion on artificial materials for tissue engineering. Physiol Res, 53 Suppl 1, S35-45.

BARLTROP, J. A., OWEN, T. C., CORY, A. H. & CORY, J. G. (1991) 5-(3-carboxymethoxyphenyl)-2-(4,5-dimethylthiazolyl)-3-(4-sulfophenyl)tetrazolium, inner salt (MTS) and related analogs of 3-(4,5-dimethylthiazolyl)-2,5-diphenyltetrazolium bromide (MTT) reducing to purple water-soluble formazans As cell-viability indicators. Bioorganic & Medicinal Chemistry Letters, 1, 611-614.

BARRY, J. J., GIDDA, H. S., SCOTCHFORD, C. A. & HOWDLE, S. M. (2004) Porous methacrylate scaffolds: supercritical fluid fabrication and in vitro chondrocyte responses. Biomaterials, 25, 3559-68.

BASHURA, C. A., DAHLGRENB, L. A. & GOLDSTEINA, A. S. (2006) Effect of fiber diameter and orientation on fibroblast morphology and proliferation on electrospun poly(D,L-lactic-co-glycolic acid) meshes. Biomaterials, 27, 5681-5688.

BAYOUSSEF, Z. (2009) Three dimensional aggregates for cell replacement therapy. Pharmacy. Nottingham, University of Nottingham.

BERGSTRÖM, L. & SJÖSTRÖM, E. (1999) Temperature Induced Gelation of Concentrated Ceramic Suspensions: Rheological Properties. ournal of the European Ceramic Society, 19, 2117-2123.

BIBLE, E., CHAU, D. Y., ALEXANDER, M. R., PRICE, J., SHAKESHEFF, K. M. & MODO, M. (2009) Attachment of stem cells to scaffold particles for intra-cerebral transplantation. Nat Protoc, 4, 1440-53.

BRANDL, F., SOMMER, F. & GOEPFERICH, A. (2007) Rational design of hydrogels for tissue engineering: impact of physical factors on cell behavior. Biomaterials, 28, 134-46.

BROSWORTH, L. & DOWNES, S. (2009) Bicompatible three-dimensional scaffolds for tendon tissue engineering using electrospinning. IN DI SILVIO, L. (Ed.) Cellular response to biomaterials. Woodhead publishing in materials limited.

CAMPBELL, P. G. & WEISS, L. E. (2007) Tissue engineering with the aid of inkjet printers. Expert Opin Biol Ther, 7, 1123-7.

CAO, X. & SCHOICHET, M. S. (1999) Delivering neuroactive molecules from biodegradable microspheres for application in central nervous system disorders. Biomaterials, 20, 329-39.

CEN, L., LIU, W., CUI, L., ZHANG, W. J. & CAO, Y. L. (2008) Collagen tissue engineering: Development of novel biomaterials and applications. Pediatric Research, 63, 492-496.

CHANG, C. W., BAYS, E., TAO, L., ALCONCEL, S. N. & MAYNARD, H. D. (2009) Differences in cytotoxicity of poly(PEGA)s synthesized by reversible addition-fragmentation chain transfer polymerization. Chem Commun (Camb), 3580-2.

CHATERJI, S., KWON, I. K. & PARK, K. (2007) Smart Polymeric Gels: Redefining the Limits of Biomedical Devices. Prog Polym Sci, 32, 1083-1122.

CHEN, M. & RUSSEL, W. B. (1991) Characteristics of flocculated silica dispersions. J. Colloid Interface Sci., 141, 546.

CHEN, Z., MENG, H., XING, G., CHEN, C., ZHAO, Y., JIA, G., WANG, T., YUAN, H., YE, C., ZHAO, F., CHAI, Z., ZHU, C., FANG, X., MA, B. & WAN, L. (2006) Acute toxicological effects of copper nanoparticles in vivo. Toxicol Lett, 163, 109-20.

CHO, Y., ZHANG, Y., CHRISTENSEN, T., SAGLE, L. B., CHILKOTI, A. & CREMER, P. S. (2008) Effects of Hofmeister anions on the phase transition temperature of elastin-like polypeptides. J Phys Chem B, 112, 13765-71.

CHOI, C., CHAE, S. Y. & NAH, J. W. (2006) Thermosensitive poly(N-isopropylacrylamide)-b-poly(epsilon-caprolactone) nanoparticles for efficient drug delivery system. Polymer, 47, 4571-4580.

CHU, P. K., CHEN, J. Y., WANG, L. P. & HUANG, N. (2002) Plasma-surface modification of biomaterials. Materials Science and Engineering: R: Reports, 36, 143-206.

CHUN, K. W., YOO, H. S., YOON, J. J. & PARK, T. G. (2004) Biodegradable PLGA microcarriers for injectable delivery of chondrocytes: Effect of surface modification on cell attachment and function. Biotechnology Progress, 20, 1797-1801.

COHN, D., SOSNIK, A. & LEVY, A. (2003) Improved reverse thermo-responsive polymeric systems. Biomaterials, 24, 3707-3714.

CORTIELLA, J., NICHOLS, J. E., KOJIMA, K., BONASSAR, L. J., DARGON, P., ROY, A. K., VACANT, M. P., NILES, J. A. & VACANTI, C. A. (2006) Tissue-engineered lung: An in vivo and in vitro comparison of polyglycolic acid and pluronic F-127 hydrogel/somatic lung progenitor cell constructs to support tissue growth. Tissue Engineering, 12, 1213-1225.

COSGROVE, T. (2010) Polymers at Interfaces. IN COSGROVE, T. (Ed.) Colloid Science: Principles, Methods and Applications., Wiley.

CRAPO, P. M., GILBERT, T. W. & BADYLAK, S. F. (2011) An overview of tissue and whole organ decellularization processes. Biomaterials, In Press, Corrected Proof.

CUKIERMAN, E., PANKOV, R. & YAMADA, K. M. (2002) Cell interactions with three-dimensional matrices. Current Opinion in Cell Biology, 14, 633-640.

CURTIS, A. & DALBY, M. (2009) Cell repsonse to nanofeatures in biomaterials. IN DI SILVIO, L. (Ed.) Cellular response to biomaterials. 1 ed., Woodhead Publishing in Materials.

DALBY, M. J., RIEHLE, M. O., SUTHERLAND, D. S., AGHELI, H. & CURTIS, A. S. (2004) Changes in fibroblast morphology in response to nano-columns produced by colloidal lithography. Biomaterials, 25, 5415-22.

DAY, R. M., BOCCACCINI, A. R., MAQUET, V., SHUREY, S., FORBES, A., GABE, S. M. & JEROME, R. (2004) In vivo characterisation of a novel bioresorbable poly(lactide-co-glycolide) tubular foam scaffold for tissue engineering applications. J Mater Sci Mater Med, 15, 729-34.

DE LAAT, A. W. M. & SCHOO, H. F. M. (1997) Reversible Thermal Flocculation of Aqueous α-Fe_2O_3 Dispersions Stabilized with Novel Poly(Vinyl Ether) Block Copolymers. Journal of Colloid and Interface Science, 200, 228-234.

DE LAS HERAS ALARCON, C., PENNADAM, S. & ALEXANDER, C. (2005) Stimuli responsive polymers for biomedical applications. Chem Soc Rev, 34, 276-85.

DERBY, B. (2008) Bioprinting: inkjet printing proteins and hybrid cell-containing materials and structures. Journal of Materials Chemistry, 18, 5717-5721.

DESAI, T. A. (2000) Micro- and nanoscale structures for tissue engineering constructs. Med Eng Phys, 22, 595-606.

DEY, S., KELLAM, B., ALEXANDER, M. R., ALEXANDER, C. & ROSE, F. R. A. J. (2011) Enzyme-passage free culture of mouse embryonic stem cells on thermo-responsive polymer surfaces. Journal of Materials Chemistry, 21, 6883-6890.

DICKINSON, E. & VAN VLIET, T. (2003) Colloidal aggregation: Mechanisms and implications. Food Colloids, Biopolymers and Materials Royal Society of Chemistry (Great Britain).

DIMITROV, I., TRZEBICKA, B., MULLER, A. H. E., DWORAK, A. & TSVETANOV, C. B. (2007) Thermosensitive water-soluble copolymers with doubly responsive reversibly interacting entities. Progress in Polymer Science, 32, 1275-1343.

DISCHER, D. E., MOONEY, D. J. & ZANDSTRA, P. W. (2009) Growth factors, matrices, and forces combine and control stem cells. Science, 324, 1673-7.

DOBSON, J. (2010) Cancer therapy: A twist on tumour targeting. Nat Mater, 9, 95-6.

DORSEY, S. M., LIN-GIBSON, S. & SIMON, C. G., JR. (2009) X-ray microcomputed tomography for the measurement of cell adhesionand proliferation in polymer scaffolds. Biomaterials, 30, 2967-74.

DRURY, J. L. & MOONEY, D. J. (2003) Hydrogels for tissue engineering: scaffold design variables and applications. Biomaterials, 24, 4337-4351.

DUARTE, A. R., MANO, J. F. & REIS, R. L. (2010) Thermosensitive polymeric matrices for three-dimensional cell culture strategies. Acta Biomater.

DUIJNEVELDT, J. V. (2010) Effect of Polymers on Colloid stability IN COSGRAVE, T. (Ed.) Colloid Science Prinicples, Methods and Applications Second ed., Wiley.

DVIR, T., TIMKO, B. P., KOHANE, D. S. & LANGER, R. (2010) Nanotechnological strategies for engineering complex tissues. Nat Nanotechnol, 6, 13-22.

DVIR-GINZBERG, M., GAMLIELI-BONSHTEIN, I., AGBARIA, R. & COHEN, S. (2003) Liver tissue engineering within alginate scaffolds: Effects of cell-seeding density on hepatocyte viability, morphology, and function. Tissue Engineering, 9, 757-766.

DYNAL (1996) Cell Separation and Protein Purification: information Booklet, Oslo, Norway.

ELAISSARI, A. (2006) Thermally sensitive colloidal particles: From preparation to biomedical applications. PROGRESS IN COLLOID AND POLYMER SCIENCE.

ELSTAD, N. L. & FOWERS, K. D. (2009) OncoGel (ReGel/paclitaxel) -- Clinical applications for a novel paclitaxel delivery system. Advanced Drug Delivery Reviews, 61, 785-794.

ENGLER, A. J., GRIFFIN, M. A., SEN, S., BONNEMANN, C. G., SWEENEY, H. L. & DISCHER, D. E. (2004) Myotubes differentiate optimally on substrates with tissue-like stiffness: pathological implications for soft or stiff microenvironments. J Cell Biol, 166, 877-87.

ESPOSITO, A., MEZZOGIORNO, A., SANNINO, A., DE ROSA, A., MENDITTI, D., ESPOSITO, V. & AMBROSIO, L. (2006) Hyaluronic acid based materials for intestine tissue engineering: A morphological and biochemical study of cell-material interaction. Journal of Materials Science-Materials in Medicine, 17, 1365-1372.

FISCHBACH, C., CHEN, R., MATSUMOTO, T., SCHMELZLE, T., BRUGGE, J. S., POLVERINI, P. J. & MOONEY, D. J. (2007) Engineering tumors with 3D scaffolds. Nat Methods, 4, 855-60.

FRANKS, G. V. (2005) Innovative applications of controlled particle interactions Chemical Engineering Research and Design, 83, 937–945.

FRAYLICH, M. R., LIU, R., RICHARDSON, S. M., BAIRD, P., HOYLAND, J., FREEMONT, A. J., ALEXANDER, C., SHAKESHEFF, K., CELLESI, F. & SAUNDERS, B. R. (2009) Thermally-triggered gelation of PLGA dispersions: Towards an injectable colloidal cell delivery system. J Colloid Interface Sci.

FRAYLICH, M., WANG, W., SHAKESHEFF, K., ALEXANDER, C. & SAUNDERS, B. (2008) Poly(D,L-lactide-co-glycolide) dispersions containing pluronics: from particle preparation to temperature-triggered aggregation. Langmuir, 24, 7761-8.

FREEMONT, A. J. & HOYLAND, J. (2006) Lineage plasticity and cell biology of fibrocartilage and hyaline cartilage: Its significance in cartilage repair and replacement. European Journal of Radiology, 57, 32-36.

FREIBERG, S. & ZHU, X. (2004) Polymer microspheres for controlled drug release. International Journal of Pharmaceutics, 282, 1-18.

FRESHNEY, R. I., B.OBRADOVIC, W.GRAYSON, C.CANNIZZARO & G.VUNJAK-NOVAKOVIC (2007) Principles of Tissue Culture and Bioreactor Design. IN R.LANZA, R.LANGER & J.VACANTI (Eds.) Principles of Tissue engineering 3ed., Elsevier.

FRISCH, S. M. & SCREATON, R. A. (2001) Anoikis mechanisms. Curr Opin Cell Biol, 13, 555-62.

GAO, J. M., NIKLASON, L. & LANGER, R. (1998) Surface hydrolysis of poly(glycolic acid) meshes increases the seeding density of vascular smooth muscle cells. Journal of Biomedical Materials Research, 42, 417-424.

GARTI, N., ROSSANO, A. & AVNI, Y. (1993) GRAFT COPOLYMERS AS EMULSIFIERS: Part I: Grafted Polyethyleneglycol on Polymethylmetacrylate. J. Disp. Sci. Techn., 14, 47-70.

GENTILE, F., TIRINATO, L., BATTISTA, E., CAUSA, F., LIBERALE, C., DI FABRIZIO, E. M. & DECUZZI, P. (2010) Cells preferentially grow on rough substrates. Biomaterials.

GIANCOTTI, F. G. & RUOSLAHTI, E. (1999) Integrin signaling. Science, 285, 1028-32.

GOLDBERG, M., LANGER, R. & JIA, X. (2007) Nanostructured materials for applications in drug delivery and tissue engineering. J Biomater Sci Polym Ed, 18, 241-68.

GUPTA, A. K. & GUPTA, M. (2005) Synthesis and surface engineering of iron oxide nanoparticles for biomedical applications. Biomaterials, 26, 3995-4021.

GURAV, N. (2009) Biocompatibility of degradable polymers for tissue engineering. IN DI SILVIO, L. (Ed.) Cellular response to biomaterials. Woodhead Publishing in Materials.

GUTOWSKA, A., JEONG, B. & JASIONOWSKI, M. (2001) Injectable gels for tissue engineering. Anatomical Record, 263, 342-349.

HAMILTON, L. G. (2008) New injectable scaffolds for cell and drug delivery. Pharmacy. Nottingham, Univeristy of Nottingham.

HARRIS, L. D., KIM, B. S. & MOONEY, D. J. (1998) Open pore biodegradable matrices formed with gas foaming. J Biomed Mater Res, 42, 396-402.

HARTGERINK, J. D., BENIASH, E. & STUPP, S. I. (2002) Peptide-amphiphile nanofibers: a versatile scaffold for the preparation of self-assembling materials. Proc Natl Acad Sci U S A, 99, 5133-8.

HE, C., KIM, S. W. & LEE, D. S. (2008) In situ gelling stimuli-sensitive block copolymer hydrogels for drug delivery. J Control Release, 127, 189-207.

HENRı´QUEZ, C., BUENO, C., LISSI, E. A. & ENCINAS, M. A. (2003) Thiols as chain transfer agents in free radical polymerization in aqueous solution. Polymer, 44, 5559–5561.

HESSE, E., HEFFERAN, T. E., TARARA, J. E., HAASPER, C., MELLER, R., KRETTEK, C., LU, L. & YASZEMSKI, M. J. (2010) Collagen type I hydrogel allows migration, proliferation, and osteogenic differentiation of rat bone marrow stromal cells. J Biomed Mater Res A.

HIGUCHI, A., SUGIYAMA, K., YOON, B. O., SAKURAI, M., HARA, M., SUMITA, M., SUGAWARA, S. & SHIRAI, T. (2003) Serum protein adsorption and platelet adhesion on pluronic (TM)-adsorbed polysulfone membranes. Biomaterials, 24, 3235-3245.

HOLLISTER, S. J. (2006) Porous scaffold design for tissue engineering. Nat Mater, 4, 518-524.

HOQUE, M. E., SAN, W. Y., WEI, F., LI, S., HUANG, M. H., VERT, M. & HUTMACHER, D. W. (2009) Processing of polycaprolactone and polycaprolactone-based copolymers into 3D scaffolds, and their cellular responses. Tissue Eng Part A, 15, 3013-24.

HU, Z., CAI, T. & CHI, C. (2010) Thermoresponsive oligo(ethylene glycol)-methacrylate- based polymers and microgels. Soft matter, 6, 2115-2123.

HUANG, H. L., HSING, H. W., LAI, T. C., CHEN, Y. W., LEE, T. R., CHAN, H. T., LYU, P. C., WU, C. L., LU, Y. C., LIN, S. T., LIN, C. W., LAI, C. H., CHANG, H. T., CHOU, H. C. & CHAN, H. L. (2010) Trypsin-induced proteome alteration during cell subculture in mammalian cells. J Biomed Sci, 17, 36.

HUCKNALL, A., RANGARAJAN, S. & CHILKOTI, A. (2009) In Pursuit of Zero: Polymer Brushes that Resist the Adsorption of Proteins. Advanced Materials, 21, 2441-2446.

HUGHES, R. (2010) An introduction to Colloids. IN COSGROVE, T. (Ed.) Colloid Science: Principles, Methods and Applications. second ed., Wiley.

HUTMACHER, D. W., SCHANTZ, T., ZEIN, I., NG, K. W., TEOH, S. H. & TAN, K. C. (2001) Mechanical properties and cell cultural response of polycaprolactone scaffolds designed and fabricated via fused deposition modeling. Journal of Biomedical Materials Research, 55, 203-216.

HYNES, R. O. (1999) Cell adhesion: old and new questions. Trends Cell Biol, 9, M33-7.

JABBARZADEH, E., JIANG, T., DENG, M., NAIR, L. S., KHAN, Y. M. & LAURENCIN, C. T. (2007) Human endothelial cell growth and phenotypic expression on three dimensional poly(lactide-co-glycolide) sintered microsphere scaffolds for bone tissue engineering. Biotechnol Bioeng, 98, 1094-102.

JAGUR-GRODZINSKI, J. (2006) Polymers for tissue engineering, medical devices, and regenerative medicine. Concise general review of recent studies. Polymers for Advanced Technologies, 17, 395-418.

JAIN, R. A. (2000) The manufacturing techniques of various drug loaded biodegradable poly(lactide-co-glycolide) (PLGA) devices. Biomaterials, 21, 2475-90.

JAKLENEC, A., HINCKFUSS, A., BILGEN, B., CIOMBOR, D. M., AARON, R. & MATHIOWITZ, E. (2008) Sequential release of bioactive IGF-I and TGF-beta(1) from PLGA microsphere-based scaffolds. Biomaterials, 29, 1518-1525.

JAMES, D. W. & TAYLOR, J. F. (1969) The stress developed by sheets of chick fibroblasts in vitro. Exp Cell Res, 54, 107-10.

JEONG, B. & GUTOWSKA, A. (2002) Lessons from nature: stimuli-responsive polymers and their biomedical applications (vol 20, pg 305, 2002). Trends in Biotechnology, 20, 360-360.

JEONG, B., BAE, Y. H. & KIM, S. W. (1999) Thermoreversible gelation of PEG-PLGA-PEG triblock copolymer aqueous solutions. Macromolecules, 32, 7064-7069.

JEONG, B., BAE, Y. H., LEE, D. S. & KIM, S. W. (1997) Biodegradable block copolymers as injectable drug-delivery systems. Nature, 388, 860-862.

JIAO, Y. P. & CUI, F. Z. (2007) Surface modification of polyester biomaterials for tissue engineering. Biomed Mater, 2, R24-37.

KHOR, H. L., NG, K. W., SCHANTZ, J. T., PHAN, T. T., LIM, T. C., TEOH, S. H. & HUTMACHER, D. W. (2002) Poly(epsilon-caprolactone) films as a potential substrate for tissue engineering an epidermal equivalent. Materials Science & Engineering C-Biomimetic and Supramolecular Systems, 20, 71-75.

KIM, B. S. & MOONEY, D. J. (1998) Development of biocompatible synthetic extracellular matrices for tissue engineering. Trends in Biotechnology, 16, 224-230.

KIM, M. H., HONG, H. N., HONG, J. P., PARK, C. J., KWON, S. W., KIM, S. H., KANG, G. & KIM, M. (2010) The effect of VEGF on the myogenic differentiation of adipose tissue derived stem cells within thermosensitive hydrogel matrices. Biomaterials, 31, 1213-1218.

KLOUDA, L. & MIKOS, A. G. (2008) Thermoresponsive hydrogels in biomedical applications. Eur J Pharm Biopharm, 68, 34-45.

KOH, A. Y. C. & SAUNDERS, B. R. (2000) Thermally induced gelation of an oil-in-water emulsion stabilised by a graft copolymer. Chem. Commun., 24, 2461-2462.

KRETLOW, J. D., KLOUDA, L. & MIKOS, A. G. (2007) Injectable matrices and scaffolds for drug delivery in tissue engineering. Adv Drug Deliv Rev, 59, 263-73.

KWON, O. H., KIKUCHI, A., YAMATO, M., SAKURAI, Y. & OKANO, T. (2000) Rapid cell sheet detachment from poly(N-isopropylacrylamide)-grafted porous cell culture membranes. J Biomed Mater Res, 50, 82-9.

LANGER, R. & VACANTI, J. P. (1993) Tissue Engineering. Science, 260, 920-926.

LARSON, R. G. (1999) The Structure and Rheology of Complex Fluids, OUP USA

LE RENARD, P. E., JORDAN, O., FAES, A., PETRI-FINK, A., HOFMANN, H., RUFENACHT, D., BOSMAN, F., BUCHEGGER, F. & DOELKER, E. (2010) The in vivo performance of magnetic particle-loaded injectable, in situ gelling, carriers for the delivery of local hyperthermia. Biomaterials, 31, 691-705.

LEE, J., CUDDIHY, M. J. & KOTOV, N. A. (2008) Three-dimensional cell culture matrices: state of the art. Tissue Eng Part B Rev, 14, 61-86.

LEE, M., DUNN, J. C. Y. & WU, B. M. (2005) Scaffold fabrication by indirect three-dimensional printing. Biomaterials, 26, 4281-4289.

LEE, P. Y., COBAIN, E., HUARD, J. & HUANG, L. (2007) Thermosensitive hydrogel PEG-PLGA-PEG enhances engraftment of muscle-derived stem cells and promotes healing in diabetic wound. Molecular Therapy, 15, 1189-1194.

LEVENTAL, I., GEORGESA, P. C. & JANMEY, P. A. (2007) Soft biological materials and their impact on cell function. Soft matter, 3, 299-306.

LI, L., CHEN, S., ZHENG, J., RATNER, B. D. & JIANG, S. (2005) Protein Adsorption on Oligo(ethylene glycol)-Terminated Alkanethiolate Self-Assembled Monolayers:â€‰ The Molecular Basis for Nonfouling Behavior. The Journal of Physical Chemistry B, 109, 2934-2941.

LI, W. J., TULI, R., HUANG, X., LAQUERRIERE, P., TUAN, R.S. (2005) Multilineage differentiation of human mesenchymal stem cells in a three-dimensional nanofibrous scaffold. Biomaterials 26,, 5158.

LI, W.-J., SHANTI, R. M. & TUAN, R. S. (2006) Electrospinning Technology for Nanofibrous Scaffolds in Tissue Engineering. IN KUMAR, C. S. S. R. (Ed.) Tissue, cell and Organ Engineering. Weinheim, WILEY-VCH Verlag GmbH & Co. KGaA.

LIU, J. C. & TIRRELL, D. A. (2008) Cell response to RGD density in cross-linked artificial extracellular matrix protein films. Biomacromolecules, 9, 2984-8.

LIU, R., FRAYLICH, M. & SAUNDERS, B. R. (2009) Thermoresponsive copolymers: from fundamental studies to applications Colloid Polym. Sci. , 287, 627-743.

LIUA, X., KAMINSKIB, D. M., RIFFLEC, J. S., CHENA, H., TORNOA, M., FINCKB, M. R., TAYLORA, L. & ROSENGARTA, A. J. (2007) Preparation and characterization of biodegradable magnetic carriers by single emulsion-solvent evaporation. Journal of Magnetism and Magnetic Materials, 311, 84-87.

LOPEZ-PEREZ, P. M., DA SILVA, R. M., SOUSA, R. A., PASHKULEVA, I. & REIS, R. L. (2010) Plasma-induced polymerization as a tool for surface functionalization of polymer scaffolds for bone tissue engineering: an in vitro study. Acta Biomater, 6, 3704-12.

LU, L., YASZEMSKI, M. J. & MIKOS, A. G. (2001) TGF-beta1 release from biodegradable polymer microparticles: its effects on marrow stromal osteoblast function. J Bone Joint Surg Am, 83-A Suppl 1, S82-91.

LU, P. & DING, B. (2008) Applications of electrospun fibers. Recent Pat Nanotechnol, 2, 169-82.

LUCIANI, A., COCCOLI, V., ORSI, S., AMBROSIO, L. & NETTI, P. A. (2008) PCL microspheres based functional scaffolds by bottom-up approach with predefined microstructural properties and release profiles. Biomaterials, 29, 4800-7.

LUO, Y., ENGELMAYR, G., AUGUSTE, D. T., FERREIRA, L., KARP, J. M., SAIGAL, S. & LANGER, R. (2007) Three-Dimensional Scaffolds. IN LANGER, R., LANZA, R. & VACANTI, J. (Eds.) Principles of tissue engineering. 3rd ed., Elsevier.

LUTOLF, M. P. & BLAU, H. M. (2009) Artificial Stem Cell Niches. Advanced Materials, 21, 1-14.

LUTOLF, M. P. & HUBBELL, J. A. (2005) Synthetic biomaterials as instructive extracellular microenvironments for morphogenesis in tissue engineering. Nat Biotechnol, 23, 47-55.

LUTOLF, M. P., GILBERT, P. M. & BLAU, H. M. (2009) Designing materials to direct stem-cell fate. Nature, 462, 433-41.

LUTZ, J. F. (2008) Polymerization of oligo(ethylene glycol) (meth)acrylates: Toward new generations of smart biocompatible materials. Journal of Polymer Science Part a-Polymer Chemistry, 46, 3459-3470.

LUTZ, J. F., AKDEMIR, O. & HOTH, A. (2006) Point by point comparison of two thermosensitive polymers exhibiting a similar LCST: Is the age of poly(NIPAM) over? Journal of the American Chemical Society, 128, 13046-13047.

MA, H. W., HYUN, J. H., STILLER, P. & CHILKOTI, A. (2004b) "Non-fouling" oligo(ethylene glycol)-functionalized polymer brushes synthesized by surface-initiated atom transfer radical polymerization. Advanced Materials, 16, 338-+.

MA, K., HYUN, K., ZHANG, Z., BEEBE, T. & CHILKOTI, A. (2005) Fabrication of biofunctionalized quasi-three-dimensional microstructures of a nonfouling comb polymer using soft lithography. Advanced Functional Materials, 15.

MA, P. X. & LANGER, R. (1999) Morphology and mechanical function of long-term in vitro engineered cartilage. Journal of Biomedical Materials Research, 44, 217-221.

MACCHIARINI, P., JUNGEBLUTH, P., GO, T., ASNAGHI, M. A., REES, L. E., COGAN, T. A., DODSON, A., MARTORELL, J., BELLINI, S., PARNIGOTTO, P. P., DICKINSON, S. C., HOLLANDER, A. P., MANTERO, S., CONCONI, M. T. & BIRCHALL, M. A. (2008) Clinical transplantation of a tissue-engineered airway. Lancet, 372, 2023-30.

MADIHALLY, S. V. & MATTHEW, H. W. T. (1999) Porous chitosan scaffolds for tissue engineering. Biomaterials, 20, 1133-1142.

MAGNUSSON, J. P., KHAN, A., PASPARAKIS, G., SAEED, A. O., WANG, W. & ALEXANDER, C. (2008) Ion-sensitive "isothermal" responsive polymers prepared in water. J Am Chem Soc, 130, 10852-3.

MAO, S., XU, J., CAI, C., GERMERSHAUS, O., SCHAPER, A. & KISSEL, T. (2007) Effect of WOW process parameters on morphology and burst release of FITC-dextran loaded PLGA microspheres. Int J Pharm, 334, 137-48.

MART, R. J., OSBORNE, R. D., STEVENS, M. S. & ULIJN, R. V. (2006) Peptide-based stimuli-responsive biomaterials. soft matter, 2, 822-835.

MARTIN, Y., ELDARDIRI, M., LAWRENCE-WATT, D. J. & SHARPE, J. R. (2010) Microcarriers and Their Potential in Tissue Regeneration. Tissue Eng Part B Rev.

MATSUDA, N., SHIMIZU, T., YAMATO, M. & OKANO, T. (2007) Tissue engineering based on cell sheet technology. Advanced Materials, 19, 3089-3099.

MEZGER, T. G. (2006) The rheology handbook : For users of rotational and oscillatory rheometers, Hannover, Germany, Vincentz Network. GMBH & Co.

MIKOS, A. G., LYMAN, M. D., FREED, L. E. & LANGER, R. (1994) Wetting of poly(L-lactic acid) and poly(DL-lactic-co-glycolic acid) foams for tissue culture. Biomaterials, 15, 55-8.

MILTENYI, S., MULLER, W., WEICHEL, W. & RADBRUCH, A. (1990) High gradient magnetic cell separation with MACS. Cytometry, 11, 231-8.

MOAD, G., RIZZARDO, E. & THANG, S. H. (2005) Living Radical polymerization by the RAFT process. Aust. J.Chem., 58, 379-410.

MOONEY, D. J. & VANDENBURGH, H. (2008) Cell Delivery Mechanisms for Tissue Repair. Cell Stem Cell, 2.

MOONEY, D. J., BALDWIN, D. F., SUH, N. P., VACANTI, J. P. & LANGER, R. (1996) Novel approach to fabricate porous sponges of poly(D,L-lactic-co-glycolic acid) without the use of organic solvents. Biomaterials, 17, 1417-22.

NA, K., PARK, J. H., KIM, S. W., SUN, B. K., WOO, D. G., CHUNG, H. M. & PARK, K. H. (2006) Delivery of dexamethasone, ascorbate, and growth factor (TGF beta-3) in thermo-reversible hydrogel constructs embedded with rabbit chondrocytes. Biomaterials, 27, 5951-5957.

NAPPER, D. (1970) Flocculation studies of sterically stabilized dispersions Journal of Colloid and Interface Science, 32, 106-114.

NAPPER, D. H. (1983) Polymeric stabilisation of colloidal dispersions Academic Press.

NAPPER, D. H. (1983a) The effects of Free Polymer on colloid Stability: Theories of Depletion Flocculation and Depletion Phase Seperation. IN NAPPER, D. H. (Ed.) Polymeric Stabilization of colloidal dispersions. Academic Press

NAPPER, D. H. (1983b) Polymeric stabilisation of colloidal dispersions Academic Press.

NETTLES, D. L., CHILKOTI, A. & SETTON, L. A. (2010) Applications of elastin-like polypeptides in tissue engineering. Adv Drug Deliv Rev, 62, 1479-85.

NEWMAN, K. D. & MCBURNEY, M. W. (2004) Poly(D,L lactic-co-glycolic acid) microspheres as biodegradable microcarriers for pluripotent stem cells. Biomaterials, 25, 5763-5771.

NG, K. W., KHOR, H. L. & HUTMACHER, D. W. (2004) In vitro characterization of natural and synthetic dermal matrices cultured with human dermal fibroblasts. Biomaterials, 25, 2807-18.

NG, K. W., LEONG, D. T. & HUTMACHER, D. W. (2005) The challenge to measure cell proliferation in two and three dimensions. Tissue Eng, 11, 182-91.

NOCIARI, M. M., SHALEV, A., BENIAS, P. & RUSSO, C. (1998) A novel one-step, highly sensitive fluorometric assay to evaluate cell-mediated cytotoxicity. J. Immunol. Methods, 213.

ODONNELL, P. B. & MCGINITY, J. W. (1997) Preparation of microspheres by the solvent evaporation technique. Advanced Drug Delivery Reviews, 28, 25-42.

PACHENCE, J. M., BOHRER, M. P. & KOHN, J. (2007) Biodegradable Polymers. IN LANZA, R., LANGER, R. & VACANTI, J. (Eds.) Principles of tissue engineering. 3rd ed., Elsevier,Inc.

PARK, G. E., PATTISON, M. A., PARK, K. & WEBSTER, T. J. (2005) Accelerated chondrocyte functions on NaOH-treated PLGA scaffolds. Biomaterials, 26, 3075-3082.

PARK, S., KIM, G., JEON, Y. C., KOH, Y. & KIM, W. (2009) 3D polycaprolactone scaffolds with controlled pore structure using a rapid prototyping system. J Mater Sci Mater Med, 20, 229-34.

PATTISON, M. A., WURSTER, S., WEBSTER, T. J. & HABERSTROH, K. M. (2005) Three-dimensional, nano-structured PLGA scaffolds for bladder tissue replacement applications. Biomaterials, 26, 2491-500.

PEK, Y. S., WAN, A. C. A., SHEKARAN, A., ZHUO, L. & YING, J. Y. (2008) A thixotropic nanocomposite gel for three-dimensional cell culture. Nature Nanotechnology, 3, 671-675.

PHAM, Q. P., SHARMA, U. & MIKOS, A. G. (2006) Electrospinning of polymeric nanofibers for tissue engineering applications: a review. Tissue Eng, 12, 1197-211.

POLAK, J. M. & BISHOP, A. E. (2006) Stem cells and tissue engineering: past, present, and future. Ann N Y Acad Sci, 1068, 352-66.

PROKOP, A. (2001) Bioartificial organs in the twenty-first century: nanobiological devices. Ann N Y Acad Sci, 944, 472-90.

QIAGEN (2010) http://www.qiagen.com/ products/genomicdnastabilizationpurification/ qiaampsystem/qiaampdnaminikit.aspx#Tabs=t1.

QUIRK, R. A., CHAN, W. C., DAVIES, M. C., TENDLER, S. J. & SHAKESHEFF, K. M. (2001) Poly(L-lysine)-GRGDS as a biomimetic surface modifier for poly(lactic acid). Biomaterials, 22, 865-72.

RAMAKRISHNAN, S. & ZUKOSKI, C. F. (2006) Microstructure and rheology of thermoreversible nanoparticle gels. Langmuir, 22, 7833-42.

RANELLA, A., BARBEROGLOU, M., BAKOGIANNI, S., FOTAKIS, C. & STRATAKIS, E. (2010) Tuning cell adhesion by controlling the roughness and wettability of 3D micro/nano silicon structures. Acta Biomaterialia, 6, 2711-2720.

RATNER, B. D. & BRYANT, S. J. (2004) Biomaterials: where we have been and where we are going. Annu Rev Biomed Eng, 6, 41-75.

REINOUT, S. (2008) Smart biomaterials for tissue engineering of cartilage. Injury, 39, 77-87.

REJMAN, J., OBERLE, V., ZUHORN, I. S. & HOEKSTRA, D. (2004) Size-dependent internalization of particles via the pathways of clathrin- and caveolae-mediated endocytosis. Biochem J, 377, 159-69.

ROBERT, J., PELHAM, J. & WANG, Y. (1997) Cell locomotion and focal adhesions are regulated by substrate flexibility. Proc. Natl. Acad. Sci., 94, 13661–13665.

RON, E. S. & BROMBERG, L. E. (1998) Temperature-responsive gels and thermogelling polymer matrices for protein and peptide delivery. Adv Drug Deliv Rev, 31, 197-221.

ROSCA, I. D., WATARI, F. & UO, M. (2004) Microparticle formation and its mechanism in single and double emulsion solvent evaporation. J Control Release, 99, 271-80.

SAFARIK, I. & SAFARIKOVA, M. (1999) Use of magnetic techniques for the isolation of cells. J Chromatogr B Biomed Sci Appl, 722, 33-53.

SAIM, A. B., CAO, Y., WENG, Y., CHANG, C.-N., VACANTI, M. A., VACANTI, C. A. & EAVEY, R. D. (2000) Engineering Autogenous Cartilage in the Shape of a Helix Using an Injectable Hydrogel Scaffold. The Laryngoscope, 110, 1694-1697.

SALEM, A. K., ROSE, F. R. A. J., OREFFO, R. O. C., YANG, X. B., DAVIES, M. C., MITCHELL, J. R., ROBERTS, C. J., STOLNIK-TRENKIC, S., TENDLER, S. J. B., WILLIAMS, P. M. & SHAKESHEFF, K. M. (2003) Porous polymer and cell composites that self-assemble in situ. Advanced Materials, 15, 210-+.

SALIH, V. (2009) Biodegradable scaffolds for tissue engineering. IN DI SILVIO, L. (Ed.) Cellular response to biomaterials. Cambridge, Woodhead Publishing Limited.

SALTZMAN, W. M. & KYRIAKIDES, T. R. (2007) Cell interactions with Polymers. IN LANZA, R., LANGER, R. & VACANTI, J. (Eds.) Principles of Tissue engineering. Third ed., Elsevier,Inc.

SCHILD, H. G. (1992) Poly (N-Isopropylacrylamide) - Experiment, Theory and Application. Progress in Polymer Science, 17, 163-249.

SCHINDLER, M., NUR, E. K. A., AHMED, I., KAMAL, J., LIU, H. Y., AMOR, N., PONERY, A. S., CROCKETT, D. P., GRAFE, T. H., CHUNG, H. Y., WEIK, T., JONES, E. & MEINERS, S. (2006) Living in three dimensions: 3D nanostructured environments for cell culture and regenerative medicine. Cell Biochem Biophys, 45, 215-27.

SCHMOLKA, I. R. (1972) Artificial skin. I. Preparation and properties of pluronic F-127 gels for treatment of burns. J Biomed Mater Res, 6, 571-82.

SCHWARZ, U. (2007) Soft matters in cell adhesion: rigidity sensing on soft elastic substrates. Soft matter, 3, 263-266.

SCOTCHFORD, C. A. (2009) Cell response to surface chemistry in biomaterials. IN DI SILVIO, L. (Ed.) Cellular response to biomaterials. Cambridge, Wooshead Publishing

SERRANO, M. C., PAGANI, R., VALLET-REGI, M., PENA, J., RAMILA, A., IZQUIERDO, I. & PORTOLES, M. T. (2004) In vitro biocompatibility assessment of poly(epsilon-caprolactone) films using L929 mouse fibroblasts. Biomaterials, 25, 5603-11.

SERRANO, M. C., PORTOLES, M. T., VALLET-REGI, M., IZQUIERDO, I., GALLETTI, L., COMAS, J. V. & PAGANI, R. (2005) Vascular endothelial and smooth muscle cell culture on NaOH-treated poly (epsilon-caprolactone) films: A preliminary study for vascular graft development. Macromolecular Bioscience, 5, 415-423.

SHAKESHEFF, K. M., EVORA, C., SORIANO, I. & LANGER, R. (1997) The adsorption of poly(vinyl alcohol) to biodegradable microparticles studied by x-ray photoelectron spectroscopy (XPS). Journal of Colloid and Interface Science, 185, 538-547.

SHAY, J. S. (1999) AQUEOUS COLLOIDAL DISPERSIONS WITH GRAFTED POLY(ETHYLENE OXIDE) CHAINS: SYNTHESIS, MICROSTRUCTURE, AND RHEOLOGY. CHEMICAL ENGINEERING. Raleigh, North Carolina State University.

SHAY, J. S., ENGLISH, R. J. & KHAN, S. A. (2000) Rheological behavior of a polymerically stabilized latex for use in water-borne coatings,. Polym. Eng.Sci., 40.

SHAY, J. S., RAGHAVAN, S. R. & KHAN, S. A. (2001) Thermoreversible gelation in aqueous dispersions of colloidal particles bearing grafted poly(ethylene oxide) chains. Journal of Rheology, 45, 913-927.

SHEN, H., HU, X., YANG, F., BEI, J. & WANG, S. (2007) Combining oxygen plasma treatment with anchorage of cationized gelatin for enhancing cell affinity of poly(lactide-co-glycolide). Biomaterials, 28, 4219-30.

SHEN, R. R. & MOONEY, D. J. (2003) Polymeric Growth Factor Delivery Strategies for Tissue Engineering

SHIN, M., ISHII, O., SUEDA, T., AND VACANTI, J.P. (2004) Contractile cardiac grafts using a novel nanofibrous mesh. Biomaterials.25, 3717.

SILL, T. J. & VON RECUM, H. A. (2008) Electrospinning: applications in drug delivery and tissue engineering. Biomaterials, 29, 1989-2006.

SINHA, V. R., BANSAL, K., KAUSHIK, R., KUMRIA, R. & TREHAN, A. (2004) Poly-epsilon-caprolactone microspheres and nanospheres: an overview. Int J Pharm, 278, 1-23.

STEINBERG, M. S., ARMSTRONG, P. B. & GRANGER, R. E. (1973) On the recovery of adhesiveness by trypsin-dissociated cells. J Membr Biol, 13, 97-128.

STEVENS, M. M., MARINI, R. P., SCHAEFER, D., ARONSON, J., LANGER, R. & SHASTRI, V. P. (2005) In vivo engineering of organs: the bone bioreactor. Proc Natl Acad Sci U S A, 102, 11450-5.

STUART, M. A., HUCK, W. T., GENZER, J., MULLER, M., OBER, C., STAMM, M., SUKHORUKOV, G. B., SZLEIFER, I., TSUKRUK, V. V., URBAN, M., WINNIK, F., ZAUSCHER, S., LUZINOV, I. & MINKO, S. (2010) Emerging applications of stimuli-responsive polymer materials. Nat Mater, 9, 101-13.

SUCIATI, T., HOWARD, D., BARRY, J., EVERITT, N. M., SHAKESHEFF, K. M. & ROSE, F. R. A. J. (2006) Zonal release of proteins within tissue engineering scaffolds. Journal of Materials Science-Materials in Medicine, 17, 1049-1056.

TADROS, T. (2009) Polymeric surfactants in disperse systems. Adv Colloid Interface Sci, 147-148, 281-99.

TADROS, T. F. (1992) Control of stability/flocculation and rheology of concentrated suspensions. Pure&Appl. Chern, 64, 1715-1720.

TADROS, T. F. (1996) Correlation of viscoelastic properties of stable and flocculated suspensions with their interparticle interactions. Advances in Colloid and Interface Science, 68, 97-200.

TADROS, T. F. (1996) Correlation of viscoelastic properties of stable and flocculated suspensions with their interparticle interactions. Advances in Colloid and Interface Science, 68, 97-200.

THANG, S. H., CHONG, Y. K., MAYADUNNE, R. T. A., MOAD, G. & RIZZARDO, E. (1999) Novel Synthesis of Functional Dithioesters,Dithiocarbamates, Xanthates and Trithiocarbonates. Tetrahedron Letters, 40, 2435-2438.

THAPA, A., WEBSTER, T. J. & HABERSTROH, K. M. (2003) Polymers with nano-dimensional surface features enhance bladder smooth muscle cell adhesion. J Biomed Mater Res A, 67, 1374-83.

VACANTI, J. P., LANGER, R., UPTON, J. & MARLER, J. J. (1998) Transplantation of cells in matrices for tissue regeneration. Adv Drug Deliv Rev, 33, 165-182.

VAN DUIJNEVELDT, J. (2010) Effect of Polymers on Colloidal Stability IN COSGRAVE, T. (Ed.) Colloid Science Principles, Methods and Applications. Second ed., Wiley

VAN TOMME, S. R., STORM, G. & HENNINK, W. E. (2008) In situ gelling hydrogels for pharmaceutical and biomedical applications. International Journal of Pharmaceutics, 355, 1-18.

VAN VLIET, T. & LYKLEMA, H. (2005) Rheology. IN LYKLEMA, H. (Ed.) Fundamentals of Interface and Colloid Science. Elsevier.

VEHRING, R. (2008) Pharmaceutical particle engineering via spray drying. Pharm Res, 25, 999-1022.

VERNON, B., SUNG, W. K. & YOU, H. B. (1999) Insulin release from islets of Langerhans entrapped in a poly(N-isopropylacrylamide-co-acrylic acid) polymer gel. Journal of Biomaterials Science, Polymer Edition, 10, 183-198.

VIHOLA, H., LAUKKANEN, A., VALTOLA, L., TENHU, H. & HIRVONEN, J. (2005) Cytotoxicity of thermosensitive polymers poly(N-isopropylacrylamide), poly(N-vinylcaprolactam) and amphiphilically modified poly(N-vinylcaprolactam). Biomaterials, 26, 3055-3064.

VIHOLA, H., MARTTILA, A. K., PAKKANEN, J. S., ANDERSSON, M., LAUKKANEN, A., KAUKONEN, A. M., TENHU, H. & HIRVONEN, J. (2007) Cell-polymer interactions of fluorescent polystyrene latex particles coated with thermosensitive poly(N-isopropylacrylamide) and poly(N-vinylcaprolactam) or grafted with poly(ethylene oxide)-macromonomer. Int J Pharm, 343, 238-46.

VON RECUM, A. F. & VAN KOOTEN, T. G. (1995) The influence of micro-topography on cellular response and the implications for silicone implants. J Biomater Sci Polym Ed, 7, 181-98.

VUORI, K. (1998) Integrin signaling: tyrosine phosphorylation events in focal adhesions. J Membr Biol, 165, 191-9.

WANG, Q., WANG, L. M., DETAMORE, M. S. & BERKLAND, C. (2008) Biodegradable colloidal gels as moldable tissue engineering scaffolds. Advanced Materials, 20, 236-+.

WANG, W., LIANG, H., CHEIKH AL GHANAMI, R., HAMILTON, L., FRAYLICH, M., SHAKESHEFF, K. M., SAUNDERS, B. & ALEXANDER, C. (2009) Biodegradable Thermoresponsive Microparticle Dispersions for Injectable Cell Delivery Prepared Using a Single-Step Process. Advanced Materials, 21, 1809-1813.

WANKA, G., HOFFMANN, H. & ULBRICHT, W. (1990) The Aggregation Behavior of Poly-(Oxyethylene)-Poly-(Oxypropylene)-Poly-(Oxyethylene)-Block-Copolymers in Aqueous-Solution. Colloid and Polymer Science, 268, 101-117.

WATSON, M. S., WHITAKER, M. J., HOWDLE, S. M. & SHAKESHEFF, K. M. (2002) Incorporation of Proteins into Polymer Materials by a Novel Supercritical Fluid Processing Method. Advanced Materials, 14, 1802-1804.

WEBBER, M. J., TONGERS, J., RENAULT, M. A., RONCALLI, J. G., LOSORDO, D. W. & STUPP, S. I. (2010) Development of bioactive peptide amphiphiles for therapeutic cell delivery. Acta Biomater, 6, 3-11.

WEI, G., JIN, Q., GIANNOBILE, W. V. & MA, P. X. (2007) The enhancement of osteogenesis by nano-fibrous scaffolds incorporating rhBMP-7 nanospheres. Biomaterials, 28, 2087-2096.

WEISSLEDER, R., STARK, D. D., ENGELSTAD, B. L., BACON, B. R., COMPTON, C. C., WHITE, D. L., JACOBS, P. & LEWIS, J. (1989) Superparamagnetic iron oxide: pharmacokinetics and toxicity. AJR Am J Roentgenol, 152, 167-73.

WILSON, C. J., CLEGG, R. E., LEAVESLEY, D. I. & PEARCY, M. J. (2005) Mediation of biomaterial-cell interactions by adsorbed proteins: a review. Tissue Eng, 11, 1-18.

WISCHERHOFF, E., UHLIG, K., LANKENAU, A., BORNER, H. G., LASCHEWSKY, A., DUSCHL, C. & LUTZ, J. F. (2008) Controlled cell adhesion on PEG-based switchable surfaces. Angew Chem Int Ed Engl, 47, 5666-8.

WOO, B. H., FINK, B. F., PAGE, R., SCHRIER, J. A., JO, Y. W., JIANG, G., DELUCA, M., VASCONEZ, H. C. & DELUCA, P. P. (2001) Enhancement of bone growth by sustained delivery of recombinant human bone morphogenetic protein-2 in a polymeric matrix. Pharm Res, 18, 1747-53.

XIE, B. J., PARKHILL, R. L., WARREN, W. L. & SMAY, J. E. (2006) Direct writing of three-dimensional polymer scaffolds using colloidal gels. Advanced Functional Materials, 16, 1685-1693.

YAMAMOTO, M., TABATA, Y. & IKADA, Y. (1999) Growth factor release from gelatin hydrogel for tissue engineering. Journal of Bioactive and Compatible Polymers, 14, 474-489.

YANEZ, J. A., LAARZ, E. & BERGSTROM, L. (1999) Viscoelastic properties of particle gels. Journal of Colloid and Interface Science, 209, 162-172.

YANG, J., PARK, S. B., YOON, H. G., HUH, Y. M. & HAAM, S. (2006) Preparation of poly epsilon-caprolactone nanoparticles containing magnetite for magnetic drug carrier. Int J Pharm, 324, 185-90.

YANNAS, I. V. (2005) Facts and theories of induced organ regeneration. Adv Biochem Eng Biotechnol, 93, 1-38.

ZELZER, M., MAJANI, R., BRADLEY, J. W., ROSE, F. R. A. J., DAVIES, M. C. & ALEXANDER, M. R. (2008) Investigation of cell-surface interactions using chemical gradients formed from plasma polymers. Biomaterials, 29, 172-184.

ZENTNER, G. M., RATHI, R., SHIH, C., MCREA, J. C., SEO, M. H., OH, H., RHEE, B. G., MESTECKY, J., MOLDOVEANU, Z., MORGAN, M. & WEITMAN, S. (2001) Biodegradable block copolymers for delivery of proteins and water-insoluble drugs. Journal of Controlled Release, 72, 203-215.

ZHANG, Y., FURYK, S., BERGBREITER, D. E. & CREMER, P. S. (2005) Specific ion effects on the water solubility of macromolecules: PNIPAM and the Hofmeister series. J Am Chem Soc, 127, 14505-10.

ZHOU, M., SMITH, A. M., DAS, A. K., HODSON, N. W., COLLINS, R. F., ULIJN, R. V. & GOUGH, J. E. (2009) Self-assembled peptide-based hydrogels as scaffolds for anchorage-dependent cells. Biomaterials, 30, 2523-30.

ZHU, Y. B., GAO, C. Y. & SHEN, J. C. (2002) Surface modification of polycaprolactone with poly(methacrylic acid) and gelatin covalent immobilization for promoting its cytocompatibility. Biomaterials, 23, 4889-4895.

ZHUA, A. P., FANGB, N., CHAN-PARKA, M. B. & CHANB, V. (2006) Adhesion contact dynamics of 3T3 fibroblasts on poly(lactide-co-glycolide acid) surface modified by photochemical immobilization of biomacromolecules. Biomaterials 27 2566–2576.